# The Creation of Nonlinear Behavioral-Level Models for System Level Receiver Simulation


Christo A. Nel

Thesis presented in partial fulfillment of the requirements for the degree of Master of Science (Electronic Engineering) at the University of Stellenbosch.

Supervisor: Dr. Cornell van Niekerk

December 2004

Declaration: *I, the undersigned, hereby declare that the work in this thesis is my own original work and has not previously in its entirety or in part been submitted at any university for a degree.*

Signed:

Date:

# Abstract

The aim of this thesis was to investigate the use of behavioral level models in receiver simulations using the capabilities of Agilent's Advanced Design System. Behavioral level modeling has become increasingly attractive because it offers faster and easier results for system level simulations.

The work in this thesis focused strongly on nonlinear measurements to characterize the various nonlinear phenomena that are present in amplifiers and mixers. Measurement automation software was developed to automate the process. An error correction technique was also developed to increase the accuracy of spectrum analyzer measurements.

The measured data was used to implement the behavioral level amplifier and mixer models in ADS. The accuracy of the models was compared to measured data and the different available models were compared.

Finally the models were combined to realize different receivers and were used to do typical receiver tests. These test include gain and gain compression, two-tone intermodulation and spurious responses. The results are compared to measured data to test the accuracy and usefulness of the models and simulation techniques.

# Opsomming

Die doel van hierdie tesis was om stelsel-vlak gedrags-modelle te ondersoek soos hulle in Agilent se Advanced Design System (ADS) aangebied word. Die modellering van die stelselvlak-gedrag van komponente en stelsels is aantreklik aangesien dit 'n hoë vlak beskrywing van komplekse kommunikasie stelsels moontlik maak. Akkurate stelsel-vlak simulasies sal lei tot vinnige ontwikkeling en evaluasie van nuwe sisteme. Die resultate wat verkry word is egter afhanklik van die beskikbaarheid van akkurate stelsel-vlak gedrags-modelle

Die tesis het baie sterk op metings staat gemaak om die nie-liniêre gedrag van versterkers en mengers te karakteriseer. Meet sagteware is ontwikkel om die verskillende metings te automatiseer. Fout korreksie vir spetrum-analiseerder-metings is ook ontwikkel.

Die gemete data is gebruik om die nie-liniêre gedrags-modelle in ADS te implementer. Die modelle is in simulasies gebruik en die akuraatheid van die simulasies is teen gemete data getoets.

Die finale deel van die tesis gebruik die modelle om tipiese ontvanger karakteristieke te voorspel. Die volgende toetse is gedoen: aanwins en kompressie, twee-toon intermodulasie en hoer orde meng produkte. Die resultate van die toetse is met gemete data vergelyk om die akuraatehied en bruikbaarheid van die verskillende modelle te vergelyk.

# Acknowledgements

I am in debt to Dr. Cornell van Niekerk for his unprecedented helpfulness and patience. I want to thank him for always being available and genuinely concerned in solving my problems. Thank you very much I really enjoyed working with you.

To everyone at the E&E, thank you for the friendliness and help. Specifically, the people at SED. Thank you to Wessel Croukamp in particular.

I want to thank my parents for support and love over the past six years. I want to thank them for the incredible opportunities they have given me.

To my friends who aided in the preservation of sanity, albeit by means of insanity.

To Elmien, your support and devotion has changed me forever. Thank you for always being there.

To the Creator of the things we can only see in part. My praise and thanks for the life that I have. We are nothing without You.

'If the solar system was brought about by an accidental collision, then the appearance of organic life on this planet was also an accident, and the whole evolution of Man was an accident too. If so, then all our present thoughts are mere accidents — the accidental by-product of the movement of atoms. And this holds for the thoughts of the materialists and astronomers as well as for anyone else's. But if *their* thoughts — i.e. of materialism and astronomy — are merely accidental by-products, why should we believe them to be true? I see no reason for believing that one accident should be able to give me a correct account of all the other accidents. It's like expecting that the accidental shape taken by the splash when you upset a milk jug should give you a correct account of how the jug was made and why it was upset.'

C.S. Lewis (1898–1963),

# Content

# Chapter 1

# Theoretical Overview of RF Simulation

## Introduction

The main object of this research was to investigate the abilities of nonlinear system level simulation for the design of RF receivers. This is a very wide topic and the aim of this chapter is to clarify the definition of nonlinear simulation in this work, and to show where it fits into the larger topic of simulation in general. For this purpose some terms will be defined to clarify their use in this work. In general, simulation means to imitate conditions of a situation, using a model, for the convenience of training or to resemble the real thing [1]. In the case of electronics and more specifically RF systems, this can be translated to mean that simulation is the numerical calculation of the response of a system under certain inputs. This usually boils down to applying various parameters to a specific algorithm [2]. This type of mathematical simulation is used to replicate almost any observable phenomenon in engineering. In the case of RF electronics there is a wide variety of mathematical techniques and strategies that have been used to do this. In the field of engineering this is usually done to simplify and speed up the design process, with the ultimate goal being to deliver a better product faster, and at lower cost. It may be valuable to keep this in mind throughout the reading of this work because the purpose of modelling and simulation is not purely the perfect reproduction of the real situation but rather a reproduction adequate to reach the goals of the user. However, this work will show that modern day communications systems require increasingly accurate results that require increasingly complicated techniques. The different simulation strategies will be discussed in this section (1.1). A basic simulation usually consists of a simulator (simulating technique) and a model. In the simplest form the model is a mathematical representation of a physical process that receives an input or inputs supplied by a simulator. However it is also possible that the physical process can be known beforehand by the simulator in which case the model can just be a collection of data on which the simulator will perform certain operations. The typical models that work with the simulation strategies described in section (1.1) will be explained in section (1.2). This work is primarily focussed on exploring nonlinear phenomenon and the models and simulation techniques that are used to describe them. Section (1.3) is an introduction to nonlinear behaviour in RF components and systems which will be very important in the later chapters. The aim of this chapter is therefore to clarify the purpose of this work and where it fits in relative to other

simulation techniques. The final section of this chapter will describe the layout of the rest of the content.

## 1.1 Simulation Techniques

The rapid development of computer technology in the past few years has significantly increased the expectations that designers have from a simulation. Before the large processing power available today, the most limiting aspect to simulations was time. Because of this many earlier simulation techniques focussed mainly on linear theory where devices are assumed to be linear around a certain operating point. While this assumption may be adequate in many cases it is a fact that all electrical circuits are nonlinear (active or passive) and therefore this assumption will eventually break down [3]. This usually happens at high frequencies or power levels. There are various older nonlinear techniques that aimed to incorporate the nonlinear behaviour of devices to different degrees. However most of them can only be applied to very specific purposes for instance load pull analyses for amplifiers, and large signal scattering parameters. These techniques basically apply linear theory to localized nonlinear data. They are often not adequate to simulate large systems and are not discussed further in this work. The basic linear approach to simulation using linear two port device descriptions like scattering parameters or port impedance parameters, can still deliver usefull, albeit limited results. This is a well known technique and computer programs like Touchtone is widely known and used. However when nonlinear behaviour is important other options need to be considered. The two basic approaches to this problem are time-domain analysis and frequency-domain analysis. There are also hybrid techniques like envelope simulation that incorporate aspects of both time-domain and frequency-domain techniques. This section aims to distinguish between the different available nonlinear simulation strategies.

### 1.1.1 Time Domain Analysis

Time domain simulation is an excellent nonlinear technique. It consists of dividing a circuit into lumped linear and nonlinear components and then determining a set of differential equations that can be solved numerically. This technique, used by simulation packages like Spice, is excellent for the design of low-frequency analog and digital circuits. It works very well with lumped elements and a limited array of distributed elements. However it cannot use frequency domain parameters, such as S-parameters, that are usually used to describe distributed element devices such as transmission lines. It also has difficulty in handling noncommensurate excitations which is specifically important in communication systems. One additional problem is that higher frequencies directly translate to smaller time steps in an analysis. This, along with the fact that many circuits have slow start-up transients, make time-domain analysis very slow and will continue to limit its application to RF and microwave circuits.

### 1.1.2 Frequency Domain Methods

The best known technique used for nonlinear frequency domain analysis is harmonic-balance analysis (HB). This technique can be applied to strongly nonlinear circuits and can handle multi frequency excitations although it is limited by computer hardware in this regard. Another very important aspect of harmonic-balance is that it can easily link nonlinear and linear circuit portions as well as distributed element sections. This is important because it makes this technique "backwards compatible" with previous industry standard techniques like linear S-

parameter simulations. This also enables the user to describe passive components by their linear two port S-parameters and nonlinear active components with more complicated nonlinear models.

There are various simulation programs that have HB capabilities of which the best known ones are ADS (Advanced Design System) from Agilent and Microwave Office (MWO) from Advanced Wave Research. Another nonlinear frequency domain technique that is supplied by MWO is called Voltera-series analysis. This technique is best when applied to weakly nonlinear circuits and it was not evaluated in this work which focussed primarily on harmonic-balance simulations.

Even though harmonic balance can handle multi-tone excitations, modulated signals soon become too complicated for efficient simulation. Primarily for this reason, envelope analysis was developed. This technique starts by determining the envelope of a modulated signal which usually has a much lower frequency than the carrier signal. The modulated waveform can then be sampled at a rate determined by the slow envelope frequency and a harmonic-balance simulation is then performed at each sample point. The result is a harmonic-balance simulation at different time steps that yield time domain results. The time domain results can be translated to the frequency domain by Fourier transform. This technique is also available in ADS. The relevant techniques will be explained in more detail in the chapters where they are used.

## 1.2 Circuit and Component Modelling for Simulation

The simulation techniques described in the previous section all need some information of the specific circuit to operate on. This information is usually supplied in the form of device models. A model is the way in which the different characteristics of a circuit is supplied to a simulator and this term is applied to a wide range of data structures, equations and equivalent circuits that are used to accomplish this. This section will describe some of the best know modelling strategies.

### 1.2.1 Linear Data Models

This type of model usually consists of some sort of port parameter that describes the linear operation of a device, such as S-parameters. These models can be very valuable in linear as well as nonlinear simulations and was used extensively in this work to describe devices such as filters, cables and attenuators. Linear data is normally used to calculate linear parameters such as port impedance or the forward gain or loss of a device. The data in these models, like S-parameters, are usually frequency domain quantities and this type of model is therefore used in frequency domain simulations.

### 1.2.2 Equivalent Circuit Models

Equivalent circuit modelling is a technique that describes a device, such as a transistor, by using lumped circuit elements including nonlinear resistors, capacitors and controlled sources. These models can be used by time-domain as well as frequency-domain simulators and is a well developed field. The structure of an equivalent circuit model is usually derived from the physical construction of the device together with the basic principles that it operates on. As an example,

Figure 1.1 shows the nonlinear controlled sources, capacitors and resistors of the Maas-Neilsen field effect transistor (FET) model [4].

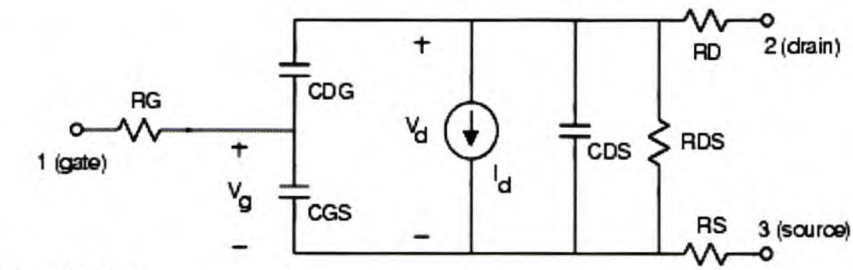


For $V_g \le VT$

$I_d = 0.0$

For $V_g > VT$

$$I_d = \tanh(T \cdot V_d) \cdot (A0 \cdot X_{rad} + A1 \cdot \sin(X_{rad}) + A2 \cdot \sin(2X_{rad}) + A3 \cdot \sin(3X_{rad}) + A4 \cdot \sin(4X_{rad}))$$

where

$$X_{rad} = \pi \frac{(V_g - VT)}{(VF - VT)}$$

Figure 1.1 The Maas-Neilsen FET equivalent circuit model is shown in this figure [4]. *VT* refers to the threshold or "pinch off "gate voltage while *VF* is the maximum gate voltage. These two voltages, as well as the parameters A0 to A4, are usually determined from measurements. The values for the capacitors and resistors are also determined from measured data. [3]

The process of determining parameter values for an equivalent circuit model from measured data is called parameter extraction. It usually requires large sets of measured data to describe a device. This data can be DC measurements such as I/V or C/V characteristics, or a combination of DC and S-parameter measurements. In some cases parameters such as CGS (gain source capacitance) in Figure 1.1 can be measure directly using a network analyzer. The most fundamental problem of this technique is that it requires extensive knowledge of the device physics. The structure of the model has to be determined beforehand and then the different parameters of the model are extracted from measured data. This type of information is often not readily available. Another problem is that devices such as small signal amplifiers may include several transistors. An equivalent circuit of a more complicated device will soon become very large and the internal circuitry of system level devices are rarely available to designers. Furthermore this type of modelling will require large amounts of human intervention to create a model of a system like an RF receiver. It is the possibility of bypassing these time consuming efforts that makes the concept of behavioral models so attractive.

The topic of equivalent circuit models and parameter extraction is a very large field, and it is not in the scope of this work.

### 1.2.3 Models

The term "behavioural models" has been applied to many different modelling schemes in the past. Basically the ideal behavioral model is a "black box" representation of a device such as an amplifier or a mixer that reproduce the device behaviour depending on the excitation. Such a model describes the device as a whole in contrast to equivalent circuit modelling where each

transistor or diode in an amplifier or mixer is described by an equivalent circuit. This is where the major difference between the two strategies is the clearest. Equivalent circuit modelling fits measured data to a rigid structure of lumped elements of an equivalent circuit model while behavioral modelling fits an equation of some sort to data that describe the operation of a device as a whole. The creator of a behavioral model does not base the model on any physical aspect of the device's internal components while this is the starting point with equivalent circuit models. The field of equivalent circuit modelling is well established and can give very accurate predictions of nonlinear device behaviour in simulations. However it is slow and become increasingly slower for more complicated devices and systems. On the other hand the field of behavioral modelling can give a varying range of performances (speed and accuracy) depending largely on the amount of effort that is put into creating a model.

In this work the various amplifier and mixer nonlinear behavioral models that are available in ADS are tested. The strategy in ADS is to use data that describe the behaviour of the device under certain excitations to determine some transfer equation from input port to output port. The data used to describe the model can come from various sources and types of measurements.

One of the ideas is to do a once-of equivalent circuit simulation of the device and capture the data. This is often called transistor level simulation because an amplifier model will be created using existing equivalent circuit models of the transistor (or transistors) used in the amplifier. This very slow but accurate simulation is then performed only once. The resulting data is then used to represent the device in larger circuits by applying the transistor level simulation data to a behavioral model. The major problem with this strategy is that the user has to know exactly what the circuit looks like and which transistors etc. were used. This type of information is usually not available to third party users of MMIC amplifiers and mixers.

The strategy that was explored in this work was to measure certain device parameters, and then apply them to the behavioral models instead of using the data from a transistor level simulation. This has the advantage that the user can measure the device under the exact operating conditions that it will be used for. Furthermore, depending on the application, this can be done fast and without any knowledge of the internal working of the device. The most obvious drawback of this method is that it relies on RF or microwave measurements. This limits the accuracy and some nonlinear measurements can be very complicated. Because these models are dependent on data they can usually only be used for excitations close to the measurements they where modelled from. This is unlike the case of equivalent circuit models that are generally applicable to a wide range of applications.

The use of behavioral level models is not a clearly defined area and the aim of this work is to investigate the possibilities of this type of modelling for receiver simulation in ADS. The chapters in this work will show the accuracy of these models and discuss the abilities as well as shortcomings and difficulties. The next section is an introduction to the nonlinear parameters and quantities that are commonly used to define nonlinear phenomenon in RF and microwave circuits and systems.

## 1.3 Basic Nonlinear Phenomenon

The concept of nonlinearity is difficult to define explicitly and even in real world measurements there is no one single parameter or quantity that can define a nonlinear device. There is rather a collection of "figures of merit" that can define different aspects of a device's nonlinear behaviour. This section will show a mathematical analysis of an arbitrary nonlinearity and use

this to define the important nonlinear parameters that will be used in this work to characterize nonlinear devices. Similar mathematical discussions of the basic nonlinear phenomenon can be found in the following references [3, 5, 6]. Figure 1.2 shows a general third order nonlinearity exited by a voltage source $V_s$.

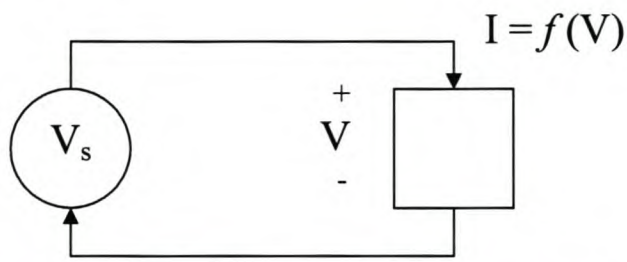


Figure 1.2 This figure shows a general nonlinearity excited by voltage source $V_s$. The circuit current is a nonlinear function of the voltage (V) across the nonlinear device.

For the purpose of this illustration there is no source resistance and therefore the current can be calculated by substituting the source voltage into the nonlinear current equation given by the following expression.

$$I = aV + bV^2 + cV^3 \qquad 1.1$$

For the purpose of this analysis $V_s$ is a two tone excitation given by equation (1.2).

$$V_s = V_1 \cos(\varpi_1 t) + V_2 \cos(\varpi_2 t) \qquad 1.2$$

If the excitation, equation (1.2), is substituted into the nonlinear equation (1.1), the resulting terms can be grouped into three sets. The first set is the result of the first term in equation (1.1) the second set is for the quadratic term while the third set is for the cubic term. The three sets are shown in equation (1.3).

$$i_a(t) = aV_1 \cos(\varpi_1 t) + aV_2 \cos(\varpi_2 t) \qquad 1.3a$$

$$i_b(t) = \frac{b}{2}\{V_1^2 + V_2^2 + V_1^2 \cos(2\varpi_1 t) + V_2^2 \cos(2\varpi_2 t) + 2V_1 V_2[\cos((\varpi_1 + \varpi_2)t) + \cos((\varpi_1 - \varpi_2)t)]\} \qquad 1.3b$$

$$\begin{aligned} i_c(t) = \frac{c}{4}\{&V_1^3 \cos(3\varpi_1 t) + V_2^3 \cos(3\varpi_2 t) \\ &+ 3V_1^2 V_2[\cos((2\varpi_1 + \varpi_2)t) + \cos((2\varpi_1 - \varpi_2)t)] \\ &+ 3V_1 V_2^2[\cos((\varpi_1 + 2\varpi_2)t) + \cos((\varpi_1 - 2\varpi_2)t)] \\ &+ 3(V_1^3 + 2V_1 V_2^2)\cos(\varpi_1 t) \\ &+ 3(V_2^3 + 2V_1^2 V_2)\cos(\varpi_2 t)\} \end{aligned} \qquad 1.3c$$

It can be seen that many new frequencies are generated by this fairly simple nonlinearity and these equations can be used to explain a number of nonlinear effects that are common in RF

devices and systems. The most important of these where used in this work to characterize nonlinear device behaviour and is explained in the following paragraphs.

### 1.3.1 Harmonic Generation

While this is a well known effect in most RF devices it is easy to forget that it is also the result of the nonlinearity of circuits and involve the generation of completely new frequencies. These terms are obvious from equation (1.3a) to (1.3c) as all integer multiple terms of the excitation frequencies, $m\omega_1$ and $n\omega_2$. The maximum harmonic order will depend on the order of the nonlinearity. In this case the maximum harmonic order is 3 generating frequencies at $2\omega_1$, $2\omega_2$, $3\omega_1$ and $3\omega_2$.

### 1.3.2 Saturation

Considering equations (1.3a) to (1.3c) for a case where only one tone is applied ($V_2 = 0$) will result in the current component at $\omega_1$ being the following:

$$i(t)=(aV_1+\frac{3}{4}cV_1^3)\cos(\varpi_1 t) \qquad 1.4$$

From this equation it can be seen that if the coefficient c is negative the current will start to saturate at a certain magnitude of $V_1$. This phenomenon is often referred to as gain compression and the topic is discussed in Chapter 3.

### 1.3.3 Intermodulation Distortion

This nonlinear phenomenon occurs when two or more input tones combine to generate frequencies at linear combinations of these tones. This will include all tones in equations (1.3a) to (1.3c) that can be calculated as $\pm m\omega_1 \pm n\omega_2$ excluding the cases where either m or n is zero. Intermodulation is normally associated with third order intermodulation where a combination of m and n has an order of three. Third order intermodulation is very important figure of merit in communications systems because these terms are very close to the input frequencies and cause intermodulation distortion (IMD). Chapter 3 will give a more detailed discussion of intermodulation.

### 1.3.4 Spurious Responses

While this effect is specifically used in mixers it is essentially the same as intermodulation. If a mixer receives an RF input and an LO input the combination of these frequencies in a nonlinear system will give the same combinations as those described by equation (1.3) to (1.5) for a two tone excitation. In this case the two tones are applied to different ports but it is the same calculation and will generate tones at $\pm m \cdot RF \pm n \cdot LO$ by replacing $\omega_1$ and $\omega_2$ with RF and LO. It is however possible to define two-tone intermodulation for a mixer by applying two closely spaced RF tones as well as an LO signal in which case even more frequencies will be generated [7]. The generation of spurious signals in mixers is discussed in more detail in Chapter 4.

### 1.3.5 AM-to-PM Conversion

This phenomenon happens when a magnitude change in the input signal causes a change in the phase response. As an example, for a case such as an amplifier, the current at one of the input tones is given by equation (1.4) which is the sum of first order and third order components at $\omega_1$. However the analysis in equations (1.1) to (1.3) is for a memoryless system and does not provide for phase differences between the first and third order tones. However if a circuit has reactive nonlinearities, this is a common occurrence and a more accurate version of equation (1.4) that allows for phase differences is given in equation (1.5). This equation is the vector sum of two phasors at this frequency.

$$I_1(\varpi_1) = aV_1 + \frac{3}{4}cV_1^3 e^{j\theta} \qquad 1.5$$

In this equation $\theta$ is the phase difference. In this vector sum the phase of the current will change if $\theta$ changes as well as when $V_1$ changes. It can also be seen that the phase change as a result of $V_1$ will become larger for increasing $V_1$ because of the cubed term. This effect can often be seen in large phase changes when devices go into gain compression.

## 1.4 Scope and Layout of this Study

The topic of nonlinear modelling and specific behavioral modelling can be a confusing area that is not always clearly defined. In this work the aim was to investigate the different possibilities in ADS that can be classified as behavioral modelling. The emphasis was placed on modelling devices from measured data using existing structures and not the creation of nonlinear behavioral models. The research was specifically based on devices that would normally be classified as "small-signal" devices such as mixers and low noise amplifiers. The amplifiers and mixers in this work were mounted on aluminium base-plates with separate power supplies [Appendix A]. The devices where therefore treated as closed systems without any internal knowledge of the device structure or external matching circuitry up to the connector plane. Because of this the behaviour of the devices where taken purely from data measured at the ports (connectors).

Chapter 2 is a discussion of the various measurement instruments that were available to characterize the different devices. This chapter is very important because of the fact that no other information of the devices where used. Chapter 3 is a detailed chapter on amplifiers. The first part of this chapter focuses on nonlinear amplifier behaviour and the important aspects of measuring these phenomena. Special emphasis is given to measurement automation procedures that where developed in an attempt to automate the characterisation process. The last part of this chapter is dedicated to amplifier models in ADS. The content of Chapter 4 is the same as Chapter 3 with the focus on aspects specific to mixer behaviour. In Chapter 5, the measurements and models that where developed in the previous chapters, are used in receiver simulations. The aim of this chapter is to use the nonlinear models in larger RF systems to predict system behaviour. This is ultimately the goal of producing such devices and therefore also the goal of modelling them.

The final chapter is an overview of the results including recommendations for future research.

# Chapter 2

# Measurement Instruments

## Introduction

Accurate simulation depends on accurate models, but these models can only be as good as the measurements they were derived from. The most common way to create nonlinear models utilizes equivalent circuits to represent the device. Equivalent circuits are made up of lumped elements that may include linear and nonlinear resistors, capacitors and controlled sources. The parameters of the various elements are usually extracted from linear measurements (scattering parameters) and DC measurements. This process is normally applied to the creation of nonlinear transistor models and is made possible because the equivalent circuit provides a set structure that relates the measured data to the transistor physical behavior [3]. However, in the case of behavioral models for system simulation, devices such as mixers and amplifiers may be constructed from many transistors and other devices. There are no fixed structures for which parameters can be extracted. Behavioral models aim to predict complete device behavior from measurements. To represent nonlinear phenomena will require nonlinear measurements. The various linear and non-linear measurements that are necessary to characterize a device require a variety of measurement instruments. Even though some modern measurement systems have the ability to do a good number of these measurements, they mostly depend on either basic spectrum analysis or network analysis techniques. This chapter discusses the available measurement instruments. Understanding measurement instruments is vital. Not only is it necessary to ensure accurate measurements, but also to maximize measurement speed and flexibility. While section 2.1 and section 2.2 look at the network analyzer and spectrum analyzer respectively, section 2.3 discusses the use of some other instruments that were used such as power meters.

## 2.1 Vector Network Analyzer

Traditionally vector network analyzers are used to measure transmission and reflection characteristics of different components and circuits. In this work, an HP8753 vector network analyzer (VNA), together with a HP85047A S-parameter test set was used. This system is capable

of making various scalar and vector measurements. These include gain, gain compression, isolation, return loss (SWR), phase and complex port impedance [9, 12]. The instrument was used to measure amplifier and mixer characteristics, but it was also valuable in determining the effects of passive components in the various measurement setups. This section describes the main aspects of making VNA measurements, as well as some of the HP8753's additional capabilities. It describes basic theory of VNA operation by showing how S-parameters are measured. It explains the VNA hardware, focusing on issues that influence measurement accuracy. Error correction through calibration is also explained briefly.

### 2.1.1 Basic Operation

Figure 2.1 is a block diagram of a general 4 channel network analyzer. S-parameters are calculated as different ratios of the incident, reflected and transmitted signals numbered $a_n$ through $b_n$ in the figure. The basic VNA operation is explained in this section but for more detail see reference [8].

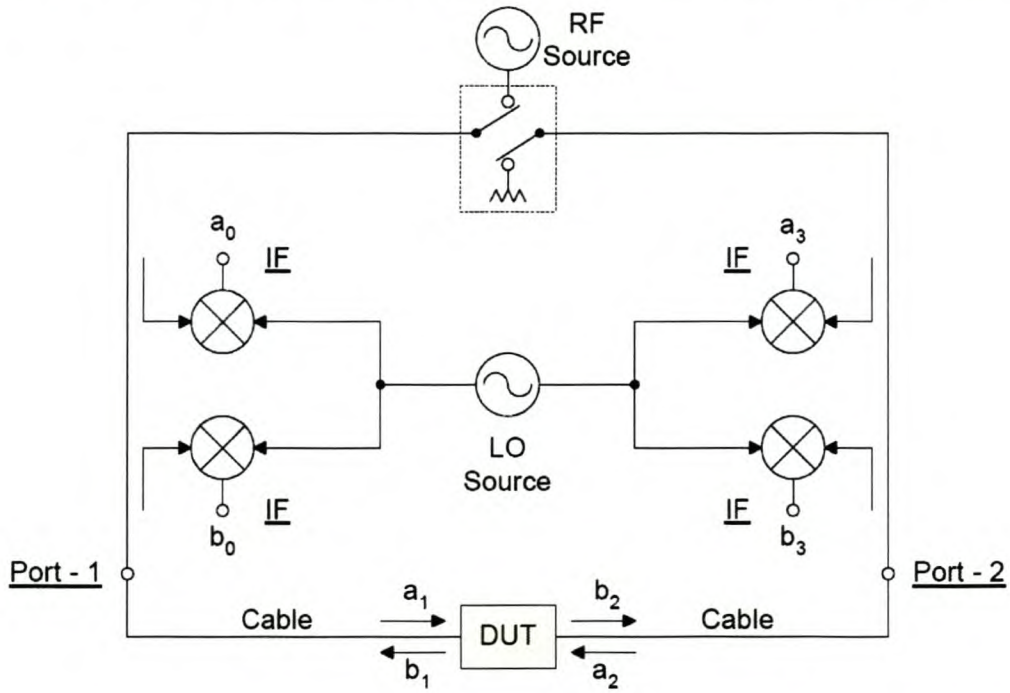


Figure 2.1 Block diagram showing a four-channel VNA. The different incident, reflected and transmitted waveforms (signals) are numbered $a_n$ through $b_n$. [10].

The RF source supplies the input signal to the device under test (DUT). The signal direction is determined with a switch to excite either port-1 or port-2 of the DUT. Directional couplers are used to separate the incident, reflected and transmitted signals in both the forward and reverse direction. Mixers are used to down convert the RF signals to a fixed IF. The LO source is tuned to the frequency of the RF + IF to ensure correct down conversion. The S-parameters of the DUT can be defined as follows:

- $S_{11} = b_1/a_1$, switch in forward direction
- $S_{21} = b_2/a_1$, switch in forward direction
- $S_{12} = b_1/a_2$, switch in reverse direction
- $S_{22} = b_2/a_2$, switch in reverse direction

As an example, the operation will be explained in the forward direction for a typical transmission measurement. Figure 2.2 shows the different available signals to determine the S-parameters from. The incident signal is sampled through the first directional coupler and down converted giving $a_0$, while the transmitted signal, $b_2$, is sampled by the third coupler and down converted resulting in signal $b_3$. The actual forward transmission, $S_{21}$, of the DUT is the ratio $b_2/a_1$. This ratio of the DUT output ($b_2$) to the DUT input ($a_1$) is the gain or loss of the device. However, the measured signals, after the coupler, down-conversion and sampling, are $b_3$ and $a_0$. The sampled IF signals, $b_3$ and $a_0$, can be used to calculate $S_{21}$ providing that the effects of the measurement setup can be removed.

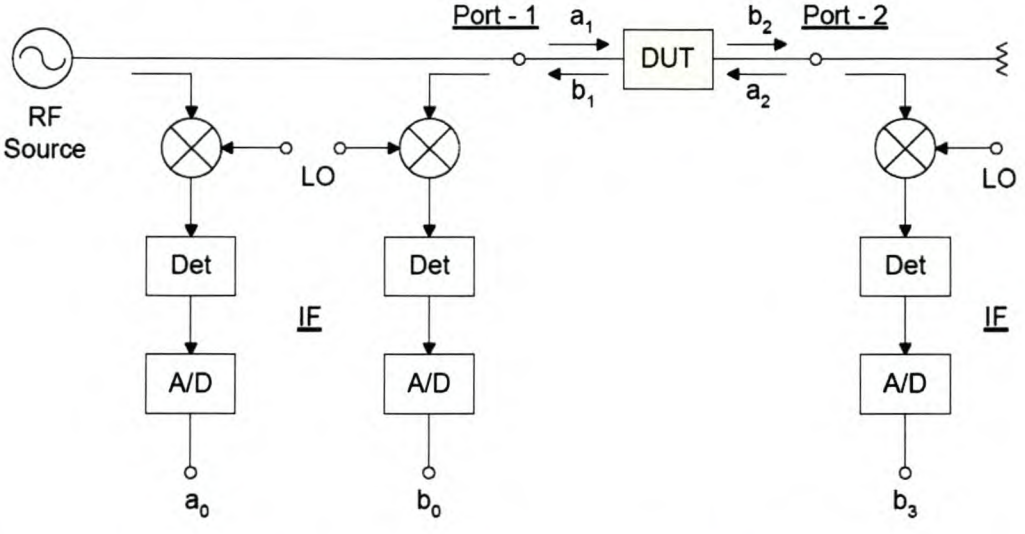


Figure 2.2 For measurements in the forward direction only three of the channels shown in Figure 2.1 are used. The necessary signals to do forward direction transmission and reflection measurements are $a_0$, $b_0$ and $b_3$ [10].

The whole signal path, from the DUT ports to the sampling of the IF signal, introduces errors to the measurement. The error between the actual ($b_1$, $b_2$, $a_1$and $a_2$) and measured ($b_0$, $b_3$, $a_0$ and $a_3$) signals are caused by the following factors:

- Imperfect impedances at VNA test ports
- Finite directivity of couplers
- Loss, phase shift and reflections caused by connectors and cables connecting the VNA and the DUT
- Internal leakage between the test ports of the VNA

These errors, including the loss, match errors and leakage errors of the network analyzer, along with that of the cables and connectors, are shown in Figure 2.3 for a reflection measurement. The

match errors cause reflections that are added to that of the DUT while the effect of unwanted loss on a signal is obvious.

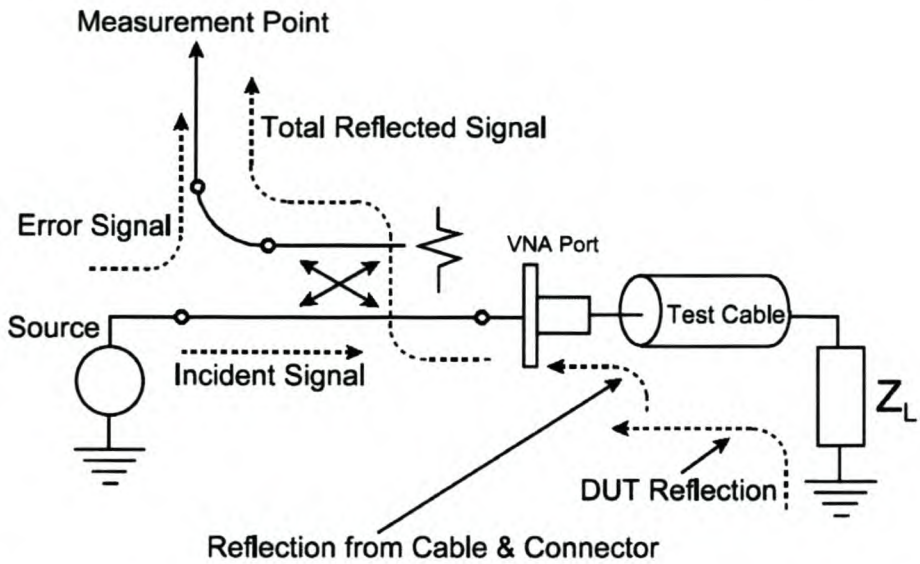


Figure 2.3 The figure shows the different signal paths that introduce error to a reflection measurement. The main sources of error are the leak signal through the coupler and the unwanted reflections from the cables, connectors etc. [11].

The errors caused by leakage are because of parasitic signal paths within the VNA and the finite directivity of the directional couplers. The directional couplers serve the very important purpose of separating the incident and reflected signals. A coupler with a high directivity will allow only a small error signal to leak through. The error signal in Figure 2.3 is part of the incident wave. The coupler should only allow the total reflected signal to pass to the down converter. The signal at the measurement point includes the leak through the coupler and various error reflections apart from the wanted signal. Errors such as these are called systematic errors. Systematic errors can be greatly reduced by calibration for most cases. There is one more type of systematic error related to the frequency response of the receiver. These errors are called transmission and reflection tracking. The process of calibration is discussed in the following section. However there are other factors that influence the VNA's accuracy such as receiver non-linearity (IF filter, A/D and detector non-linearities) and the system noise. These factors will be discussed in a following section.

### 2.1.2 Calibration

Calibration is the process by which systematic errors are removed from a measurement mathematically. These systematic errors are a result of imperfections of the VNA and the test setup. Assuming they are time invariant, they can be characterized with a calibration process and their effect removed from the measured data [10, 11]. The calibration process is described in this section.

For the purpose of calibration, the VNA is assumed to be perfect, and the systematic errors due to the VNA and test setup are lumped in an error adaptor. This linear error adaptor is then added mathematically to the measurement setup as shown in Figure 2.4. The error adaptors relate the DUT S-parameters to the data measured inside the perfect VNA. By this process the effects of the systematic errors can be "cancelled out" or removed.

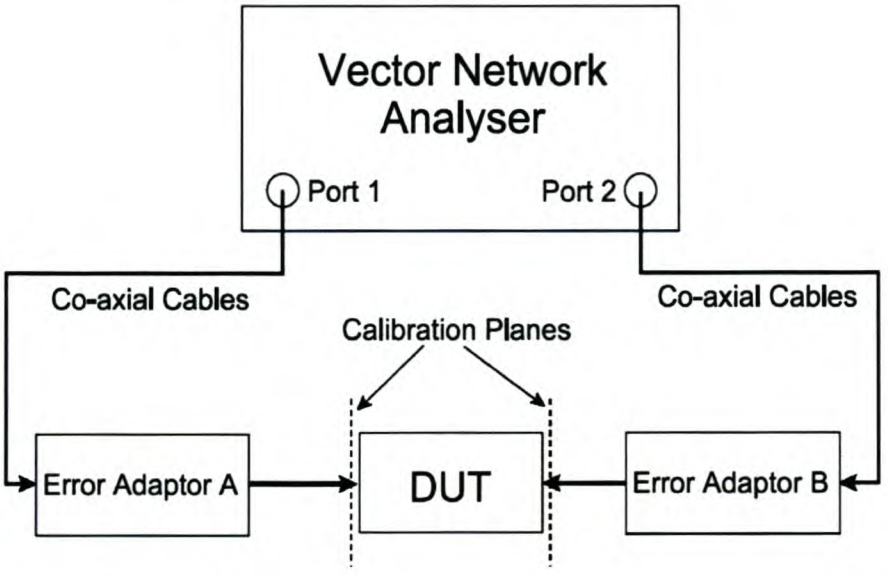


Figure 2.4 Calibrated VNA showing error adaptors used to remove systematic errors mathematically to produce calibration planes. If a DUT is measured at the calibration planes, a calibrated network analyzer can use the error adaptors to minimize the measurement error [11].

The error adaptors are determined by measuring calibration standards. A calibration standard is a network or impedance whose response is known exactly. The VNA can then calculate the error adaptors from the difference between what it expected (from the calibration standard) and what it actually measured. Calibration establishes a calibration plane. If the DUT is measured at the calibration plane, the calibrated VNA will be able to correct for systematic errors up to that plane. There are two basic types of calibration:

- Response Calibration
- One or Two Port Vector-Calibration

Response calibration uses only a through calibration standard. This type of calibration removes the effect of tracking errors by measuring the VNA response with this through connection instead of the DUT. A through connection basically connects the two calibration planes. The VNA then stores this reference trace in memory to normalize the measured DUT data. It can store either a vector or scalar reference trace to correct for tracking errors. A scalar reference trace will only be able to correct amplitude errors while a vector trace can be used to compensate for amplitude and phase errors.

Vector calibration includes response calibration but also measures additional calibration standards. The most common is the SOLT calibration involving short, load, open and through calibration standards. Vector calibration can compensate for tracking errors as well as errors resulting from mismatch, finite directivity and leakage (isolation) problems as discussed previously. Full two port vector error correction should be used where possible to ensure maximum accuracy. Calibration is discussed in detail in reference [10]. There are however some additional aspects of VNA measurements that can influence measurement accuracy. These include the effects of power levels on the receiver linearity as well as effects of spurious signals in measurements involving frequency translating devices. The next section discusses these issues in more detail.

### 2.1.3 Receiver Linearity and Bandwidth Issues

After the signals traveling in the forward or reverse direction have been separated by the couplers, they need to be down converted and sampled. Figure 2.5 displays a tuned receiver of a VNA. The tuned receiver uses a local oscillator to mix the RF down to the IF. The LO is synchronized with the RF to ensure that the receivers in the VNA are always tuned to the RF signal present at the input. The IF signal is bandpass filtered. Narrowing the receiver bandwidth in this way greatly improves sensitivity and dynamic range of the instrument. It also provides rejection of harmonic and spurious signals. The signal is then digitized with an analog to digital converter (ADC). It should also be remembered that the digitizing hardware also influence the signal.

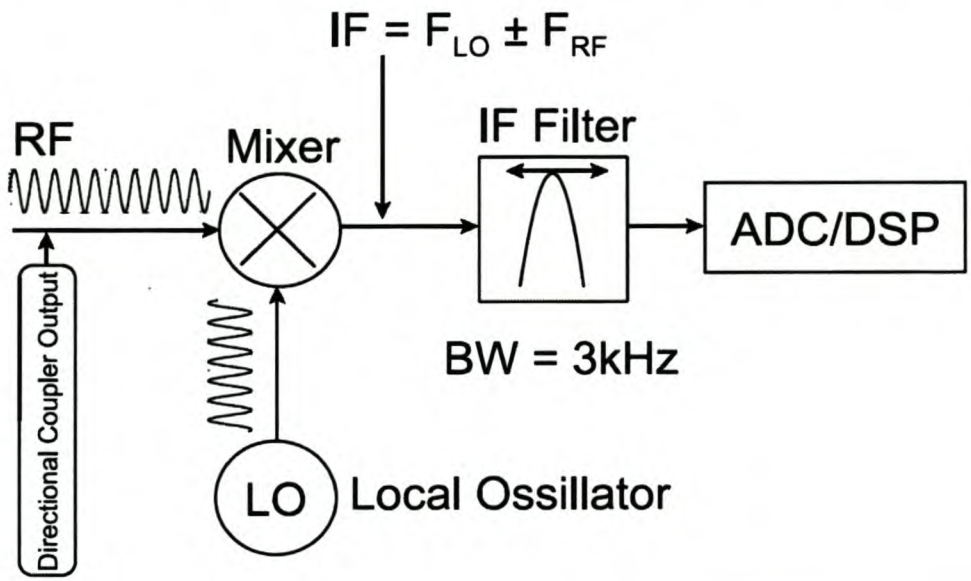


Figure 2.5 After a signal has been separated by the directional coupler, it is down-converted with a narrow band tuned receiver. The mixer's LO is synchronized with the RF and the IF is filtered. The IF filter is a narrow bandpass filter with a default bandwidth of 3kHz for the HP8753. After the IF has been filtered it is sampled and the signal is processed [11, 13].

Typical receiver imperfections in VNA receivers are:

- Spurious responses and compression caused by the mixer (non-linear mixer behavior)
- Local oscillator phase noise can degrade the spectral purity of the IF signal
- Local oscillator stability
- Dynamic range, spurious response and linearity of the ADC are also important aspects to consider

The influence of some of these problems can be minimized. The dynamic range and receiver linearity can be controlled to a certain extent while the LO characteristics and linearity of the ADC are hardware limitations. For instance narrowing the IF filter's bandwidth will increase the dynamic range and may reduce the effects of spurious signals in some cases. For example, changing the HP8753's IF bandwidth from 3kHz (default) to 10Hz decreases the noise floor from -90dBm to -100dBm [12]. This type of improvement is however dependent on the specific instrument used. Also some spurious signals can not be avoided or are too big to be completely removed by the IF filter. Reducing the IF filter bandwidth decreases the noise floor but increases the sweep time. The important considerations that need to be taken into account to ensure that the VNA is operating in the linear region are discussed next.

The VNA receiver's non-linear behavior, such as internally generated spurious signals and compression, can be minimized by selecting proper power levels in the test setup. In the case of the HP8753 the most important power specifications are [12]:

- Mixer input power levels should not exceed a certain maximum power level to ensure operation in the mixers linear region. For the HP8753 this is -10dBm.
- The power level at the reference channel should not be too small to ensure receiver phase lock on the desired signal. For the HP8753 this must be larger than -35dBm.

The HP85047A test set is shown in Figure 2.6 along with the HP8753's three receiver channels. The HP8753 switches the RF source to eliminate the necessity for a fourth channel. The power specifications at the reference port and channels A and B is shown. If all the power specifications in the figure are met, the VNA non-linear behavior is negligible for most applications. From the figure the signal paths for typical transmission and reflection measurements are shown along with the attenuations that need to be taken into account. The directional couplers in the HP85047A test set have 16dB attenuation from the port to the mixer input. If this is not enough additional attenuation has to be supplied as for the case at port two in the figure.

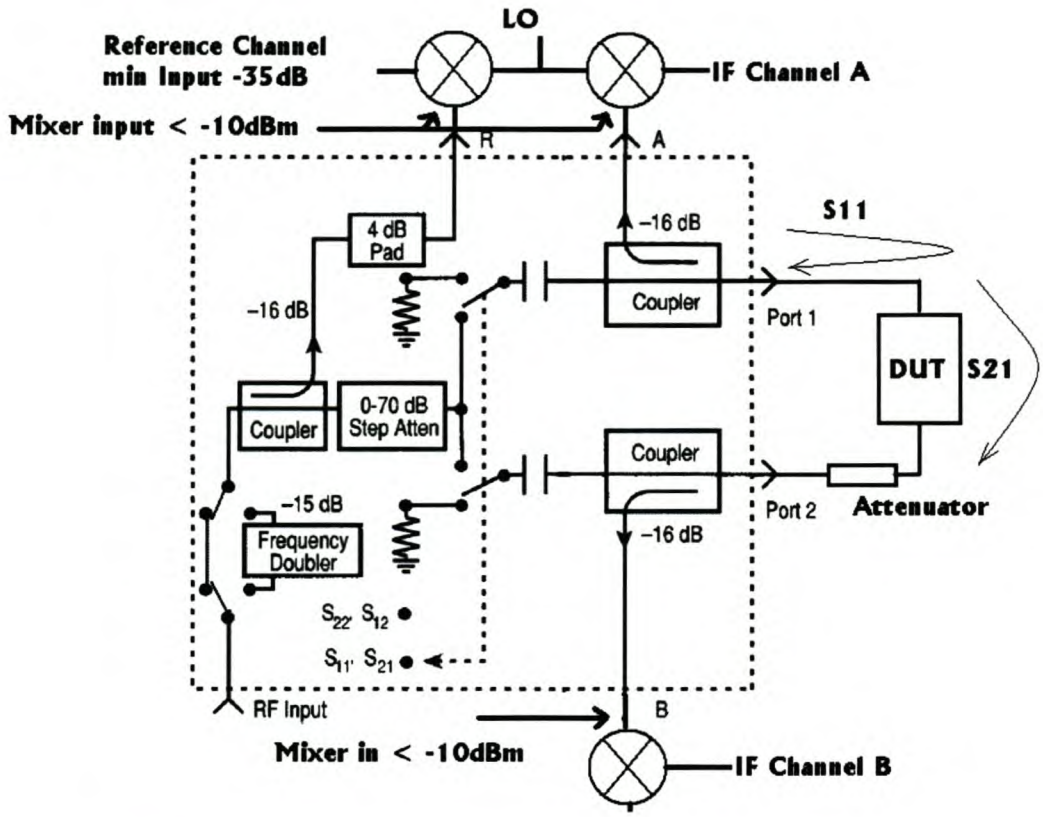


Figure 2.6 This figure shows the various important power levels that need to be considered to ensure operation in the linear region for the combination of a HP8753 VNA and a HP85047A test set. The maximum power level at any mixer should be less than -10dBm for linear operation [9].

The process of selecting power levels through the setup can be better explained with an example for the HP8753. The HP8753 controls internal power levels by changing the RF input power level, adjusting the built in step attenuators (0 to 70 dB in 10 dB steps) and by adding additional attenuation to the external setup. Consider a power sweep to determine swept power gain for an amplifier in the setup of Figure 2.7. Suppose the maximum input power of the amplifier is 0dBm. The RF source can sweep from -5dBm to 20dBm requiring more than 20dB attenuation to protect the amplifier. The nominal loss through the test set to Port 1 is 3dB. Adding these attenuations will result in a power sweep of -28dBm to -3dBm ignoring cable loss. If the DUT is an amplifier with a gain of 20dB this will result in the input power at Port 2 being from -8dBm to 17dBm. The coupler has a coupling factor of 16dB resulting in the power at mixer B being between -14dBm to 1dBm. This is much more than the maximum level of -10dBm required for linear operation of the receiver. The problem can be fixed by adding more than 11dB of attenuation between the amplifier output and Port 2. This signal path is shown in Figure 2.7 for an amplifier with 20dB gain and an external attenuator of 20dB.

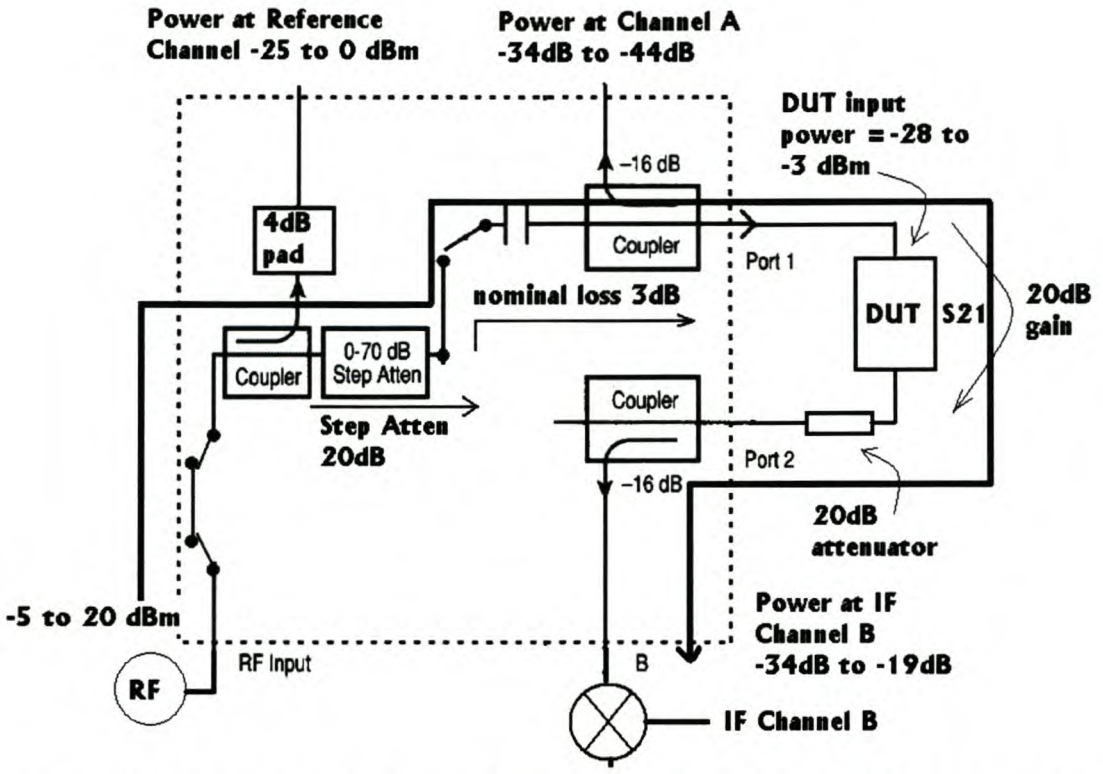


Figure 2.7 The various important power levels for a swept power amplifier gain measurement are shown. The dark line shows the RF signal path through the measurement setup. The power at the reference channel is large enough to ensure receiver synchronization. The input power at Port 2 will be too large if an external attenuator is not included in the circuit [9].

This section has shown that the hardware limitations of the VNA need to be taken into account to ensure accurate measurements. A thorough knowledge of the VNA's internal receiver will enable the user to minimize or eliminate the possible sources of error mentioned at the start of this section. When a VNA is used to perform mixer measurements, there are other problems that will be discussed in chapter 4 section 1.

### 2.1.4 Conclusion

The most important aspect of VNA measurement is the fact that it supplies phase data as well as amplitude data. It is mostly used to do small signal measurements but some network analyzers have the ability to do certain non-linear measurements. Specific measurements that were done with the HP8753 will be presented in chapter 3 and chapter 4. The VNA was very useful because of its ability to do error corrected S-parameter measurements. These measurements give important insight into device characteristics but were also used extensively to characterize measurement setups and passive devices. In chapter 3 the VNA was also used to do power sweeps on amplifiers. This is an important measurement ability that can show an amplifier's phase response to different input power levels (AM-to-PM). In chapter 4 it is also shown that the VNA can be used to do important mixer measurements such as determining isolation and port impedances. In summary, vector network analyzers are invaluable in characterizing RF devices.

## 2.2 Spectrum Analyzer

The basic purpose of a spectrum analyzer is to examine signals in the frequency domain. Ideally, it should operate as a perfect receiver, meaning it should not distort the signal in any way. Spectrum analyzers are mostly used to measure modulation, distortion and noise [13]. In this case the spectrum analyzer was used to measure distortion such as compression, intermodulation, harmonics and spurious emissions. However, no receiver is perfect and the spectrum analyzer introduces additional distortion into the system. Understanding the operation of the spectrum analyzer is important to ensure that its influence on the measured signal is negligible or known. This section describes the various techniques used to produce reliable, accurate data with a HP8562A spectrum analyzer. The basic operation of a spectrum analyzer is discussed section 2.2.1 followed by an explanation of measurement uncertainty section 2.2.2. The measurement uncertainty is different for absolute and relative measurements section 2.2.3 and the application of an accurate measurement automation procedure is presented in section 2.2.4. Error correction can be done for spectrum analyzer measurements through response calibration referenced to a known signal and this is explained in section 2.2.5.

### 2.2.1 Basic Operation

Spectrum analyzers are RF receivers that sweep over a specified frequency band displaying all the received signals within the band. The major components in a spectrum analyzer are the RF input attenuator, pre-select filter, mixer, IF gain, IF filter, detector, video filtering, local oscillator, sweep generator and the CRT display. The paragraphs in this section will describe the operation of a spectrum analyzer referring to the various components mentioned above and shown in Figure 2.8.

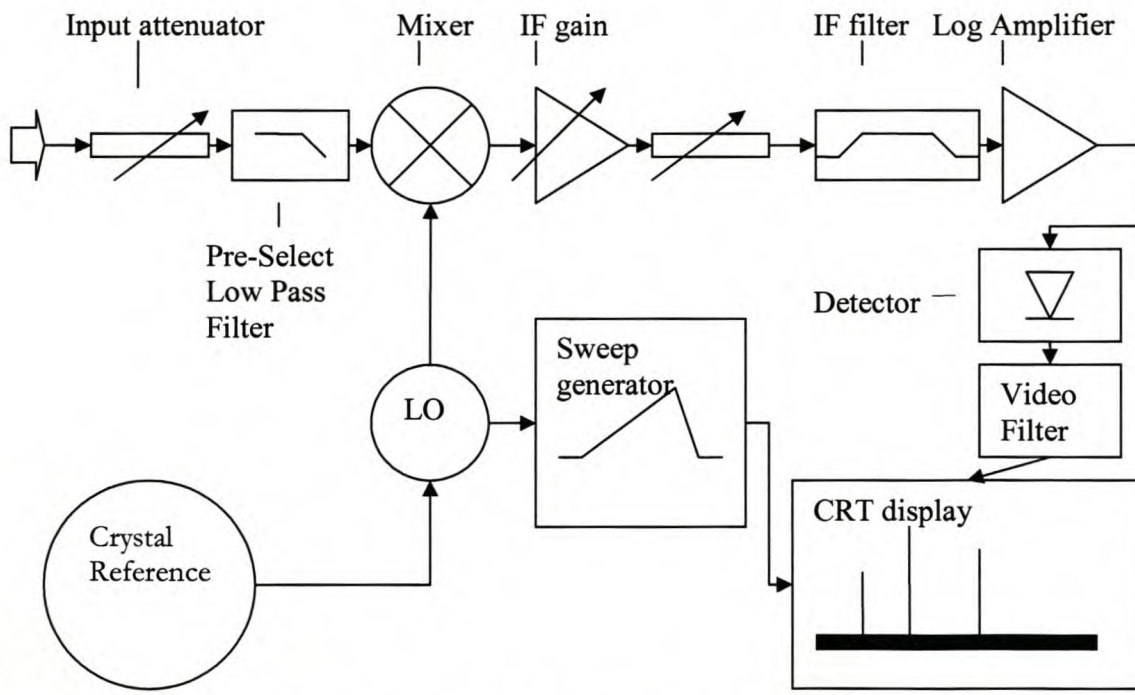


Figure 2.8 This spectrum analyzer block diagram shows all the necessary components that are important to spectrum analyzer operation.

The spectrum analyzer is basically a superheterodyne receiver that sweeps across the desired frequency span. To do this the LO input to the mixer in Figure 2.8 is swept to down convert the desired frequencies at the input port. The mixer converts the RF spectrum to an IF spectrum that can be filtered, amplified and detected. The sweep generator controls the LO frequency with a voltage ramp. The same voltage ramp is used to sweep the CRT display ensuring that the IF frequency and the display is in tune. Some spectrum analyzers have the ability to work in different frequency bands. For example in the case of the HP8562 these bands are 3KHz to 3GHz, 3GHz to 6GHz etc. The first band is accessed by sweeping the LO frequency across the band. Higher bands are accessed by sweeping the harmonics of the LO frequency which are at higher frequencies. Because the harmonics are generally smaller and have inferior phase noise when compared to the fundamental, the noise floor is increased for each higher band that is accessed.

The IF filter is a bandpass filter that is used to select the desired signal from the frequency spectrum at the mixer's IF port. The bandwidth of the IF filter is called the resolution bandwidth (RBW). This can be changed from the front panel and the effect of the resolution bandwidth can be seen in Figure 2.9. This figure shows repeated measurements of the same signal with only the RBW changed between measurements. Reducing the RBW increases the frequency selectivity (ability to resolve signals), and can improve signal to noise ratio. This however increases the sweep time. For a specific measurement, the resolution bandwidth setting is a trade-off between the resolution (selectivity) and measurement speed.

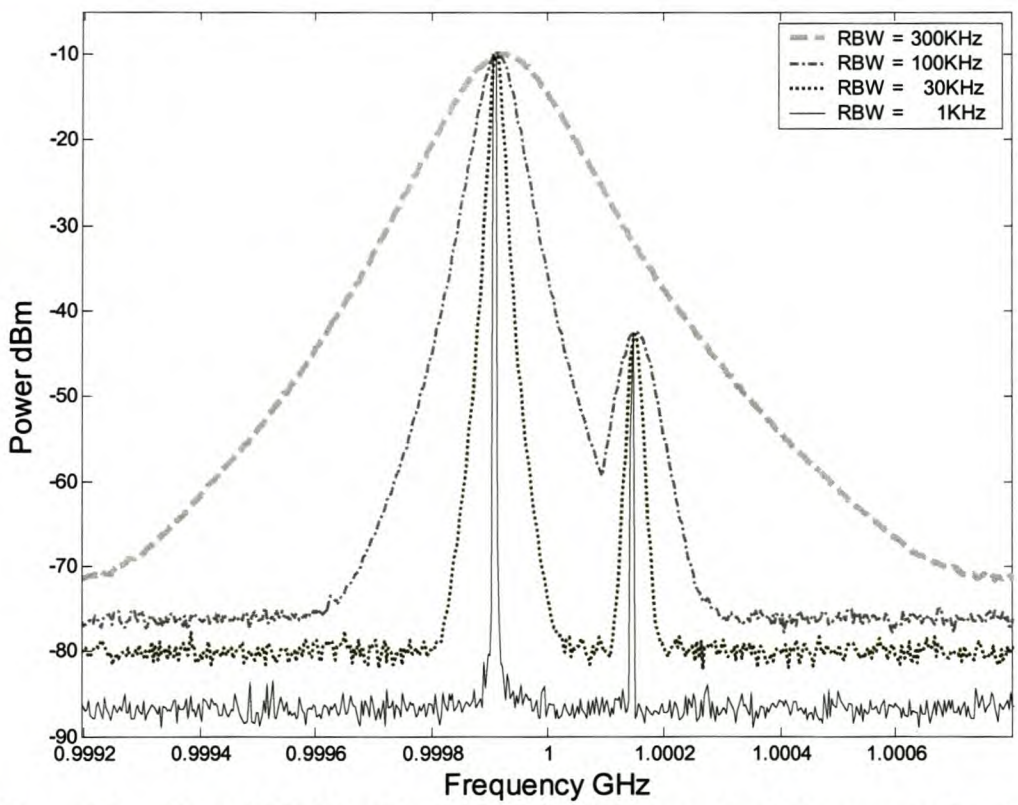


Figure 2.9 The effect of RBW on frequency selectivity can clearly be seen in this figure. The same signal was measured with different RBW settings showing the increase in frequency selectivity and decreased noise floor. All the measurements in this figure were done with a VBW of 1KHz.

The analyzer must convert the IF signal to a baseband signal so that it can be displayed on the screen. This is accomplished through the logarithmic amplifier and envelope detector. The baseband signal, containing the desired signal plus the noise in the IF bandwidth, is displayed on the screen. If a signal is close to the noise floor, the noise will make the signal difficult to read because of poor signal to noise ratio. To compensate for this there is another filter called the video filter. The video filter is a digital filter that effectively adds averaging to the measurement. By decreasing the bandwidth of the video filter, called the video bandwidth (VBW), the peak-to-peak variations of the noise can be decreased which will result in smoothing the display output. This is possible because noise generally has a uniform power distribution which means that the average noise power is zero. Therefore the effect of noise can be reduced by averaging. However decreasing the VBW does not increase frequency selectivity and therefore sensitivity. It does however improve discernability and repeatability of low signal-to noise ratio measurements. This can be seen in Figure 2.10.

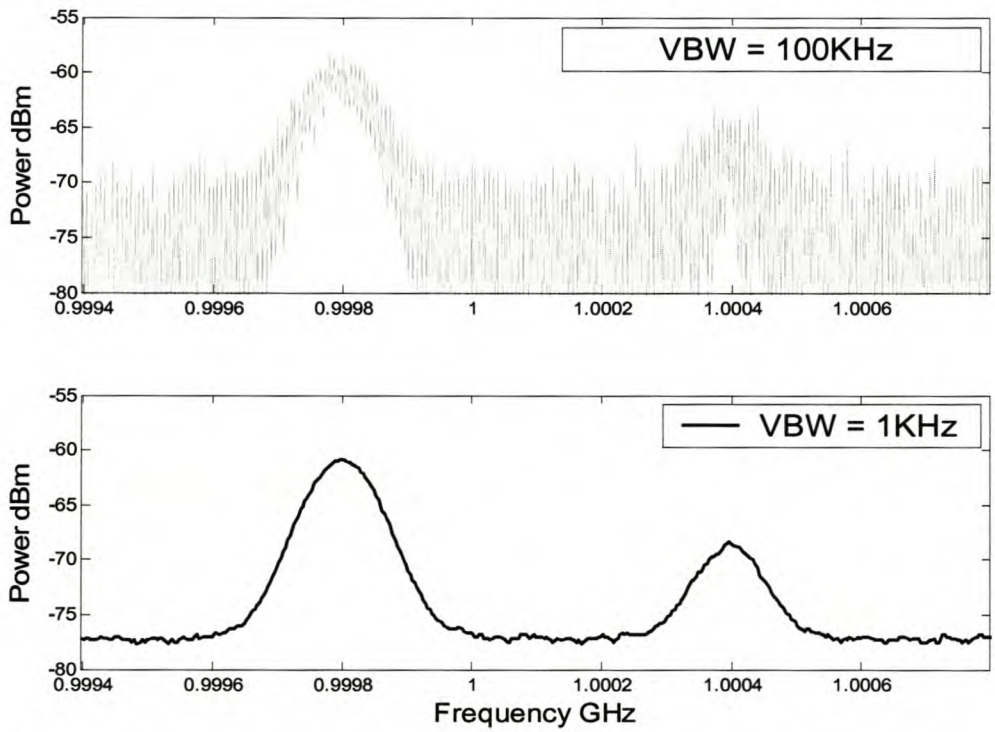


Figure 2.10 The effect of reducing VBW can be seen in this figure. The same input signal was measured with two different VBW settings showing a decrease in display noise. This enables easier identification of low level signals and greater amplitude accuracy and measurement repeatability.

The input attenuator in Figure 2.8 is a step attenuator that is used to adjust the level of the input signal. This is done to prevent mixer distortion and gain compression due to large input signals. The attenuator is linked to the IF gain. The IF gain determines the position of signals on the CRT by adjusting the reference level. The spectrum analyzer will change the IF gain, and therefore the reference level, automatically if the input attenuator is changed. This is done so that signals remain stationary on the display even if the attenuation has been changed. Increasing the input attenuator by 10dB also increases the noise floor by 10 dB.

After the input signal has been downconverted and filtered, it is detected indicating the magnitude of the signal component at the spectrum analyzer's tuned frequency. The output voltage of the detector is sampled using an analog to digital converter (ADC). The detected power level is used to drive the vertical axis of the display. This is the amplitude while the horizontal axis, the frequency, is determined by the sweep generator. This ensures synchronization of the horizontal axis of the display and the LO signal. The result is the amplitude vs. frequency of spectral components of all incoming signals. Spectrum analyzer operation is discussed in detail in reference [13]. The spectrum analyzer's components work together to present a very flexible measurement instrument. This flexibility however, comes at the price of measurement uncertainty which is the topic of the next section.

### 2.2.2 Measurement Uncertainty

Spectrum analyzer accuracy is influenced by all the components described in the previous section. Depending on the setting, each component adds an uncertainty to the measured result. The analyzer makes both frequency and amplitude errors. The effect of frequency errors is not critical for the work in this thesis and it will not be discussed. To understand the effect of the amplitude uncertainties, it is important to differentiate between absolute and relative amplitude measurements. The spectrum analyzer uses markers to read out the amplitude or frequency of a specific spectral component. For relative measurements, two markers are used. The relative amplitude is the difference, in amplitude, between the two markers in dB where for absolute measurements the output is the marker amplitude in dBm. This is discussed more thoroughly in [13]. Some of the measurement uncertainties influence absolute and relative measurements differently. The specifications used to quantify the various uncertainties for relative measurements are:

- Frequency response of the receiver between markers.
- Display fidelity. This includes linearity of the detector and ADC as well as uncertainty related to the log amplifier (how true the amplifiers logarithmic response is). This is influenced by the relative amplitude placement of two signals on the screen.
- Increasing or decreasing the input attenuator between two measurements adds uncertainty. This happens because the attenuator has a finite repeatability introducing uncertainty each time it is changed.
- Changing the reference level, which in effect changes the IF gain, introduces uncertainty.
- Adjusting the resolution bandwidth between measurements adds uncertainty because the IF filter's (RBW) insertion loss changes for different settings.
- Changing the CRT scaling between measurements may also introduce uncertainty between the two measurements. This is also as a result of the log amplifier being an approximation of a perfect log amplifier.

The last four items only add uncertainty to the measurement if they are changed between two measurements. For absolute amplitude measurement (only one signal giving an output value in dBm) the uncertainties are:

- The accuracy of the internal calibrator is limited. Absolute amplitude measurements are relative measurements referenced to a calibration signal. For the HP8562 this calibration reference is at 300MHz, -10dBm ±0.3dBm.

- The frequency response between the marker and the calibration signal. The absolute frequency response uncertainty is normally larger than the relative frequency response uncertainty.
- Reference level uncertainty is a result of the calibration technique used. The top line of the CRT is compared to the calibration signal and adjusted accordingly. Therefore the top of the screen is directly related to the calibration signal and all other amplitude levels on the screen are displayed relative to the reference level. This process introduces uncertainty for signals that are not at the reference level.

Therefore, the maximum accuracy you can expect is if you measure a signal at the calibration signal's frequency and power level. If the frequency settings or reference level (IF gain) is changed to accommodate a certain signal, the measurement uncertainty will increase. There are some additional factors that may influence both types of measurements:

- IF alignment uncertainty occurs when the resolution bandwidth gets too narrow, the frequency error can cause the signal and the resolution bandwidth filter to be misaligned. This will result in unwanted and unknown attenuation of the signal.
- Saturation of the receiver can be a result of a single tone as well as a combination of signals. The total power at the mixer input is important and large signals that are not displayed on the screen can cause mixer compression and other forms of distortion. It is therefore important that the signal level should be low enough. This can be done by changing the input attenuation or including external attenuation. The HP8562A has an input 1dB compression point of -5dBm and therefore the signal level at the internal mixer of the spectrum analyzer should be kept well below this.
- Distortion products resulting from mixer nonlinear behavior. For example, the spectrum analyzers mixer will produce intermodulation if two tones are applied to the input port. If these tones are large enough the spectrum analyzer will display the measured signals as well as any intermodulation products generated by its own nonlinear characteristics.
- Mismatch at the input port of the spectrum analyzer will cause unwanted reflections that will influence the accuracy of the measurement.
- Noise may also influence the measurement in various ways.
- Frequency band switching. The spectrum analyzer frequency band is divided in blocks. The first block is up to 3GHz. The second is from 3 to 6 GHz. The blocks for higher frequencies have larger frequency response uncertainties.

To make accurate measurements, it is important to understand how the spectrum analyzer works and how different settings influence the spectrum analyzers accuracy. For some applications dynamic range and sensitivity is important while other applications may require a wide frequency span. To measure distortion such as intermodulation, often requires high dynamic reach. Accommodating these requirements often results in a measurement setup with a large sweeptime. If a measurement with a significant sweeptime has to be repeated for different frequencies or powers the total time needed can soon become very large. Another factor to take into consideration is the time needed to change the front panel settings to ensure maximum accuracy for each new signal. For this reason a set of procedures were developed to automate spectrum analyzer sweeps. It is important that these procedures produce accurate and repeatable data using either absolute or relative amplitude measurements. The following section quantifies the differences between absolute and relative amplitude measurements for the HP8562. It also justifies the choice of

measurement technique that was used to create the measurement software which is described in section (2.2.4).

### 2.2.3 Absolute versus Relative Amplitude Measurement

In Section 2.2.2 all the different sources of measurement error and uncertainty were discussed. It was seen that absolute and relative measurements are influenced by different factors. This section quantifies the measurement uncertainties for the HP8562.

The different sources of uncertainty (section 2.2.2) are all results of systematic errors in the measurement setup and the instruments. Random errors as a result of noise also influence the measurements and although there are ways to minimize the influence of noise, the noise uncertainty can not be characterized or removed completely. The effect of random errors is that measurement accuracy is degraded by the effective level of display noise [13]. Measurements are more accurate for larger signal to noise ratios and this is directly affected by the noise level. The effective level of display noise is a function of the input attenuator setting, the RBW setting and the VBW setting. The effect of noise (random error) can therefore be minimized by careful selection of these settings. It should be noted that the input attenuator setting is mostly dictated by signal power level and that the RBW and VBW settings are a trade off between signal to noise ratio and measurement speed. These settings depend on the specific measurement and will not be discussed in this chapter.

There are two basic types of measurement that can be performed with the HP8562 namely relative amplitude measurements and absolute amplitude measurements. The first, relative measurement of two signals, uses the built in delta marker of the spectrum analyzer. It measures the difference in power level of the two signals in dB. The second method entails doing absolute measurements of one signal giving a power level in dBm. This technique can also be used to do relative measurements by subtracting the results of two absolute measurements to give a power difference in dB. These two types of measurement are affected by different measurement uncertainties. As an example, to compare the two techniques for the HP8562, the amplitude uncertainty of both techniques was calculated. The calculation assumes the worst case error from the datasheet specifications of the different uncertainties. Many of these uncertainties are as a result of finite repeatability when a setting is changed between two measurements.

The sources of systematic error discussed in section 2.2.2 are usually described by a number quantifying the uncertainty added to a measurement in dB. The total uncertainty of a measurement is the sum of the uncertainties added by the different sources of section 2.2.2. The uncertainty is calculated for a relative amplitude measurement between two signals for both types of measurement. The aim of this comparison is to give insight into the effect of the different measurement aspects on measurement uncertainty.

Option 1: Relative delta marker measurement

For this measurement the delta marker function is used. Two markers measure the signals and the difference in power level is calculated in dB. It can not produce absolute power levels in dBm which may be required. The total datasheet uncertainty is calculated as follows:

| | |
|---|---|
| Display fidelity | ± 0.4 dB uncertainty for each 4dB between signals to a total of ± 1.5 dB over 0 to 90 dB range |
| Frequency response | ± 1dB |
| Δ Input attenuator | ± 0.6 dB for each 10 dB step, 1.8 dB maximum |
| Δ Resolution bandwidth | ± 0.5 dB |
| Δ CRT scaling | ± 0.5 dB |
| | = ± 5dB maximum error |

The last three factors only add uncertainty to the measurement if they are changed from one tone to the next to accommodate the second signal.

Option 2: Absolute measurements at the reference level

This method measures both signals as accurately as possible in dBm and the relative power is calculated from these measurements.
Uncertainty:

| | |
|---|---|
| Frequency response | ± 1.5dB |
| IF Gain uncertainty | ± 1.0dB |
| (Reference level uncertainty) | |
| Calibrator uncertainty | ± 0.3dB |
| Δ Input attenuator | ± 0.6 dB for each 10 dB step, 1.8 dB maximum |
| Δ Resolution bandwidth | ± 0.5 dB |
| Δ CRT scaling | ± 0.5 dB |
| | = ± 5.6dB maximum error |

The last three factors only add uncertainty to the measurement if they are changed from one tone to the next to accommodate the second signal while the reference level uncertainty applies to signals that are not at the top of the screen.

Although the first method can give very accurate relative measurement in cases where the signals are closely spaced in frequency and amplitude, there are other cases where it can have a datasheet uncertainty of ± 5dBm. The uncertainty is largely affected by the attributes of the two input tones. If for instance a power sweep is done the uncertainty will change for each measurement in the sweep depending on the amplitude difference and relative frequency for each measurement. For this reason the second method was chosen. Even though the total worst case uncertainty is larger, it allows for greater flexibility. Furthermore, many of the sources of uncertainty for this method can be avoided consistently, ensuring that two consecutive measurements in a sweep will have the same uncertainty. In addition to this it can produce either power levels in dBm or power differences in dB. In other words it can be used for absolute measurements and relative measurements.

The measurement uncertainty of ±5.6dB is very large. Many of the sources of uncertainty that amounts to this number can be avoided. It is possible to measure signals of different amplitudes accurately by only changing the reference level (assuming they are in the same frequency band). Less changes between measurements cause less uncertainty. If only the reference level and frequency settings are changed this method eliminates the last three sources of uncertainty bringing

the total datasheet uncertainty to ±2.8dB. If the reference level is changed so that the signal is at the top of the screen the reference level uncertainty is also eliminated giving total uncertainty of ±1.8dB. The accuracy of the second method can be further enhanced by calibrating it at the desired frequency with an external reference signal. This process characterizes the spectrum analyzer measurement error. This can reduce the errors associated with the single calibration tone. The calibration process will be discussed in section 2.2.5.

This section described the difference between absolute and relative amplitude measurement and quantified the sources of uncertainty section 2.2.2 for the HP8562. The following section describes the implementation of such a measurement procedure in MATLAB.

### 2.2.4 Measurement Automation through Remote Instrument Operation

Spectrum analyzer measurements are affected by many factors that often result in a playoff between settings. In the previous sections it was seen that accuracy and sweeptime is often opposing outcomes as a result of random errors. Some of the sources of systematic errors are as a result of changing a certain setting. It was seen in section 2.2.3 that doing all measurements without changing attenuation, RBW or VBW will give lower measurement uncertainty. Therefore a procedure was proposed that change only the frequency and reference level settings to measure any given signal. The initial RBW and VBW settings are chosen to minimize random errors. Unfortunately this results in large sweeptimes. Doing sweeps over power or frequency including many measurement points can soon become very time consuming and for this reason the measurement process was automated using an instrument control interface called GPIB. The GPIB interface enables the user to control measurement instruments from a PC. MATLAB has a toolbox enabling the user to send commands to an instrument from a complex MATLAB procedure using the GPIB interface. Data can also be read from the instrument via the GPIB bus and this ability enables the user to write control software to automate measurement sequences. This section describes the basic measurement procedures that were used to ensure accurate and repeatable measurements.

For this work there were two types of sweeps that the spectrum analyzer was used for, namely swept input power at one frequency (typically to obtain an amplifier power curve) and measuring signals at various frequencies and unknown amplitude (typically mixer spurious response measurements). However both of these require at some point the measurement of a signal for which only the approximate power level is known. This section describes a measurement technique that was used to do this kind of absolute measurement as accurately as possible. It also shows an example of the use of this procedure in a power sweep.

The basic measurement setup is shown in Figure 2.11 showing PC control of the measurement instruments. In any measurement the desired signal is applied to the DUT by the signal generator as specified by the PC. The next step is to adjust the spectrum analyzer to measure the resulting DUT output.

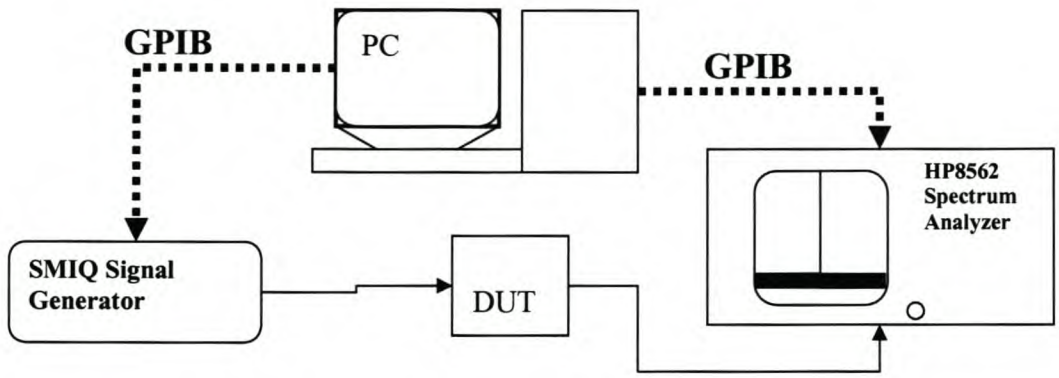


Figure 2.11 This figure shows a PC controlling instruments over the GPIB interface.

A basic procedure was developed that is used to measure a signal of which only the approximate amplitude is known. In order to have maximum accuracy, the reference level should be changed to match the signal level as closely as possible. This is because the reference level of the spectrum analyzer is directly related to the calibration signal, and measuring at the reference level eliminates the reference level uncertainty as mentioned in section 2.2.3. This procedure is normally used in larger programs that adjust the other spectrum analyzer settings to suit the type of sweep.

Once the correct spectrum analyzer settings have been established and the desired input tone is applied to the DUT the measurement procedure is started. The procedure can only change the frequency and reference level to measure a signal. Therefore the procedure starts with the maximum reference level and measures the output power level. This value includes the reference level uncertainty because the power level will be somewhere below the top of the screen. The next step is to reduce the reference level to the measured value and so doing reducing the reference level uncertainty. This happens because the signal will now be very close to the top of the screen. The signal is measured again and the reference level is again adjusted to this new, more accurate measurement of the signals power level. The first adjustment brings the signal and the reference level within ±1.5dB. The uncertainty for signals so close to the reference level is very small and so the second reference level adjustment brings the signal very close to the top of the screen. The repeatability of this method is high because the recursive level adjustment will bring any signal, regardless of its original amplitude relative to the reference level, very close to the top of the screen. This will result in near equal uncertainty for all power levels. After the two adjustments of the reference level to match the signal level, the signal power level is measured and the data is returned to the larger sweep procedure. This technique will be referred to as the recursive measurement procedure in the rest of this work. The basic use of the procedure is described with the flowchart in Figure 2.12.

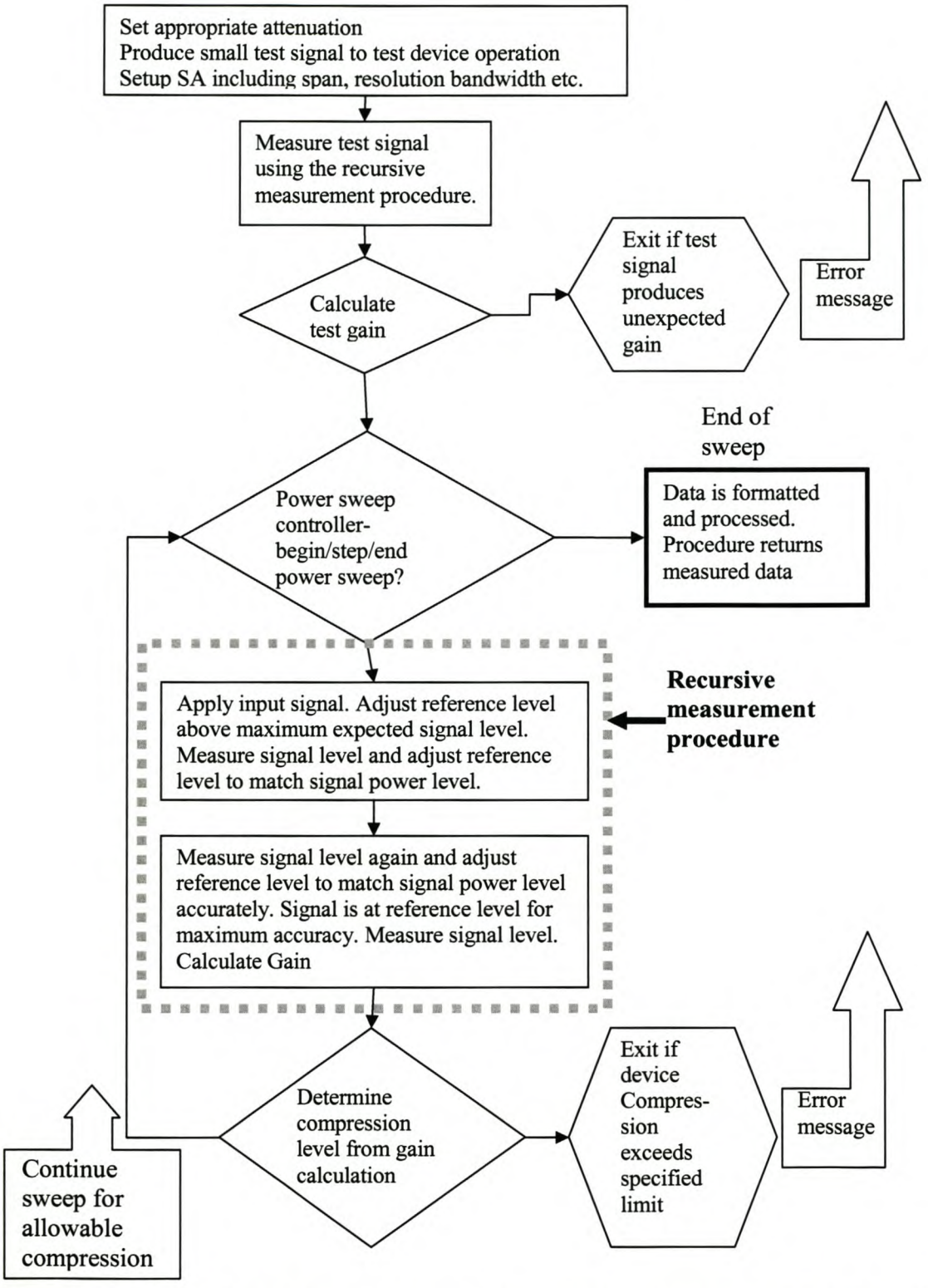


Figure 2.12 This figure shows the use of the recursive measurement technique in a larger procedure that does power sweeps. Maximum accuracy is assured by measuring at the reference level.

The power sweep procedure's input parameters are: input power, expected gain, maximum allowable compression and frequency. A Signal generator (or generators) is used to produce an input signal at the desired frequency and power level. Because the procedure knows the expected gain, the approximate signal level at the spectrum analyzers input port is known. From this data the appropriate attenuation levels can be set for the largest expected signal in a sweep. This is done to prevent spectrum analyzer damage or compression. A safety measure to prevent damage to the DUT is also implemented. This is done by specifying the maximum compression that should be allowed from the specified gain. This gain is updated for each new measurement enabling the procedure to stop as soon as unacceptable levels of compression are measured.

The power sweep procedure of Figure 2.12 starts with the reference level more than 10dB above the maximum expected signal level. It determines if the device is operating correctly by calculating gain from a test measurement. If the device is working properly the procedure continues to sweep through the input power vector. After each step the device compression is determined and compared to the maximum allowable compression specified. If the device doesn't work or the compression is too high the procedure will stop to prevent damage. Accuracy is assured by adjusting the reference level to match the signal level with the recursive measurement procedure. In this way only the reference level is adjusted between power steps. The procedure allows large measurement sweeps to be done without operator intervention and can be adjusted to suit various spectrum analyzer applications. It was found that a 300KHz span, 3kHz resolution bandwidth and 1KHz video bandwidth produced fast and accurate measurements. These settings can be adjusted to suite the specific measurement application. However, it should be noted that a resolution and video bandwidth of less than 1kHz introduce additional filter alignment uncertainty.

Using this measurement strategy yields repeatable measurements. The absolute accuracy can be further enhanced by characterizing the absolute frequency response of the spectrum analyzer. This process is described in the following section.

### 2.2.5 Error Correction through Frequency Response Characterization

The HP8562's internal calibration has two drawbacks. Firstly its accuracy of ±0.3dB and secondly the fact that it is at one frequency and power necessitating measurements to be referenced to this point for calibration. Using an accurate external signal source, the spectrum analyzer can be characterized at any desired frequency and power level within hardware capabilities. The technique used to accomplish this is discussed in this section.

To compensate for the measurement error, given a certain instrument state (constant attenuation, span, RBW and VBW), the spectrum analyzer can be characterized for each power level and frequency expected at its input port. If the input to the spectrum analyzer is known the error can easily be found as the difference between the measured value and the applied value. By this process an error grid can be set up to correct data measured with the spectrum analyzer. The effectiveness of this calibration procedure depends strongly on the accuracy of the applied reference signal. The accuracy of a Rhode&Schwarz SMIQ signal generator was measured with a HP436A power meter using a HP8481A power sensor. The uncertainty of the power meter measurement is discussed in section 2.3.2. It is dependant on the source SWR and the power sensor SWR. The source SWR is less than 1.5 resulting in a maximum power meter uncertainty of

±0.06dB. The result of the power meter measurements are shown in Figure 2.13. It can be seen that the signal generator error is less than ±0.05 dB for output power levels below 10dBm. The SMIQ signal generator's output is also stable over time and very repeatable.

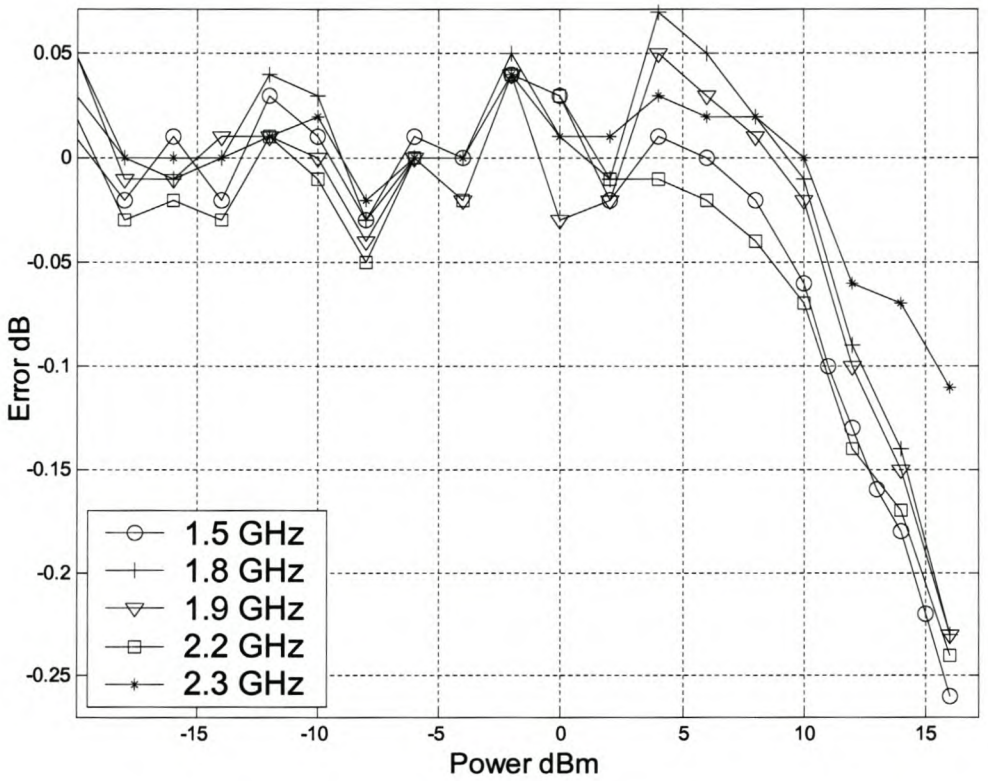


Figure 2.13 This plot shows the output power error for the Rohde&Schwarz SMIQ signal generator at various frequencies. The output is very accurate for power levels below 10dBm.

Figure 2.14 shows the HP8562's measured error for a certain instrument state. It can be seen that the error is relatively constant over power except when measuring near the noise floor. The frequency band switching at 3GHz also increases the error. This error can be used to correct measured data. However, there remains a residual error of seemingly random nature that can not be characterized.

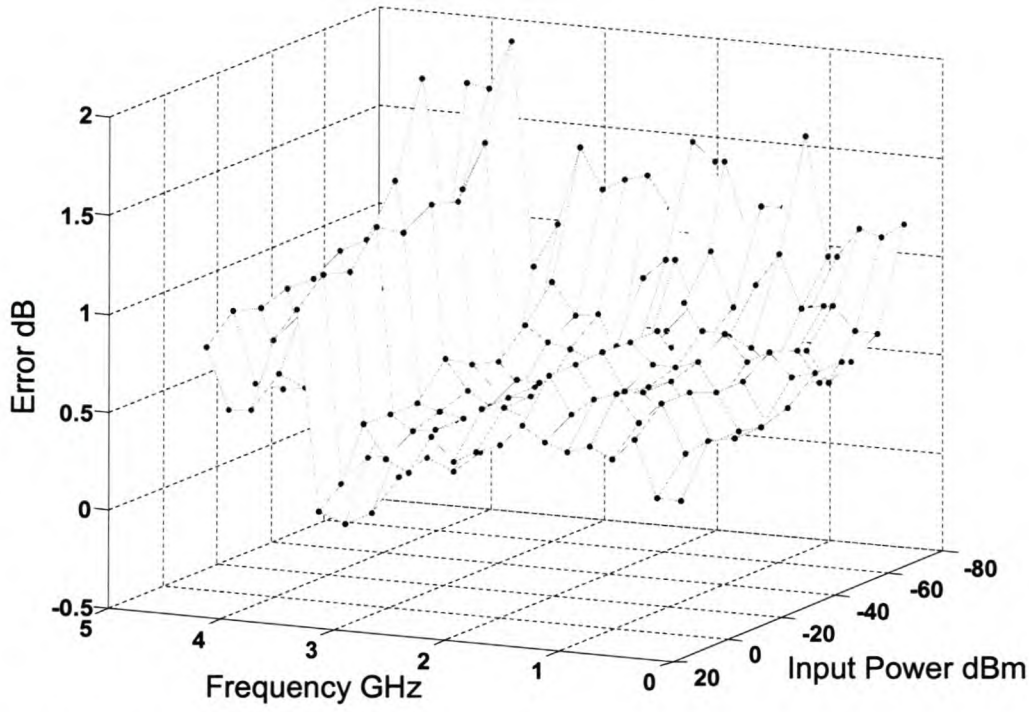


Figure 2.14 The HP8562 spectrum analyzer's error is fairly constant. The error increases close to the noise floor, in this case below 60dBm, and for frequencies above 3GHz.

This type of error correction can characterize the systematic errors in a system to a certain extent (like in Figure 2.14), and then compensate to remove them from a measurement. The random errors resulting from noise can not be removed from a measurement in this way. It is also true that the measurements that were used to characterize the systematic errors were also done with instruments that have both types of error uncertainty. Therefore the accuracy of the measurements done to determine the spectrum analyzer error, is also limited. Any measurement has a basic limit to accuracy as a result of systematic errors after imperfect calibration and noise. However it is usually possible to reduce these remaining errors to acceptably small values.

This noisy characteristic of the spectrum analyzer error is a result of these accumulated random errors and the physical accuracy limits of the various instruments in the process. This puts a limit on the maximum accuracy of the error correction that can be achieved. In the process of measuring the error, the amplitude is measured with the spectrum analyzer and referenced to a known source. Any uncertainty in the measurement setup used to calculate the calibration error, will remain unknown and will therefore limit the calibration accuracy. This residual uncertainty of the error is caused by the following two factors:

- The uncertainty of VNA measurements used to remove the effects of passive components (filter, cables etc.) from the measurement together with the SMA connector repeatability. The setup is shown in Figure 2.15.

- SA measurement uncertainty. This is influenced by the frequency response and calibration uncertainties as well as signal generator repeatability. The spectrum analyzer accuracy is also influenced by noise which will change for each RBW and VBW setting.

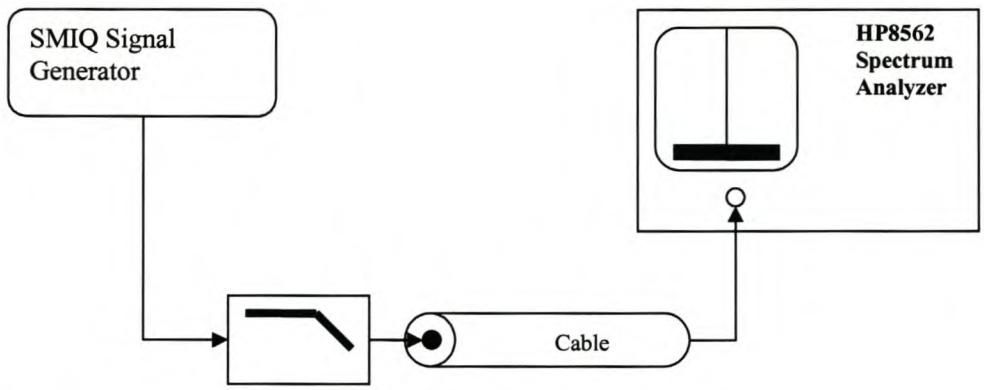


Figure 2.15 This figure shows the measurement setup used to determine the spectrum analyzer error. The effect of the filter and cable is removed by using VNA measurements while the signal generator output is characterized with a power meter.

The noisy nature of the error data can be reduced by averaging. Averaging will have an effect on the random errors in the system. To illustrate Figure 2.16 shows three error measurements and their average at 1.9GHz. Figure 2.17 illustrates the deviation from average for the same three measurements, from the average of those three measurements. From these figures it can be said that if spectrum analyzer data is corrected by the average error of Figure 2.16, the data should be correct to within the maximum deviation from that average shown in Figure 2.17. The certainty of this statement can be increased by averaging over more data sets. In this case only three measurements are shown to illustrate the principle.

By taking the average of three measurements the expected uncertainty, after error correction, can be reduced from ±1.8dB (section 2.2.3) to:

- Spectrum Analyzer Uncertainty from Figure 2.17 = ±0.15dB
- SMA Connector Repeatability (measured) = ±0.06dB
- VNA Measurement Uncertainty (data sheet) =±0.075dB
- Power Meter Uncertainty (calculated)
  for Reference Source Uncertainty Measurement = ±0.06dB

The accumulation of these factors will result in a total measurement uncertainty of ±0.345dB for error corrected spectrum analyzer data.

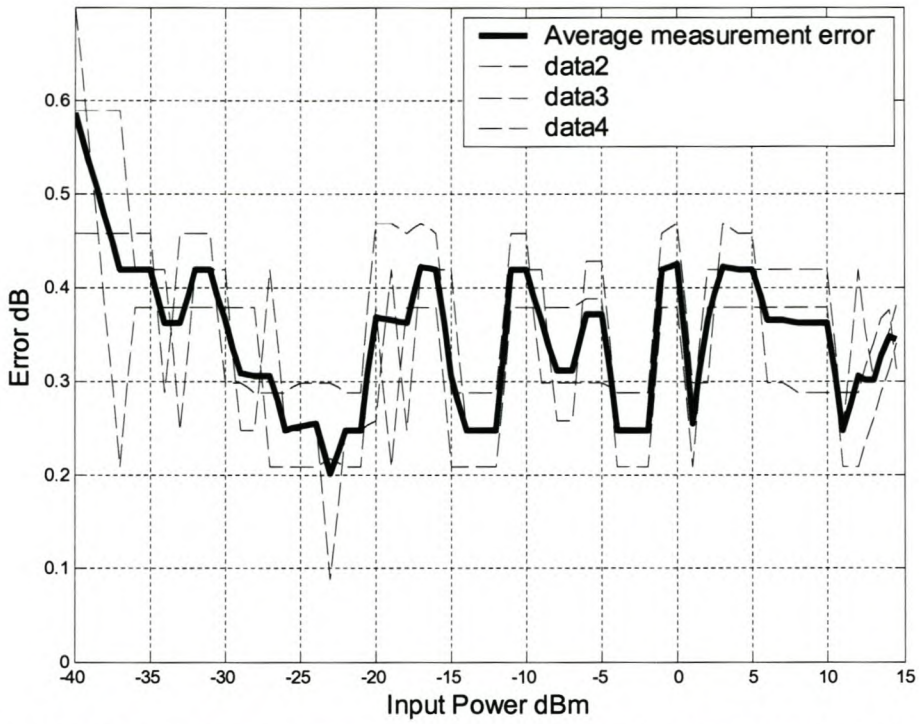


Figure 2.16 This figure shows three error measurements for the HP8562 at 1.9GHz and the average of the three measurements.

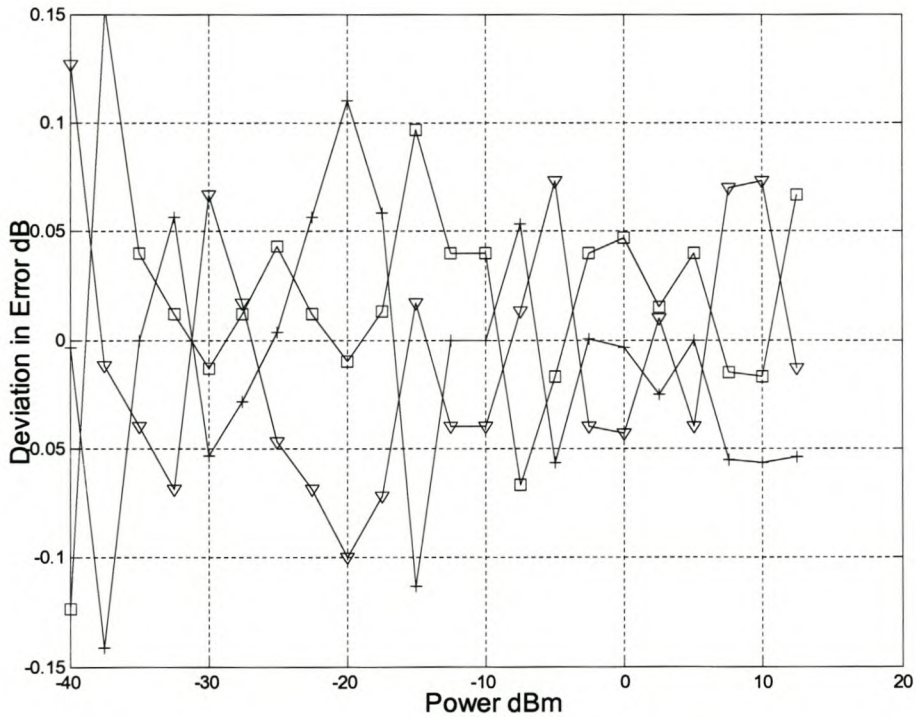


Figure 2.17 The deviation from average for the 3 measurements in Figure 3.16 is shown in this figure.

From the above mentioned results it can be said that two consecutive measurements of the same signal will differ at most by 0.69dB. If this average error is used to do data correction of a measurement, the maximum error after correction will be ±0.345dB. Because the error changes for different spectrum analyzer states (noise is dependant on RBW and VBW) the average error is usually calculated from a limited number of data sets. Figure 2.19 shows a gain verses power plot of an ERA33 amplifier for different stages of error correction for the setup in Figure 2.18.

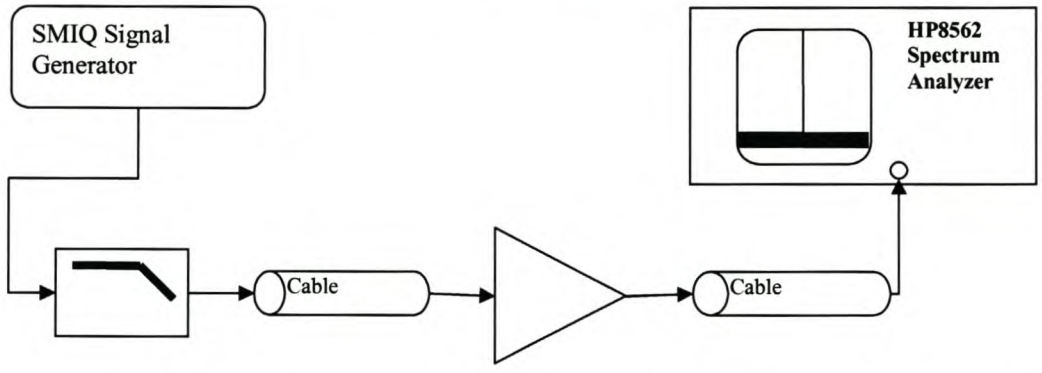


Figure 2.18 This figure shows the measurement setup for amplifier measurements. The effect of the loss introduced by the two cables and the lowpass filter must be removed from the measured data.

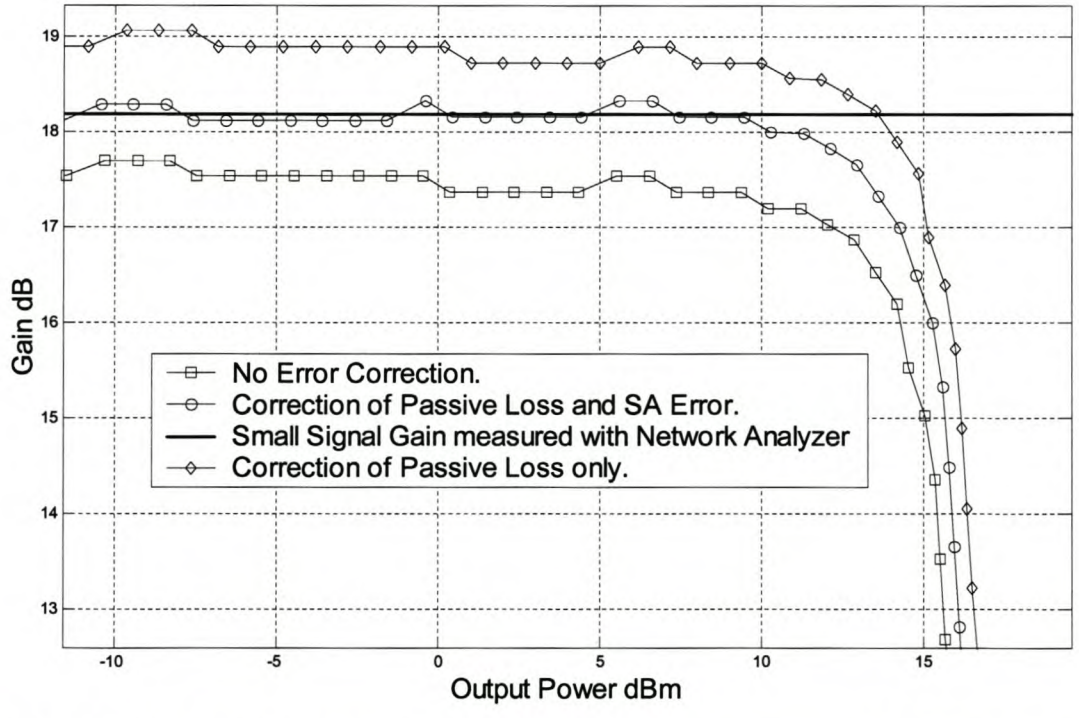


Figure 2.19 This figure shows the different stages of error correction for spectrum analyzer (SA) measurement of the Gain for an ERA33 amplifier.

The first step in error correction is removing the effect of passive components in the circuit (cables, filters etc.). This is done by calculating the frequency dependant loss from VNA measurements of cables, filters and so on. The second step is removing the spectrum analyzer error as explained above. Comparing the result to the small signal gain, measured with a HP8753 VNA, shows the increased accuracy. It was found that this method of error correction works well and usually gives data with a maximum absolute error of ±0.25dB.

Figure 2.20 shows the same process used to measure the pass band of a 2.4GHz low-pass filter. This type of measurement is usually done with a VNA. It can be seen that the error correction enhances the accuracy of spectrum analyzer measurement to match the VNA measurement accurately over all frequencies.

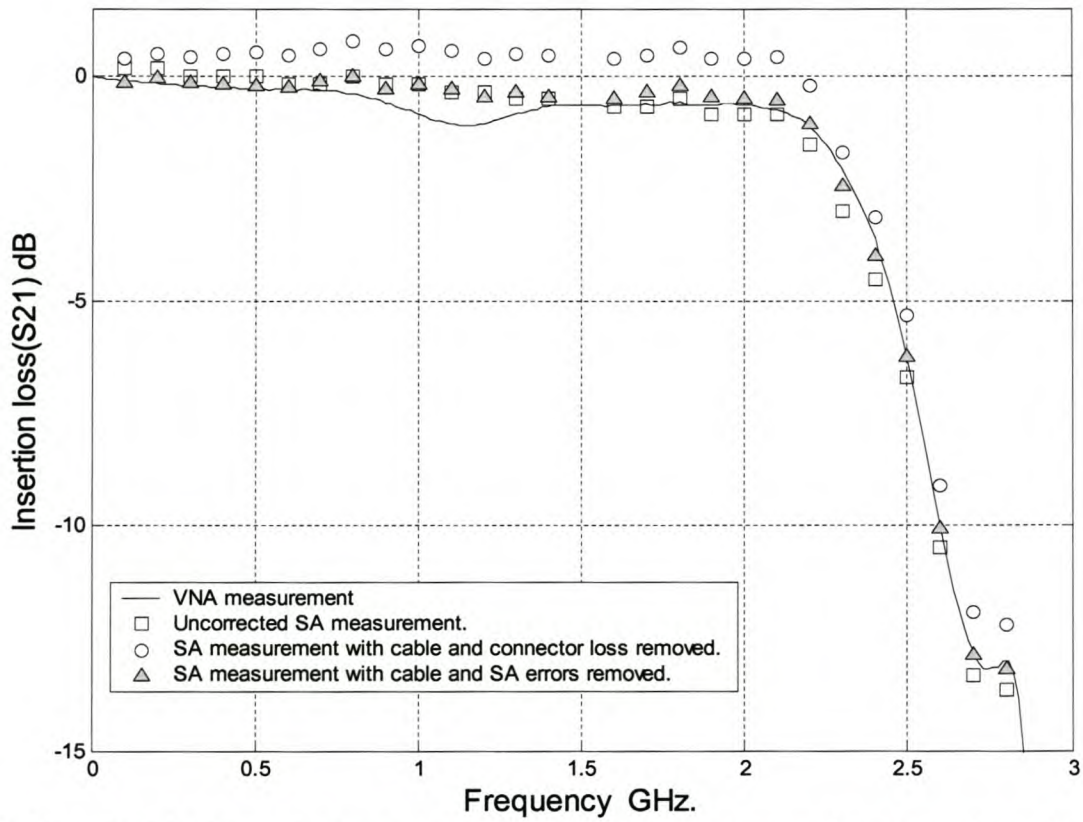


Figure 2.20 In this figure the spectrum analyzer (SA) measurement is compared to the VNA measurement of a 2.4GHz lowpass filter. The different stages of error correction can be seen to greatly enhance the measurement accuracy.

## 2.2.6 Conclusion

Using GPIB to control the spectrum analyzer together with signal sources has many advantages. As shown with Figure 2.19 and Figure 2.20 the setup is very flexible and it can be used to do power sweeps as well as frequency sweeps. The accuracy is also greatly enhanced by the error correction described. The setup is also fully automated by GPIB control from a PC and therefore demands no operator attention once a measurement has started. To change all the settings after a power step will take an operator at least one minute. The program does this accurately in 20

seconds. But most importantly it can do it for large sweeps. The most significant shortcoming of the spectrum analyzer is its inability to measure phase data. The spectrum analyzer was used to characterize mixers and amplifiers (chapters 3 and 4) and is the only instrument that can be used to investigate the spurious response of a mixer (section 4.1.3).

## 2.3 Other Instruments

Two additional measurement instruments were used namely the Anritsu Scorpion vector network measurement system and a HP436A power meter. Measurements made with these instruments were used mainly for comparison. Signal generators were used in most of the measurements and they are discussed briefly in section 2.3.3. One additional instrument was used to confirm the validity of the measurements performed in the RF and Microwave Laboratory of the E&E department at Stellenbosch University. This instrument, called a Nonlinear Network Measurement System (NNMS) or Large Signal Network Analyzer (LSNA), is located at the Katholieke Universiteit Leuven and is discussed in section 2.3.4.

### 2.3.1 Anritsu Scorpion vector network measurement system

This machine was only available for a short time. The MS462 Scorpion is primarily a high performance VNA that performs S-parameter measurements. The MS462 is especially innovative because it can also perform measurements not typically associated with a VNA. These measurements include noise figure, intermodulation distortion (IMD), and harmonics. The ability to perform these other measurements typically requires four additional instruments besides the VNA namely, a noise figure meter, two synthesizers, and a spectrum analyzer. The MS462 can integrate these five instruments into a single system: a Vector Network Measurement System. The Scorpion was used to do the following measurements:

- Three-port, error-corrected measurements of mixers. A single connection provides all 9 S-parameters simultaneously.
- Intermodulation distortion (IMD) measurements versus frequency. CW-type measurements are simple for the MS462, but it can also measure IMD, calculate third-order intercept (TOI), and display the results versus frequency referenced to input or output and relative to upper or lower tones.
- Vector Harmonic measurements where S-parameters are used to correct for source harmonics. Similar to IMD measurements, the harmonic measurements can be displayed versus frequency referenced to input or output.
- Simplified mixer measurements for fixed LO and fixed IF measurements, for instance conversion loss.

A limited range of measurements were performed with this instrument and they serve mainly as reference for comparison with the spectrum analyzer and HP8753 measurements in chapters 3 and 4. For more information see [14].

### 2.3.2 Power Meter

Power meter measurements are considered to be the most accurate method to measure amplitude. However, there are many different kinds of power meters and power sensors or power heads. This is in part to accommodate different kinds of power measurements. The instrument that was used to do power measurements is the HP436A with a HP8481A power sensor. The setup is designed to do average power measurements on CW signals. The purpose of the power meter measurements is to serve as a reference to determine the accuracy of measurements done with other instruments. Even though the power meter is very accurate it is slow and demands constant operator presence and is therefore not suitable to do large sweep.

Power meters have known errors that can be quantified by specific uncertainties. They also have errors as a result of mismatch between the power sensor and the source of the signal being measured. The coaxial cable used to connect the power source and the power sensor will also cause reflection. To determine the total error involves calculating the known error according to the incident power level and frequency, and calculating the mismatch uncertainty. The known sources of uncertainty for the HP436A are:

- Instrumentation uncertainty ±0.02dB
- Power reference uncertainty ±0.03dB
- Calibration factor switch resolution ±0.02dB

  Total ±0.07dB

To calculate the mismatch uncertainty requires the SWR of the source as well as the power sensor. From these values the mismatch uncertainty can be calculated with the following steps [15].

1. Calculate reflection coefficient from the SWR. This depends on the DUT and cables. For the purpose of illustration the SWR of a Mini-Circuits ERA33 amplifier was used. The mismatch can be improved by an attenuator between the DUT output and the power sensor.
2. Calculate relative power uncertainty.
3. Determine the measurement uncertainty in dB

The ERA33's VSWR is 1.25 and the HP8481A power sensor has a reflection coefficient, $\rho_{sensor}$, of 0.012 at 2GHz. First calculate the reflection coefficient of the amplifier's output port:

$$\rho = \frac{SWR-1}{SWR+1} \qquad 2.1$$

$$\rho_{amp} = 0.111$$

From this the relative power uncertainty is calculated:

$$PU = [1 \pm (\rho_{sensor}\rho_{amp})]^2 \qquad 2.2$$

PU = 1.00266 and 0.9973

The calculated values result in a measurement uncertainty of:

$$MU = 10[\log_{10}(\frac{PU}{1})] \; for \; PU > 1 \qquad 2.3$$

MU = 0.0112dB and -0.0117dB

The total uncertainty is the sum of the known uncertainties of the instrument and the mismatch uncertainty. Although the power meter is very accurate (±0.018dB total measurement uncertainty in this case) it can not distinguish between frequencies. If the signal contains harmonics or distortion the power reading will include them. The details of power meter measurement are further discussed in [16].

### 2.3.3 RF Sources

Signal sources provide precise, highly stable test signals for test applications. Signal generators add precision modulation capabilities, and are used to simulate system signals for receiver performance testing [17]. To ensure the accurate and correct measurement of device characteristics, it is important to know what is going into a mixer or amplifier. Ideally a signal source should produce an infinitely stable and pure sinusoid with the desired frequency and amplitude. Although modern signal generators give high quality test signals, there are selected signal generator aspects that need to be considered. This section includes basic descriptions of signal purity and some hardware aspects that may cause problems in certain measurements.

The various factors that degrade signal quality or purity are phase noise, spurious signals and residual frequency modulation (FM). Phase noise defines spectral purity. It is the most common and meaningful method of specifying short-term stability and is usually presented as a plot of the signal generator's single-sideband (SSB) phase noise in a 1 Hz bandwidth versus the offset from the carrier (desired singular frequency component). In signal generators spurious signals refers to non-random or deterministic signals created from mixing and dividing signals to get the carrier frequency. If these signals are harmonically related to the carrier they are called sub-harmonics. The non-harmonic spectral components are called spurious signals. Residual FM is the undesired angular modulation or FM inherent in a signal generator with all the modulation turned off. It includes the effects of both spurious signals and phase noise. For detailed description of these signal generator signal purity issues see reference [18].

As mentioned previously two Rohde&Schwarz signal generators were used in this work namely the SMIQ and SML03 models. For most measurements the Rohde&Schwarz signal generators spectral purity was sufficient except for harmonic levels. Another problem is the output VSWR. The easiest way to remove the effects of these two problems is to add filters and attenuators to the output. Lowpass filters will suppress the harmonics while attenuators will reduce the effect of source mismatch.

When two signal generators are combined to perform two tone intermodulation measurements, the test system can introduce errors. Figure 2.21 shows a typical output circuit of a signal generator.

To ensure stable output power levels the generators employ a technique called automatic level control (ALC) which is basically a feedback system.

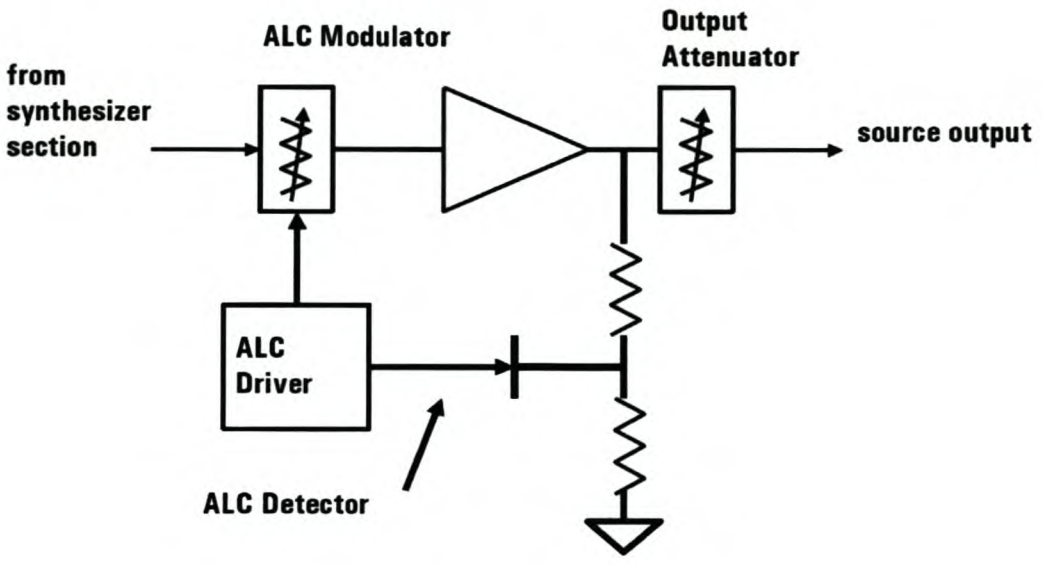


Figure 2.21 This figure shows the ALC feedback circuit for a signal generator. It is used to ensure a constant output power [19].

Whenever two signals are input to a combiner, the nonlinearities of the sources will create intermodulation products. This happens if the two sources are not adequately isolated. If a signal from a different signal generator leaks into the output circuit shown in Figure 2.21, it may affect the ALC if it falls within the ALC bandwidth. The additional power of the signal is combined with the feedback power and detected by the ALC detector. The two closely spaced tones will in effect cause AM modulation of the ALC circuitry. This will cause intermodulation in the output signal. The intermodulation created by the ALC will interfere with the measurement because the intermodulation products created by the test system are at the same frequencies as those created by the amplifier under test. This effect can be avoided by adding additional attenuation between the two signal generators as shown in section 3.1.3.

There are additional signal generator imperfections that may be important in other applications and they are discussed in reference [19].

### 2.3.4 Nonlinear Network Measurement System

This instrument was initially developed by Agilent Technologies. It has the unusual ability to calibrate and measure nonlinear component characteristics. The instrument at K.U. Leuven was used to measure the Hittite mixer and the ERA33 amplifier to serve as an external reference. The

measurements performed at the University of Stellenbosch are compared to these measurements as an additional test of accuracy. The basic capabilities of the instrument are explained in this section.

The NNMS, shown in Figure 2.22, has the ability to measure the phase and amplitude of all spectral components of both the incident and reflected signals at the device ports. The signals ($a_1$, $b_1$, $a_2$, $b_2$) that are measured are actually the incident and reflected traveling power waves. From these measured traveling voltage waves the current and power waveforms can be calculated. This information represents the large-signal or nonlinear behavior of the device. The system also has two sources that can simultaneously excite both ports of the device. Figure 2.22 shows the two sources as well as the input and output waves each consisting of multiple harmonics. Because it measures the complete multi-tone input and output the DUT's nonlinear behavior can be extracted from this information. The instrument gives vector calibrated measurements and the fact that it was located in a different laboratory makes it a good reference to compare the local measurements to.

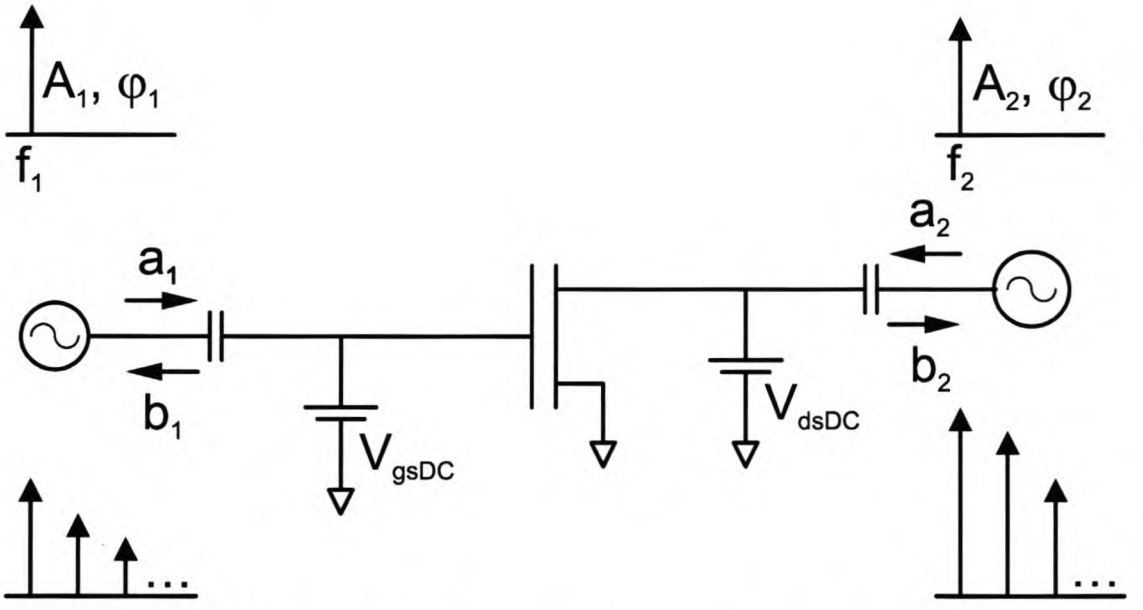


Figure 2.22 This figure shows the basic components and waveforms necessary to understand the capabilities of this instrument [20].

## 2.3.5 Conclusion

Using these instruments along with the VNA and the spectrum analyzer enabled the measurement of a wide variety of nonlinear and linear characteristics. The most important factor of using different measurement instruments is the ability to compare the results which was the primary reason for the power meter, Scorpion and NNMS measurements. The comparisons are shown in the following chapters. The VNA and spectrum analyzer combination is able to do most of the measurements required by the ADS models to describe certain device characteristics. The most significant shortcoming is the spectrum analyzers inability to measure vector data. However with the different measurement automation software that was developed (shown in following chapters) the spectrum analyzer is the only viable instrument to do certain measurements because of the

measurement time compared for example to the power meter. The automated measurement setup can do large sweeps without operator presence. More detail of these aspects will be given in following chapters. Even though instruments such as the Scorpion and other modern measurement systems have increasingly complicated nonlinear capabilities, a thorough understanding of the basic principles of network and spectrum analysis is important to ensure the correct interpretation of measured data.

# Chapter 3

# Amplifiers

## Introduction

Amplification is one of the most important functions in wireless receivers and transmitters. Specifically for the case of receiver systems, small-signal amplifiers are usually required to have low noise figure and linear gain within a desired operating bandwidth. In the process to design such an amplifier, the active device (transistor) is viewed as a two port described by small signal parameters such as S or Y parameters. The two-port is then matched to the desired impedance of the system. However, apart from this small signal operation of the amplifier or transistor, the nonlinear nature of transistors will also cause distortion phenomena of which saturation, intermodulation distortion, harmonic distortion and AM-to-PM conversion are of the greatest concern. These were described in chapter one. The amplifier models in ADS all require the small signal parameters to describe the device operation in the linear region. If nonlinear behavior is important there are various options to create models that will reproduce the different desired nonlinear phenomena. These models require various nonlinear parameters. This chapter describes the measurement of these nonlinear characteristics of amplifiers specifically for the purpose of simulation in ADS. In this chapter, section 3.1 describes various nonlinear amplifier measurements looking at measurement technique and accuracy, while section 3.2 describes system level simulation of amplifiers in ADS.

## 3.1 Amplifier Measurements

This section describes the measurement of gain compression and intermodulation related phenomena. Harmonic distortion was also measured but this is a simple extension of the gain compression measurements of section 3.1.1. AM-to-PM data is inherently available from VNA measurements of gain compression and this will be shown later. It was also mentioned that the small signal parameters (S-parameters) are important and the procedures to do accurate S-parameters measurements were already described in chapter 2 and will not be repeated.

### 3.1.1 Amplifier Gain Compression Measurements

Amplifier gain compression is a nonlinear phenomenon. The most common way to specify gain compression is the 1dB gain compression point. This is the point where the actual measured gain is 1dB less than the gain in the small signal or linear operating region. With amplifiers, compression is usually specified as the output power at which gain compression occurs. The dashed line in Figure 1 represents the output for an ideal amplifier with no saturation (compression). The solid line represents actual or measured response of an amplifier. From Figure 3.1 it can also be seen that the gain saturates for very large input powers.

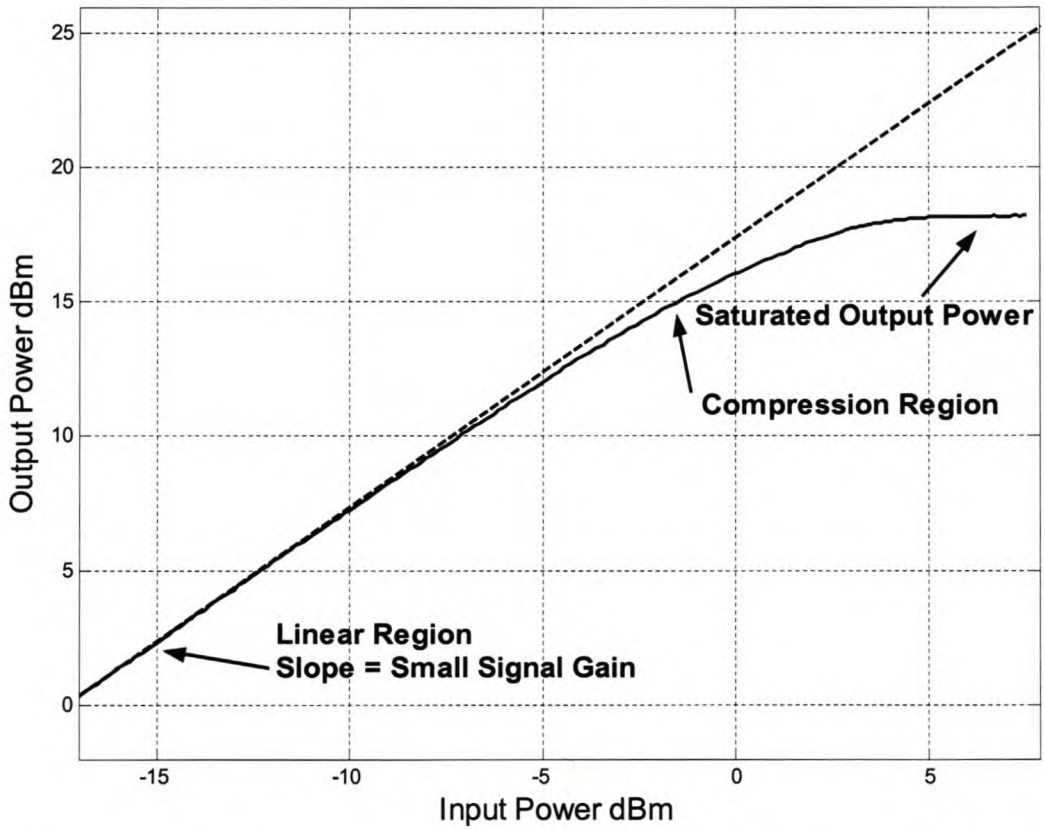


Figure 3.1 Amplifier gain compression can clearly be seen in this figure. It shows the output versus input power levels for an ERA33 amplifier at 2.3GHz. The amplifier's gain is equal to the small signal gain for low input power levels, but gradually decreases until the gain saturates for large input power levels.

Measuring gain compression requires swept input power measurements. The 1dB compression point can be determined from these measurements. Three instruments for measuring fundamental non-linear amplifier output power was used. A vector network analyzer (VNA) HP8753, a spectrum analyzer (SA) HP8562A and an Anritsu vector network measurement system with nonlinear measurement options. Some reference measurements were also done with a HP436A

power meter to test the accuracy of the various methods. Each of the methods presented its own problems. The following sections describe these problems and compare results of measurements done on two Mini-Circuits RF MMIC amplifiers.

### 3.1.1.1 Non-Linear VNA power sweep

Measuring gain with the VNA essentially means measuring $S_{21}$. When this is done with an input power ramp it is possible to see the non-linear gain of the amplifier. With VNA measurements S21 is the ratio of the Port 2 and Port 1 power levels in Figure 3.2.

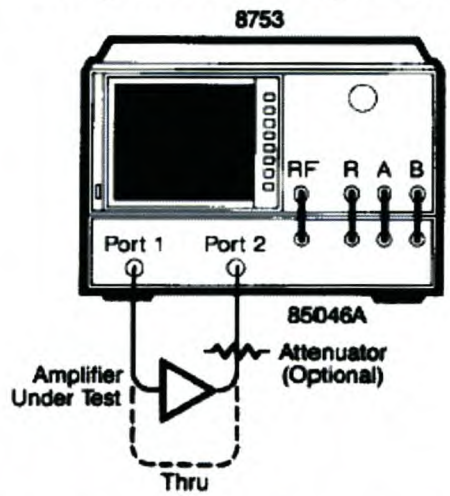


Figure 3.2 The swept power gain compression measurement procedure is explained in [9]. This application note describes the fairly complex process but the basic idea is shown in this figure which was taken from the text.

For this ratio to accurately represent the DUT's power gain from input to output, the input power ramp and loss through the measurement setup need to be taken into account. To do this requires a response calibration and measuring the actual power level at input B of the VNA. This is done with a specific procedure to enable the instrument to give absolute power readings instead of power ratios. The response calibration is done to measure the signal path without the DUT as displayed in Figure 3.2. The setup and steps to do absolute power measurements are described in [9]. It is important to note that the VNA is a narrow band tuned receiver with an adjustable IF as explained in chapter 2. The IF bandwidth default is 3KHz and the measured power is therefore only the power at the fundamental frequency.

Measurements were made on the two Mini-Circuits amplifiers with the following datasheet specifications:

| *AMP* | *FREQ GHz* | *GAIN* | *P1dB* |
|---|---|---|---|
| ERA33 SM | DC-3 | 17.4dB@2GHz | 13.5dB @2GHz |
| ERA6 SM | DC-4 | 11.3dB@2GHz | 17.9dB @1GHz |

Swept frequency, small signal calibrated VNA measurements were also done. These measurements were made with optimum power levels at the VNA's internal mixer (smaller than -10dBm) and

with full two port calibration as described in chapter 2. This is a very accurate measurement of the small signal gain of the amplifier. The swept power measurement has the disadvantage that the power level at the output will change throughout the measurement. The setup was done so that the power level would be less than -10dBm for the maximum expected output power in the sweep. Figure 3.3 displays the output versus. input power for the ERA 33. It can be seen that the two measurements compare closely in the amplifiers linear operating region. The measurement was done at 2GHz to compare with the datasheet specifications.

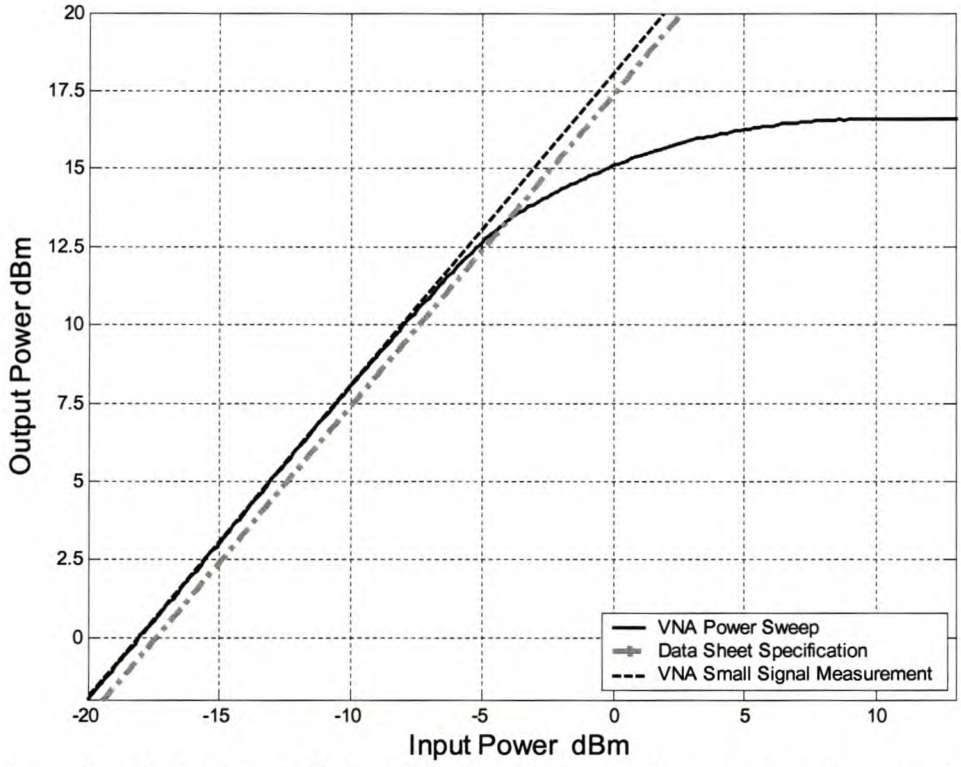


Figure 3.3 Results in the small signal region illustrates the necessity of measuring the device. The data sheet gain is 17.4dB while the measured small signal gain is 18.1dB. The power sweep gain in the small signal region is 18.2dB at 2GHz.

The gain is effectively a numerical differentiation of the output versus input curve. This has the effect of accentuating differences between the nonlinear and small signal measurements. For power levels well into the small signal range the two measurements should produce exactly the same gain in an ideal measurement setup. This is not the case as can be seen in Figure 3.4 which shows the gain versus. output power for the ERA6 at 1.9GHz. There are many factors which could produce this discrepancy. These include noise, connector repeatability, VNA receiver errors and mismatch errors as a result of only doing a response calibration in the case of the VNA power sweep.

Although there is uncertainty about the accuracy of the VNA power sweep it is the only instrument that measures vector data. The phase change introduced by an amplifier can be very important in some applications. Figure 3.5 shows the gain and phase versus. output power for the ERA33 at 1.9GHz. It can be seen that the phase response is constant in the linear region but starts to deviate drastically from this as the amplifier goes further into compression. However the phase response of the ERA6 is very different from that of the ERA33 as can be seen in figure 3.6.

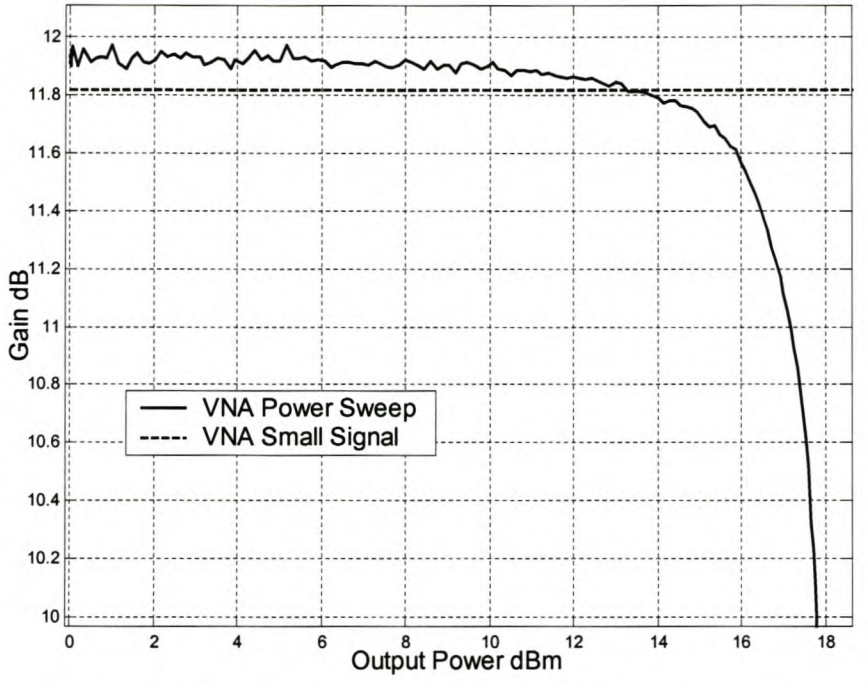


Figure 3.4 From this figure the difference between the small signal measurement and the swept power measurement in the linear region can be seen at 1.9GHz. There is an error of approximately 0.1dB in the swept power measurement.

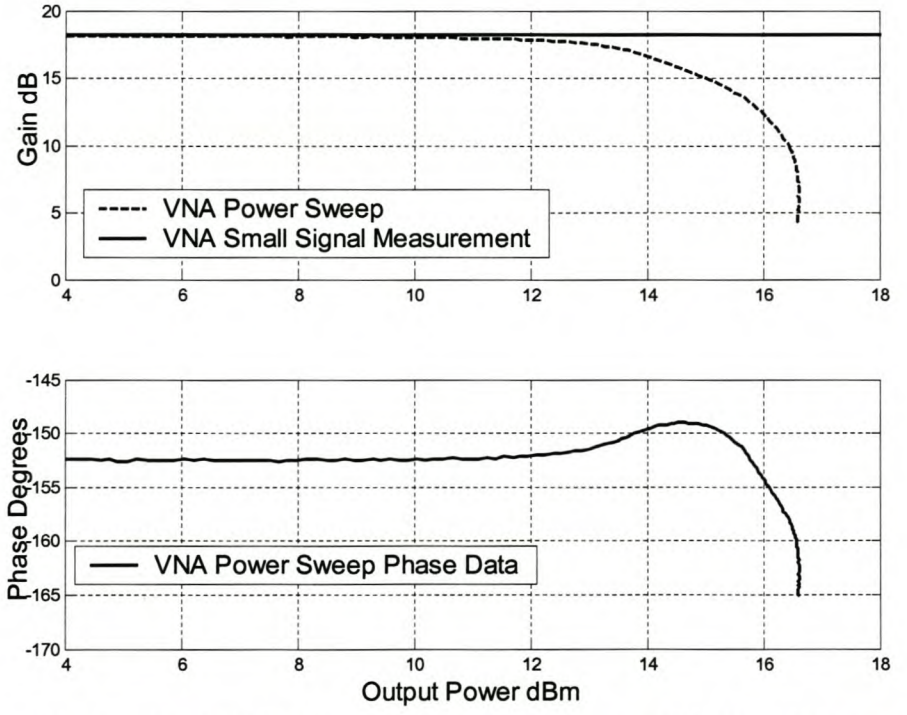


Figure 3.5 In many applications an amplifiers phase response is very important and may be crucial to system design. This figure shows the phase response of the ERA33 for a power sweep at 1.9GHz. AM-to-PM data is inherent to this measurement.

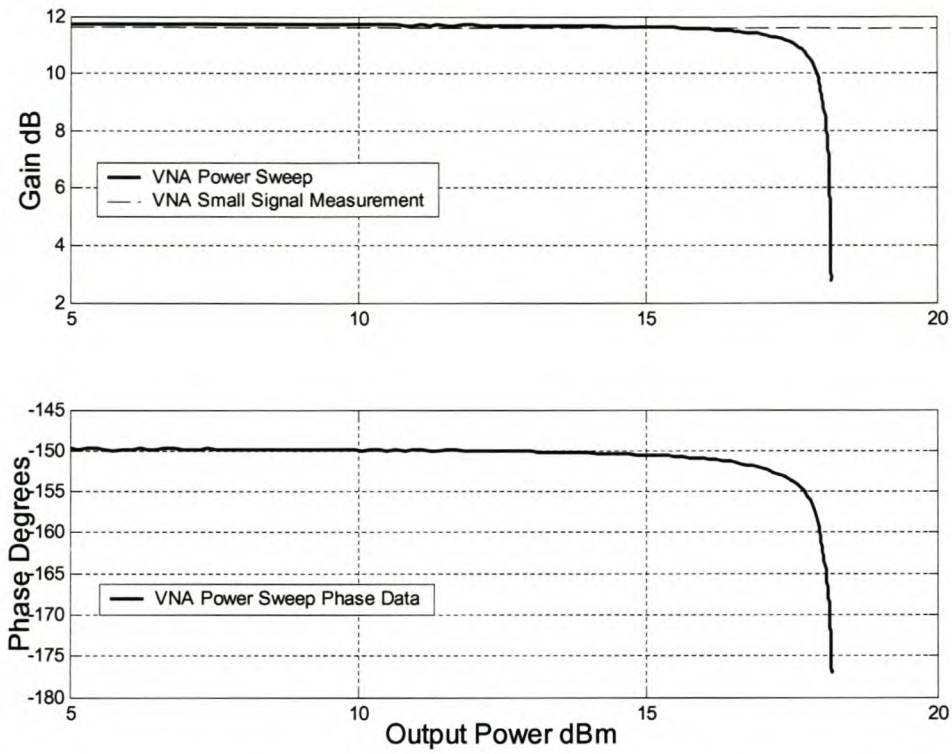


Figure 3.6 The gain compression and phase response for the ERA6 at 1.9GHz is shown. The difference in phase response between the ERA33 (Figure 3.5) and ERA6 is obvious and may be important for certain applications.

Phase data from Figure 3.5 and Figure 3.6 shows the difference in the two amplifiers phase response in the compression region. In applications where phase data is important, this type of comparison can be very valuable in deciding between two amplifiers.

### 3.1.1.2 Spectrum Analyzer Power Sweep

The basic setup for swept power gain measurements with the HP8562 spectrum analyzer and a signal generator is shown in Figure 3.7. There are many factors that influence the accuracy and repeatability of this setup and they are discussed in Chapter 2 along with error correction of the measured data. This section will present further results displaying the abilities of this setup. The repeatability and accuracy are discussed in section 3.1.1.2 A while the post processing to calculate the 1dB compression point is discussed in section 3.1.1.2 B.

### 3.1.1.2A Measurements

Apart from the spectrum analyzer accuracy and repeatability the most important aspect of the setup in Figure 3.7 is the spectral content of the input signal. The low pass filter must ensure that the levels of the signal generators harmonics are low enough. This is important to ensure that the response measured at the fundamental frequency is not influenced by signals at higher frequencies.

Harmonic input levels of more than 60dBc below the carrier were considered to be negligible in this work.

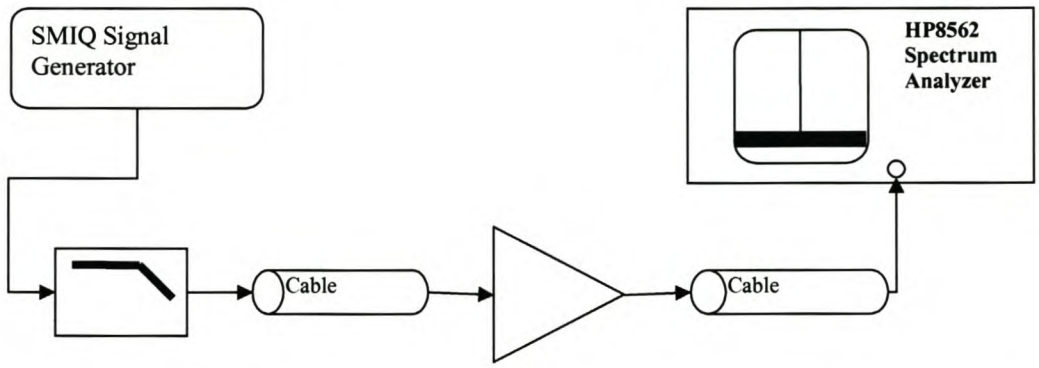


Figure 3.7 Measurement setup for swept power amplifier measurements showing lowpass filter and cables.

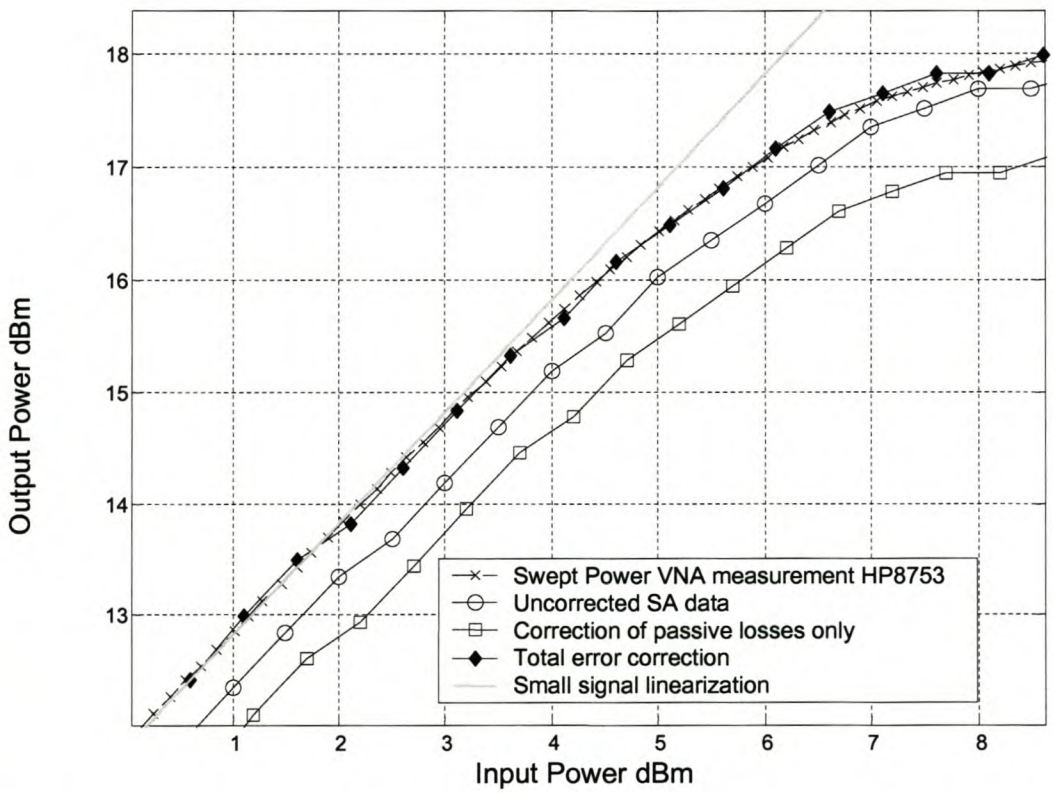


Figure 3.8 The input versus output power levels for the ERA6 at 1.9GHz is shown in the compression region. The different stages of error correction are shown. The uncorrected data is marked with circles. After the effect of the cables and filter are removed the trace is marked with a square. The final result is the trace marked with diamonds showing a good match with VNA data.

The input versus output plot in Figure 3.8 shows excellent agreement with the small signal VNA measurement. This confirms the validity of the error correction procedure. The repeatability of the measurement can be seen in Figure 3.9. This figure shows the gain versus output power for the ERA33 at 2.3 GHz for three consecutive measurements. It can be seen that they all match the small signal VNA measurement well. The maximum difference between two measurements is 0.4dB although it is mostly within 0.2dB.

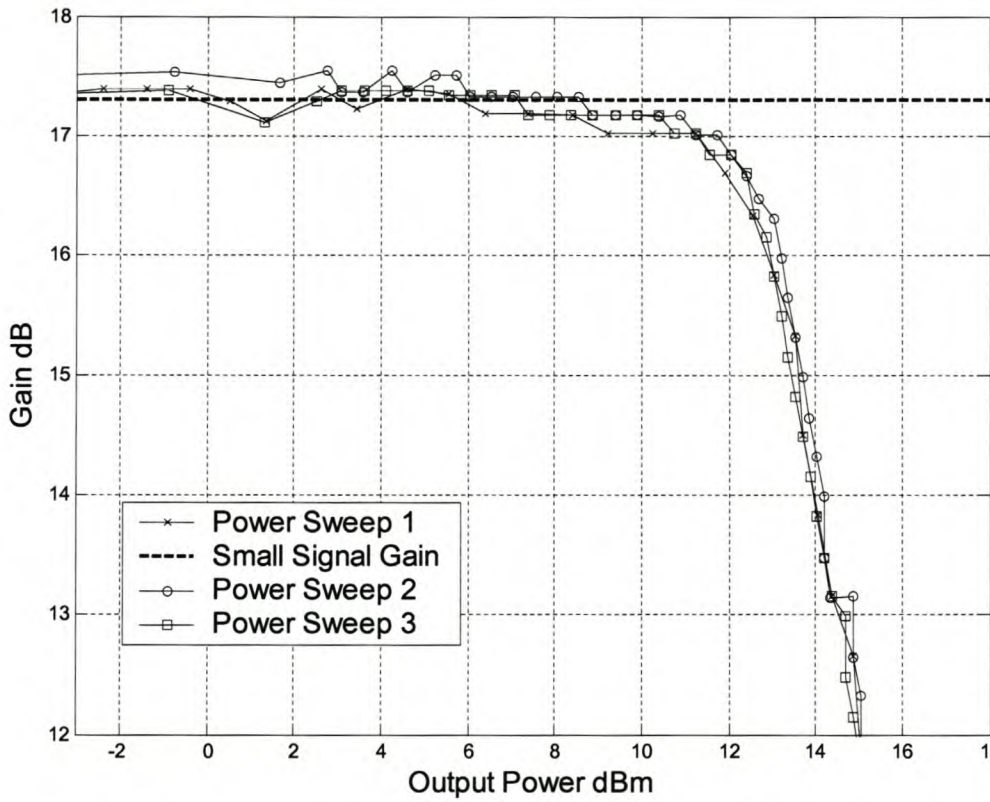


Figure 3.9 Three consecutive measurements were made of the ERA33 at 2.3GHz showing the measurement repeatability. It can be seen that all three measurements agree closely to the small signal VNA measurement in the linear operating region. In the compression region the three measurements compare very closely.

The automated spectrum analyzer measurement setup along with the error correction described in section 2.2, give repeatable and accurate compression measurements as seen from Figure 3.8 and Figure 3.9.

### 3.1.1.2 B Post Processing of Measured Data

There are two parameters that need to be calculated from these measurements namely the 1dB compression point and saturation output power. The measurement automation described in chapter 2 consists of two different MATLAB procedures: one for measurement automation and one that does the post processing of the data. The second procedure includes the error correction as well as calculating the 1dB compression point.

The spectrum analyzer error correction procedure's input parameters are the measured power levels and the input power levels, the S-parameters of all the passive components and the error matrix for the spectrum analyzer measurement error. The procedure starts by doing the error correction for both types of error as described in section 2.2.5. This results in an input power vector and an output power vector. From this data the 1dB compression point can be calculated. The basic steps are shown in Figure 3.10. It is important to choose the minimum and maximum input powers of the measurement carefully. The power sweep must start well in the linear region to ensure accurate calculation of the small signal gain. It should also drive the amplifier far enough into the compression region at the high end. This usually requires a power sweep that changes over a minimum of 20dB which puts a limit on the minimum step size. A practical solution that gives accurate measurements in reasonable times uses larger step sizes in the linear region (2.5dB to 5dB) and reduces the step size in the compression region to as low as 0.5dB. The user has to select the step size manually. Because of the measurement uncertainty steps smaller than 0.5dB does not increase the accuracy.

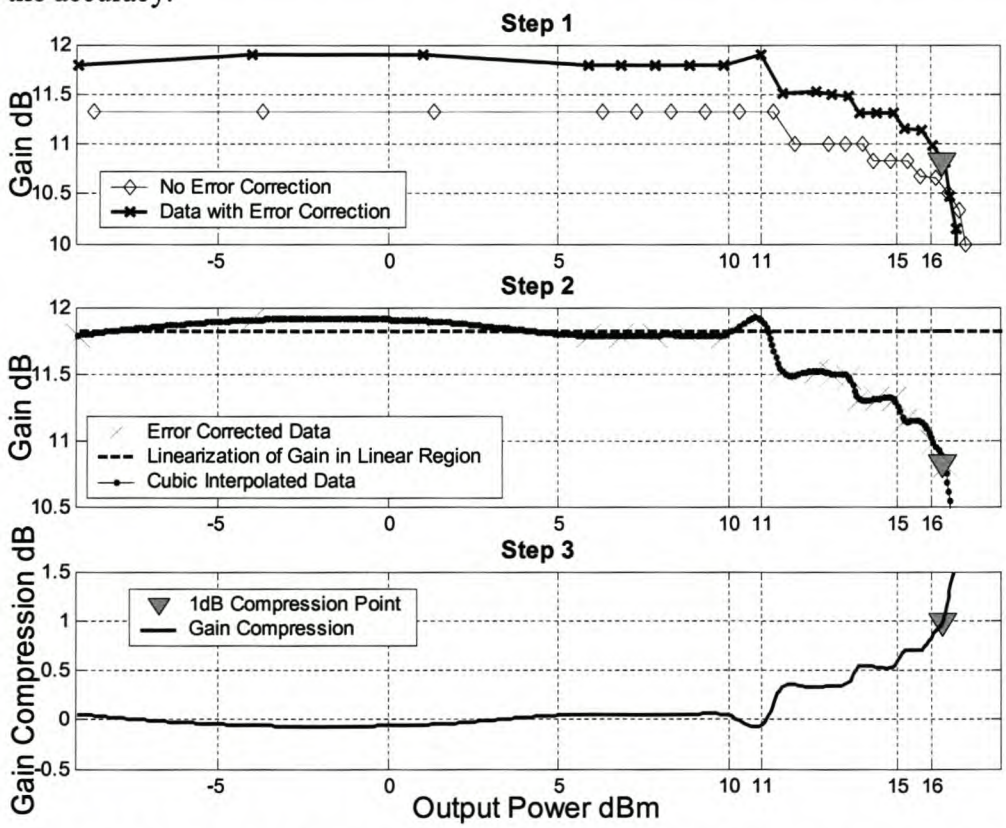


Figure 3.10 The three steps that are necessary to calculate the 1dB gain compression point are shown in this figure for the ERA6 at 1.9GHz. The small signal gain is 11.8dB as measured with the VNA. Step one shows error correction and determining the linear region from the gain's rate of change. Step two shows the interpolation of the gain curve and the linearization of the small signal gain. Step 3 shows the gain compression curve.

Step 1 in Figure 3.10: After error correction the procedure determines the linear operating region. This is done by first calculating the gain (gain = output power – input power) and then doing numerical differentiation of the gain data. The differentiated gain is the rate of change in the gain between consecutive data points and can be seen as the angle of the gain curve. In the linear region

the gain should theoretically not change between two consecutive points while it will by definition change between two points in the compression region. In reality however the gain changes in the linear region because of measurement uncertainty. To compensate for this the procedure determines the end of the linear region from the rate of change of the gain. If the absolute value of the angle (rate of change) is larger than a specified value, the device is going into compression and that marks the end of the linear region. In Figure 3.10, Step 1 shows that the linear region is up to 11dBm output power where the gain's rate of change is clearly increased.

Step 2 in Figure 3.10: The purpose of the procedure is to accurately determine the 1dB gain compression point. This will be the point where the gain deviates 1dB from the gain in the linear region. With the specific instruments the user will usually not choose a step size smaller than 0.5dB and because of this the data has to be interpolated to increase the resolution for the 1dB point calculation to more than the minimum step size. This is done by using cubic interpolation of the input versus output curve shown as Step 2 in Figure 3.10. The small signal gain is the average of the portion of the data determined to be the linear region in Step 1.

Step 3 in Figure 3.10: The final step to determine the 1dBc point, the gain at each point is calculated. This can be done by subtracting the interpolated nonlinear data from the linear extrapolation of the small signal gain. This will give the gain curve, including the compression region, which can be used to get the compression value in dB as shown in Step 3. From the gain compression curve the 1dB compression point can easily be found. This will give an output power value and a gain value from which all other parameters can be calculated. The procedure was implemented in MATLAB. The interpolation is done to a resolution of 0.1dB. The saturation point is determined graphically from the input versus output power plots.

Results of the spectrum analyzer measurements including the calculation of the 1dB compression points are compared to other techniques in section 3.1.1.4.

### 3.1.1.3 Anritsu Scorpion Vector Network Measurement System MS462

This machine was only available for a short time. It has built in non-linear measurement capabilities designed to do some of the more common non-linear measurements. For the amplifier compression measurements there were two options. The first option is similar to the swept power VNA measurement. It is essentially the same measurement except that the Scorpion does a calibrated power sweep. The second option is to do power sweeps at various specified frequencies. The instrument then automatically looks for the 1dB compression point at each frequency. The measurement output is the input and output powers at the 1dB compression point for each frequency. An example of this measurement is shown in Figure 3.11.

The measurements were done without source calibration but with full two port calibration. The specified accuracy for this measurement and the calibration used is:

- Source Accuracy ($< \pm 0.5$dB)
- Receiver Accuracy ($< \pm 0.1$dB)
  = Total Uncertainty ($\leq \pm 0.6$dB)

The next section compares data from the different measurement techniques including the Scorpion data and measurements done with the Agilent 436 power meter.

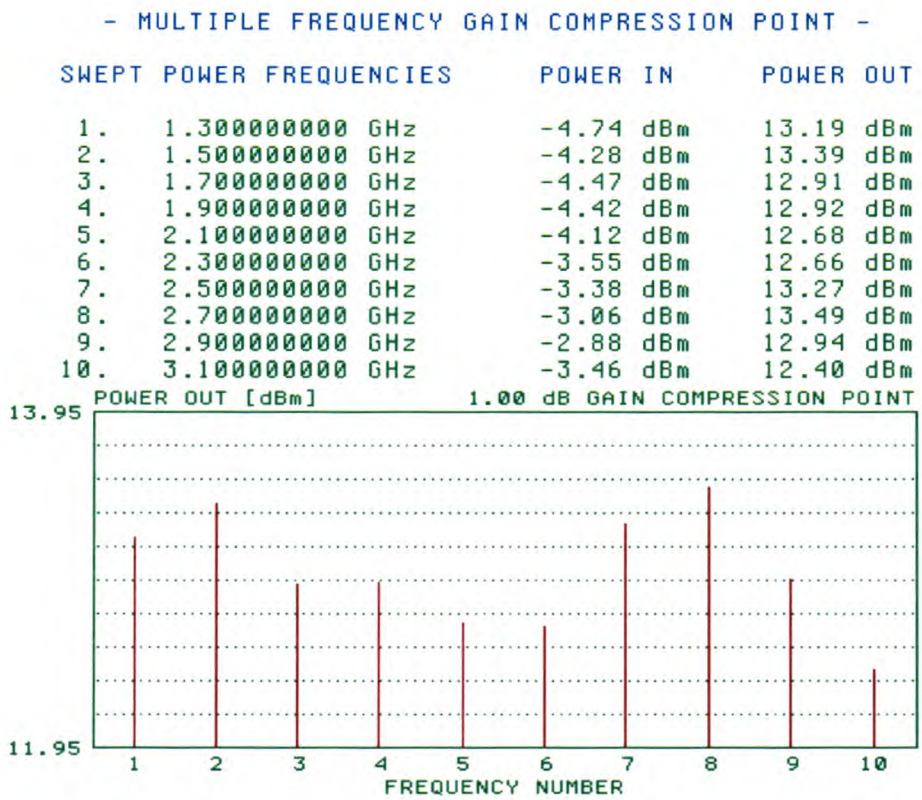


Figure 3.11 This figure shows a screen grab from the Scorpion measurement system for the multiple frequency 1dB compression measurement. The measurement was done for the ERA33.

### 3.1.1.4 Measurement Comparison

To compare the different measurement machines and techniques, measurements for the two amplifiers were done at two different frequencies. A one tone power sweep was done at 2.3 GHz for the ERA33 and at 1.9 GHz for the ERA6. The measurement was repeated as closely as possible with each instrument. This experiment was done to determine the accuracy of the various methods. The greatest accuracy was expected from the power meter and Scorpion measurements. Nevertheless it is important to remember that the power meter measurement will include the total power including the power in the harmonic tones. In most cases the effects of the harmonics were negligible. In other cases filtering the input tone can remove the harmonics. Harmonic levels of more than 35dBc below the fundamental was considered to be negligible.

The input power versus output power plot for the ERA 33 measurements is displayed in Figure 3.12. At this frequency and power level the SA is in very good agreement with both the power meter and Scorpion measurements. The accuracy for the 1dB compression point is within 0.3dB

for the different instruments. In the linear region all the techniques are very close to the small signal VNA measurement. The swept power VNA measurement starts to make significant errors as the amplifier goes into compression while all the other methods remain in good agreement.

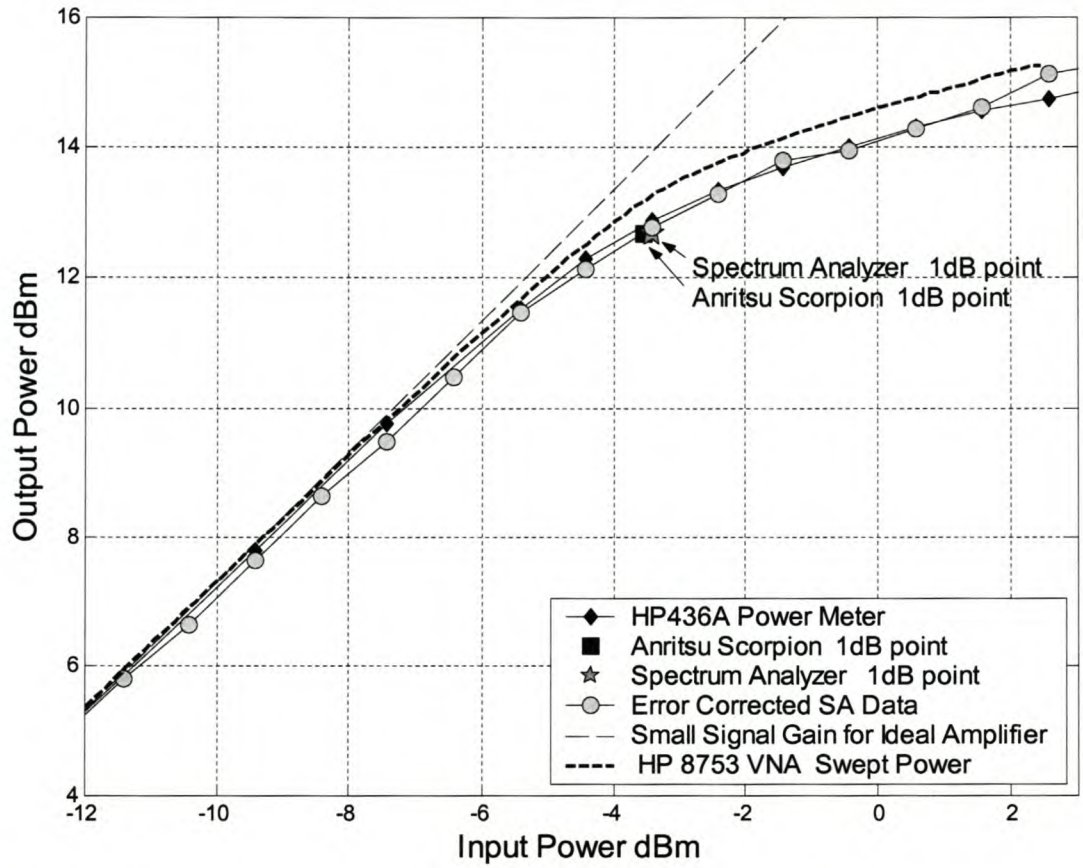


Figure 3.12 There is excellent correlation between the spectrum analyzer, power meter and Scorpion measurements but the VNA deviates from these in the compression region.

The same measurement was repeated with the NNMS at the K.U. Leauven. For this measurement the specific ERA33 amplifier was shipped and measured there and the data was returned to Stellenbosch. In Figure 3.13 the result of this measurement is compared to power meter and spectrum analyzer measurements.

From this comparison it can be seen that the NNMS data matches the power meter and spectrum analyzer measurements very well. This accurate match of the same measurement performed by different machines and people in different laboratories serve as an excellent confirmation of the accuracy of these measurements. Additionally to the accurate nonlinear measurement of the fundamental input/output power transfer characteristics, the NNMS also measured the various harmonics produced in the setup. The data also includes the phase of each harmonic. This was however not compared to any other measurement instrument since this ability is unique to the NNMS system.

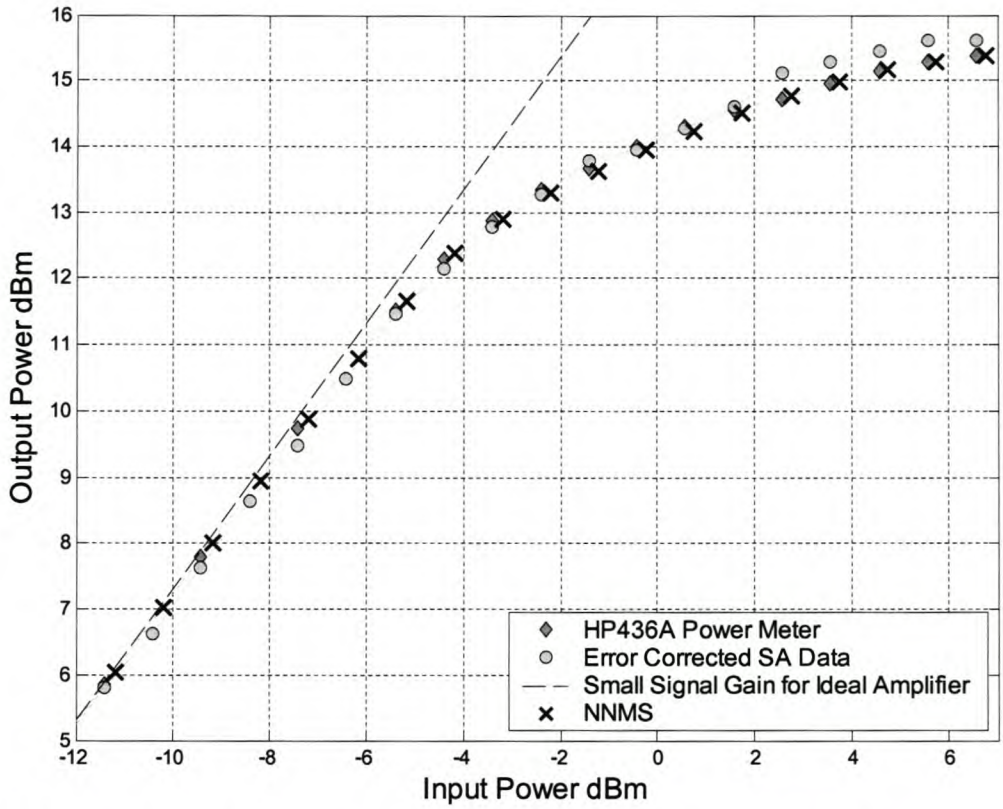


Figure 3.13 This figure compares the power meter and spectrum analyzer measurements with a measurement performed with the NNMS

For the ERA 6 measurement the gain versus output power is displayed in Figure 3.14. From Figure 3.14 it can again be seen that all the techniques match the small signal VNA measurement closely in the linear region. The deviation is never more than 0.25dB but mostly it is much less. However, for this case both the SA and VNA make larger errors in the compression region while the power meter and Scorpion measurements match very closely. The spectrum analyzer measurement deviates considerably from the other measurements in the region between 11dBm and 14dBm output power. The spectrum analyzer error correction described in chapter 2 assumes that the signal generator error is negligible. However the error for the Rohde&Schwarz SMIQ, shown in Figure 2.13, is considerably larger in the region between 1dBm and 4dBm output power. Bearing in mind the ERA6 has a gain of approximately 11dB this will result in the input to the spectrum analyzer being between 12dBm and 15dBm which is the power range where the error in Figure 3.13 is the largest. The unusually large error in this measurement is a result of the larger than expected signal generator error between 1dB and 4dB that is not taken into account when error correction is done. The power levels that are necessary to drive the ERA 6 into saturation are on the edge of the capabilities of this measurement setup. Nevertheless the 1dB compression point matches the power meter and Scorpion measurements well. The spectrum analyzer data also matches the power meter data for measurements further into the compression region up to the saturation point. For the measurement in Figure 3.13 the error in the saturation region is 0.22dB.

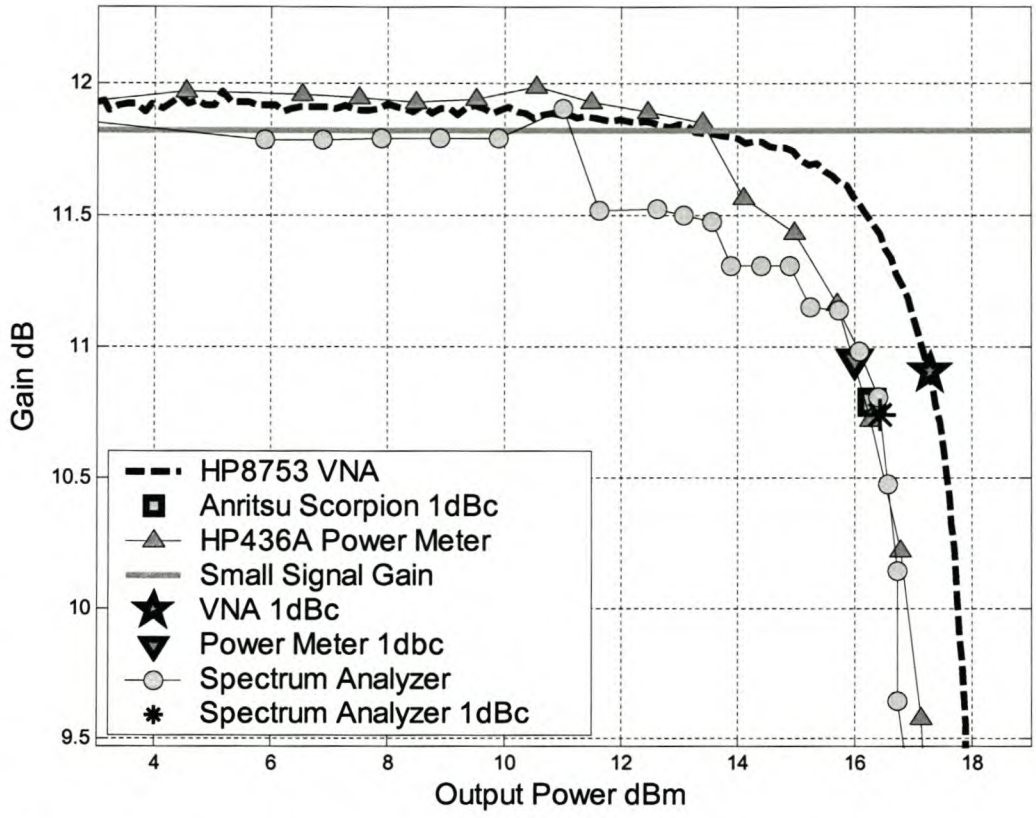


Figure 3.14 Gain versus output power for the ERA6 is shown in this figure. The 1dB compression points for the spectrum analyzer, power meter and Scorpion measurements compare very well. It can be seen that the spectrum analyzer measurement has a large error in the region between 11dBm and 15 dBm. This is caused by the signal generator that has an unusually large error in the input power region corresponding to these output powers.

These comparisons showed that the spectrum analyzer and Scorpion measurements, although they can not produce phase information, are accurate and repeatable if they are compared to the power meter measurement. Because they are the only two techniques that give a practical solution for doing large sweeps, they are compared to each other in Figure 3.15. This figure compares the gain and output power for the two measurement instruments at the 1dB compression point over a frequency range. The figure also shows the small signal gain so that the accuracy of the gain at the 1dB gain compression point can be evaluated. From this figure it can be seen that both instruments match the compressed gain (small signal gain – 1) closely. The output power at the 1dB compression point is also shown to match reasonably well for the two instruments. The maximum difference between the two is 0.5dB at 2.2GHz.

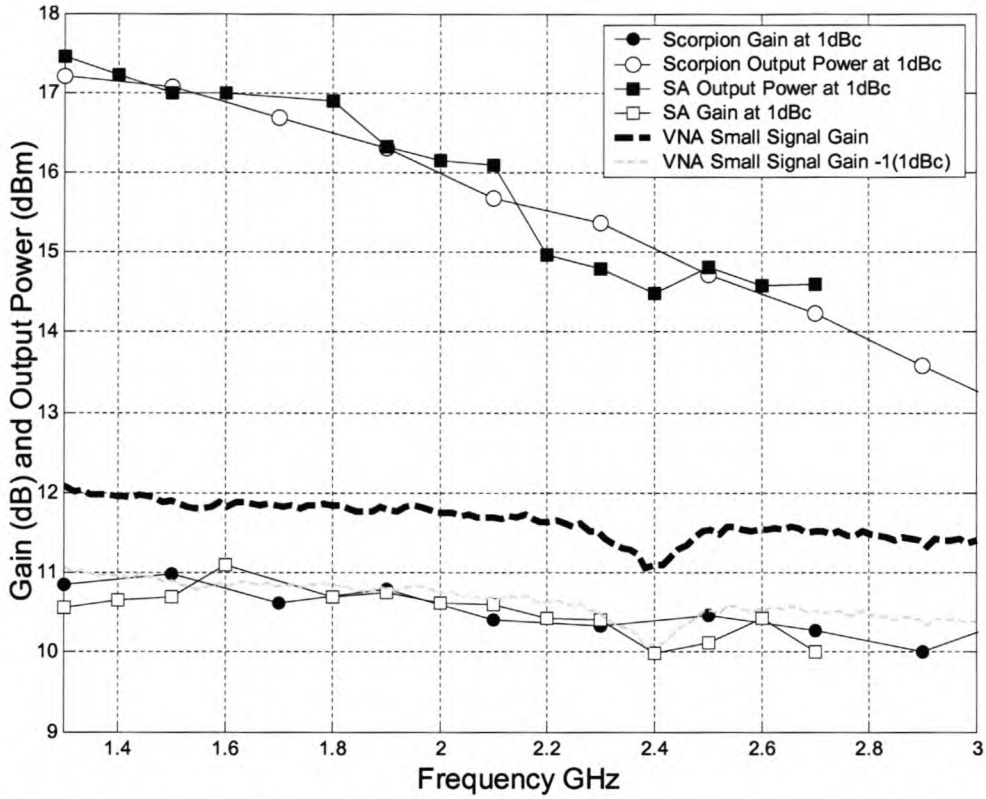


Figure 3.15 Both gain and output power at the 1dB compression point for the ERA6 are shown in this figure. The small signal gain versus frequency, as measured with the VNA, is also included to determine the accuracy of the 1dB gain compression.

From the many comparisons in this section the spectrum analyzer was seen to give reliable results for gain compression. The accuracy is significantly enhanced by the error correction and the repeatability of the measurements is high. It also gives reliable data well into the saturation region which the VNA measurement does not. The results were used to create models for system level simulation which will be described in section 3.2. The following section describes two-tone measurements on amplifiers.

### 3.1.2 Intermodulation Distortion in Amplifiers

Intermodulation distortion (IMD) is a term used to describe signals that are generated from the nonlinear transfer function of a device under the condition of two or more input tones at different frequencies that are not harmonically related. In amplifiers this is normally quantified with a figure of merit called the third-order-intercept (IP3 or TOI) for two input tones. This section starts by describing intermodulation distortion in amplifiers including the TOI. It continues to discuss techniques for measuring IMD and concludes with results of measurements for the ERA33 and ERA6.

### 3.1.2.1 Two-Tone Intermodulation Distortion and TOI

Intermodulation in amplifiers normally refers to two-tone intermodulation. In chapter 1 the response of a general third order nonlinear transfer function was expanded for the case of a two-tone excitation. This however assumes that a third order power series is adequate in describing the amplifiers transfer function. For most small signal amplifiers this is usually the case. Keeping with this assumption and substituting a two-tone input signal equation (3.1) into a third order nonlinearity equation (3.2)

$$Vin = V_1 \cos(\omega_1 t) + V_2 \cos(\omega_2 t) \qquad 3.1$$

$$I = aVin + bVin^2 + cVin^3 \qquad 3.2$$

will produce the output response in equations (1.3a) to (1.3c) in chapter 1. A closer examination of the frequencies that are generated by this process shows that they are a result of linear combination of the two excitation frequencies $\omega_1$ and $\omega_2$. A third order transfer function under two-tone excitation will yield output products at the following frequencies:

$$\omega_{M,N} = \left| \pm M\omega_1 \pm N\omega_2 \right| \qquad 3.3$$

for M and N any integer values 0, 1, 2, 3... and $\omega_1$ and $\omega_2$ not harmonically related. The order of a given intermodulation product is defined as |M| + |N|. Figure 3.16 shows the output spectrum of a third order amplifier with two input tones at $\omega_1$ and $\omega_2$. The figure includes only second and third order intermodulation products.

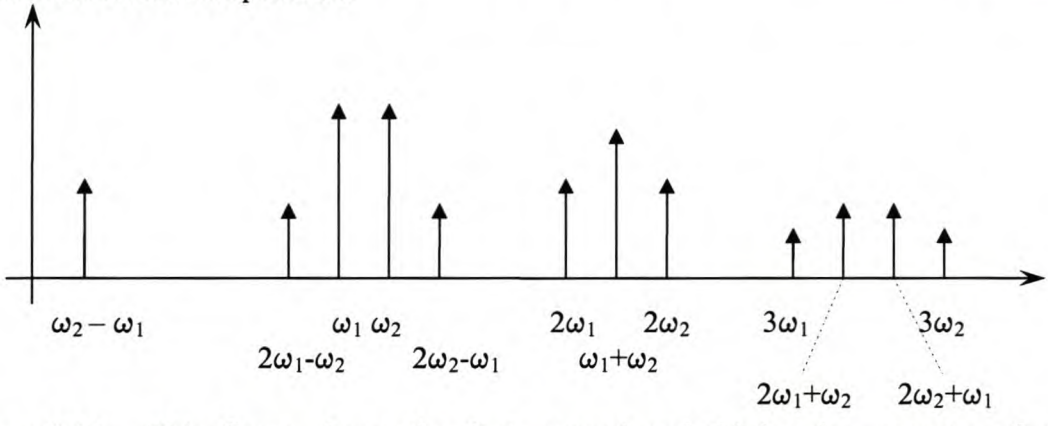


Figure 3.16 This figure shows the first, second and third order response of an amplifier described by the third order nonlinear transfer function represented by equation (3.2).

Normally in amplifiers the two frequencies $\omega_1$ and $\omega_2$ are closely spaced relative to their respective RF frequencies. The size of intermodulation products is also related to the order of the product with amplitude decreasing as the order increases. Even though this is the case the second order products are located far from $\omega_1$ and $\omega_2$ at $2\omega_1$, $2\omega_2$, $\omega_2 - \omega_1$ and $\omega_1 + \omega_2$ and are typically not a problem in most receiver systems. The third order products are located at the following frequencies $3\omega_1$, $3\omega_2$, $2\omega_2 + \omega_1$, $2\omega_1 + \omega_2$, $2\omega_2 - \omega_1$and $2\omega_1 - \omega_2$. From Figure 3.16 it is clear that the first four frequencies are also far removed from $\omega_1$ and $\omega_2$ at frequencies even higher than the second order

products. However the last two are very close to $\omega_1$ and $\omega_2$. These two in-band intermodulation responses may cause distortion in a system. The distortion caused by these third order products is called third order intermodulation distortion. Although it is possible that higher order responses ($5^{th}$, $7^{th}$ etc) may also add in band distortion, third order IMD is the most troublesome. It should also be noted that the response at the frequencies $2\omega_2 - \omega_1$and $2\omega_1 - \omega_2$ may also include higher order responses at this frequency that simply add to the effect.

The most common way to specify third order intermodulation is by a figure of merit called the third order intercept point (IP3 or TOI). It is the point where the third order intermodulation output power is at the same power level as the fundamental output tones. Since power saturation occurs, the intercept point cannot be measured directly. TOI is taken as the intercept of the two extrapolated power curves under the assumption that in a weak nonlinear third order system, the third order intermodulation products change by 3 dB for each dB change in the input power. This also assumes that the system has no memory. Figure 3.17 illustrates this definition of the TOI figure of merit. The utility of the TOI number is in comparing and quantifying the linear performance of amplifiers. In addition the relative suppression of a third order product to the fundamental power level can be calculated easily at a desired output power level (assuming the power level is in the linear region of the circuit).

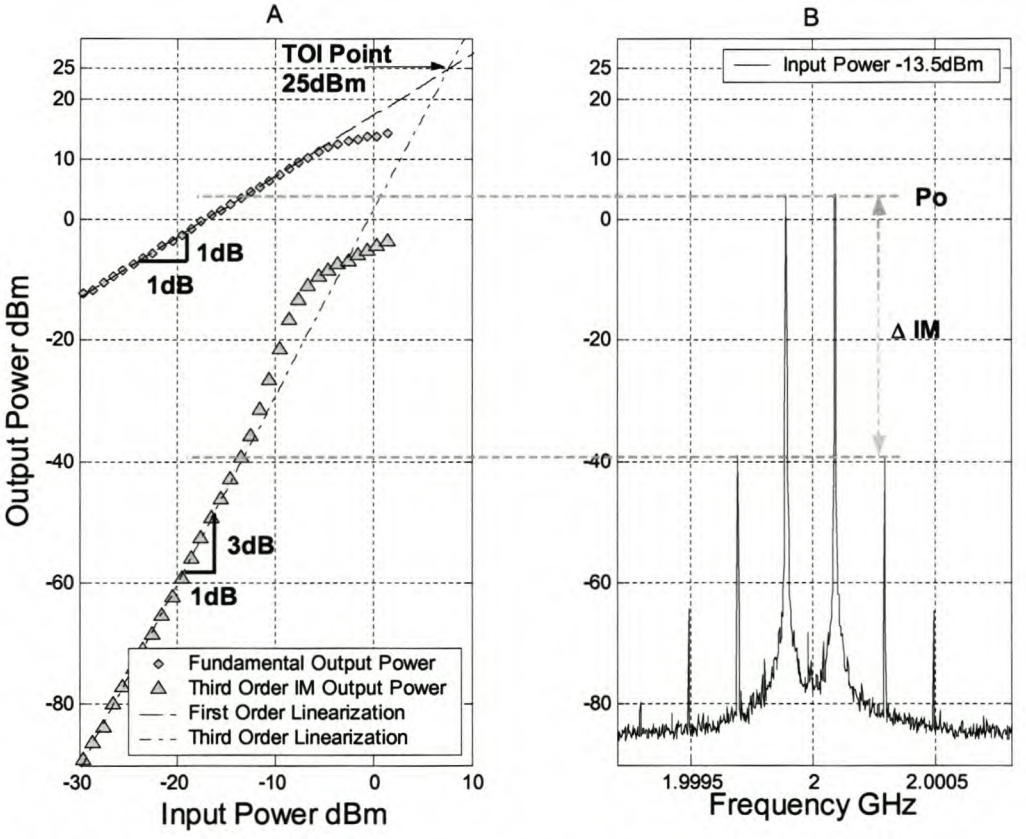


Figure 3.17 This figure shows the input versus output power curves as well as the output tones versus frequency for the case of -13.5dBm input power. In part B the $5^{th}$ and $7^{th}$ order intermodulation products can be seen. From this figure the link between the swept power measurement and the output spectrum for a certain input power can be seen. The TOI is taken as the output power where the fundamental curve and the third order intermodulation curve intersect.

From Figure 3.17 it can be seen that linear extrapolations of the fundamental output curve and the third order intermodulation curve intersect at 25dB output power. The TOI can also be calculated from the power versus frequency graph with the following equation:

$$TOI(IP3) = Po + \frac{\Delta IM}{2} \qquad 3.4$$

For the case in Figure 3.16B this will give a value for TOI = 25.125dBm. This value compares very well with the value obtained by the graphical linearization method. However, each point in the power sweep will give a different answer for the TOI from this equation. In the linear region the values calculated should all be the same as the TOI from the graphical technique in Figure3.16A. However measurement uncertainty may cause a TOI value calculated at a specific power to be different from the graphical value. There are many aspects to consider when doing IMD measurements and calculating TOI. The next section describes the measurement setup and sources of error that may cause problems. Section 3.1.2.3 describes a MATLAB procedure that automates the process for swept power IMD measurement as well as a procedure to accurately calculate TOI. Measurement results are discussed in section 3.1.2.4.

### 3.1.2.2 Intermodulation Measurement Setup

Measuring intermodulation requires a test setup that can deliver two closely spaced tones of equal amplitude at the DUT input port. This requires two signal sources and a device to combine the two signals. The preferred method for combining the two signal generator outputs is to use a resistive power combiner. A resistive combiner has the advantages of being well-matched at all three ports and presents a constant, power-independent impedance to both of the signal sources as well as the device under test. In addition, a resistive combiner is frequency insensitive (broadband) and being virtually completely linear, creates no intermodulation products of its own. One of the most important considerations in making intermodulation measurements is to provide adequate isolation between the two signal generators. If the two signal generators are not well isolated from one another, their circuits can interact in such a way as to produce excessive intermodulation products not related to the DUT. The isolation is achieved with a combination of attenuators and low pass filters. The test setup is shown in Figure 3.18.

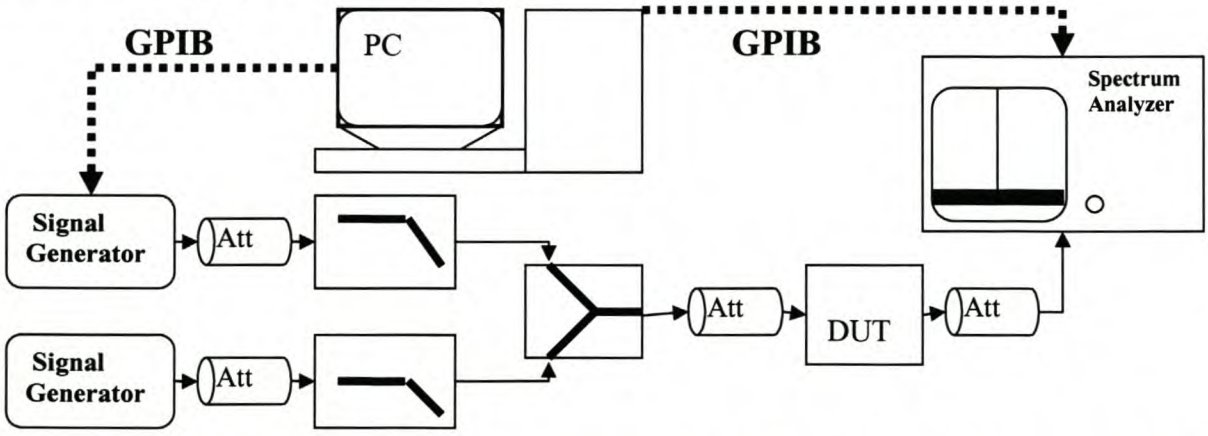


Figure 3.18 This figure shows the measurement setup for two-tone intermodulation measurements. The signal sources and spectrum analyzer are controlled by a PC through GPIB.

Another technique to increase the isolation between the signal sources is to replace the attenuator/filter combination in Figure 3.18 with ferrite isolators. This may in some cases give superior isolation but is normally a narrowband solution and also much more expensive. This will present a problem if measurements at various frequencies are to be done.

The accuracy and reliability of the measurements done with this test setup can be influenced by the following [21, 22]:

- Intermodulation and distortion caused by the measurement instruments. Both the signal generators and the spectrum analyzers may cause intermodulation.
- The loss in the two signal paths as a result of the cables, attenuators, power combiner and filters influences the measurement. The important power levels are the powers at the DUT input and output ports.
- The two signal sources and signal paths may not be symmetrical resulting in two non-equal signals at the DUT input port.
- Repeatability and accuracy of the spectrum analyzer measurement will introduce errors.

These sources of error are discussed in the following paragraphs. For the purpose of illustration, the test setup that was used for most of the measurements is shown in Figure 3.19 for the part of the setup up to the DUT input port. The attenuator at the output port depends on the DUT. It is only necessary if the DUT is poorly matched at the output port or if the output power is very large. The measurement results used to describe the important aspects of the two-tone test setup in the following paragraphs is for the components in Figure 3.19.

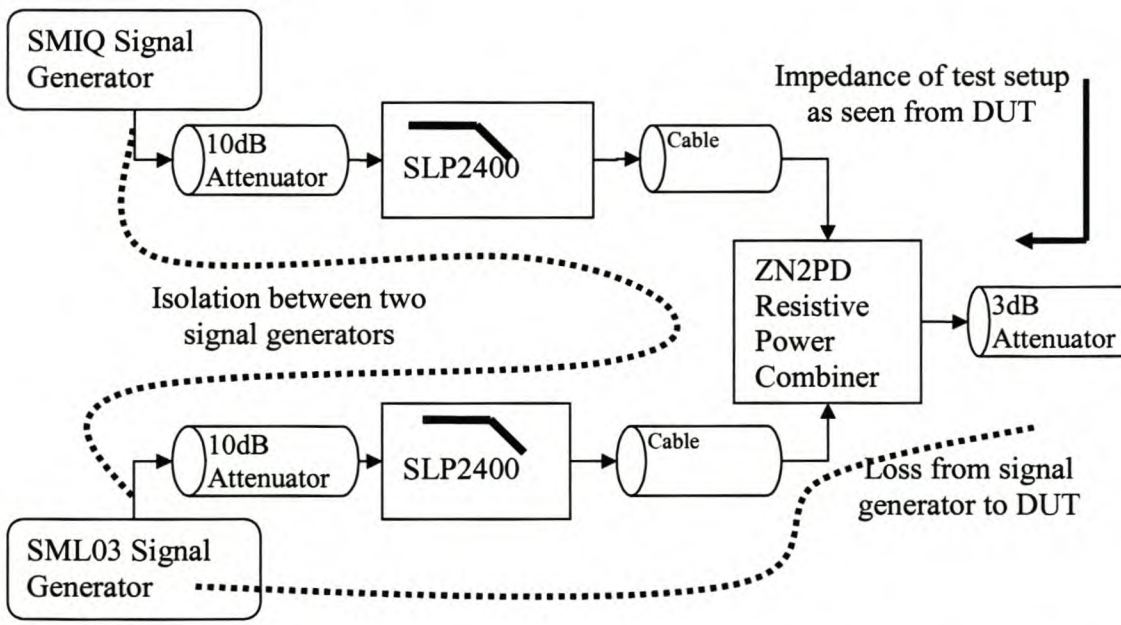


Figure 3.19 This is a typical combination of attenuators, filters and power combiner used to produce a clean two-tone signal at the DUT input port. The isolation between signal generators and the loss from signal generator to the DUT is shown with dotted lines. The impedance as seen from the DUT is also indicated.

Adequate isolation between the two sources is very important. If the isolation is not enough, signals may leak into the signal generator output ports. The signal generator's ALC circuitry may cause intermodulation in such a situation. Isolation between signal sources is therefore one of the most important aspects of intermodulation measurements. For the example in Figure 3.19 this is achieved by the combination of 10dB attenuators, lowpass filters ($f_c$ = 2.4GHz) and a power combiner. Choosing the right power combiner is also important to ensure good isolation. Figure 3.20 shows the isolation with attenuators and filters and without for the ZN2PD resistive combiner.

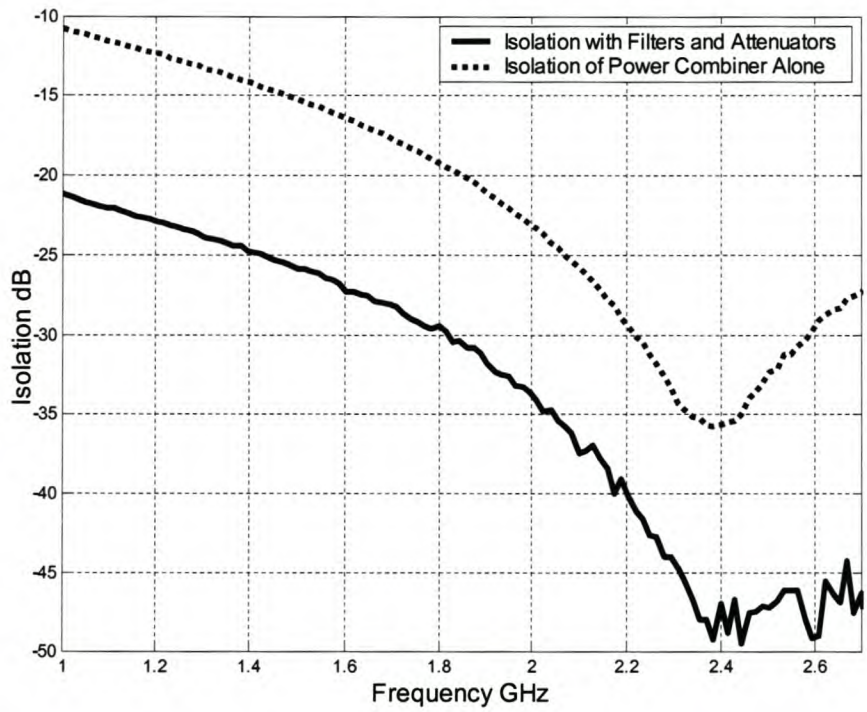


Figure 3.20 The isolation between the two signal generators in Figure 3.18 is shown for two cases. It can be seen that the power combiner (Mini-Circuits ZN2PD) already has excellent isolation around 2.4GHz. However the isolation is greatly improved by adding the attenuators and filters. With the setup of Figure 3.19 the isolation is more than 20dB over the entire bandwidth in this figure.

From the figure it can be seen that the isolation between the two signal generators is larger than 20dB for all frequencies between 1GHz and 3GHz.

Although power combiners give good isolation and impedance at the input ports the return loss looking into the sum port may often not be good enough. The attenuator between the power combiner sum port and the DUT is there to reduce this mismatch problem. In the setup of Figure 3.19 a 3dB attenuator is used and the improved return loss looking from the DUT is shown in Figure 3.21. The power combiner was designed to work from 1.5GHz to 3.5GHz. This can be seen in the return loss as well as the isolation. The 3dB attenuator increases the quality of the test setup in regions where the combiner is not at its optimum performance. This reduction of the mismatch between the DUT and power combiner will increase the measurement accuracy.

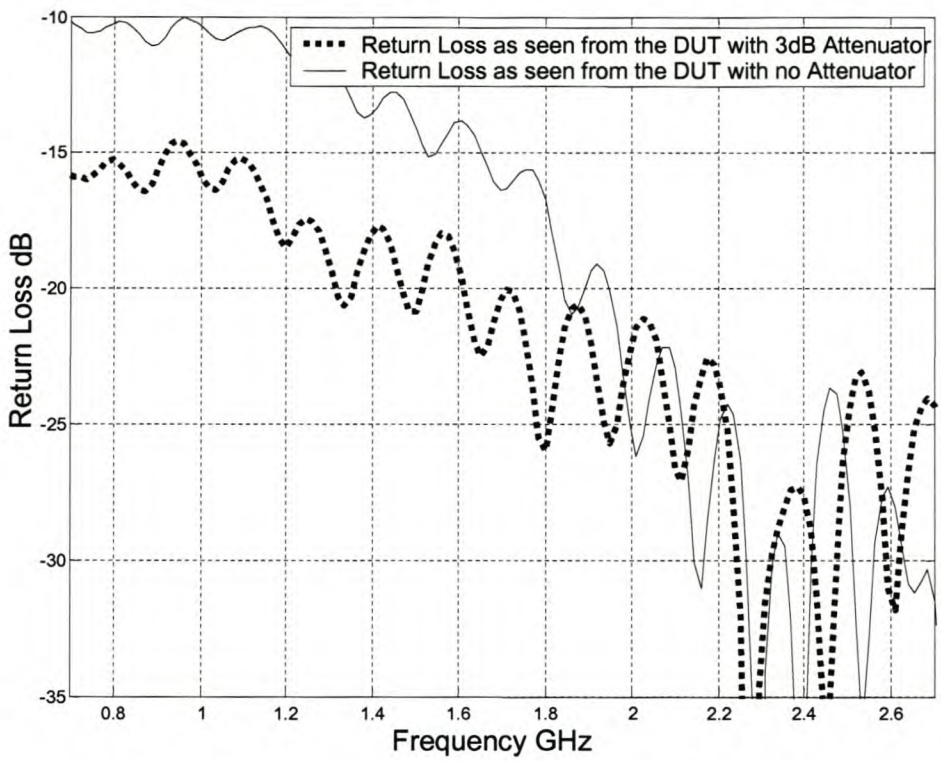


Figure 3.21 The effect of impedance mismatch at the sum port of the power combiner can be reduced by an attenuator. For the case in Figure 3.19 the addition of a 3dB attenuator reduced the return loss seen from the DUT significantly in the region below 1.8GHz.

Another factor that may influence the measurements is the symmetry of the two signal paths up to the DUT input. For example if the attenuator, filter and power combiner path between the SMIQ signal generator and the DUT, and the path from the SML03 signal generator to the DUT, is not completely identical, the two-tones at the DUT will have different amplitudes. This will happen even if the two signal generators produce equal amplitudes to start with. Figure 3.22 shows the loss for the two signal paths in Figure 3.19 from the signal generator output ports up to the DUT input. It can be seen that the loss for the alternate signal paths are very closely matched in the passband. However the cut-off frequencies of the two filters show a clear difference. It is possible to compensate for non-symmetrical signal paths by adjusting the signal generators output power. If the difference in attenuation between the signals paths is *x*dB, the signal generator for the path with the *x*dB larger attenuation must produce a signal that is *x*dB larger than the other signal generator. In this way the power level of the two tones at the DUT input port can be equal.

If the setup is used in the region where the two signal paths are closely matched the effect is very small. However, in addition to this, the two signal generators do not produce exactly equal amplitudes. The cumulative error may be quite large in some cases. The measurement algorithm described in the next section compensates for non-symmetrical systems.

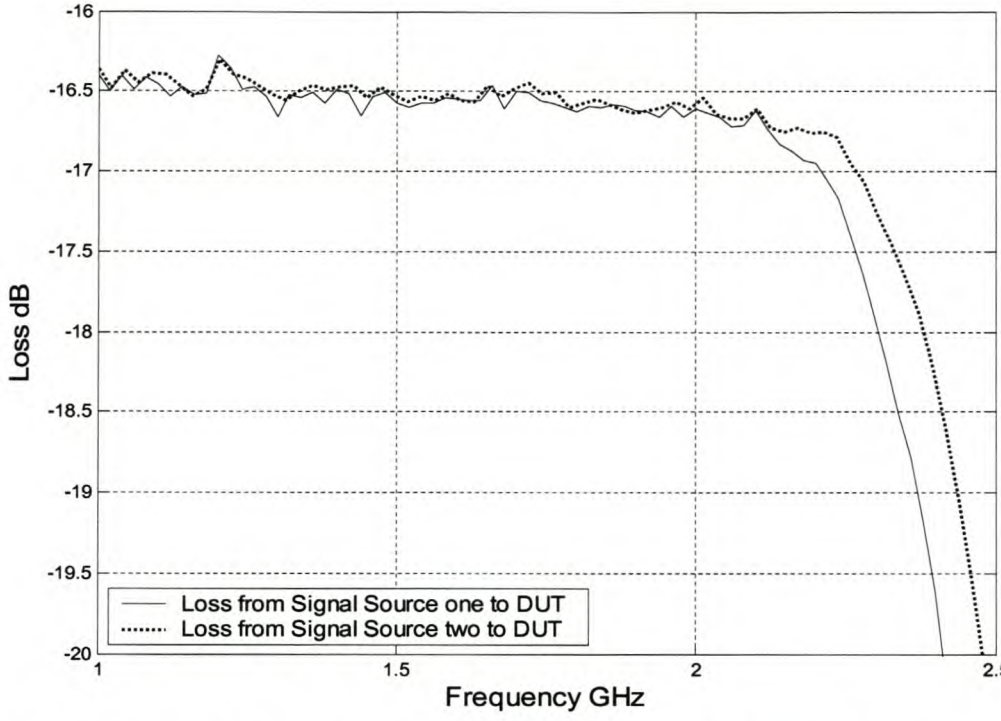


Figure 3.22 The setup in Figure 3.18 is highly symmetrical in the passband.

The final source of error is the problems introduced by the measurement instruments. In chapter two issues concerning the spectrum analyzer accuracy were discussed in detail. There is however one practical problem that is present for intermodulation measurements. In many cases intermodulation products are very small. The spectrum analyzer dynamic range is therefore very important. Optimizing measurement speed and dynamic range is also discussed in the next section as it forms an integral part of the measurement algorithm. It is also necessary to correct the measurements for the loss in the system. This is done in the same way as for the compression measurements and is discussed in the next section. The loss in the system may also introduce a problem concerning the signal generators maximum output power. As seen in Figure 3.22 the loss is in the range of 16.5dB for a setup like the one shown in Figure 3.19. Depending on the DUT it may be impossible to produce input tones with adequate amplitude at the DUT input port because of this loss. The loss can be reduced at the price of less isolation between the sources by using smaller attenuators.

The different factors mentioned above can make it difficult to design a test setup for intermodulation measurements. Figure 3.23 shows the final results of the various important characteristics for the setup in Figure 3.19. The setup will produce excellent measurements in the region between 1.6GHz and 2.4GHz. In this region the signal paths are highly symmetrical. The isolation is larger than 27dB and the return loss as seen from the DUT is less than -20dB. The setup can be changed by using different filters, combiners and attenuators to suite a specific frequency band.

The measurement algorithm that will be explained in the next section can compensate for the type of error introduced by the filters in the region between 2.2GHz and 2.4GHz.

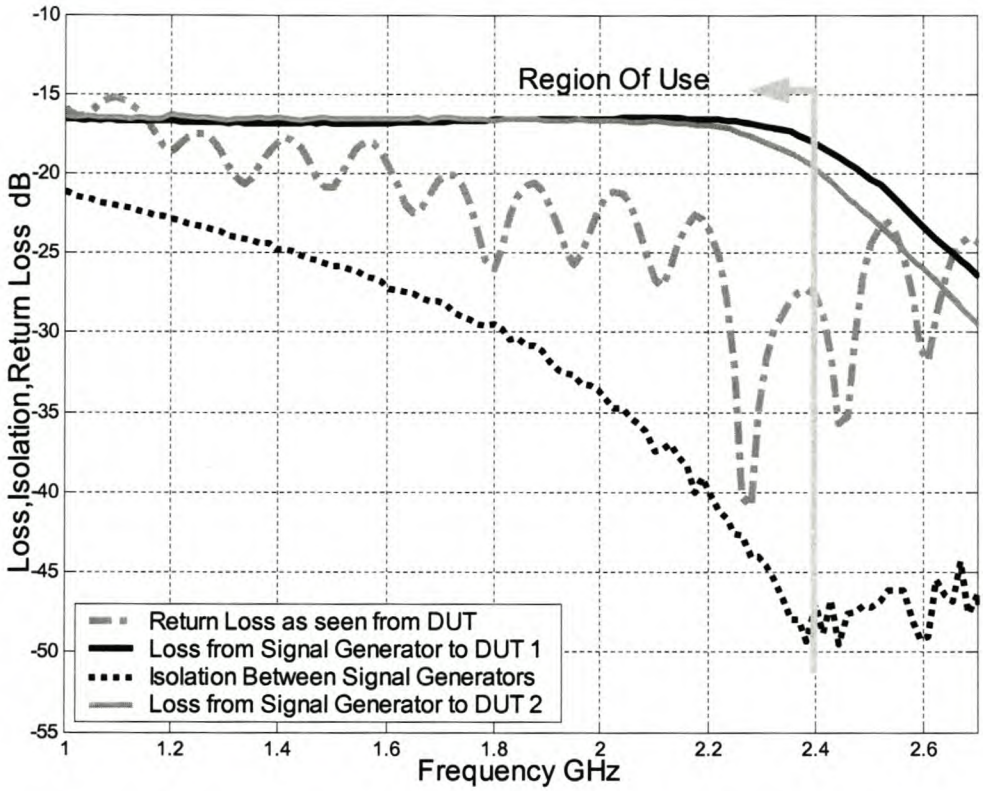


Figure 3.23 The most important aspects of the intermodulation measurement setup are shown in this figure for the setup of Figure 3.19. It shows excellent isolation, return loss and symmetry.

### 3.1.2.3 Measurement Automation and Data Processing

The previous two sections described intermodulation and the important aspects of measuring intermodulation. The concept of TOI and different ways to determine it were also shown. To be able to accurately determine the TOI and also to get additional insight into an amplifier's nonlinear characteristics, swept power two-tone intermodulation measurements are necessary. Such a power sweep introduces many problems considering that each power level and frequency combination will require adjustments of the signal generators and spectrum analyzer resulting in a time consuming operation. The measurement setup also introduces loss and error to the measurements. To enable repeatable and accurate swept power intermodulation measurements requires two steps. The first is the automation of the measurement process through GPIB and MATLAB. The second is to do error correction on the data to remove the effect of the measurement setup. This procedure also calculates the TOI from the data. This section describes the two procedures that were used.

The output data of the measurement procedure is two matrices of the form shown in Figure 3.24. One of the matrices is for first order fundamental response and the other one is for third order intermodulation response. The matrices consist of the output powers for each input power and frequency combination. The matrix output structure makes it easy to do error correction etc.

| | $f_1$ | $f_2$ | .....$f_y$ |
|---|---|---|---|
| $Pin_1$ ⋮ ↓ | $D_{11}$ | $D_{12}$ | $D_{1y}$ |
| $Pin_x$ | $D_{x1}$ | $D_{x2}$ | $D_{xy}$ |

Figure 3.24 This figure shows the structure of the measured output power matrices for both the fundamental and third order intermodulation responses for two-tone measurements. The row index is the input power while the column index is the frequency. The data points are the relevant output power levels.

In this way the procedure can step through a set of frequencies doing a power sweep at each frequency. The measurement procedure was designed to have the following input parameters: frequency array, input power array and the desired tone spacing. The important measurement aspects are all built into a single frequency power sweep procedure that is repeated for each new frequency value in a larger frequency sweep structure. The power sweep procedure is shown in Figure 3.25 and the different steps are explained below.

1. The procedure sets the signal generators to the desired frequencies and power levels to produce the two-tone input. The tones usually do not have equal amplitude because of signal generator errors and the two non-symmetrical signal paths as mentioned in section 3.1.2.2. The procedure turns one signal source off. The remaining source will be the reference source. Its amplitude is measured with the recursive measurement technique described in chapter 2. The reference signal is then switched off and the other signal generator is switched back on. This signal generator's output is adjusted until it matches the reference generators output at the spectrum analyzer reference level. Assuming the amplifiers gain is constant over the narrow band between the two frequencies this will produce two signals of equal amplitude at the DUT input. This assumption is valid if the spacing is small enough. For a tone spacing of 1MHz the difference in gain for the two amplifiers is less than 0.1dB/MHz for frequencies above 200MHz.

2. The next step is to determine the gain. This will be very far from the amplifiers actual gain because of the loss in the setup. The purpose of the gain measurement is to determine when the device is going into compression as a safety measure and therefore the actual gain does not matter. Once more than three measurements have been done the procedure starts to differentiate the output power curve to get the gain versus input power curve. From this the linear region and the compression region can easily be seen. The power sweep is aborted when unacceptable gain compression is observed. Another important function of the gain measurement is to determine the approximate input power to the spectrum analyzer. To do this the loss between the DUT and the spectrum analyzer must be known. If the input power to the spectrum analyzer is too large the internal mixer may produce intermodulation of its own that will be indistinguishable from the DUT's intermodulation. The HP8562 produces third order intermodulation at -105dBm for mixer power levels of -28dBm. The procedure takes this into account and ensures that the power level at the mixer is always below -30dBm. This introduces additional uncertainty as a result of changing the attenuator setting between measurements. However it is necessary to have maximum dynamic range at small input powers and is therefore unavoidable.

3. The intermodulation power level will usually be much smaller than the fundamental. To measure this small signal the procedure zooms in on the frequency where the intermodulation product is expected. For accuracy as well as time reasons the RBW and VBW is initially set to relatively large values. If a signal is found to be more than 6dB above the noise floor, the procedure uses the recursive measurement technique (chapter 2) to do an accurate amplitude measurement at the reference level of this intermodulation signal. If the signal is smaller than this, the RBW and VBW are adjusted to increase the signal to noise ratio by reducing the noise floor. This process is repeated until the signal can be clearly measured or the spectrum analyzer's limits are reached. If a signal is still not found the noise floor is taken as the measured value.

4. The procedure returns to step one and repeats the process for a larger input power until the maximum value is reached or the safety rules are violated.

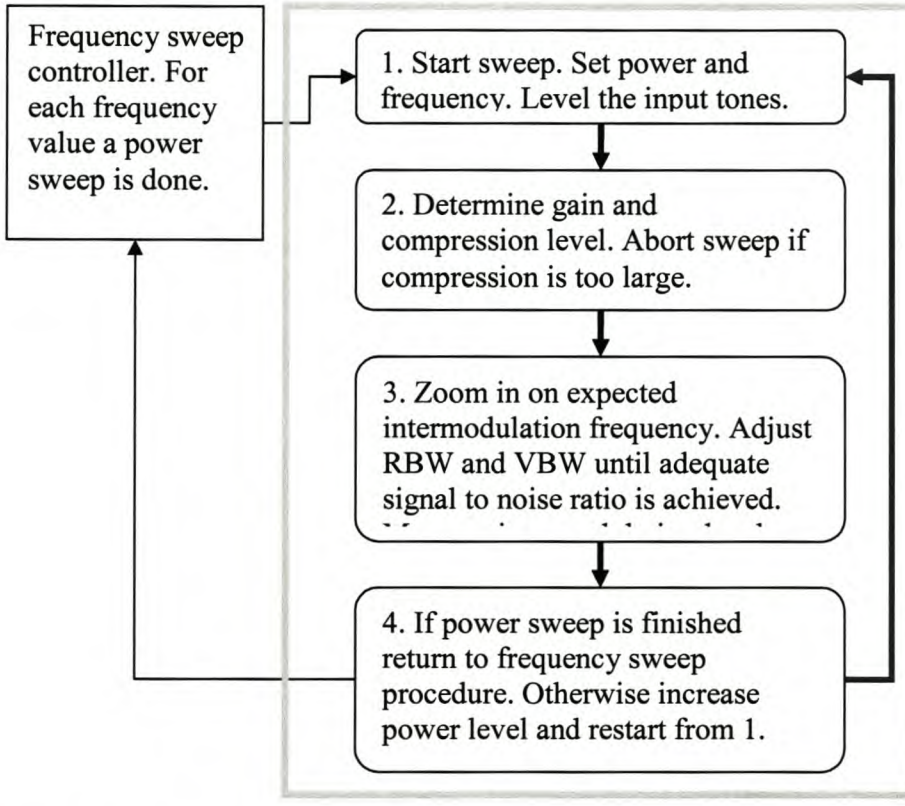


Figure 3.25 This figure shows the basic steps in the procedure used to measure IM. The procedure consists of a power sweep procedure within a frequency sweep loop.

Once the data has been measured, error correction has to be done before the TOI can be calculated. Error correction is done with a procedure that uses the S-parameters of all the components in the test setup to correct for the loss in the signal path. By this method the actual power levels at the DUT ports can be calculated. The procedure operates at one frequency at a time producing the input power array at the DUT input port, the fundamental output power array at the DUT output port and the third order intermodulation output power at the DUT output port. The upper and lower intermodulation products ($2\omega_2$ - $\omega_1$and $2\omega_1$ - $\omega_2$) are measured separately. After the error correction, the procedure implements two methods to determine the TOI point. The first is the

graphical method explained in section 2.1.2.1. This method determines the linear operating region by the same method that was used in section3.1.1.2 to determine the 1dB gain compression point for one tone measurements. In short it differentiates the power curve to get a gain curve. The region where the gain is constant (within limits to compensate for measurement error) is taken as the linear region. A straight line is fitted to the linear region to extrapolate the gain in the linear region. The same is done for the intermodulation measurements. The third order intermodulation power curve often starts to deviate from a straight line before the fundamental goes into compression. Therefore the process has to be repeated for both curves. The TOI is the output power where the two extrapolated straight lines intersect. The second method is to calculate the TOI from equation (3.4). Results of the two techniques are discussed in the next section along with measurements.

### 3.1.2.4 Measurement Results

Measurements of intermodulation were done with two instruments namely the HP8562 spectrum analyzer and the Anritsu Scorpion. Figure 3.26 is a spectrum analyzer measurement of intermodulation at 2GHz. The tone spacing for all measurements is 1MHz. This figure shows the third, fifth and seventh order intermodulation resulting from the two-tone input. It is important to note that the upper and lower intermodulation responses are not equal in amplitude. Another aspect that can be seen in this measurement is the effect of the reference spurs on the measurement. The SML03 signal generator (left input tone) has reference spurs at -75dBc at 100KHz from the carrier. If intermodulation measurements were done for tone spacing in this range (KHz) these spurs will influence the measurement.

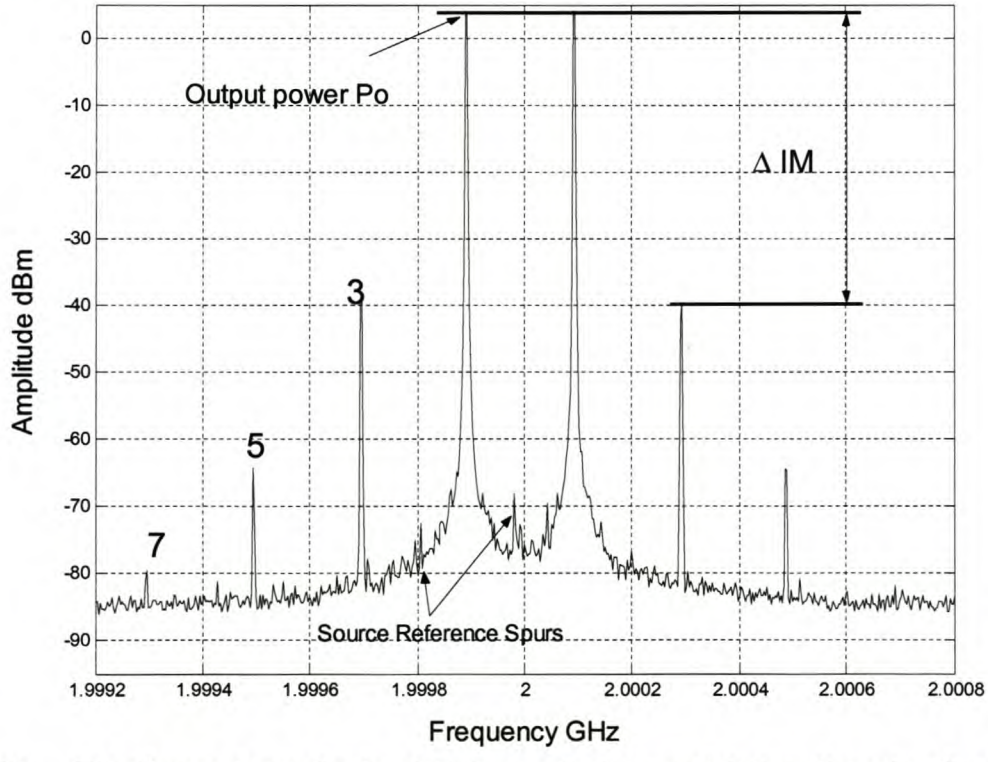


Figure 3.26 This figure shows third and higher order intermodulation distortion for the ERA33 amplifier at 2GHz with a tone spacing of 1MHz. It is important to notice that the upper and lower intermodulation tones are not exactly equal in amplitude.

Figure 3.27 and Figure 3.28 are the result of swept power intermodulation measurements. The setup of Figure 3.19 was used and error correction was done. The TOI points for both amplifiers are also shown in the figures. The result for the two-tone power sweep at 2.3GHz for the ERA33 is shown in Figure 3.27. The two methods for determining the TOI point discussed in the previous section can be compared in this figure. The figure also shows the linear region of the device. It is important to notice that the third order intermodulation curve deviates from the linear assumption at -13dBm input power while the fundamental curve goes into compression at -5dBm. This must be taken into account for the graphical method as discussed in (section 3.1.2.3).

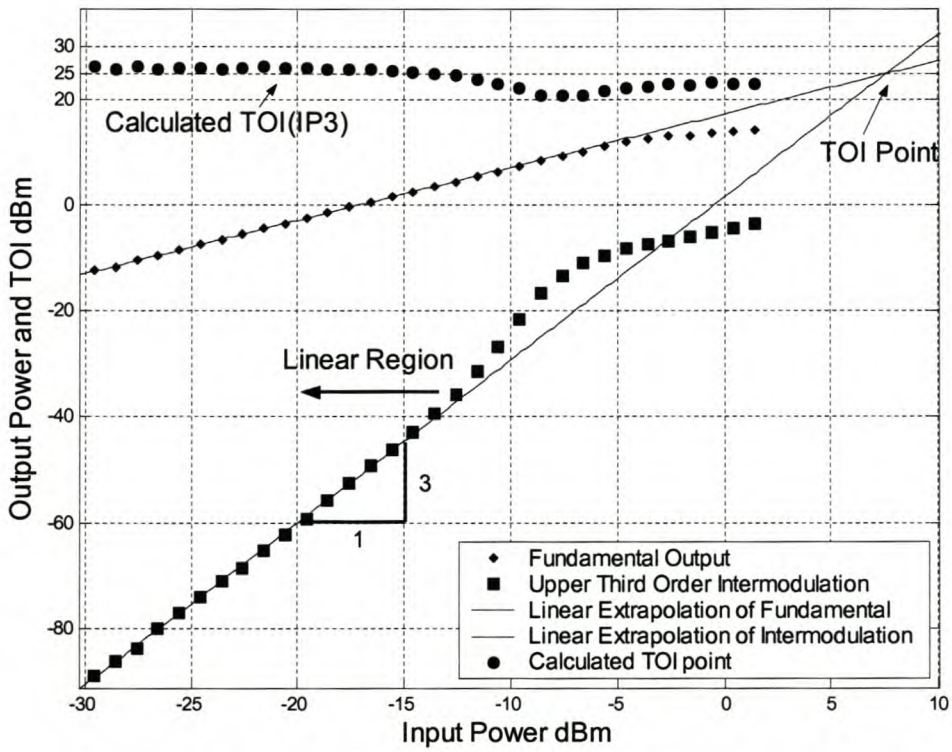


Figure 3.27 The fundamental output curve as well as the output power versus input power of the upper third order intermodulation tone ($2\omega_2 - \omega_1$) is shown. The figure shows the linear extrapolation of the two curves intersecting in the TOI point. The calculated values for IP3 agree well with the result from the graphical method. It can be seen that the assumption that the intermodulation will increase by 3dB for each 1dB increase in input power is only valid in the linear region.

The two methods are strongly matched in the linear region of the third order response and both give a TOI of 25.3dBm. However, the calculated value obviously deviates from this from -12.5dBm input power up. At this point the output versus input power relationship no longer adheres to the 3dB to 1dB assumption for a third order system. The linearization technique is built on this assumption and was implemented to work in the linear region only. It will therefore not give the same results as the equation that was implemented over the whole input power range. However the TOI is defined as a parameter that describes the non-linear behavior of a device in the region where the third order assumption is valid, and therefore the values obtained in this region are the correct values. The datasheet value for TOI is 27dBm for the ERA 33 at 2GHz.

Figure 3.28 shows the results for the same measurement for the ERA6 at 1GHz. The ERA 6 has a higher IP3 value of 36dBm at this frequency. However the figure will show that the linear extrapolation method gives a value of only 30dBm. The figure also shows that the calculated values for TOI changes with the input power from about 38dBm to 34dBm for input power values in the linear region.

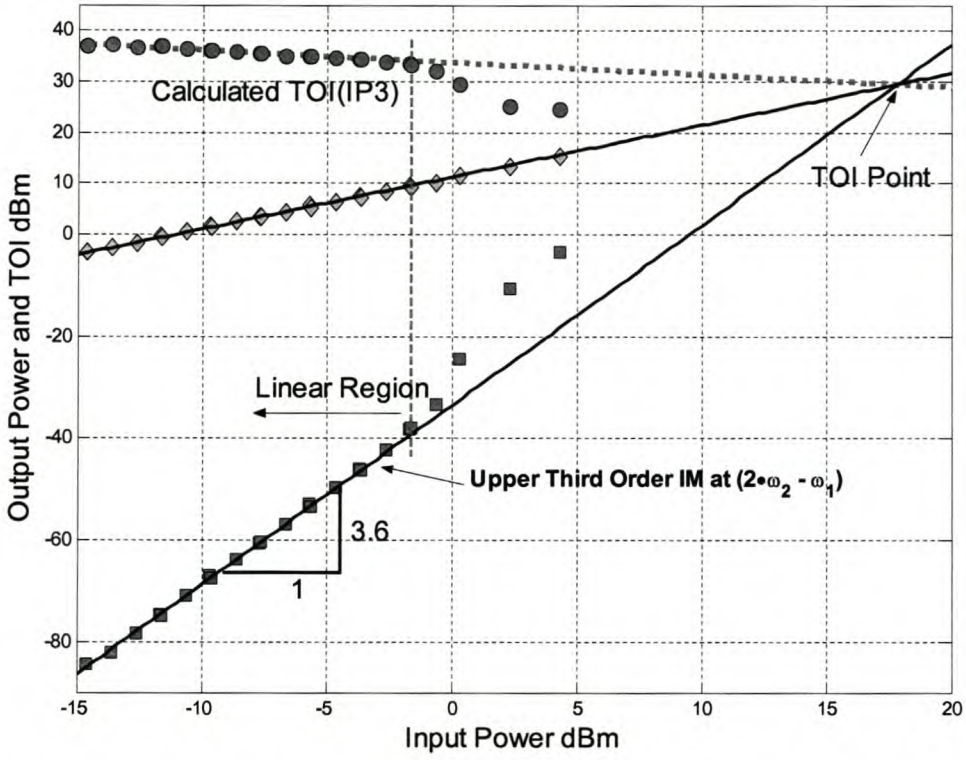


Figure 3.28 The fundamental output curve as well as the output power versus input power of the upper third order intermodulation tone ($2\omega_2$ - $\omega_1$) is shown. The figure shows the linear extrapolation of the two curves intersecting in the TOI point. It can be seen that the ERA6 does not adhere to the assumption of a third order system with the slope of the third order intermodulation being 3.6dB to 1dB instead of the required 3dB to 1dB relationship.

The ERA6 does not adhere to the third order assumption. Because of this the linearization technique gives poor results because it effectively uses the average of the various points in the linear region which has in a 3.6dB to 1dB relationship. Calculating the TOI point by point with the equation gives a local value for TOI at that point. The datasheet value of 36dBm was probably calculated by this method for an input value in the range of -10dBm. Notice that the level of the third order intermodulation increases significantly long before the compression region is reached.

The Scorpion measurement system has two sources and is therefore capable of doing two-tone measurements. The setup for the Scorpion intermodulation measurements is basically the same as for the spectrum analyzer and signal generator case except that all the instruments are in the same box. The isolation and combining of the two signals is exactly the same as for the case in Figure 3.19. The Scorpion system has the ability to give the power level of the third order intermodulation

in dBc relative to the fundamental output power. From this the TOI can be calculated. This measurement technique gives the output power level in dBc over frequency for a specific input power level. The two instruments are compared in Figure 3.29. The measurement was repeated for the same input power and external components (filters, combiner etc.) for both instruments. From the results it can be seen that the spectrum analyzer setup matches the Scorpion system closely over the frequency band. The input power at the DUT input port was in the range of -14dBm which is well in the linear region.

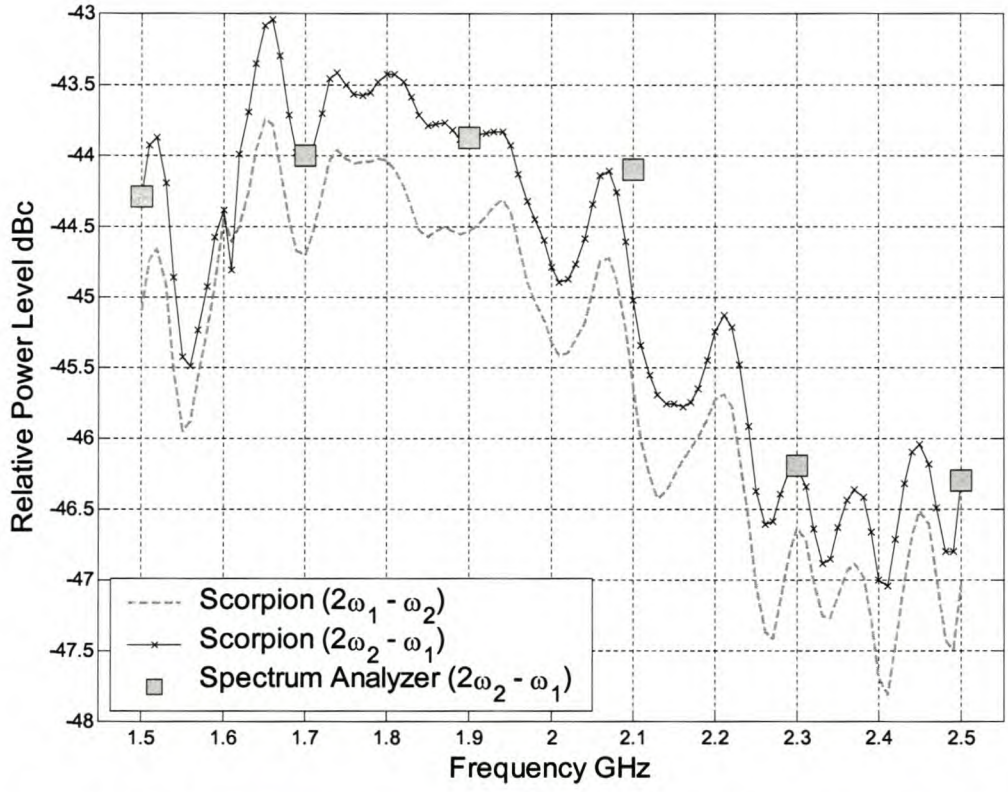


Figure 3.29 This figure compares the spectrum analyzer two-tone setup with the Scorpion measurement system. The third order IM's relative power level to the fundamental output power is shown in dBc. It can be seen that the result are in excellent agreement. Also note that the upper and lower intermodulation products are not equal.

### 3.1.3 Conclusion

This section described the important issues regarding intermodulation and compression that may occur in a nonlinear system. Both the 1dBc and the TOI figures of merit were explained. The necessary steps and precautions to measure these phenomena in amplifiers were also described in detail. Finally results show that measuring nonlinear figures of merit is important as the datasheet specifications may often be far off the mark and only give limited information of the complicated effects they describe. It was also shown that the one and two-tone measurement techniques that were developed for the spectrum analyzer give results that compare very well to other measurement instruments especially the Scorpion measurement system's built in intermodulation

measurement capabilities. The results that were obtained from the measurements in this section were used to create nonlinear models for use in simulation. That is the topic of the following section.

## 3.2 Amplifier Simulation

In chapter one a brief discussion of the various strategies that are commonly used to analyze device and system behavior showed that there are many options for system simulation. One of the approaches used widely today is harmonic balance analysis. This is, among other reasons, because it is applicable to a wide variety of problems. Modern day communications receivers are becoming more complicated and simulations of such systems can become a significant problem. Computer aided engineering (CAE) programs such as ADS have the ability to simulate systems using harmonic balance techniques. This section describes the different models and simulation strategies available in ADS to do small signal amplifiers simulations. Many different amplifier models are available depending on the specific system level behavior that is of importance. The models that are relevant to receiver design are described, evaluated and tested against measurements. However the basic modeling principles used in ADS to describe nonlinear amplifier behavior is discussed first.

### 3.2.1 System Level Amplifier Models in ADS

The perfect system level amplifier model should exactly reproduce the linear and nonlinear behavior of the amplifier. It should work under small-signal and large-signal excitation, correctly reproducing transfer characteristics as well as important parameters such as port impedance. Although there is no one such universal model, ADS has a collection of amplifier models that gives it the ability to model the important amplifier phenomena albeit not all at the same time and with separate simulations. With this approach, the amplifier model is chosen to suite the specific non-linear phenomenon that is being examined. There are two basic approaches to the modeling problem in ADS. These are parameter-based behavioral models and data-based behavioral models. In parameter–based models the device behavior is modeled from a small number of independent parameters. In the case of data-based models the behavior is extracted from a simulation or measurement of a transistor level circuit. Although this technique was not employed, many of the data-based behavioral models can be used in the same way as the parameter-based models.

In a simulation of a RF system the circuit will generally have a large number of linear and nonlinear circuit elements. These two basic types of circuit elements are grouped together as shown in Figure 3.30, resulting in a N+2-port network where N is the number of nonlinear elements. For this figure the source and load impedances has been absorbed into the linear network. In the simplest form, harmonic balance simulation will analyze the circuit in Figure 3.30 by finding a set of port voltages that will produce the same current components in both the linear and nonlinear subcircuits [3]. This is done by analyzing the linear portion in the frequency-domain and the nonlinear portion in the time-domain. The results of the nonlinear time-domain analysis is then transformed to the frequency domain and compared to the time domain results. The purpose of this analysis is to find solutions for the circuit in the two domains that will result in the linear currents ($I_1$ to $I_N$) and the nonlinear currents ($I_1$ to $I_N$) being equal or within a certain margin. From

this it can be seen that models for nonlinear simulation must provide the simulator with both linear and nonlinear descriptions of the circuit's properties. Generally for the behavioral models in ADS the linear subcircuit is described as a multiport matrix containing small signal parameters such as Z or S parameters. The nonlinear sections are modeled by some nonlinear transfer function such as the device's I/V or Q/V characteristics.

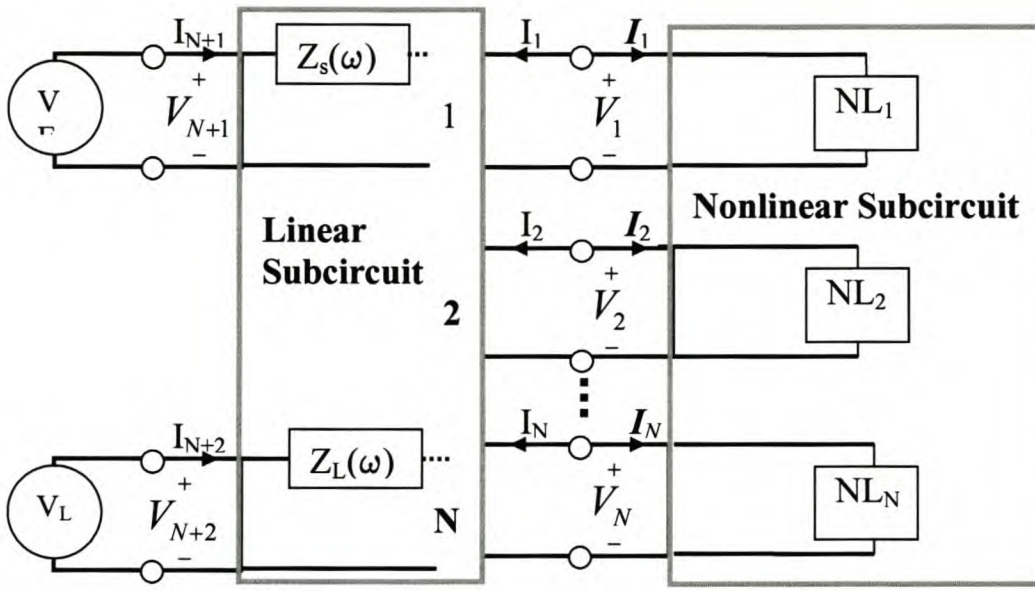


Figure 3.30 A nonlinear circuit can be divided into linear and nonlinear subcircuits with the source and load impedances $Z_s(\omega)$ and $Z_L(\omega)$ absorbed into the linear circuit. Harmonic-balance simulation of such a circuit will aim to find a set of port voltages $V_{1\text{to N}}$ that will give matching currents for the linear ($\mathbf{I_{1\text{ to N}}}$) and nonlinear ($\boldsymbol{I_{1\text{ to N}}}$) subcircuits.

In the case of transistor level simulations the nonlinear transfer characteristic of the circuit is described by a number of nonlinear circuit elements in the equivalent circuit model for the device (transistor). These may include nonlinear resistors, capacitors and sources that describe a transistor's I/V characteristics. The main problem with this type of simulation is the fact that each transistor can have many nonlinear components in its equivalent circuit. In addition to this, modern MMIC amplifiers and mixers can have a number of transistors. A receiver system can contain many amplifiers and mixers resulting in a large number of nonlinear elements causing very slow simulations. It is for this reason that behavioral model aim to represent the nonlinear transfer characteristic of a complete amplifier or mixer with a less complicated technique. Generally for nonlinear devices, the current and port voltage relationship can be described by the following equation:

$$I(V) = aV + bV^2 + cV^3 + dV^4 + \ldots \qquad 3.5$$

where a, b, c, d etc. are constant real coefficients. In ADS there are two basic modeling strategies used for determining the form of (3.5) that fit a specific device's nonlinear behavior. This is where the difference between parameter-based and data-based behavioral models is most obvious. For the case of data-based system level behavioral models the nonlinear transfer equation is deduced from

a large data set. The data set is usually the result of a nonlinear transistor level simulation of the device. In the transistor level simulation in ADS a device called a device setup component is used. This component is an extractor that is designed to do circuit characterization and generates data sets that describe the device's nonlinear characteristics. The data-based model can then use these datasets in simulations to reproduce the nonlinear behavior at system level. This technique is much faster than the transistor level equivalent. The transistor level simulation is done only once to give a rich dataset for the data-based model to work from in following simulations. The problem with this approach is that it requires detail knowledge of the device's internal working and of the transistors etc. that are used. This kind of information is usually only available to designers (IC designers). The parameter-based models give a solution to this problem. In this case the nonlinear behavior of the device is presented by a polynomial similar to that in equation (3.5) that characterizes the device's output power as a function of some port parameter such as voltage or current equation (3.6). In this strategy the user does not need to know anything about the internal working of the device and views it at the system level. The simulator uses the polynomial in equation (3.6) to describe the entire device's nonlinear power transfer characteristics (from input port to output port) by fitting it to a set of parameters.

$$P(x) = ax + bx^2 + cx^3 + dx^5 + \ldots \qquad 3.6$$

Because the parameters that the polynomial is fitted to are common nonlinear parameters such as P1dB, IP3 and saturation power (defined as power), the equation is in the form of a power-transfer nonlinearity. The power can be as a result of either voltage or current represented by $x$ in equation (3.6). In most cases the coefficient for the squared term, b, is zero and the equation is a combination of odd terms only. This is based on an assumption that only odd-order nonlinearities will generate in-band distortion. This is not always the case which justifies the inclusion of the second order term for specific cases where it is relevant [22].

For data-based models equation (3.6) is fitted to the datasets created from the transistor level simulation. However for the parameter-based models the polynomial's order and the values of the coefficients (a, b...), are determined from the parameter combinations in Table 3.1.

| **Parameters** | **Order of Polynomial** |
|---|---|
| TOI | 3 |
| TOI & AM2PM | 3 |
| SOI & TOI | 3 $b \neq 0$ |
| PndB | 3 |
| PndB & AM2PM | 3 |
| Saturation Power (Psat) | 5 |
| TOI & PndB | 5 |
| PndB & Psat | 7 |
| TOI & Psat | 7 |
| PndB & TOI & Psat | 9 |

Table 3.1 Parameter combination and matching polynomial order of equation (3.6) for the RF system amplifier models [23].

In this table PndB refers to gain compression of *n*dB with the common default parameter being the 1dB compression point ($n$ = 1). The coefficients are determined from the values of the various parameters. The linear data needed to describe the device for HB simulation is usually specified by S-parameters for both parameter-based and data-based models in ADS.

In this section the ADS amplifier models were implemented and tested with the data obtained from the nonlinear measurements in (sections 3.1.1 and 3.1.2). The basic idea is to see how well the models reproduce the amplifier behavior from measured parameters and also to improve the results where possible. The purpose of this section is to show the abilities of the various amplifier models so that they can be used in system simulations in chapter 5. Some of the amplifier models were not tested but short descriptions of their abilities are included.

### 3.2.1.1 Parameter-Based Behavioral Models

The circuit components in ADS are divided into pallets. The parameter based behavioral models for amplifiers and mixers are located in the system models palette while the data-based models are in the system data models pallet. The system model pallet contains, along with some other components, the following amplifier models: RF system amplifier, voltage controlled amplifier and three logarithmic amplifiers. In this section only the RF system amplifier will be discussed. The basic use of this parameter model is discussed and important simulation results are shown. The amplifier is shown in Figure 3.31 with the data acquisition components that are used to import the necessary data into the amplifier's parameter variables.

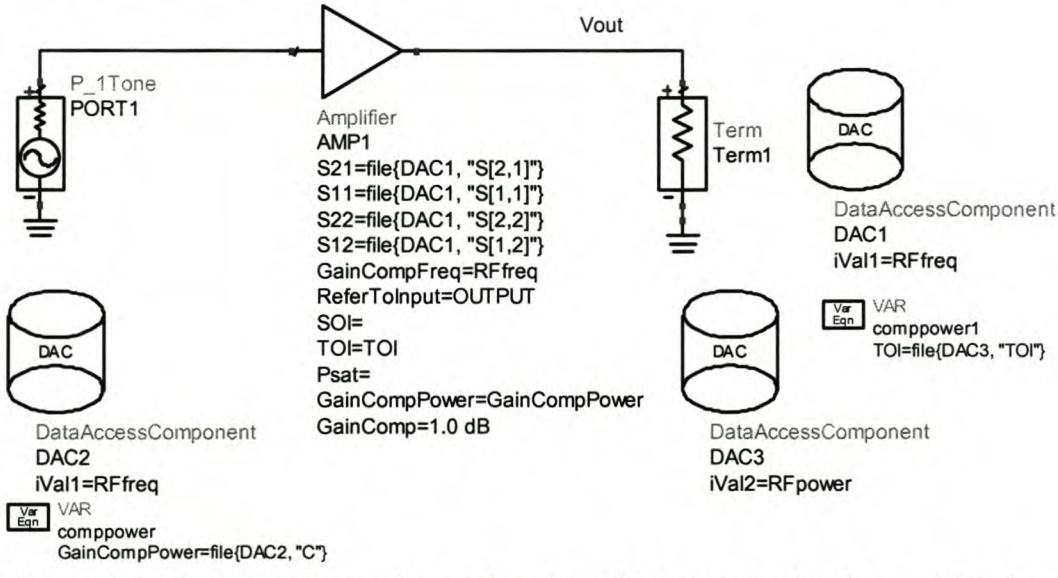


Figure 3.31 This schematic shows the application of the system level amplifier in a basic simulation. The DACs (data acquisition components) are used to access data from files. For this simulation the S-parameters are accessed with DAC1. The variable "GainCompPower" is assigned a value from DAC 2 depending on the frequency while "TOI" is dependant on the input power "RFpower" and retrieved with DAC3. The parameters are referenced to the output port.

The following input parameters were used for simulations done with the parameter-based RF system level amplifier:

- $S_{21}$ = forward transmission gain
- $S_{11}$ = port 1 reflection
- $S_{22}$ = port 2 reflection
- $S_{12}$ = reverse transmission gain
- $Z_1$ = reference impedance for port 1 (real or complex number)
- $Z_2$ = reference impedance for port 2 (real or complex number)
- ReferToInput = specify gain compression with respect to input or output amplifier port
- SOI = second order intercept, in dBm
- TOI = third order intercept, in dBm
- Psat = power level at gain saturation, in dBm
- GainCompSat = gain compression at gain saturation, in dB
- GainCompPower = power level in dBm at gain compression for *x*dB (default compression is 1dB) compression point, specified by GainComp, in dBm
- GainComp = gain compression at GainCompPower, in dB (default is 1dB)

The model also has the ability to import noise parameters and AM-to-PM parameters but this was not implemented for this model. The parameters can be entered directly into the model but this limits the parameter to one value corresponding to a specific set of conditions. If a simulation sweeps the input power or frequency the model will only be valid in a small region where the parameter is a valid representation of the device behavior. To make the model better suited for swept simulations will require the model to change according to the specific excitation. The DAC components can be used to do this. They can import data from files (mainly Touchtone and Citi files) depending on the value of a circuit parameter such as a port power or the simulation frequency. Touchtone files contain S-parameters as a function of frequency while the citi-file format is a general multidimensional file format that is used to store data. In this way the device can receive the correct parameter values for different excitation conditions. For instance, the correct S-parameters for each frequency point in a simulation are automatically read from a Touchtone file containing S-parameter data at many frequencies. The DAC components also have the ability to interpolate between data points. This is important because the measurements needed to determine parameters such as TOI and P1dB are time consuming. For this reason the nonlinear parameters are usually only measured at a limited number of points and the simulator has to interpolate or extrapolated for areas where the data is not available explicitly. An example of this will be shown in this section.

It was shown in table 1 that the order of the polynomial used to describe the nonlinear operation of the amplifier depends on the combination of parameters. If no nonlinear parameters are entered into the model it operates like a linear small-signal model using only the S-parameters to determine gain and port impedance. The following three different combinations of nonlinear parameters were used in simulations to determine the best combination:

| | Parameter | Polynomial Order |
|---|---|---|
| 1. | 1dB compression point (P1dB) | Third order polynomial |
| 2. | P1dB and third order intercept (TOI) | Fifth order polynomial |
| 3. | P1dB, TOI an saturation power (Psat) | Ninth order polynomial |

The result of a one tone swept power HB simulation for the ERA33 at 1.9GHz is shown in Figure 3.32 for these three parameter combinations. It can be seen that all three combinations give good results up to the 1dB compression point. The ninth order model gives the best result when compared to the measured data and this combination was used in most of the simulations. The fifth order model shows poor performance in the hard nonlinear region.

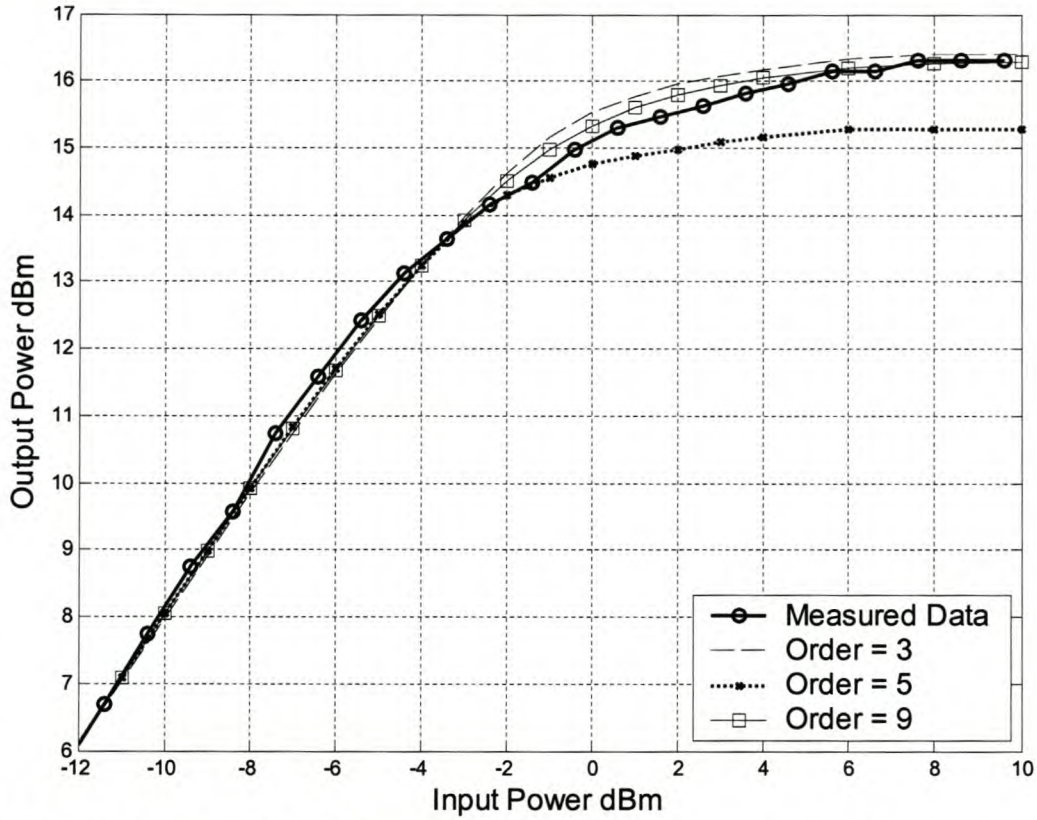


Figure 3.32 In this figure the results of three simulations are compared with measured data. The ERA33 model was simulated at 1.9GHz with a third, fifth and ninth order nonlinear model. The third order model show reasonable accuracy in this power range while the fifth order model does not work well under hard nonlinear conditions. The ninth order model gives the best results and predicts the amplifier's nonlinear behavior accurately up to 10dB gain compression. The maximum input power for the ERA33 is 13dBm and P1dB is 13.5 dBm where the gain is 17dB. All models give excellent prediction in the small-signal region.

One of the most valuable attributes of this model is the ability to easily change parameter values to suite a simulation using DAC components. This enables the model to be used for swept frequency simulations. As an example the ERA 6 was simulated over a frequency range of 1GHz to 2.7GHz. The parameters (TOI, P1dB and Psat) were supplied at all frequencies between 1.3GHz and 2.5GHz with 100MHz intervals. The simulation frequency step was 21MHz. This means that the DAC components have to interpolate the nonlinear parameter data for frequency values between 1.3GHz and 2.5GHz and extrapolate the parameter data for frequency values outside of this range. The simulator will generate a different nonlinear polynomial at each frequency point in the sweep depending on the parameter values at that frequency. If a specific frequency is not available from the parameter files, the DAC component will interpolate the available data using one of the

different interpolation options. Cubic and cubic-spline interpolations generally give good results and they were compared for the simulation shown in Figure 3.33.

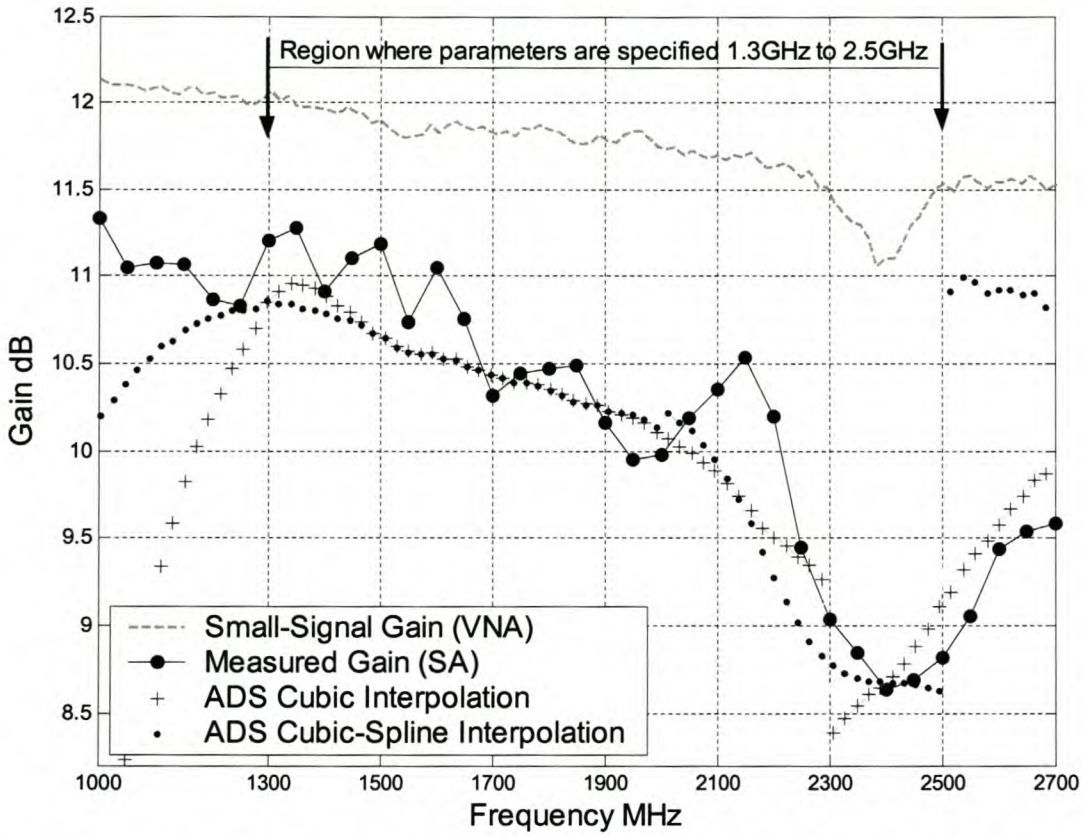


Figure 3.33 This figure shows the performance of the ERA6 for an input tone of 6.6dBm swept from 1GHz to 2.7GHz. The nonlinear parameters were only available from 1.3GHz to 2.5GHz in 100MHz increments. The parameter data was interpolated using cubic and cubic-spline interpolation and compared to measured data. Both methods of interpolation yield good results in the region between 1.3GHz and 2.5GHz. At this input power the gain compression ranges between 1dB and 2.5dB depending on the frequency and it is seen that this model gives accurate gain prediction under compression conditions.

From Figure 3.33 it can be seen that both interpolation methods (cubic and cubic-spline) give good results in the region where the nonlinear parameters are valid. The cubic interpolation is seen to respond slightly faster to parameter changes. However the results are very poor below 1.3GHz and above 2.5GHz. The interpolation also causes the simulation to ignore the abrupt change in amplifier behavior at 2.15GHz which can be seen from the measured data. Cubic interpolation was used for most simulations. The various available interpolation techniques are discussed in [2]. This simulation shows the flexibility and accuracy of the parameter-based system level amplifier model when used with the DAC components giving good results for both frequency and power sweeps. If better accuracy is needed at one frequency the interpolation can be removed. If the parameter for that frequency is available, the simulator will fit the nonlinear polynomial to the exact parameter values resulting in the accuracy seen in Figure 3.32 which is slightly better than Figure 3.33.

### 3.2.1.2 Data-Based Behavioral Models

The system data models palette has various amplifier models. These include AmpH1H2 (amplifier with fundamental and second harmonic), Amplifier P2D (large signal S-parameter amplifier), AmplifierS2D (polynomial model for nonlinearity) and Amploadpull (load-pull data for matching network design). The Amplifier S2D model was used in this work. It has the ability to recreate the amplifier's nonlinear behavior from a transistor level simulation dataset. However in this work it was used with S2D files that contain small signal S-parameters and selected nonlinear parameters. The model fits a polynomial to this data to describe the nonlinear transfer curve. This will be shown later. If used in this way the results are almost identical to the parameter-based models. The AmpH1H2 model has the ability to predict the second harmonic that is not available from the odd-order polynomial models. The AmpH1H2 needs a transistor level dataset to predict nonlinear behavior other than second order harmonics. The second order harmonic can also be described by a gain equation supplied by the user. The large signal S-parameter model requires large signal S-parameters to operate and this will not be discussed further. The load pull amplifier is specifically intended for use by amplifier designers and not for system level simulations.

The fundamental difference between the parameter-based and data-based models has already been discussed in this chapter. This difference can also be seen in the description of the two modeling strategies as top-down (parameter-based) and bottom-up (data-based) system models by the ADS literature [2]. Parameter-based models are called top-down models because the model behavior is dependant on a few parameters, usually the design specifications of the component in a system. The data-based models are described as bottom-up because the data the behavior is modeled from is usually taken from transistor level simulations of the circuit at design level. In this work however the parameter–based models as well as the data-based models use measured system level parameters. Using the models in this way removes the above mentioned classifications of bottom-up or top-down since both where implemented with measured parameters for use in system level simulations. It was found that these two models, if they receive the same parameters, give virtually identical results. The exact implementations are different and there are some other differences that will be shown in this section but the polynomial order for the data-based model is the same as that for the parameter-based model (Table 3.1).

The S2D model uses a *.s2d files that include S-parameters and one of seven GCOMP data blocks. The GCOMP data blocks can have a combination of the parameters in (table 3.1 section 3.2.1) resulting in polynomials of the same order as for the parameter model. The *.s2d files are equivalent to Touchtone files with the exception that the nonlinear parameters are included in the GCOMP data blocks. The GCOMP data blocks are just a format to specify nonlinear parameters in the same file as the linear S-parameters. The file structures are explained in detail in [2]. There is one additional GCOMP block that allows the user to specify the amplifiers nonlinear characteristics by listing the gain and phase as a function of input power. The gain and phase measured with a VNA can be used for this giving a data-based model with the ability to predict phase changes. This is called a GCOMP7 data block with GCOMP1-6 using only the parameters in (table 3.1). Because the S2D data-models give the same results with these parameters as the parameter-bases system model, only the GCOMP7 data block was used. The reason for choosing to use the parameter system model is the simplicity with which the parameters can be changed using the DAC components. The *.s2d files can have S-parameters at many frequencies but the data in the GCOMP1-6 blocks can only be for one frequency. To do a simulation at different frequencies requires a separate file for each frequency. Changing the file for each frequency in a

simulation is much more trouble than changing the parameters for the parameter-model. However, the GCOMP7 block has abilities that the parameter model does not (phase as a function of input power). To demonstrate this, the GCOMP7 block was implemented for the ERA33 from VNA data at 2GHz. The result of the simulation is compared to the measured data used in the data-model in Figure 3.34.

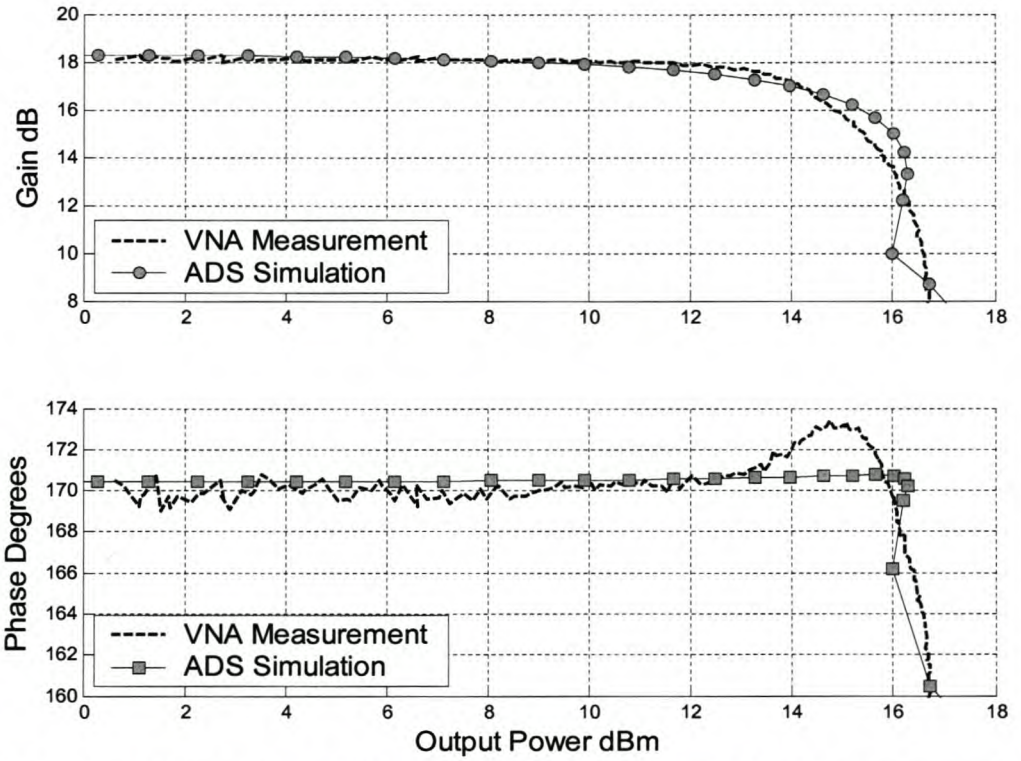


Figure 3.34 Simulation with the S2D data-based model using GCOMP7 gives reasonable results for amplitude and phase response. The GCOMP7 model uses the gain/phase data from nonlinear VNA measurements to model the amplifiers characteristics. It can be seen that the model is not very accurate in the hard nonlinear region. It does however correctly predict the major trends in the phase.

Overall the S2D data-based amplifier model gives near similar results to the parameter based model for the case where both use the measured nonlinear parameters. However the parameter-based model is much more flexible and therefore most simulations were done with the parameter-based model called simply "RF Amplifier" for the rest of this work. The next section will discuss the abilities and limitations of these models.

### 3.2.2 Capabilities and Limitations of Amplifier Simulation in ADS

This section aims to show the capabilities of system level simulation using the system level RF Amplifier model. The model was implemented to operate over a wide bandwidth and for changing input power. However for most applications specifying the parameters at the centre frequency of operation is normally sufficient.

The basic difference between linear and nonlinear simulation is illustrated by Figure 3.35 for a two-tone input signal. The top two plots show the output spectrum for a small-signal model (S-parameters) while the bottom two plots show the output spectrum for the nonlinear parameter based model. This figure shows the vast increase in information gained from nonlinear simulation of both narrowband and wideband applications.

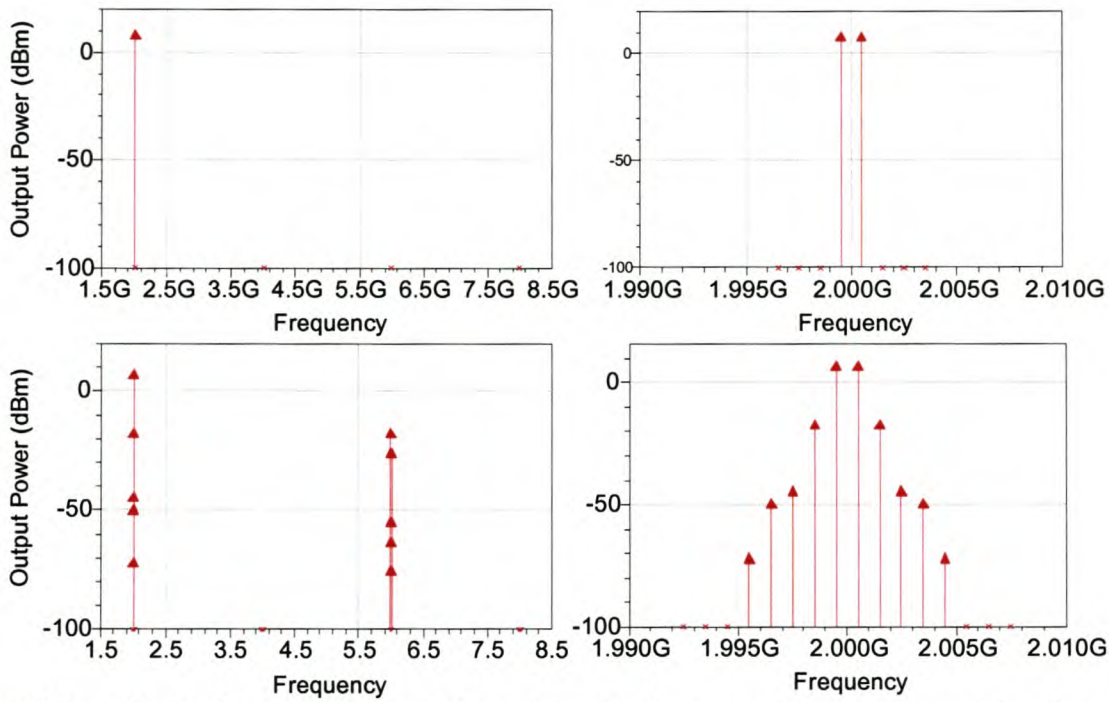


Figure 3.35 These plots show the output spectrum for the same simulation comparing linear and nonlinear models. The left hand plots are a wideband view while the right hand plots show a narrowband portion around the input frequency.

Although the nonlinear models are clearly superior in their ability to predict circuit behavior they are limited and can produce errors in some cases. The following paragraphs discuss the performance of the models in simulations specifically showing problem areas.

### 3.2.2.1 One-Tone Simulations

The accuracy of the one tone simulations are generally very good as was shown in Figure 3.32. The frequency sweep demonstrated in Figure 3.33 also gave very accurate simulations over a wide frequency band for an amplifier in the compression region. The GCOMP7 model also showed reasonable accuracy in Figure 3.34. However the most basic problem with these models is that they produce only odd order output terms according to equation (3.6) and table 3.1. Because of this the model can not predict the second harmonic. A one-tone simulation was done for the ERA 6 at 1.9GHz and the fundamental and third harmonic is compared to measured data in Figure 3.36. The plot also shows the measured second harmonic. The models inability to predict the second harmonic and the very poor prediction of the third harmonic is a significant problem for wide band

systems. The error for the third harmonic simulation is more than 20dB in some cases. The AmpH1H2 model can be used for accurate prediction of the second harmonic but this model requires either a transistor level simulation or an equation supplied by the user. If only the equations are use the amplifier predicts the second harmonic but no other nonlinear behavior and its use is therefore limited.

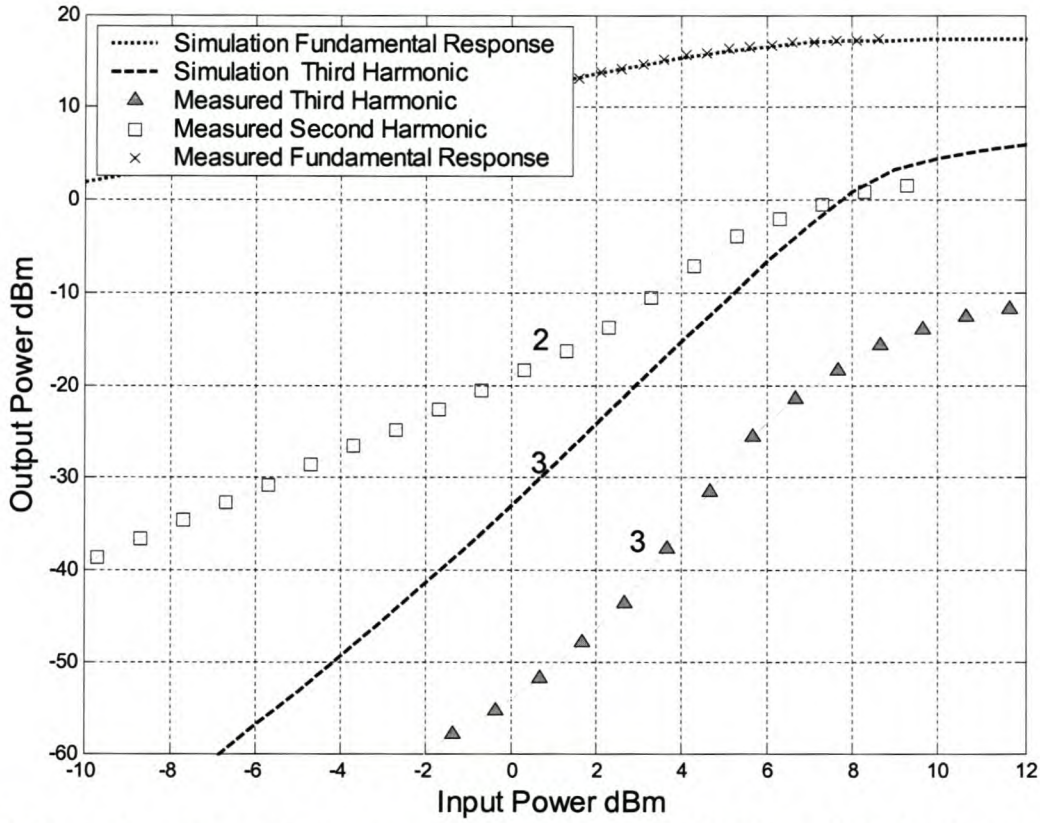


Figure 3.36 The result of a one-tone simulation of the ERA6 at 1.9GHz is compared to measured data in this figure. While the prediction of the fundamental output is excellent the third and second harmonics do not compare well. The odd order polynomial does not produce a second harmonic while the accuracy of the third harmonic is very poor when compared to measured data.

### 3.2.2.2 Two-Tone Simulation

When the models are used for two-tone simulations, the setup in Figure 3.31 is used with the same parameters but with the only difference being the addition of another tone at the input port. Figure 3.37 shows the output power versus input power plot for one of the fundamental tones, the upper third order intermodulation and the upper fifth order intermodulation. The RF Amplifier model was set up to produce a ninth order polynomial. The simulated data is compared to the two-tone measurements that were used to calculate the TOI parameter. The results show that the model gives excellent prediction of the third order intermodulation while the fifth order intermodulation is mostly within 5dB of the measured data.

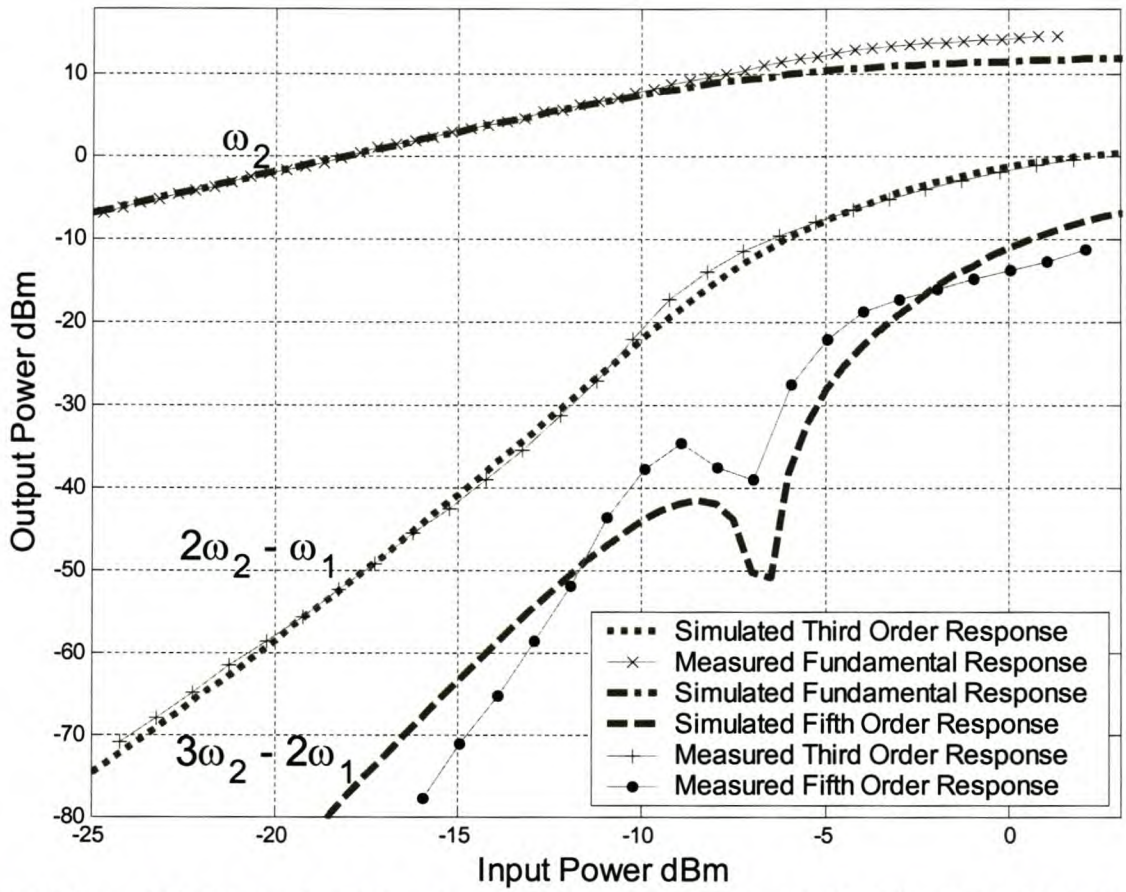


Figure 3.37 This figure shows the parameter-based amplifier models ability to predict IM. The third order intermodulation is very accurate and can be seen to match the measured data well. The fifth order intermodulation is not as accurate but the simulated data and the measurement is seen to have the same trend.

Although the simulation in Figure 3.37 shows excellent prediction of the third order intermodulation of the amplifier, it can be seen that the model does not give accurate prediction of the fundamental output in the compression region. This effect can be seen more clearly in Figure 3.38. This figure shows the fundamental response for both one-tone and two-tone measurements. It also shows the fundamental response for one-tone and two-tone simulation with the RF Amplifier. An obvious discrepancy can be seen in this plot. Both the measurements agree very well and they are also matched closely by the one-tone simulation. However the same model gives a different fundamental response under two-tone excitation. After numerous tests it was found that the 1dB compression point obtained with two-tone excitations was 3dB lower than that obtained for one-tone simulations. It would seem that the model assumes that the tone-spacing is so narrow that the average power of the two tones will be the sum of their respective power levels. If the tones are equal this will explain the 3dB difference. However this explanation is not stated anywhere in the ADS literature. Furthermore this assumption is not valid for either the ERA33 or the ERA6. Both these amplifiers were insensitive to tone spacing. In reality, if the tone spacing becomes very small the total power will be the sum of the two tones. However the relative phase of the two signals will determine the final power level of the combination of the two signals. In the case of simulations

the tone spacing does not have an effect on the fundamental output power. This effect is a specific shortcoming of these models. The problem is that the model does not take into account the effect of tone spacing and relative phase which are both important factors when two-tone measurements are done. For the case of 1MHz tone spacing that was used in the simulations the amplifiers gain is not affected by the addition of another tone and the simulation makes a clear mistake in this case.

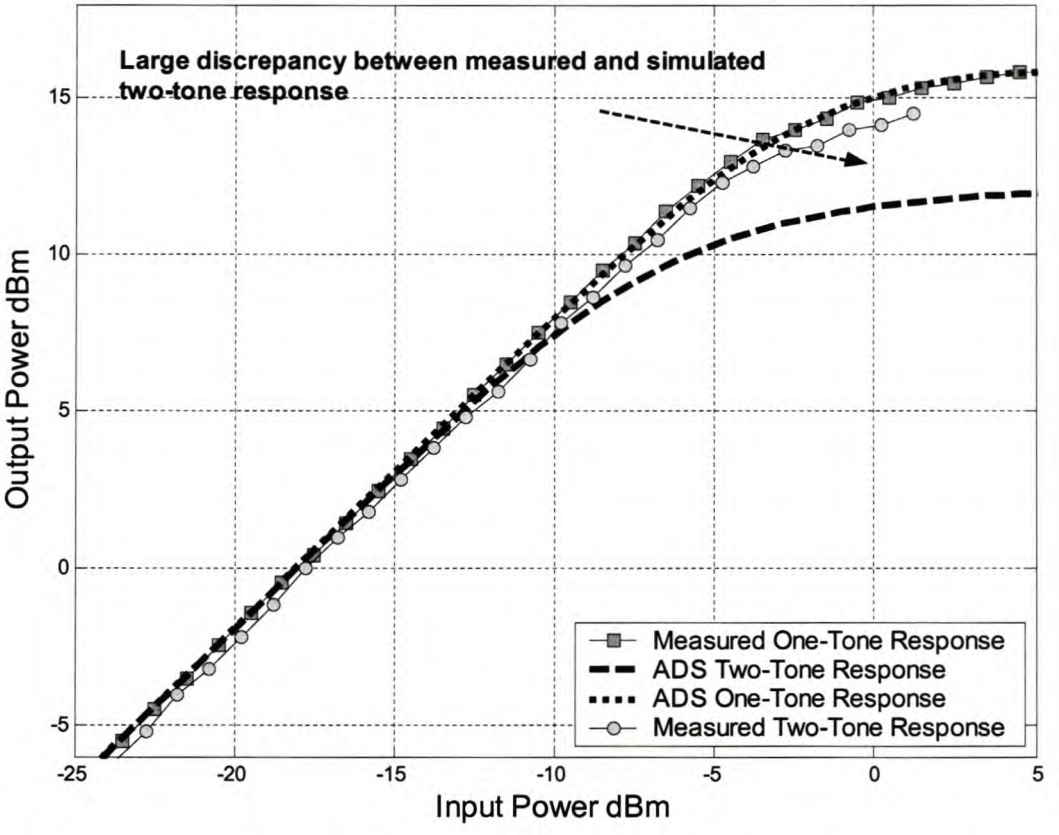


Figure 3.38 This figure shows the fundamental input versus output power for the ERA6 under different excitations. For the case of a two-tone simulation the ADS model makes a fundamental error. It can be seen that although the measured values for the one-tone and two-tone excitations give the same results as the one-tone simulation, the two-tone simulation makes a large error.

Another clear shortcoming in the two-tone simulations is the fact that the TOI parameter assumes that the upper and lower intermodulation products are symmetrical or equal. In reality the two third order intermodulation products at ($2\omega_2 - \omega_1$ and $2\omega_1 - \omega_2$) rarely have exactly equal values. The TOI parameter is calculated from measured data. Normally either the upper or the lower intermodulation product is used resulting in an upper or lower TOI point. This will lead to an obvious error in the simulation which will produce exactly equal products at both frequencies according to the specified TOI parameter. This effect can be seen in Figure 3.39 which shows the level of the third order intermodulation products relative to the fundamental output in dBc. The measurements and simulation was done over swept frequency with a two-tone input signal of constant power. The simulation was done with TOI calculated from $2\omega_1 - \omega_2$ and it can be seen that the simulation matches this tone slightly better. From the measured intermodulation it can be seen

that the upper and lower third order products are not equal. However for this case the difference is small and the accuracy obtained from the simulation is in the same order as the difference between the tones. This effect will be more severe in any case where the upper and lower intermodulation is significantly different. Nevertheless the results of this swept frequency two-tone simulation is within 1.5dB of both tones over a 1GHz bandwidth.

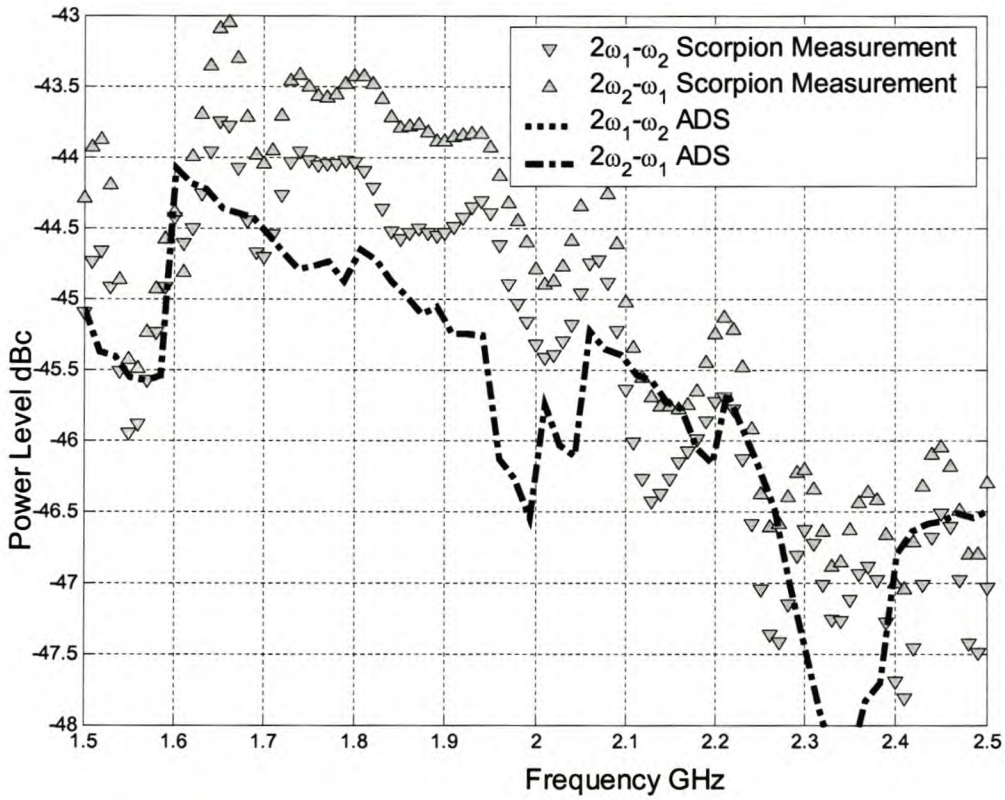


Figure 3.39 This figure compares the outcome of a swept frequency simulation of the ERA33. The upper and lower third order intermodulation relative to the fundamental output power in dBc is shown (fundamental power level – intermodulation level). This figure shows a very important shortcoming of the Amplifier model that is the fact that it will always produce symmetrical intermodulation products. In other word the upper and lower intermodulation will be exactly equal according to the simulation while this is not the case for the actual amplifier as shown in the measured data.

### 3.2.3 Conclusion

This chapter showed the measurements and techniques that are necessary to create nonlinear behavioral models in ADS. Depending on the polynomial order both gain compression and third-order intermodulation are accurately predicted. However the models are very reliant on data and extrapolated results are not always reliable. This was the case for frequency or power dependant parameters. Harmonic generation is another weak point of these models as well as the error in fundamental output power in the compression region for a two-tone excitation. Once the measurements and the data structures etc. in ADS are understood, it is possible to create an

accurate model fairly quickly. Depending on the range of frequencies and powers the models will be used for, this is a reasonably quick way to get nonlinear system level results.

# Chapter 4

# Mixers

## Introduction

Mixers are critical component in modern RF systems. Because mixers are usually among the first devices following the antenna in RF receivers, the performance of the mixer is crucial to the overall operation of a communication system. Such important mixer parameters as dynamic range, conversion loss, bandwidth, noise figure, isolation between ports and port impedance must be optimized to produce the level of device operation required by sophisticated RF systems. This chapter describes the important parameters and measurements used to characterize mixer behavior. The parameters are used in ADS to perform mixer simulations. Accurate measurement and simulation is important for understanding the effect mixer behavior has on a communication system.

## 4.1 Mixer Characteristics and Measurements

A Mixer converts RF power at one frequency into power at other frequencies [5]. Mixers achieve this frequency translation by utilizing the nonlinear characteristics of a device such as a diode or transistor. Ideally a mixer will combine the input signal having the desired information with a local oscillator signal (LO). This process yields upper and lower sidebands, each containing the identical information present in the input signal. The upper sideband is the sum of the input and the local oscillator frequencies, and the lower sideband is the difference between the input and the local oscillator frequencies. The upper or lower sideband, whichever is selected for use, is called the intermediate frequency (IF). In most receiving systems, the lower sideband (the down converted product) is used, whereas in transmitter systems the upper sideband (the up converted product) is used. The LO signal can be either above or below the frequency of the input signal. If the LO is

higher in frequency than the input signal, it is called high-side injection (HSI) while low-side injection (LSI) refers to a LO that is below the input signal in frequency. In both cased the frequency offset between the input signal and the LO signal is the desired IF frequency. This "mixing" process is shown in Figure 4.1 for a downconverting mixer using HSI.

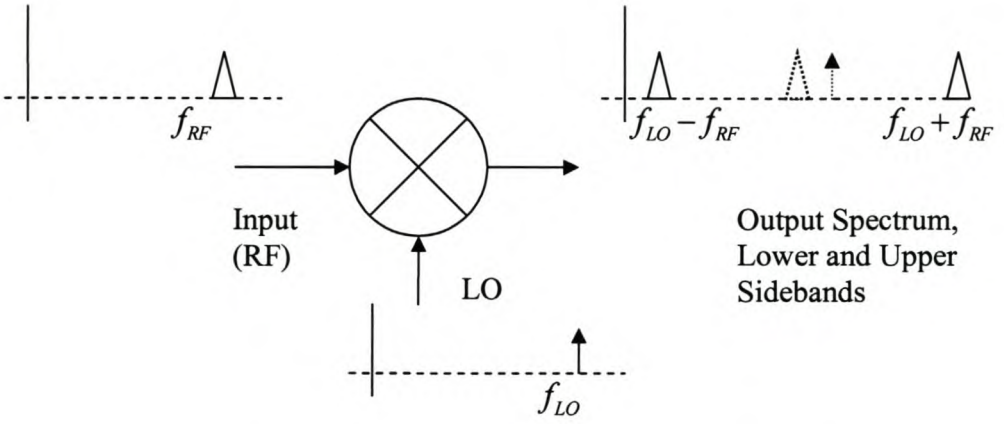


Figure 4.1 This figure shows basic mixer operation. The LO and RF combine to produce signals at the sum and difference frequencies $f_{LO} - f_{RF}$ and $f_{LO} + f_{RF}$ for the case where $f_{LO} > f_{RF}$.

However in reality, for a single input tone at the RF and LO ports respectively, a mixer will produce signals of varying power levels at the following frequencies:

$$f_{out}(IF) = \left| \pm M f_{LO} \pm N f_{RF} \right| \qquad 4.1$$

where M and N can be any integers (0,1,2,....) [3, 7, 24]. Figure 4.2 shows that a mixer can produce many signals apart from the desired IF output as described by equation (4.1). The higher order mixing products possible for equation (4.1) causes multiple responses that are generally separated by a minimum of half the IF frequency. The example in Figure 4.2 shows this phenomenon clearly. Take as an example the signal at 300MHz. While the IF frequency is the result of equation (4.1) with M = 1 and N = -1, the signal at 300MHz (100MHz above the IF frequency) is the result of equation (4.1) with M = -8 and N = 9.

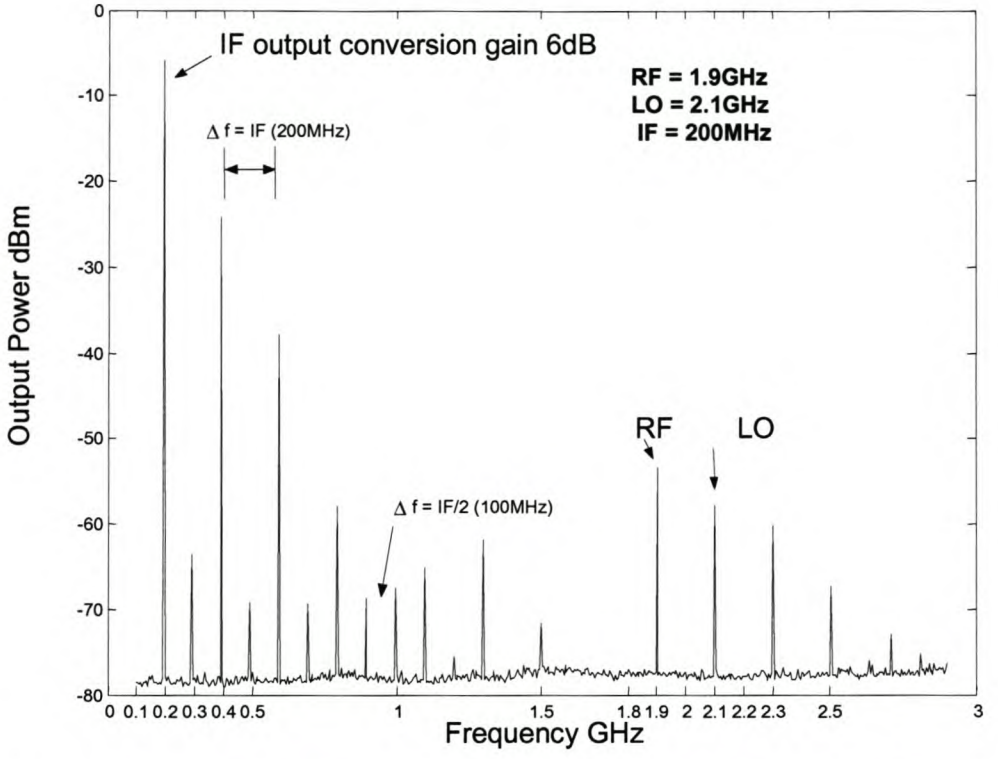


Figure 4.2 The result of applying RF (1.9GHz) and LO (2.1GHz) signals to an Agilent IAM 91563 mixer shows that many of the spectral components predicted by equation (4.1) are present at the IF port.

In addition to the frequencies of equation (4.1) the various frequencies present at the RF and LO ports are not completely isolated from the IF port and will influenced the output spectrum. These may include any signal, other than the desired signal, that are present at the input, as well as harmonics and other distortion products caused by the amplifier (preceding the mixer in a receiver) and the LO in a receiver system. These and other factors are very important when characterizing a mixer. The following sections describe the various parameters and measurements used to characterize a mixer for simulation in ADS.

### 4.1.1 Port Impedance and Return Loss

Port impedance is important to determine the mixer's return loss at various frequencies. A vector network analyzer is the best tool for measurement of complex port impedance [26]. Since even for a mixer, the reflected signal of interest is at the same frequency as the excitation signal, routine VNA calibration can be used. The measurement setup can be seen in Figure 4.3 for the case of a RF port measurement. The impedance measurements were all done with the HP8753 because it can deliver fast calibrated measurements of the different port impedances. The lowpass filter and attenuator at the LO port reduces the effects of mismatch and ensures that the LO signal's harmonics are low.

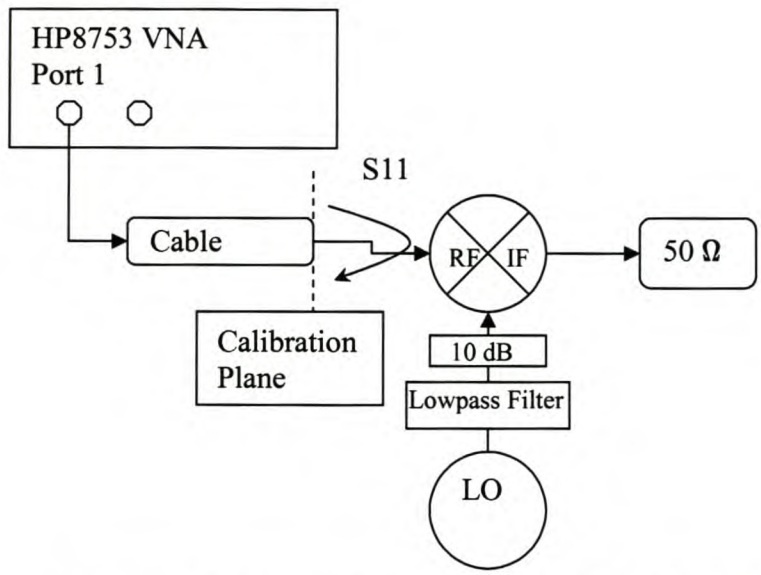


Figure 4.3 The setup for measuring port impedance with the HP8753 VNA is shown in this figure. Note that the correct LO drive level must be present at the LO port.

There are a few important aspects of mixer operation that need to be considered. When the parameter of interest is the RF port impedance or the IF port impedance, the LO port needs to be supplied of the proper operating drive level as mixer operation is strongly dependent on the power in the LO signal. Because of this the RF or IF port impedance measurement is made with two signals applied to the mixer; the RF and the LO signals. Figure 4.4 shows the RF port return loss for an Agilent IAM 91563 down converter matched for a RF frequency of 1.9GHz, LO of 2.1GHz and resulting in an IF frequency of 200MHz. The measurement was repeated for two different LO power levels. It can clearly be seen that the measurement is effected by the LO power in both amplitude and frequency.

Another problem arises from all the mixing products described by equation (4.1) and shown in Figure 4.2. These signals may be present at any of the mixer's ports. Problems will occur when the RF excitation frequency for the reflection measurement coincides with either a mixing product, (equation 4.1), or the LO frequency and its harmonics. Figure 4.5 shows the RF port return loss for the same Agilent mixer. The solid line measurement was done with an LO of 2.1GHz at -5dBm at the LO port (taking attenuation and cable losses into account). It can be seen that the LO signal leaks through to the RF port and influences the $S_{11}$ measurement at 2.1GHz. To compensate for this the VNA's IF bandwidth was reduced from 3kHz to 100Hz and the LO frequency was changed from 2.1GHz to 2.11GHz. By doing this the LO signal can be avoided in the VNA's internal IF circuitry. This can also be done by changing the number of measurement points or by specifying measurement points that do not coincide with known problem frequencies. Note however that changing the LO frequency may change the port impedance which is the parameter under test. This technique assumes that a small change in LO frequency will not change the device characteristics significantly. Additionally, for RF and IF port measurements, an attenuator should be used at the LO port to ensure a good match, and the third port must also be terminated in a matched load.

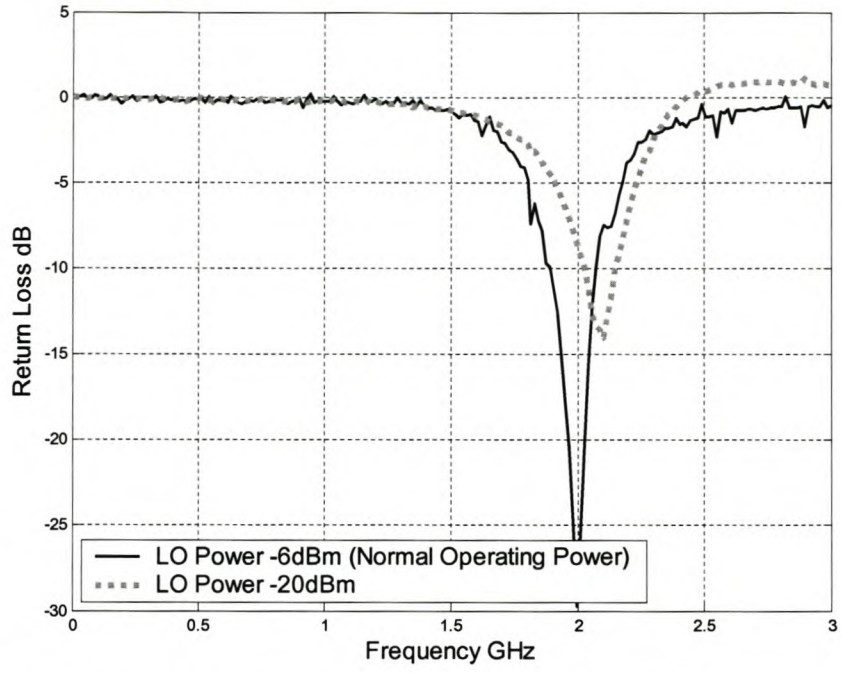


Figure 4.4 This figure shows the sensitivity of port impedance to LO power level.

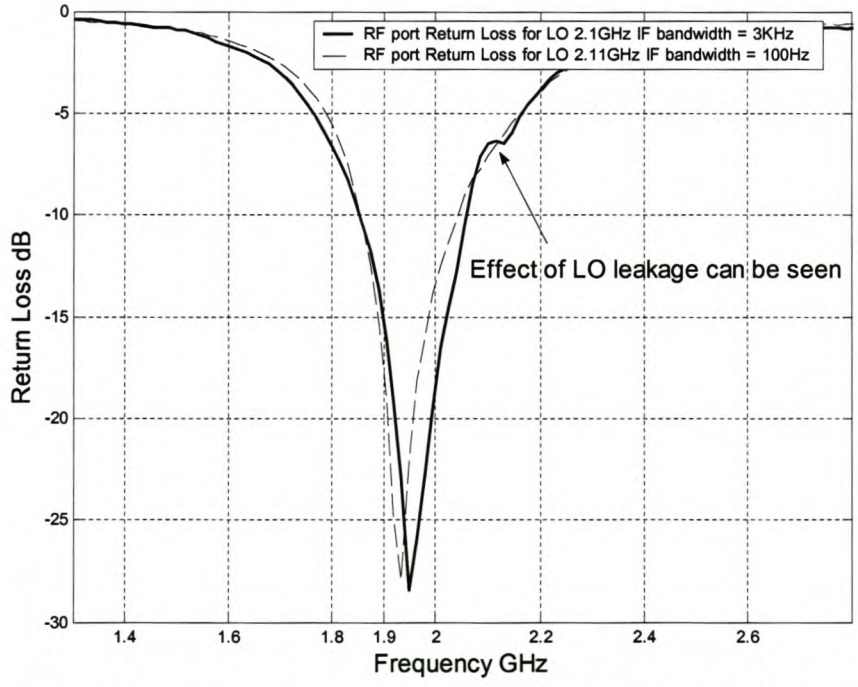


Figure 4.5 The effect of the LO signal leaking through to the RF port in this VNA measurement of the RF port impedance can be seen. The RF port was matched at 1.9GHz and it can be seen that the measurement with the 100Hz IF bandwidth gives better results.

When the parameter of interest is the LO port impedance, the RF drive level of the VNA measurement signal must be the same as the LO drive level expected under operation. Supplying

adequate drive level for excitation of the LO port can be a problem for mixers that require higher drive levels than the VNA can supply. Amplifiers can be added to some VNA configurations, but this also adds complexity, and it depends on the specific VNA model used.

### 4.1.2 Isolation

Isolation is the measure of signal leakage in mixers [5, 26]. Usually the most important isolation parameters are the LO to IF feed through and RF to IF feed through. For most mixers the LO signal will be large and therefore the LO to IF leakage signal will usually be the most degrading to system behavior.

Two techniques were used to do isolation measurements. With a spectrum analyzer the measurement is made by first observing the power level at the RF or LO port. The mixer is then connected and the power level at the specific output port is measured. It is important to compensate for frequency dependant loss through cables etc. As an example, in Figure 4.6, the LO to IF isolation is the difference in dB between the LO input power level at the LO frequency, $P_{LO}$ ($f_{LO}$), and the IF power level, $P_{IF}$ ($f_{IF}$), at the IF frequency:

$$LO\ to\ IF\ \ Isolation\ =\ P_{IF}(f_{LO}) - P_{LO}(f_{LO}) \qquad 4.2$$

The same applies for RF to IF and LO to RF isolation. In all cases the LO drive level should be the correct operating power level.

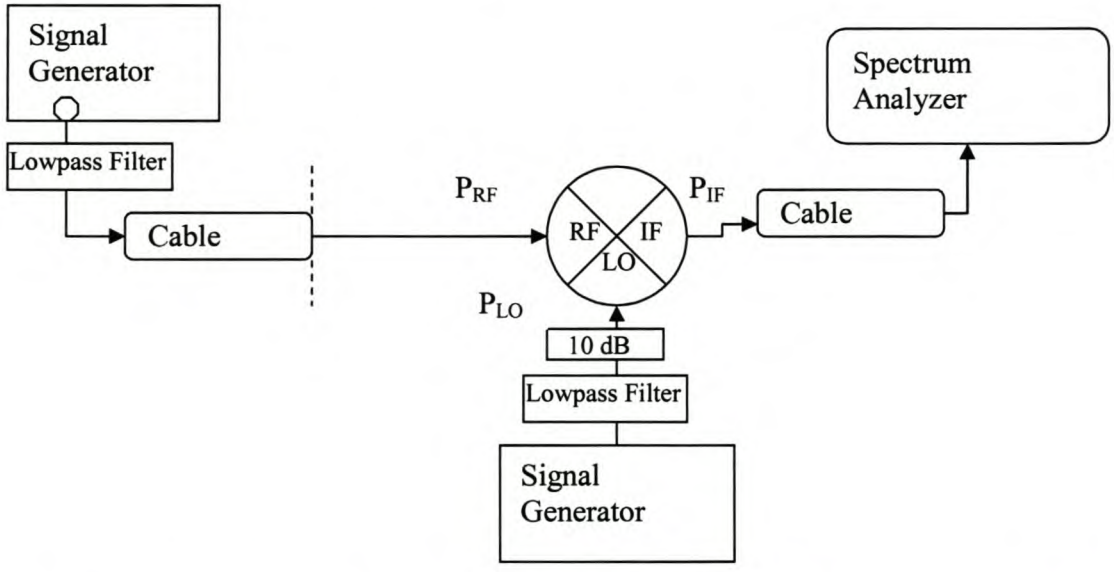


Figure 4.6 In this figure, the different power levels that are needed to determine isolation are shown. For example, substituting the power levels in this figure into equation (4.2) will give the LO to IF isolation.

When using a VNA to measure RF to IF isolation, a conventional two-port VNA calibration is used. The isolation measurement is taken as the $S_{21}$ measurement with the calibrated VNA test

ports connected to the RF and IF ports of the mixer for RF to IF isolation. Because the LO signal as well as the VNA signal are both present when making this measurement, errors can occur if the VNA measurement frequency coincides with a mixer product or the LO frequency. The LO to IF and LO to RF isolation can be measured similarly on the VNA, however, in this case the VNA power level must be comparable to the operating LO drive level to ensure the correct mixer operation is measured. The additional port is terminated in a matched load. The setup for doing isolation measurements using a VNA is the same as Figure 4.3 with the IF port connected to Port 2 of the VNA. To illustrate the different sources of error, two measurements were made on an Agilent mixer matched for an RF frequency of 1.9GHz with an IF of 200MHz. The mixer was designed for high side injection.

RF to IF isolation was measured with a LO drive level of -5dBm at the LO port. The LO signal was supplied through an attenuator to ensure a good mach at the LO port. The measurement was repeated with both the HP8753 VNA and the HP8562 spectrum analyzer. Figure 4.7 compares the measurement results for the two instruments.

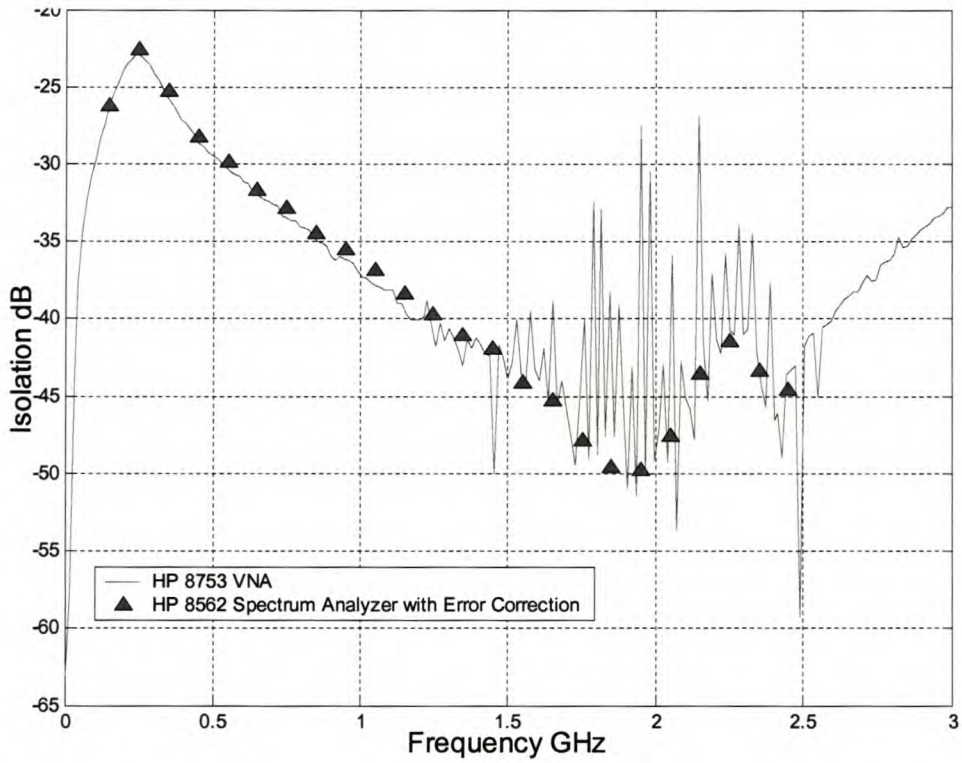


Figure 4.7 The effect of the LO signal on the measurement of RF to IF isolation can be seen along with distortion caused by multiple spurious signals from the VNA's internal mixer. The LO frequency was 2.1GHz at -5dBm and the mixer was the Agilent IAM 91563. Reducing the VNA's IF bandwidth did not reduce the problem significantly.

For the measurement in Figure 4.7 the LO frequency was kept constant at 2.1GHz where it was designed to operate. The VNA applies a signal at the mixer's RF port (201 measurement points) and measures the isolation of the signal from the RF port to the IF port. The most significant problem with VNA mixer measurements is the spurious and leakage signals encountered at various frequencies. This was also a problem in the impedance measurement of section 4.1.1. These

signals will result in disturbances in the VNA measurement. Normally a leakage signal, such as LO to IF leakage, will cause a spike in the VNA measurement as could be seen in Figure 4.5. However in this case the problem is more severe. The excessive distortion in the RF to IF isolation measurement seen in this example is predominantly caused by several of the DUT's spurious output signals downconverting to the VNA's IF in the instruments receiver.

To explain this phenomenon it is necessary to examine the HP8753 and specifically its receiver in more detail. In Chapter 2 the basic principles of VNA operation were explained. Figure 2.5 showed a VNA receiver that down-converts the RF signal coming from the directional coupler. The most important components in this receiver are the VNA receiver's mixer and the LO signal necessary to convert the input signal to the IF frequency. The IF signal is filtered with a narrow, bandpass filter and is then converted with the ADC. Even though the operation of VNA receivers are usually described to look something like that of Figure 2.5, vector network analyzers like the HP8753 use a down-converting system called a sampler-based receiver. Sampler-based receivers use a tuned oscillator to drive a pulse generator. The pulse generator in turn drives a sampler or switch. If the oscillator is tuned correctly this will result in similar operation as a mixer, downconverting the desired signal to an IF frequency. For a more detailed explanation see [27]. This concept can be seen in Figure 4.8 showing the LO input to the VNA mixer consisting of a signal with many harmonics (as would be expected from a short pulse generated by the pulse generator). The mixer can then be locked to any of the harmonics to increase the bandwidth of the instrument without having a very wideband oscillator. If there is only one signal at the receiver, this signal will mix with one LO harmonic and it will be properly downconvert to 1 MHz. However, if there are multiple signals that are 1 MHz away from any of the LO harmonics, these signals will also be downconverted to 1 MHz causing distortion in the measurement. It was seen from Figure 4.1 that mixers can produce many harmonic and other non-harmonic spurious signals at the IF output port. The distortion in Figure 4.7 is a result of these spurious signals mixing with any one of the VNA's LO harmonics. The IF frequency of the HP8753 is 1MHz.

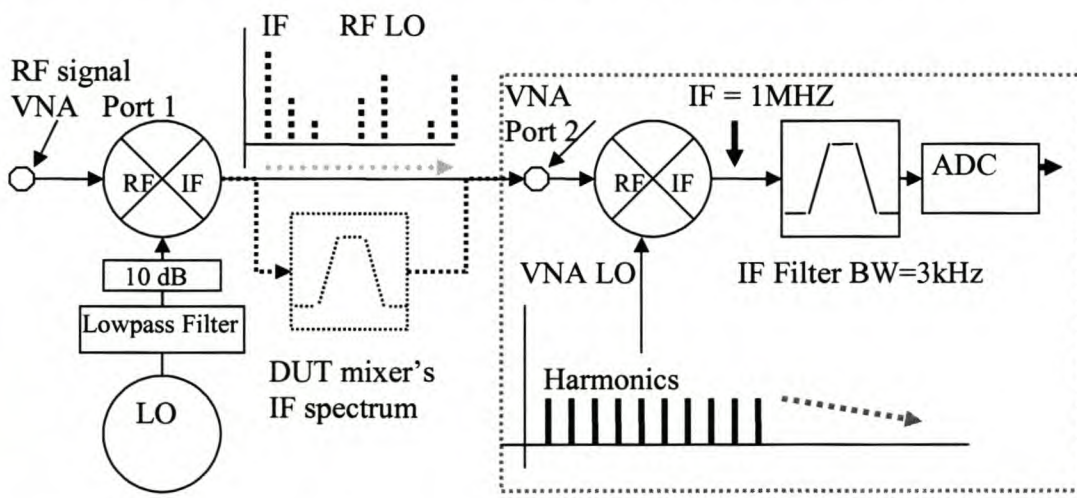


Figure 4.8 The VNA receiver produces a LO signal with many harmonics. The figure also shows a typical IF output from a mixer. In many cases some of the spurious signals may mix with one of the VNA LO signal's harmonics to produce an erroneous IF response. This effect can be reduced by filtering the DUT IF spectrum.

To determine if this was indeed the cause of the distortion in Figure 4.7 the possible spurious frequencies for the measurement were calculated. For each of the frequency points in a VNA sweep the possible spurious responses can be calculated from equation (4.1). The LO signal is constant throughout the sweep and the RF signal is the VNA test signal from Port 1. The VNA LO frequency can be calculated from the following equation:

$$F_{LO} = \frac{F_{RF} - 1MHz}{n} \qquad 4.3$$

In this equation $n$ depends on the frequency of the measurement. If $n = 2$ the second harmonic will be used etc. This signal and its harmonics is applied to the mixers LO port as shown in Figure 4.8. To calculate the possible spurious frequencies $n$ was taken as two and the DUT mixer's spurious responses was compared to the first 4 harmonics of this LO signal calculated with equation (4.3). Any of the DUT mixer's spurious responses that is closer than 1MHz from any of these harmonics can produce a spurious IF signal. The results of this calculation are shown in Figure 4.9. The calculations correlate well with the measured results even though the calculation is only approximate and does not include all possible spurious combinations. The calculations predict that there is a large possibility of spurious distortion in the area between 1.4GHz and 2.5GHz and this is clearly the case from the measurement. The squares, triangles and diamonds in the figure show the possible RF frequencies that may produce a spurious response in the VNA.

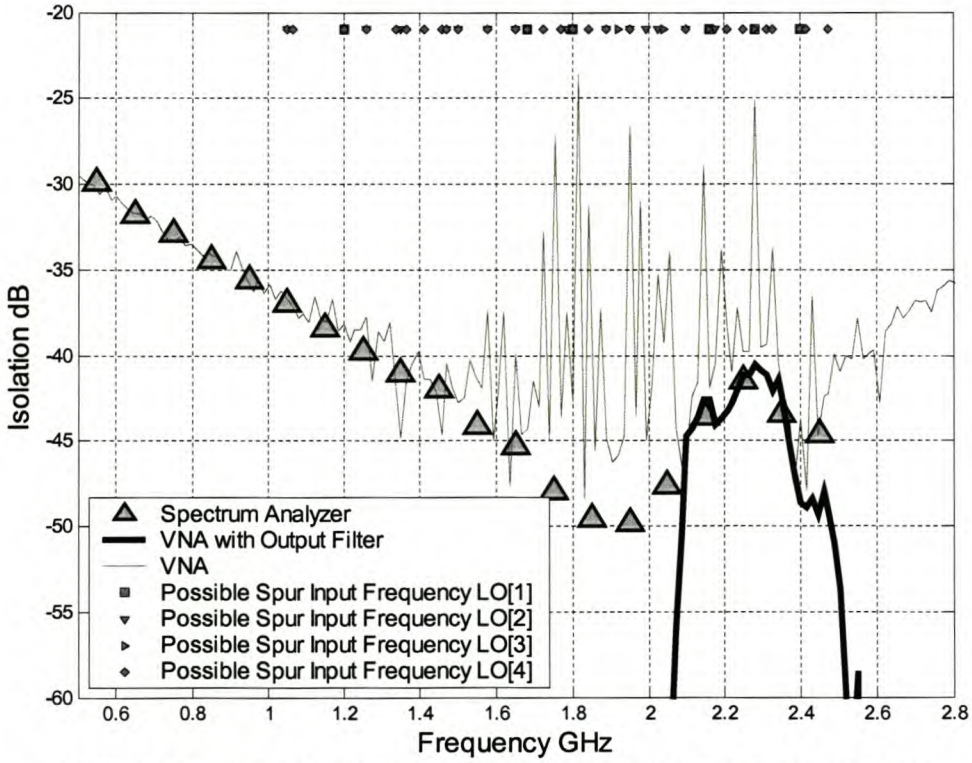


Figure 4.9 This figure shows the frequencies where possible spurious responses can occur for VNA LO harmonics up to the 4th and for all possible spurious responses calculated from equation (4.1) up to order 17. The figure also shows the results of the same VNA measurement with a bandpass filter before VNA port 2. It can be seen that this measurement matches the spectrum analyzer results well because the effects of the spurious signals have been removed.

This problem can be avoided by proper filtering of the DUT mixer's IF output. However this will greatly reduce the measurement bandwidth because mixers produce spurious responses both above and below the RF input frequency. This necessitates the use of a bandpass filter at the desired frequency. The effect of adding a bandpass filter between the mixer IF and the VNA input is shown in Figure 4.9. Although the bandwidth is reduced to that of the available filter, the distortion is much less. This problem is most severe in RF to IF isolation measurements. The possible addition of a bandpass filter in the test setup is shown in Figure 4.8.

When LO to IF isolation is measured, it is important to remember that mixers are usually very sensitive to LO power level. It is therefore important that the drive level of the VNA or the signal generator gives the desired operating drive level at the device port. Figure 4.10 displays the LO to IF isolation measured with both the VNA and the spectrum analyzer. The two spectrum analyzer plots show the effect of the cable loss on the LO signal. The cable loss is not very big but it still has a significant effect on the device operation. The RF port is terminated with a matched load. The same procedures can be used to measure LO to RF isolation. The cable loss influences the LO power level more at higher frequencies as can be expected. This can be seen in larger errors for the spectrum analyzer measurement at higher frequencies. For the VNA measurement it is important to remember that the loss through the S-parameter test set can be larger than 3dB. The calibration will correct the $S_{21}$ measurement for this loss but the absolute power level at the mixer's LO port will be smaller than that specified on the screen. This loss was taken into account for the measurement in Figure 4.10 by increasing the VNA power by 3dB. In some cases it may be necessary to apply a power ramp to compensate for the cable loss. In this case however the cable loss for the VNA and the spectrum analyzer measurements were the same (same cable was used). A constant term was added to the LO power so that the power level at 2.1GHz would be exactly -7dBm. Figure 4.10 shows the VNA plot compared to a spectrum analyzer measurement.

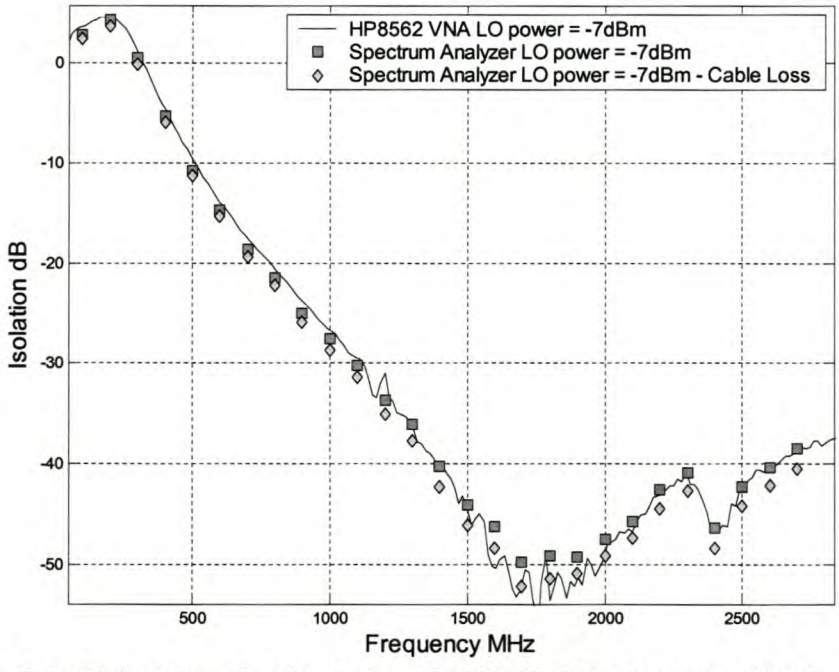


Figure 4.10 LO to IF isolation for the Agilent IAM 91563 is shown in this figure. The effect of the cable loss on the LO power can be seen to be significant for larger frequencies. In the trace marked with squares the LO power was increased to compensate for the cable loss.

For most of the isolation measurements the spectrum analyzer as well as the VNA gives good results. The VNA data is usually chosen because it includes phase information. However in cases where spurious responses or leak signals cause the VNA data to be unusable (RF to IF isolation) the spectrum analyzer measurements produce a good alternative. The spectrum analyzer (controlled by MATLAB) can also do many repeated measurements with different settings (LO power, RF power etc.) with minimal operator intervention. However in the case of the VNA each new set of measurement parameters may require a separate calibration. Because mixers are so sensitive to LO power, isolation measurements at different power levels may be required for comparison and this can be done very fast with the spectrum analyzer setup. A MATLAB procedure was developed that used the same measurement procedure discussed in chapter 2. The procedure can receive arrays of LO power and frequency as well as RF power and frequency. It then proceeds to apply the correct signals to the mixer by controlling two signal generators. The effect of the applied signals is then observed with the spectrum analyzer and measured as accurately as possible. Even though the VNA gives accurate vector data in most cases, the spectrum analyzer may present a better alternative if the mixer is to be measured under different conditions because it requires less operator time. This is a significant advantage as the number of measurements may soon become very large because of mixers additional complexity.

### 4.1.2 Conversion Gain

Conversion loss or gain is the effect the frequency translation process has on a signal's amplitude. Referring again to Figure 4.6, equation (4.4) shows this relationship to be:

$$Conversion\ Gain = P_{IF}(f_{IF}) - P_{RF}(f_{RF}) \qquad 4.4$$

If the IF output $P_{IF}$ ($f_{IF}$) is larger than the RF input $P_{RF}$ ($f_{RF}$) the conversion gain will be a positive number in dB. For an active mixer this will be the case, while for passive mixers, the conversion gain will be a negative number indicating an actual loss in signal power.

There are various methods that can be used to measure conversion gain. Spectrum analyzer measurements are the most intuitive [26]. In this section spectrum analyzer measurements are compared to calibrated measurements that were performed with the Scorpion VNA measurement system [14]. Even though the HP8753 has the ability to measure conversion gain [25], the measurement is un-calibrated and requires specific Agilent signal generators. Instead of this, the Scorpion has several built in mixer measurement functions that enable it to do calibrated, swept frequency mixer measurements. It incorporates the latest three-port VNA techniques specifically intended for, among others, mixer measurements. The spectrum analyzer measurements were done using a MATLAB procedure. The procedure uses the two signal generators to apply the correct signals to the RF and LO ports. It then observes the signal level at the IF frequency by employing the recursive measurement procedure described in chapter 2. The error correction is done with a different procedure once the data has been measured. Figure 4.11 compares conversion gain measurements done with the spectrum analyzer and the Scorpion. It can be seen that the two instruments compare reasonably well.

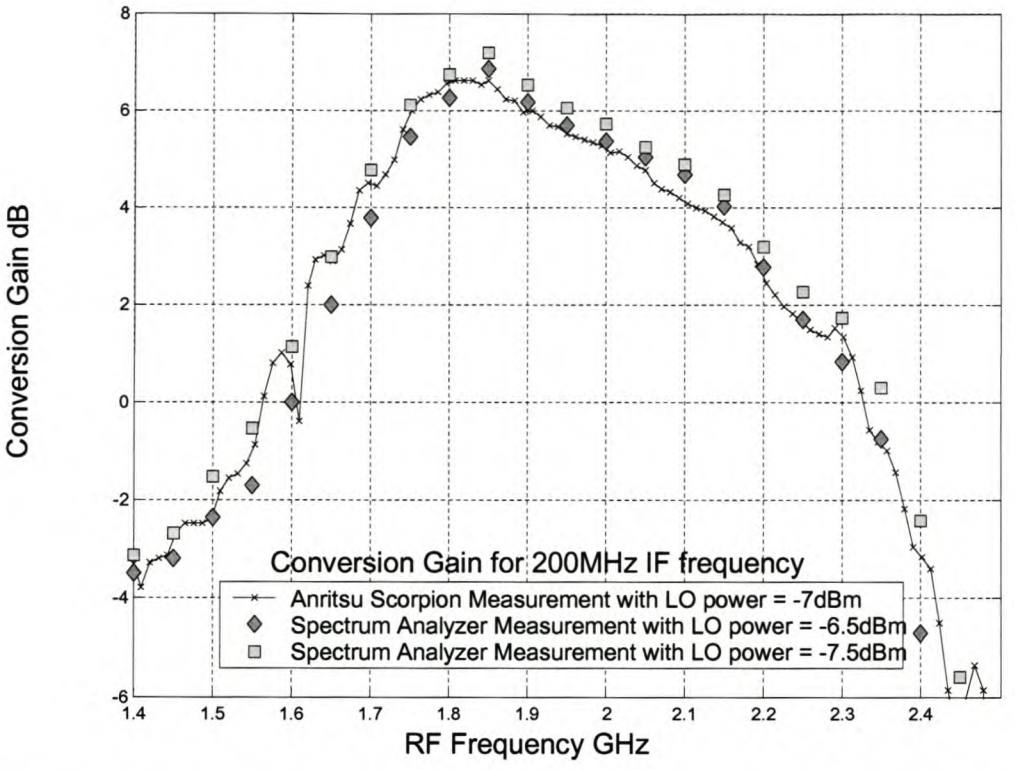


Figure 4.11 Conversion gain for the Agilent IAM 91563 mixer with swept RF and LO is shown. The IF frequency is 200MHz with high-side injection of the LO.

When doing conversion gain measurements, the LO power level is very important. In an actual measurement, the exact LO power changes with frequency. This is a result of frequency dependant loss through any measurement setup (cables etc.). Because the two systems are not identical, the actual LO power at the mixer's LO input port will not be identical. It is possible to correct this problem to some extent but it greatly increases the measurement time and complexity. Figure 4.11 compares the conversion gain for the IAM mixer measured with the spectrum analyzer and Scorpion setups. For the Scorpion the LO power level was specified as -7dBm. The spectrum analyzer measurement was repeated for two LO levels showing good agreement with the Scorpion measurement. To show the difficulty introduced when measurements over wide frequency bandwidths are done, Figure 4.12 shows the actual power level at the mixers input port for the case in Figure 4.11 with an LO power level of -6.5dBm at the signal generator. Adding the loss from the cables and filters will give a LO power smaller than -7dBm. Therefore the conversion gain for the -6.5dBm LO power matches the Scorpion measurement in Figure 4.11 the closest.

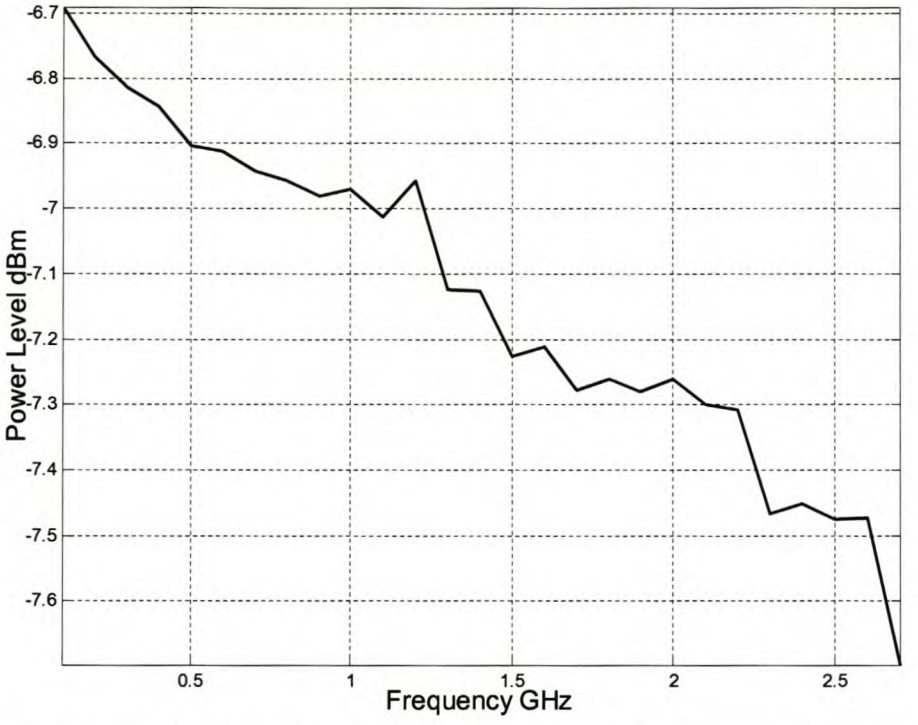


Figure 4.12 The power level at the mixer's LO port for a signal generator setting of -6.5dB is shown. The loss through the cables and filters can have a significant effect on the LO power level and therefore the measured mixer characteristics.

The mixer can also go into gain compression as was the case for amplifiers. However mixer compression is normally avoided in receiver systems. Figure 4.13 shows the conversion gain when the mixer is in compression. The two measurement techniques still compare well. The difficulty in matching LO power level exactly for the two measurements accounts for the larger than usual discrepancy between in the results. The conversion gain for RF input power of -10dBm is compared to the small signal case where the RF input power is -20dBm. The 1dB compression point for mixers is normally specified as an input power level (sometimes as output power for active mixers) as opposed to amplifiers where it is specified as an output power level. Because mixers are normally poorly matched (requiring matching circuits at the design frequency) and are very sensitive to LO power, the datasheet specification is normally of limited use. Manufacturers will typically give the 1dB compression point for a specific application frequency and matching circuit. Mixer compression was not regarded as very important in this work and therefore only selected examples are shown.

In this case of conversion gain measurement the Scorpion was used to check the accuracy of the spectrum analyzer data. Although it can not produce phase information it delivers accurate amplitude measurements. The MATLAB procedure also gives the user a lot of flexibility to change parameters (such the LO power) and observe the effect of this much faster than with the Scorpion.

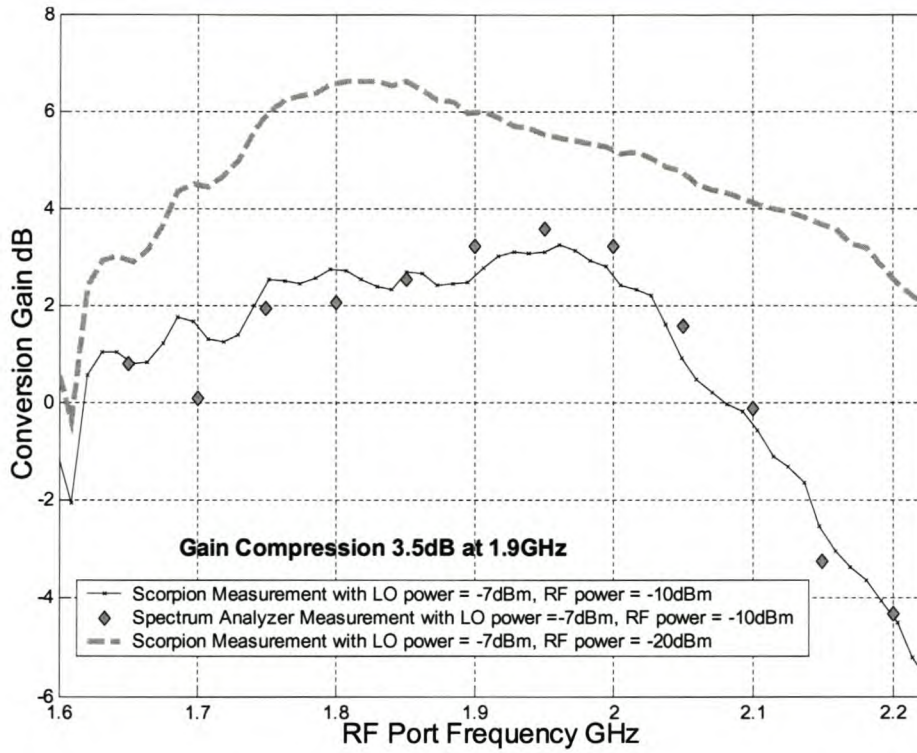


Figure 4.13 Conversion gain for the Agilent IAM 91563 mixer under gain compression is shown. The spectrum analyzer measurement agrees well with the Scorpion measurement showing 3.5dB gain compression at 1.9GHz for an RF input power of -10dBm. The input power for 1dB gain compression at 1.9GHz is -15dBm according to the datasheet [28].

### 4.1.3 Spurious Responses

In general terms something that is spurious is false, counterfeit or not genuine [29]. When this word is applied to a receiver, a spurious response refers to any output other than the desired output. There are many sources of unwanted signals that are referred to as spurious. Within an RF subsystem, spurious signals are generated by mixers, nonlinear amplifiers, and spectrally impure oscillators. In mixers, spurious signals are due to the harmonic mixing of RF and local oscillator (LO) input signals. More will be said on mixer spurious responses later in this section. In nonlinear amplifiers, spurious signals are due to the nonlinear distortion of the input RF signal. This distortion results in both the harmonics of RF tones and the intermodulation frequencies produced by multiple input tones. In oscillators, spurious signals are due to harmonics of the fundamental oscillation frequency, as well as to unwanted spurious modulation sidebands at the oscillator output sometimes referred to as spurs. This section describes the sources of spurious signals in mixers. Mixer spurious response charts and figures of merit are discussed and finally the use of intermodulation tables in ADS is shown.

### 4.1.3.1 Origin of Spurious Responses in Mixers

The paragraph above mentioned that the term spurious response is used to describe many different signals in various devices. In the case of mixers alone there are still different causes for signals called spurious. These include:

- Signals appearing to be received on frequencies to which the mixer is tuned when in fact they are transmitted on different frequencies. This happens when intermodulation between the LO or its harmonics and any input signal other than the desired RF input produce a signal that coincides with the desired IF output.
- Intermodulation of the LO and RF signals, other than the first order response that the mixer was designed for, that produce a signal at the IF frequency section 4.1.
- If the RF to IF and LO to IF isolation is not enough, signals will break through to the IF stage (or elsewhere) at these frequencies.
- Cross-modulation from a strong signal. This process involves the stronger signal transferring its modulation onto the weaker signal.
- Signals may appear to be received at the mixer input but actually originate with the LO. This is as a result of non-harmonically related spurious (LO spurs) in the LO output.

Cross modulation will not be discussed in this work. For more information see [3]. The rest of these phenomena that are termed spurious responses can be divided into two groups:

A. Signals that appear at the desired IF frequency ($f_{IF}$) because of RF input signals that are not at the desired input frequency $f_{RF}$. The image frequency is the best known example of this phenomenon and it is called congruence by Carson [29].
B. The term spurious response is also used to describe all the output signals (at any frequency) at the IF port resulting from intermodulation or leakage of the desired input signal at $f_{RF}$ and the LO signal at $f_{LO}$. Some of these signals may also fall on the desired IF frequency as a result of intermodulation of the RF and LO signals and their harmonics. This case is called coincidence by Carson.

The aim of this section is to distinguish between the above mentioned types of spurious responses. The different techniques that are used to predict them are also discussed as well as techniques to measure spurious responses for simulation purposes.

### 4.1.3.1A Spurious Responses in Mixers: Congruence

Two well known examples of the first kind of spurious response are the image frequency and half IF responses. To explain these two spurious responses the case for a mixer used as a receiver (down conversion) with high side injection of the LO is used. The explanation is extended to include all possible cases in [29]. For this case mixer operation (the fundamental response from RF to IF) can be expressed using equation (4.1) with M = 1 and N = -1 as:

$$f_{out}(IF) = \left| f_{LO} - f_{RF} \right| \qquad 4.5$$

[3, 5, 26, 29] Now consider a signal at a frequency called the image frequency $F_{IM}$.

$$f_{IM} = f_{LO} + f_{IF} \tag{4.6}$$

In this equation $f_{IF}$ refers to the desired IF frequency and not the entire IF response. Substituting equation (4.6) into $f_{RF}$ in equation (4.5) yields $f_{out} = |-f_{IF}| = f_{IF}$. A signal at the image frequency will also down-convert to the desired IF frequency $f_{IF}$. This may result in interference if the image frequency can not be filtered out of the RF input band. Because the IF frequency is usually low, the image frequency is not far removed from the RF frequency. In fact the image frequency is $2 \cdot f_{IF}$ above the RF frequency. Depending on the IF frequency it is often impossible to filter out the image frequency forcing the use of two stage down converters.

The second example of the first type of spurious response is called the half IF spurious response. The half IF response occurs for the case where M=2 and N=-2 for high side injection and M=-2 and N=2 for low side injection. This response is sometimes called the 2×2 spurious response [30]. From equation 4.1 with M=-2 and N=2

$$f_{out}(IF) = \left| 2f_{LO} - 2f_{RF} \right| \tag{4.7}$$

The RF port input frequency that will result in the half IF spurious response at the desired IF frequency is given by (4.8) for high side injection.

$$f_{halfIF} = f_{RF} + \frac{f_{IF}}{2} \tag{4.8}$$

Substituting equation (4.8) into $F_{RF}$ in equation (4.7) yields the following:

$$\begin{aligned} & -2f_{halfIF} + 2f_{LO} \\ &= -2(f_{RF} + \frac{f_{IF}}{2}) + 2(f_{RF} + f_{IF}) \\ &= -2f_{RF} - f_{IF} + 2f_{RF} + 2f_{IF} \\ &= f_{IF} \end{aligned} \tag{4.9}$$

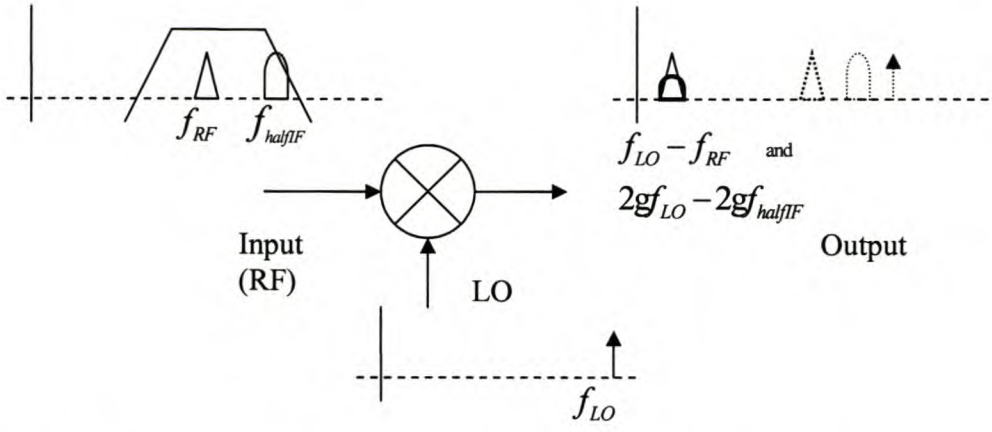


Figure 4.14 This figure shows the source of the half-IF spurious response in the output IF band. It is a result of the RF input signal at the half-IF frequency given by equation (4.8). The higher order mixing products (M=2, N=2) will result in the half IF response being smaller than the desired IF.

The reason that the half-IF spurious response is important is because it is normally very close to the desired input signal. It is only half of the IF frequency removed, unlike the image frequency which is removed by double the IF frequency. This makes it very difficult to filter out for most applications. It is specified in dBc below the desired output signal for equal input signal amplitudes at the designed RF and half-IF frequencies. Because it is a result of higher order mixing, the amplitude of the half IF response will be lower than the designed IF response as can be seen in Figure 4.14.

In the above examples of congruence, the input frequencies that will produce spurious responses were known. The standard method to determine which input frequencies may cause this kind of problem is to use a spurious response chart. However the above mentioned cases are the two most troublesome because they are both relatively close to the desired RF input frequency. In the case where measurements are done for device characterization this type of spurious response is normally not a problem because they are usually the result of signals other than the desired signal. In measurement setups these signals are usually not present and therefore this type spurious response is not a problem. Spurious response charts to predict congruence will not be discussed in this work.

### 4.1.3.1B Spurious Responses in Mixers: Coincidence

In the above two examples of congruence, the spurious response problem arises from RF input frequencies other than the desired input frequency. In most cases the problem can be avoided by filtering. Conversely, in the case of coincidence the RF input signal that causes the spurious response is the desired RF signal. The internal non-linear operation of a mixer causes intermodulation of the RF and LO signals described by equation (4.1). An example of the many output signals causes by a RF and LO signal can be seen in Figure 4.2. This results in signals at many output frequencies all harmonically related to the IF frequency. The most important of these spurious responses are the different combinations of RF and LO input that produce the IF frequency other than the desired first order mixing term (M = 1 and N = -1 in equation (4.1)). However, some wideband applications may be interested in the spurious emissions in a certain IF

band. Coincidence is therefore an important aspect of mixer nonlinear behavior that has to be incorporated into models and simulations. It is especially important for system simulations and wideband applications. In this section the use of spurious response charts to predict mixer performance is explained. The use of intermodulation tables in simulation is also explained along with the necessary measurements to create these tables.

The standard method to determine the spurious content of a mixers output port is the use of spurious response charts. The most common of these is the frequency ratio spur chart. It is a manual graphical method but numerous software implementations of the technique exists for instance one from Hittite corporation [24]. There are also some spreadsheet applications that essentially do the same thing as the graphical solutions. The basic operation of the frequency ratio spur chart, a portion of which is shown in Figure 4.15, will be explained next.

The lines for the possible spurious responses shown on the chart (Figure 4.15) are derived from the mixer equation (4.1). Derivation of the straight line equations is shown in equation (4.10) and plotted in Figures 4.15 for the case where a mixer is used as a down-converter with HSI. The same process can easily be extended to the other cases [29].

$$f_{IF} = \pm M f_{LO} \pm N f_{RF}$$
$$\frac{f_{IF}}{f_{LO}} = \pm N \frac{f_{RF}}{f_{LO}} \pm M \qquad 4.10$$

Equation (4.10) can be recognized as a straight line equation of the form $y = \pm N x \pm M$. The higher orders of the RF and LO signals are caused by the nonlinear behavior inside the mixer and do not need to be present at the respective mixer ports.

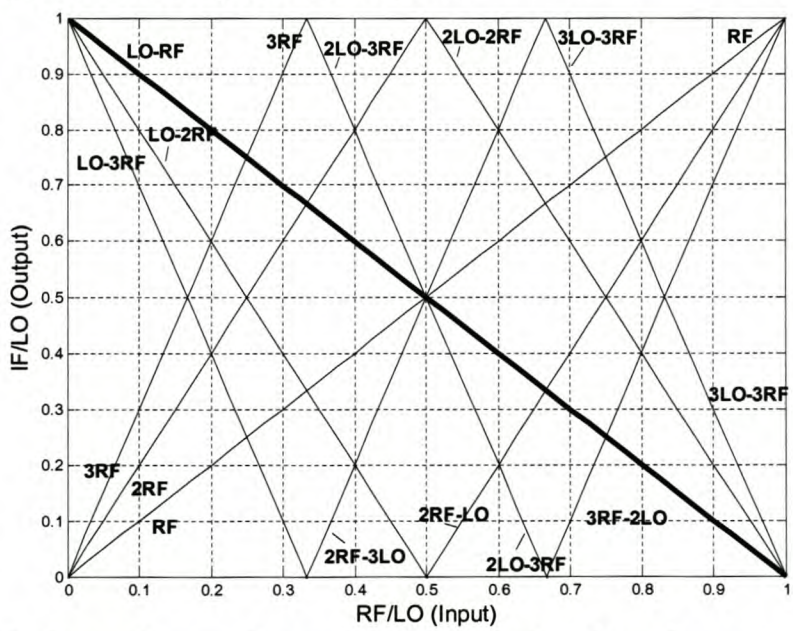


Figure 4.15 This figure shows a frequency ratio spur chart for a down-converting mixer with high side injection. Spur lines up to order 6 are shown (M+N=5 in equation (4.1)). The desired IF response is indicated with the darker line labeled LO-RF as can be expected.

The result of equation (4.10) is a family of straight lines representing the possible spurious responses. Figure 4.15 is the result of plotting equation (4.10) for all possible combinations of M and N up to order 5 (M+N=5) and some of the lines for order 6 (M=3, N=3). For low side injection (LSI) the RF/LO axis will include values of RF/LO larger than one. The chart in Figure 4.15 can be used to predict the possibility of a spurious signal falling on or close to the desired IF frequency. As an example consider a mixer that tunes the RF band from 0.6GHz to 2.3GHz to an IF of 500MHz. This down-conversion process is plotted in Figure 4.16 as a dark line and starts at the point (0.54, 0.45) and ends at the point (0.82, 0.178) on the line labeled LO-RF. The coordinates are of the form (RF/LO, IF/LO). This line corresponds to equation (4.1) with M=1 and N = -1. The line is crossed by three of the spur lines namely the 2RF-LO, 3RF-2LO and the 4RF-2LO lines. The points of coincidence are point 1 (0.67, 0.34), point 2 (0.75, 0.25) and point 3 (0.6, 0.4). These points represent RF and LO values that will produce spurious signals at the IF frequency. The points (Figure 4.16) predict spurious responses at the following frequencies:

1. 2RF-LO
   RF = 985.3MHz, LO = 1470.58MHz, IF = 2(985.3)-1470.58 = 500.02MHz
2. 3RF-2LO
   RF = 1500MHz, LO = 2000MHz, IF = 3(1500)-2(2000) = 500MHz
3. 4RF-2LO
   RF = 750MHz, LO = 1250MHz, IF = 4(750)-2(1250) = 500MHz

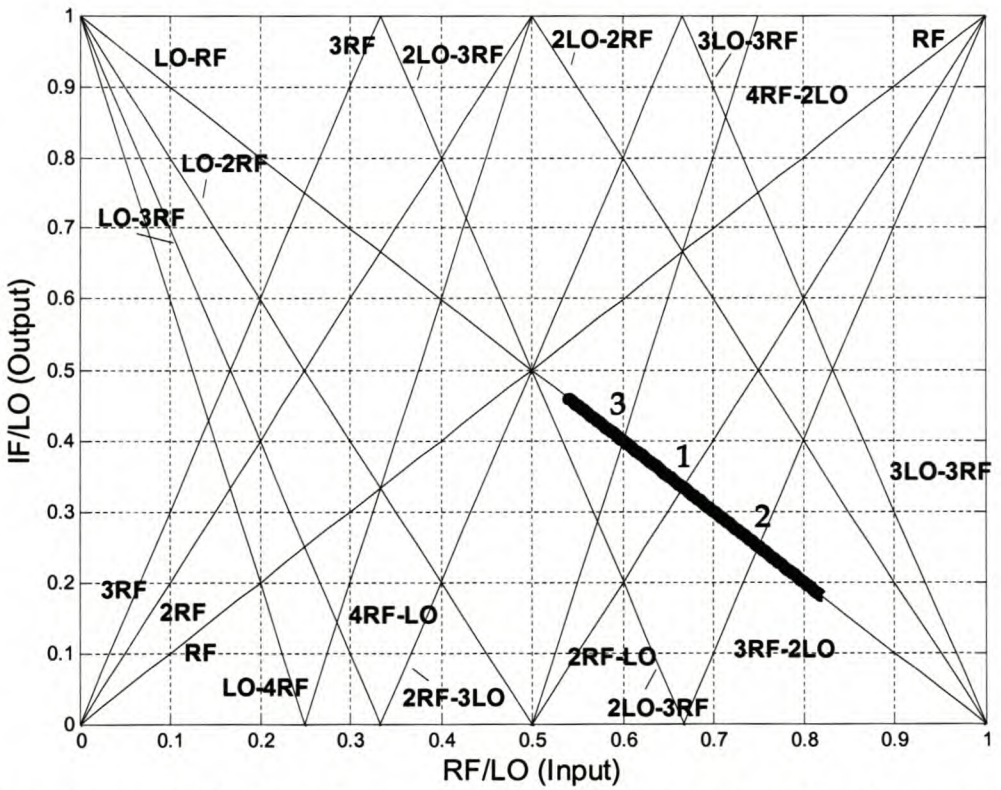


Figure 4.16 Points 1 to 3 shows the examples of coincidence discussed in the text. If any higher order response crosses the IF response line (LO-RF), it will also result in a signal at the IF frequency. The severity of the problem depends on the amplitude of the spur with lower order spurious signals generally having higher power levels.

From this example it is clear that there will be spurious responses of different orders and at different frequencies in the RF tuning band all resulting in spurious IF signals. What remains unknown is the level of these signals. Higher order responses generally have lower signal levels and will cause less interference. Although there are ways to calculate the power levels for spurious responses, the results are highly dependant on the specific mixer. Double balanced diode mixers will produce different spurious levels than single balanced active mixers and so on. Even if the exact device is known this type of calculation is still not very accurate. Another limitation of spurious response charts is the fact that they only predict responses at the IF frequency. The technique can be extended to accommodate swept IF, LO and RF cases, [24] but does not supply information of all the signals emanating from the mixer output port.

Although spurious response charts and specifically software versions of the technique can be very valuable tools in frequency planning, they have some shortcomings. As mentioned above they normally provide no estimated of the amplitude of spurs. While spurious response charts can give insight into possible system behavior it is limited and time consuming. This, among other reasons, is why modern simulation packages such as ADS use a method of spur prediction that use intermodulation tables to predict mixer spurious responses from measured data. This subject will be discussed in the following section.

### 4.1.3.2 Intermodulation Tables for Mixer Simulation

The previous sections described the different sources of spurious signals in receivers and specifically mixers. The type of spurious responses discussed in section 4.1.3.1A and B are all the product of intermodulation of the signals at the RF and LO ports. The term intermodulation is also used to describe this product of non-linear behavior in Agilent's ADS. The technique described in section 4.1.3.1B, is usually used to determine if the desired RF and LO signals will produce higher order mixing products at or close to the IF frequency. Although this technique can be very useful it is limited and for many applications a more comprehensive evaluation of spurious emissions is needed. Some simulation programs have developed a technique that uses intermodulation tables to predict the entire (limited to a practical intermodulation order) frequency content at the IF port. While they give a solution to the amplitude problem, spur charts have some limitations. The most obvious is that they are only usable in a small region close to the specific signals (power and frequency) that they were measured for. Another problem is that they are symmetrical. A spur chart will give identical values when used as an up or down converter. This section describes the use of IMT tables and the measurements necessary to construct them. The application of these IMT tables in system level simulation is discussed in section 4.2.

ADS uses intermodulation tables in the form of *.imt files. Figure 4.17 shows an IMT table with a maximum mixing order of 15 ($|M| + |N| = 15$) for the Hittite HMC170C8 passive double balanced mixer. IMT tables contain information related to mixers intermodulation generating properties as a result of single tone excitations of the RF and LO ports. Each position in the intermodulation table is occupied by the amplitude in dBc relative to the desired output frequency expected at the mixer output. This is the output for M=1, N=-1 in equation (4.1). All other possible outputs of (4.1) for different combinations of M and N are specified in dBc relative to this output power. Note that the values for M and N in the chart are absolute values.

M × LO

| N × RF | 0 | 1 | 2 | 3 | 4 | 5 | 6 | 7 | 8 | 9 | 10 | 11 | 12 | 13 | 14 | 15 |
|---|---|---|---|---|---|---|---|---|---|---|---|---|---|---|---|---|
| 0 | 65.00 | -4.67 | 99.00 | 99.00 | 99.00 | 99.00 | 99.00 | 99.00 | 99.00 | 99.00 | 99.00 | 99.00 | 99.00 | 99.00 | 99.00 | 99.00 |
| 1 | 5.66 | 0.00 | 21.16 | 99.00 | 99.00 | 99.00 | 99.00 | 99.00 | 99.00 | 99.00 | 99.00 | 99.00 | 99.00 | 99.00 | 99.00 | |
| 2 | 61.66 | 71.00 | 64.01 | 56.01 | 99.00 | 99.00 | 99.00 | 99.00 | 99.00 | 99.00 | 99.00 | 99.00 | 99.00 | 99.00 | | |
| 3 | 99.00 | 66.17 | 65.50 | 67.84 | 65.33 | 99.00 | 99.00 | 99.00 | 99.00 | 99.00 | 99.00 | 99.00 | 99.00 | | | |
| 4 | 99.00 | 99.00 | 66.16 | 66.83 | 66.00 | 65.83 | 99.00 | 99.00 | 99.00 | 99.00 | 99.00 | 99.00 | | | | |
| 5 | 99.00 | 99.00 | 99.00 | 65.67 | 66.83 | 66.67 | 66.33 | 99.00 | 99.00 | 99.00 | 99.00 | | | | | |
| 6 | 99.00 | 99.00 | 99.00 | 99.00 | 66.66 | 66.66 | 66.83 | 66.33 | 99.00 | 99.00 | | | | | | |
| 7 | 99.00 | 99.00 | 99.00 | 99.00 | 99.00 | 65.83 | 66.83 | 64.33 | 64.17 | | | | | | | |
| 8 | 99.00 | 99.00 | 99.00 | 99.00 | 99.00 | 99.00 | 65.67 | 67.17 | | | | | | | | |
| 9 | 99.00 | 99.00 | 99.00 | 99.00 | 99.00 | 99.00 | 99.00 | | | | | | | | | |
| 10 | 99.00 | 99.00 | 99.00 | 99.00 | 99.00 | 99.00 | | | | | | | | | | |
| 11 | 99.00 | 99.00 | 99.00 | 99.00 | 99.00 | | | | | | | | | | | |
| 12 | 99.00 | 99.00 | 99.00 | 99.00 | | | | | | | | | | | | |
| 13 | 99.00 | 99.00 | 99.00 | | | | | | | | | | | | | |
| 14 | 99.00 | 99.00 | | | | | | | | | | | | | | |
| 15 | 99.00 | | | | | | | | | | | | | | | |

Figure 4.17 IMT tables show the level of an intermodulation product relative to the first order IF mixing term at M=1, N=1 for the table. The value at the IF is 0dB with all other values specified in dBc below the desired IF output. In this case the mixer was a Hittite HMC170C8 mixer with an LO signal of 2.1GHz, 13dBm and an RF signal of 1.9GHz, -10dBm. The conversion gain is -12dBm resulting in an IF power level of -22dBm. It can be seen that significant intermodulation products with order 15 is present in the table at (M=8, N=7) and (M=7, N=8). The power level of these intermodulation products are -87dBm ($P_{IF} - P_{IM}$ for an IF output power of -22dBm and intermodulation levels in the region of - 65dBc).

The vertical column number N (0,1,2 to 15) shows the harmonic number of the input signal while the horizontal row number M (0,1,2 to 15) shows the harmonic number of the LO signal. A zero (0) appears in the table at the position of the fundamental signal (N = 1, M = 1). The frequency corresponding to this position could be either the sum or difference frequency depending on the application. For the case of a down converter this will be the signal at LO-RF=IF. As mentioned before all other entries are compared to this value. The entry at (N=1, M=1) therefore is 0 and if a signal has a power level that is less than this desired output signal (IF), the entry will be a positive value in dBc. If a signal is larger than the desired IF output the entry will be a negative number. In Figure 4.14 this can be seen at (N=0, M=1). The value at this entry is -4.67dBc indicating that the LO leak signal at 2.1GHz is 4.67dB larger than the IF output power. For combinations of M and N where the power level is too small to measure the table has a default value of 99dBc showing the noise floor of the measurement.

The IMT file applies to a specific power level for both the RF and LO signals. If one or both of the input signals have a different power level than the power levels that the IMT data was measured for, extrapolation is performed in ADS from the measured data. The ADS literature recommends a power range around the measured power values for which the IMT file should give accurate results. The validity of this extrapolation range will change for different devices. The recommended range that a specific IMT file can be used for is:

- RF power $\leq$specified RF power + 3
- Specified LO power – 10 $\leq$LO power $\leq$specified LO power + 3.4

For the best results, custom IMT files for a specific mixer must be constructed for specific input power levels of the RF and LO signals. This requires measuring all the possible intermodulation products at the IF port for a specific mixer setup. This can soon become a large number of measurements. The process was automated in MATLAB. The measurements were performed with two signal generators and a spectrum analyzer. A MATLAB procedure was developed that goes through the following steps:

1. The procedure receives the following input parameters: LO power, RF power, LO frequency, RF frequency and the maximum required intermodulation order (|M+N|). From this data all the possible frequencies where intermodulation products can occur is calculated by using equation (4.1).

2. The desired LO and RF signals are applied to the mixer and the spectrum analyzer settings are adjusted to ensure that the power level at the internal mixer is not too high. This limits the dynamic range of the measurement because the maximum allowable power level for the HP8562 is -30dBm. If the power is larger than this the mixer will produce its own spurious signals. For this reason most measurements were performed with input attenuation of 30dB. For these settings a dynamic range of 0dBm to -90dBm can be achieved.

3. The procedure steps through the various frequencies calculated in step 1. At each frequency a recursive search technique is used to measure the power level of the intermodulation product at that frequency. The technique starts with large RBW and VBW settings for maximum measurement speed. If however no signal is found these settings are adjusted (resulting in lower noise floor) until the signal can be measured or the minimum setting is reach. If the signal is too small too be measured the procedure assigns a default value of -99dBm to the measurement.

4. The last step is processing the data and writing the IMT file in the correct text format that can be used in ADS.

By applying this technique, accurate measurements of the mixer's spurious emissions can be made. Figure 4.18 shows the results for the Hittite HMC170C8 with an LO power of 13dBm and an RF power of 0dBm. This figure compares the measurements performed with the above described procedure with a single spectrum analyzer sweep. The plot shows the increased dynamic range that is possible by zooming in on each spurious frequency. The small differences in Figure 4.18 are a result of the logarithmic amplifier error mentioned in chapter 2 which is present in the single wideband sweep. The MATLAB procedure is also faster and produces data that is ready to write into an IMT file. The IMT files can be used in ADS to do simulations with accurate prediction of intermodulation in mixers. The following sections look at mixer simulation in ADS.

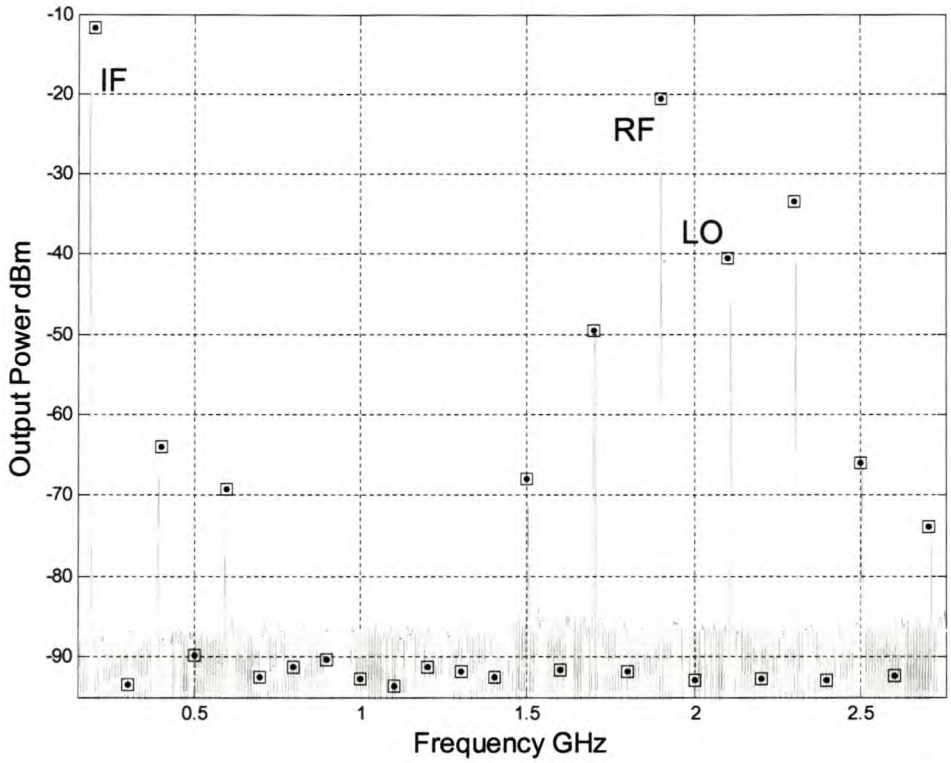


Figure 4.18 Two techniques were used to do intermodulation measurements for the Hittite HMC170C8 mixer. The wide single sweep measurement, shown in the solid line, gives reasonable accuracy but does make larger errors at the bottom of the screen. On closer inspection the error at 600MHz is 1dB. The bandwidth is also limited and it is slow. The MATLAB procedure, shown with squares, also increases the dynamic range as can be seen from the figure.

### 4.1.4 Conclusion

This section described the many challenges and problem encountered when performing mixer measurements. In all cases the measurement techniques were compared to show that the different instruments give accurate data. One of the most important aspects that was not mentioned explicitly is the time and effort needed to do a measurement and to have data that can be used in the ADS simulation package. For port impedance and isolation measurements the VNA is the easiest and fastest instrument. However in certain cases where the VNA measurement was affected by spurious and leak signals the spectrum analyzer data was used. The spectrum analyzer and the supporting error correction and automation software were best for gain conversion measurements. The spectrum analyzer is also the only device suitable for the intermodulation measurements. It should also be noted that, because mixers are very sensitive to the LO signal, it may sometimes be necessary to repeat a certain measurement under different conditions. Because the mixer operation is affected by many more parameters than was the case for amplifiers (because of three ports and nonlinear operation), the number of measurements can soon become very large. The automated measurement procedures that were developed for the spectrum analyzer provide a solution for this problem. However, the most important aspect that need to be taken into account with mixers is the fact that the device operation changes drastically with LO power and frequency. It is therefore of

utmost importance to ensure that all measurements are performed with the correct LO signal. The next section will show how the measurements in this section can be used in ADS to do nonlinear mixer simulations.

## 4.2 Mixer Simulation

The previous part of this chapter has shown the complicated nature of mixer operation. This complexity is a direct result of the fact that mixers are inherently nonlinear and always need at least two input signals to operate. The previous section showed measurements of some of the many parameters that characterize mixers. These parameters can be used to characterize a mixer for simulation purposes. However, as was the case for amplifiers, there is no single "does it all" mixer model available from ADS. This chapter will present the basic strategies available from ADS to simulated mixer behavior, showing the intended areas of use for each different model. The mixer characterization process was limited to the parameters measured in the previous section.

### 4.2.1 Mixer Models in ADS

In ADS the two basic system level models are the parameter-based and data-based models. The distinctions between these were discussed in chapter 3 for the case of amplifiers. In the case of mixers both of the model palettes have a mixer model. These are the Mixer1 and Mixer2 models for the parameter-based palette while the data-based models are called MixerData and MixerIMT respectively. While the two parameter-based models are very similar to the amplifier models as far as input parameters are concerned, the MixerData model can not be characterized by a user specified file as was the case for the S2D amplifier models. The only data-based model that could be used was the MixerIMT model which utilizes measured IMT files to predict intermodulation in a simulation. This section will describe the capabilities of the Mixer2 and MixerIMT models. Results and comparisons will be used to show the various strengths and shortcomings of the two models. This section also aims to show that the choice of model will depend on the type of simulation as well as the specific system which the mixer will be used in.

#### 4.2.1.1 Parameter-Based Models

As mentioned before, there are two parameter-based mixer models in the system models palette in ADS namely Mixer1 and Mixer2. According to the ADS literature the two models are very similar with the main distinction being that the Mixer1 model supports small signal frequency translation simulations and Mixer2 does not [23]. Because this work is focused on nonlinear behavior the small signal option is not of importance. Mixer2 was used in the simulations because it is more robust as far as convergence is concerned. This section will discuss the parameters that are necessary to use this model as well as its abilities and performance.

Apart from the fact that the mixer has three ports and is used to achieve frequency translation, its parameters are very similar to those of the amplifier models. The only two differences are the additional small-signal scattering parameters resulting from the extra port and the conversion gain specification from RF to IF. However it should be remembered that most of a mixer's parameters

are dependant on the LO power and frequency and are therefore only applicable to a specific excitation at the LO port. The Mixer2 model is shown in Figure 4.19.

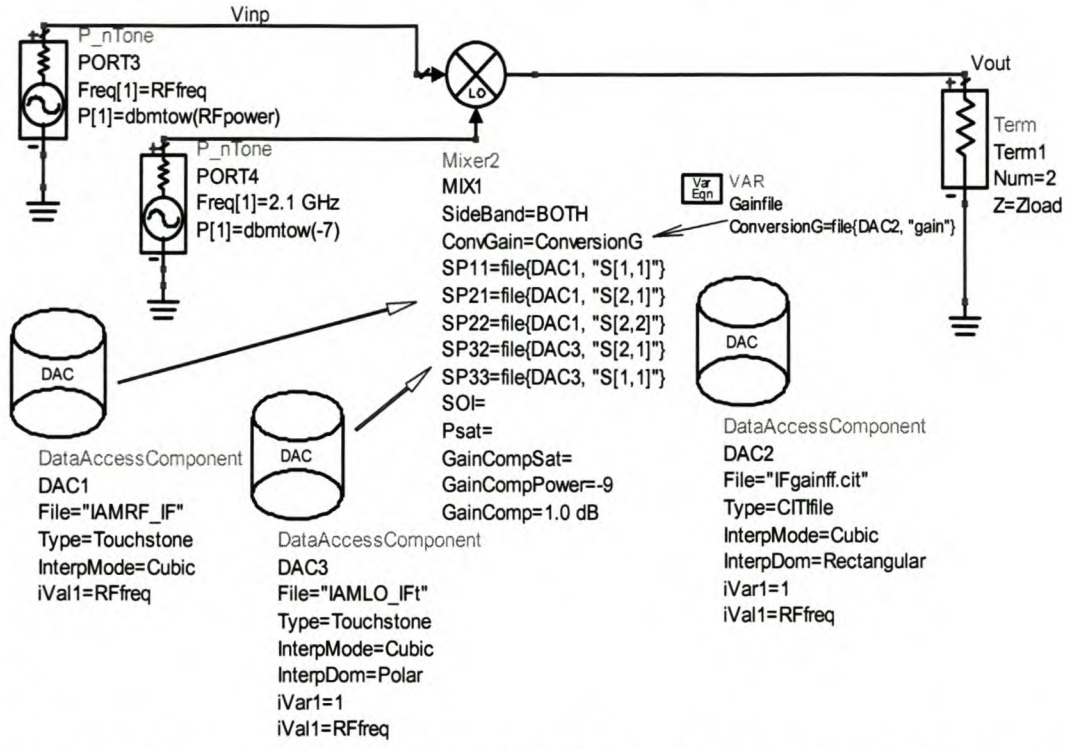


Figure 4.19 This figure shows the implementation of the Mixer2 model in ADS. The SP11 to SP33 parameters are imported with DAC1 and DAC3 depending on frequency while the conversion gain is imported with DAC2 also as a function of the simulation frequency called RFfreq in the figure. The mixer's gain compression parameters are specified for one frequency only which is the chosen operating frequency of 1.9GHz.

The Mixer2 model of Figure 4.19 has the following possible input parameters [23]:

- SideBand = produce UPPER, LOWER, or BOTH sidebands
- ConvGain = conversion gain
- SP11 = RF port reflection
- SP12 = IF port to RF port leakage
- SP13 = LO port to RF port leakage
- SP21 = RF port to IF port leakage
- S22 = IF port reflection
- SP23 = LO port to IF port leakage
- SP31 =RF port to LO port leakage
- SP32 = IF port to LO port leakage
- SP33 = LO port reflection
- PminLO = minimum LO power before starvation, in dBm
- SOI = second order intercept, in dBm
- TOI = third order intercept, in dBm
- Psat = power level at saturation, in dBm
- GainCompSat = gain compression at Psat, in dB

- GainCompPower = power level in dBm at gain compression specified by GainComp
- GainComp = gain compression at GainCompPower, in dB (default is 1dB)
- AM2PM = amplitude to phase modulation in degrees, dB
- PAM2PM = power level at AM2PM in degrees

The model also has the ability to import noise parameters which is not shown. For the case in Figure 4.19 the S-parameters for the mixer model are imported with DAC1 and DAC3 in the same way as for the amplifiers using touchtone files. The DAC components use cubic interpolation of the simulation frequency, RFfreq, to access the correct parameter values. For most applications isolation parameters such as the RF to LO isolation and the IF to RF isolation are not important and need not be specified. The most important impedance and isolation parameters are specified in Figure 4.19.

A very specific difference between the amplifier and mixer models is the ConvGain (conversion gain) parameter. In the case of mixers, $S_{21}$ is not the small signal gain but the isolation of the RF to LO port at the RF frequency. The conversion gain is the translation of the RF frequency to the IF frequency and therefore it has to be specified separately. In the case of Figure 4.19 the model was implemented with the conversion gain changing according to input frequency by importing the ConvGain parameter from a citi-file using DAC2. In this work it was assumed that mixers will generally not be used in their hard nonlinear region and less detail was included for the mixers compression behavior. The 1dB gain compression is specified in Figure 4.19 as -9dBm for the centre frequency of operation. This will result in a nonlinear polynomial mixer model of third order (see Table 3.1). The model operation is not effectively affected by the LO power level in the simulation, unless parameters are imported as a function of LO power. This can easily be done but the model does not incorporate LO sensitivity automatically and it has to be included in the data.

The process of characterizing mixers with measurements is much more complicated than amplifiers. For instance, depending on the specific application, a mixer can have a certain IF frequency, an input RF band and a tunable LO to downconvert the RF to the desired IF. In other applications it might be possible that the RF, LO and IF frequencies can take on different values. Because of this the user needs to decide what configuration the mixer will be used for and then the model can be set up to suit the specific situation. This distinction can dictate which model is used and how it is used. The Mixer2 model was implemented to operate as a narrow-band down-converter while the IMT model was implemented for a more wideband application.

To show the performance of the Mixer2 model, it was implemented for an Agilent IAM-91563 mixer matched at the RF port for 1.9GHz, LO port for 2.1GHz and at the IF port for 200MHz. The measurements and simulations presented where all done assuming that the LO frequency and power will stay constant and that the desired RF frequency was 1.9GHz. These constraints greatly reduce the number of measurements that are needed to characterize the mixer. Figure 4.20 shows the result of a power sweep applied to the simulation setup in Figure 4.19.

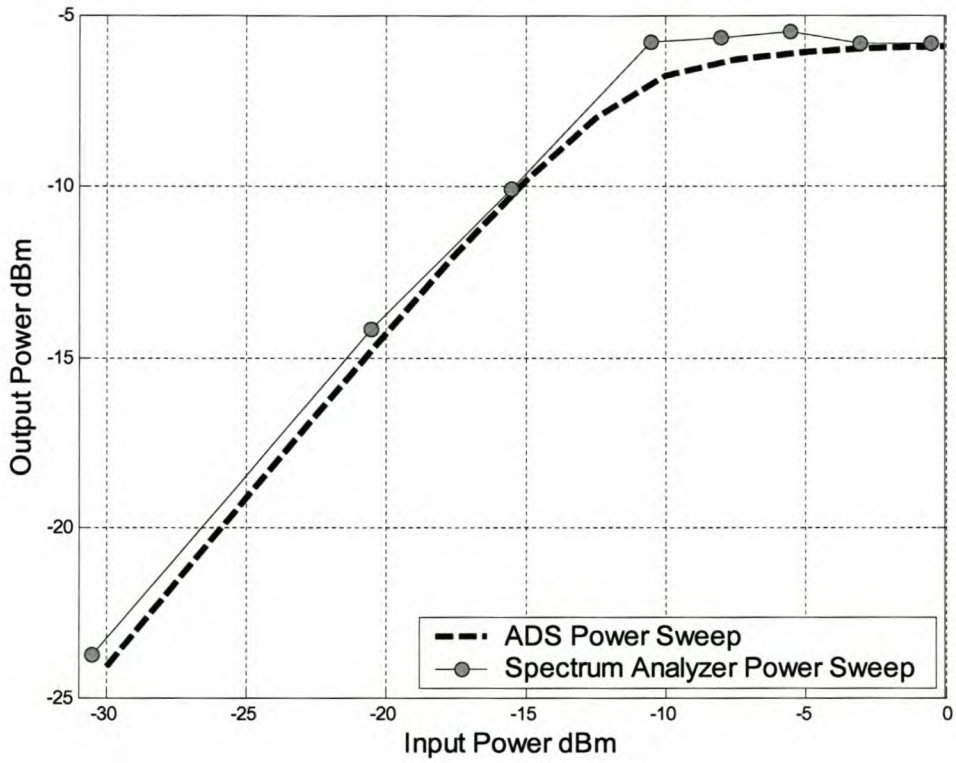


Figure 4.20 This figure shows a power sweep at 1.9GHz for the mixer implemented in Figure 4.19. It can be seen that the third-order polynomial model gives a reasonably good prediction of the mixer's gain in the compression region. Note that the small-signal gain of the simulation does not match the measured data exactly. This is because the 1dB compression parameter was calculated from a spectrum analyzer sweep while the small signal gain was measured over frequency with the Scorpion.

The 1dB compression parameter for this model was calculated from the spectrum analyzer sweep shown in the figure. Notice that less measurement points were included than was the case for amplifiers. This results in a less accurate calculation of the 1dB compression point. The small signal gain was taken from a frequency sweep performed with the Scorpion VNA. There is a clear discrepancy in the small-signal region between the measured spectrum analyzer data and the simulated data. However the simulated data is determined by the Scorpion measurement and this difference is therefore a result of limited measurement accuracy when the two measurement instruments are compared. Ideally the compression parameters as well as the small-signal parameters should be taken from the same data. Even though much less effort was taken than was the case for amplifiers, the simulation can be seen to be a good representation of the mixer even in its compression region.

Figure 4.21 shows the Mixer2 model's performance under swept frequency conditions. From this measurement the LO frequency and power was constant while the input signal was swept from 1.4GHz to 2.6GHz. The result of the simulation is compared to a Scorpion measurement under the same excitation.

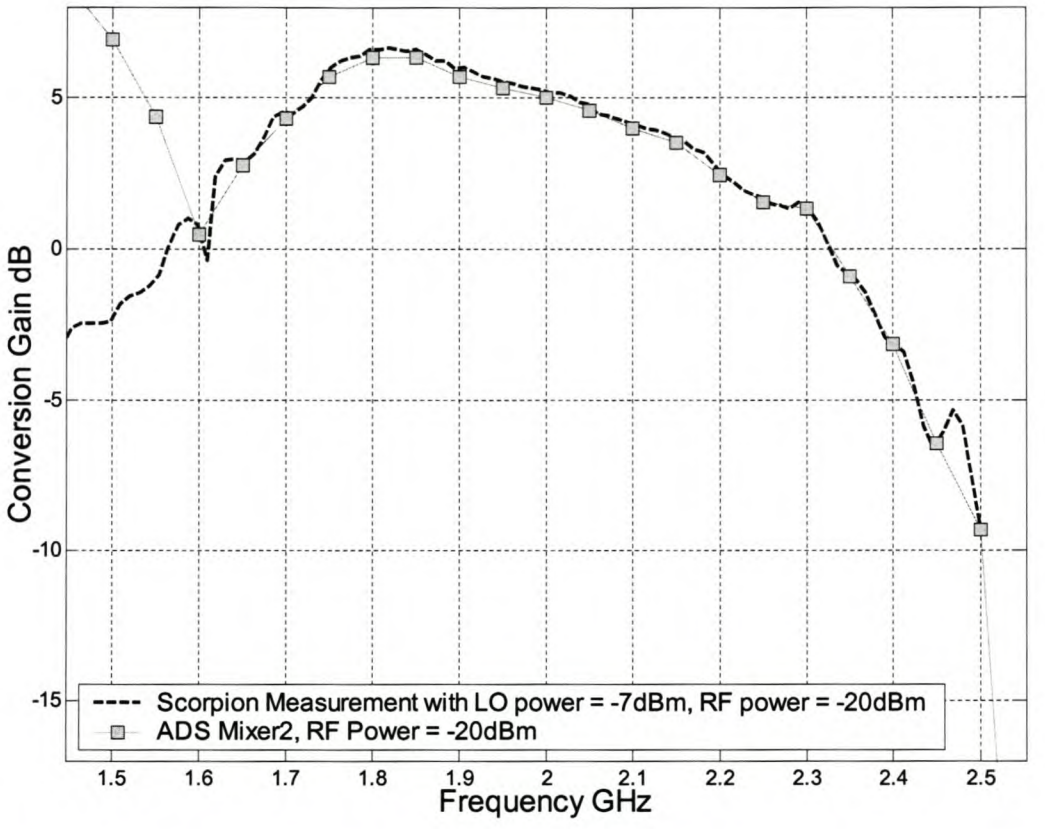


Figure 4.21 This figure shows the models performance under swept frequency conditions. The conversion gain for the model was specified from 1.6GHz to 2.5GHz in 50MHz steps. Cubic interpolation was used and from the figure it can be seen that the simulation matches the measured data very well. The two areas where there are problems are outside the specified range and at 2.45GHz where the interpolation does not track the measurement very well.

Figure 4.20 and Figure 4.21 show that the Mixer2 model can give excellent results for both swept frequency and power simulations although the results depend strongly on the range of the specified parameters. To illustrate this effect more clearly the model was used in a swept frequency simulation for a large-signal excitation. The input signal that was used was well into the mixer's compression region. Figure 4.22 shows three traces. The first trace is exactly the same as Figure 4.21 showing the mixer's performance for a frequency sweep under small-signal conditions (-20dBm input power). The second trace shows measured results for the mixer in the compression region with more than 2dB gain compression at 1.9GHz (-10dBm input power). The third trace shows the result of an ADS simulation of the setup in Figure 4.19 for an input power of -10dBm (the 1dB compression point at the input is approximately -14dBm).

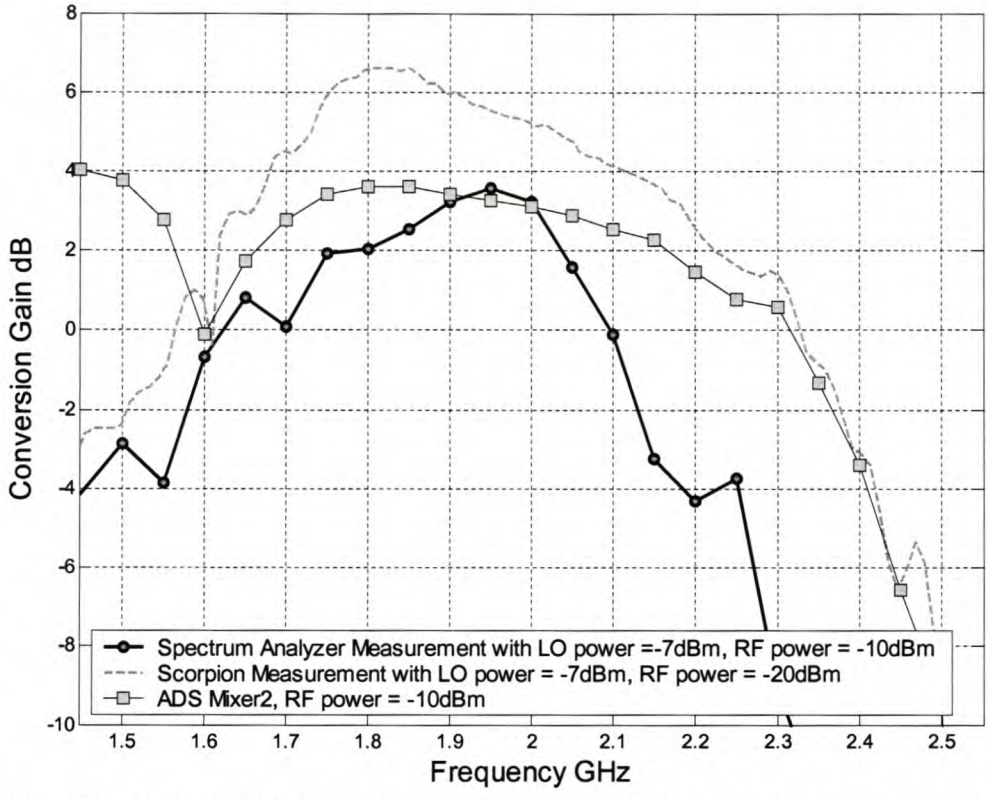


Figure 4.22 To illustrate the Mixer2 model's dependence on the input parameters this figure compares two measurements with a simulation. The Scorpion measurement shows the conversion gain under small-signal conditions. The spectrum analyzer measurement shows the conversion gain of the mixer for an input power of -10dBm (more than 2dB gain compression). The ADS simulation was performed for exactly the same excitation as the spectrum analyzer measurement. The simulated trace matches the measurement very closely in the region close to 1.9GHz where the compression parameters are specified.

From this experiment it can be seen that the model performs very well where the necessary data is supplied but deviates significantly from the measured data in all other regions. For frequency values other than 1.9GHz the model still uses the 1dB compression parameter for this frequency resulting in large errors where this value is no longer applicable. The severity of this error will differ depending on the specific characteristics of the device being modeled.

Another important aspect of mixer behavior that was also explained in the previous chapter is intermodulation. In section (2.1) the process that is necessary to measure the output spectrum of a mixer was discussed along with the creation of IMT tables from this data. However the Mixer2 model does not have the ability to use IMT tables. It does however create a nonlinear polynomial model of the device operation and therefore it also creates mixing terms other than the desired RF to IF mixing term. Using the setup shown in Figure 4.19 a simulation was performed for the Agilent IAM mixer with an LO power of -6dBm at 2.1GHz and a RF input signal of -10dBm at 1.9GHz. This excitation is in the compression region of the mixer. A portion of the output spectrum at the mixer's IF port is compared to measured data in Figure 4.23.

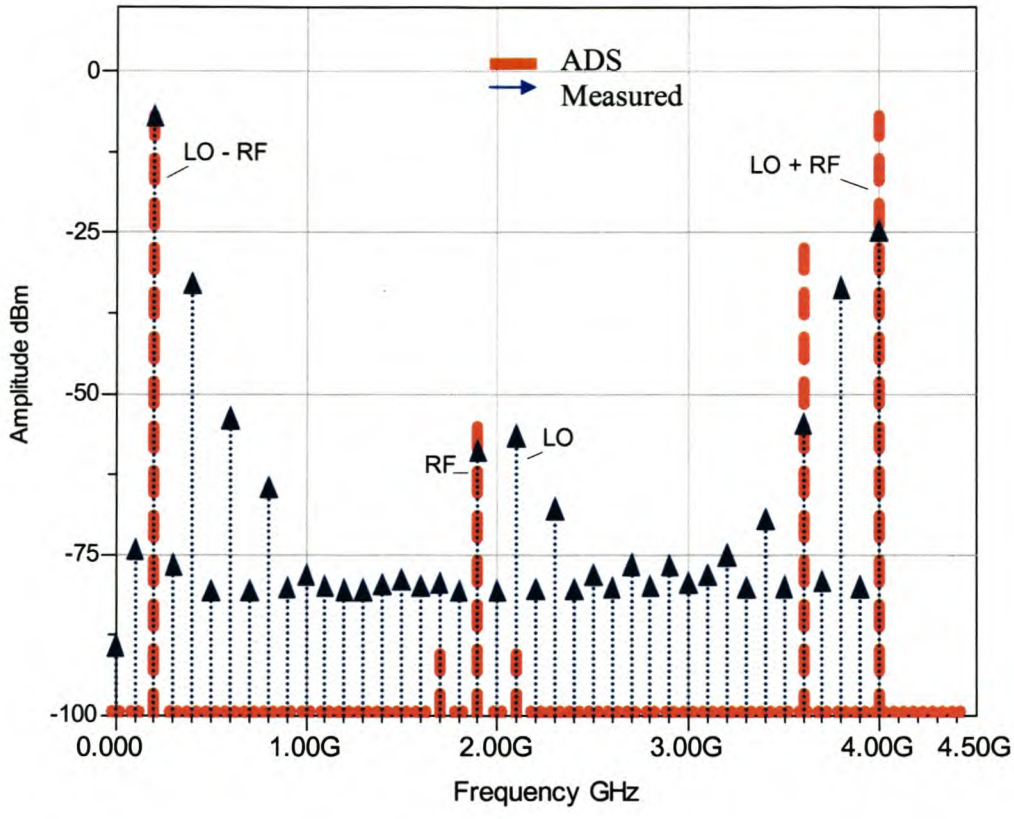


Figure 4.23 This figure compares the output spectrums of an HB simulation using the Mixer2 model to measured data. The mixer's SideBand parameter was set to produce both the upper and the lower mixing terms. The simulation shown in this figure was for a third order polynomial model.

While the Mixer2 model gives excellent prediction of the conversion gain from RF to IF, Figure 4.23 shows that there are some fundamental shortcomings in this model. The first of these is the isolation. It is clear that both the RF to IF and LO to IF isolation is not correct in the HB simulation. The data supplied to the model specifies isolation in the range of -50dB at 2GHz. The RF leakage signal at the IF port is 5dB larger than it should be and the LO signal is 30dB smaller than what would be expected. The error is not a result of incorrect data.

Another important shortcoming is the model's ability to predict higher order mixing products clearly visible in the measured data. Figure 4.24 shows the exact same simulation for a fifth order model (TOI parameter included) which slightly improves the prediction of two spurious responses (1.6GHz and 3.6GHz). Even so, the result for the total IF spectrum leaves much to be desired. The intermodulation order of the simulation was 13 with both the RF and LO tones being considered up to the seventh harmonic. Some of the tones at higher order mixing frequencies are generated but their power levels are very low (below 120dBm). Another important aspect of the Mixer2 operation is the sideband setting which determines whether the mixer should produce the sum term (RF +LO), the difference term (LO-RF) or both. The simulation in Figure 4.23 was set to produce both terms while the simulation in Figure 4.24 was set to give only the difference term. It can be seen that in the case for both terms the sum and difference terms have exactly the same amplitude. This will always be the case as the model can not distinguish whether the specified conversion

gain is for up-conversion or down-conversion. It is clear from the comparison with the measured data that both with and without the upper term there is a large error for this frequency (4GHz). However for most applications this type of error will be well out of the operation band.

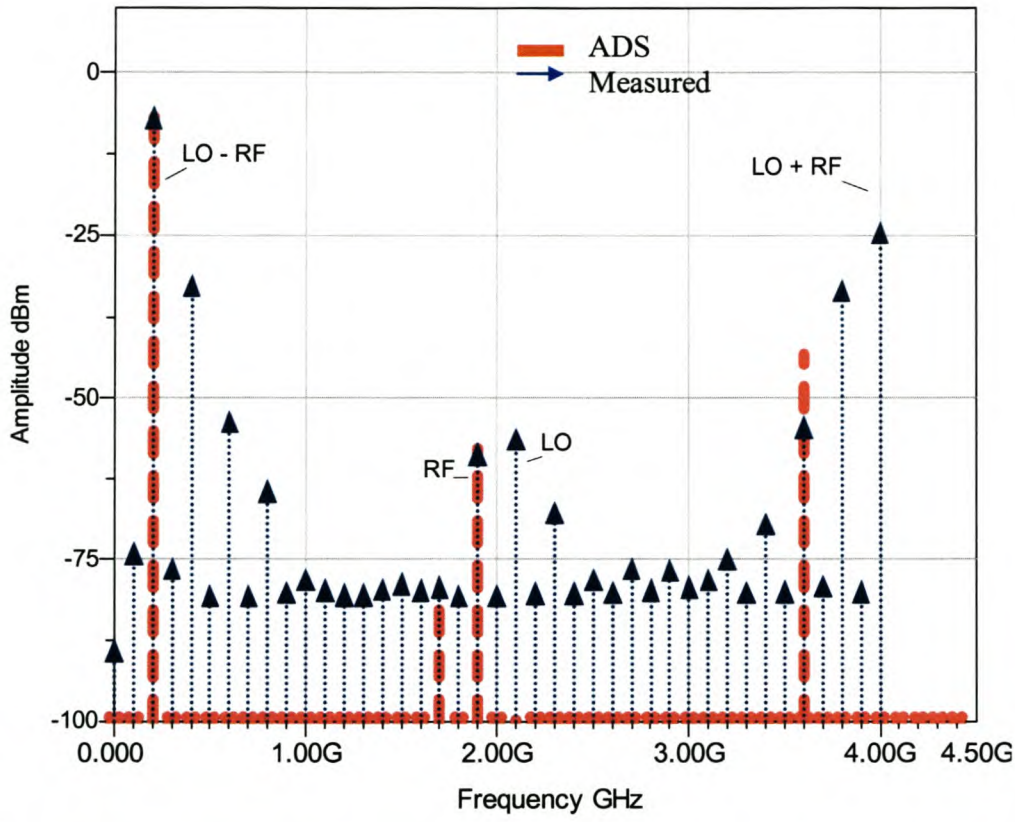


Figure 4.24 The simulation plotted in this figure was for a fifth order Mixer2 model with the SideBand setting configured to produce only the difference term. The higher order polynomial increases the accuracy of the spurious prediction at some frequencies. Notably the RF to IF isolation is exactly the same as the measured data.

From these two comparisons of the IF output spectrum of simulations to measured data it is clear that while higher order polynomials may give slightly better spurious prediction the model is still far from the measured data. It does however give excellent prediction of the first order difference mixing term from RF to IF. This model is very flexible and can be configured to suite a variety of applications from a simple third order polynomial to the maximum ninth order polynomial. The next section will describe the data-based model called MixerIMT which uses IMT tables for accurate simulation of spurious responses.

#### 4.2.1.2 Data-Based Models

It was stated previously that the only data-based model that can be implemented using VNA and spectrum analyzer measurements is the MixerIMT model. This model is intended for situations where the spurious response of a mixer is important and it uses IMT tables first discussed in section 4.1.3.2 do achieve this. The process to create custom IMT files from a mixers measured spurious responses is also discussed in that section. The aim of this section is to show the abilities and limitations of this model.

The MixerIMT model appears identical to the Mixer2 model shown in Figure 4.19. However the MixerIMT model is a data-based model and therefore its operation is not described by a set of parameters which was the case for the parameter-based model. The MixerIMT model can receive the following input data [23]:

- ConvGain = Conversion gain (real or complex number)
- SP11 = RF port 1 reflection
- SP12 = IF port to RF port leakage
- SP13 = LO port to RF port leakage
- SP21 = RF port to IF port leakage
- SP22 = IF port reflection
- SP23 = LO port to IF port leakage
- SP31 = RF port to LO port leakage
- SP32 = IF port to LO port leakage
- SP33 = LO port reflection
- NF = input double sideband noise figure, in dB
- Rn = equivalent noise resistance
- M_RF = IMT order for RF port
- N_LO = IMT order for LO port
- IMTValueType = IMT value type (dB value or dBm value)
- IMT_File = file containing intermodulation table

From this list it can be seen that the MixerIMT data-based model uses a number of similar input parameters as the parameter-based model. These include all the S-parameters as well as the conversion gain. The difference between the models is the inclusion of the IMT_File input for the data-based model instead of the compression parameters. This is the file containing the IMT table for the mixer. Although there are two built-in, default IMT tables in ADS, the best results are achieved when custom measured data is used to produce this data input. The operation of MixerIMT model is strongly focused on the IMT data. Figure 4.25 shows the Mixer IMT model implemented for the Agilent IAM mixer. It shows the DAC component used to import the conversion gain as well as the IMT file specified in the model.

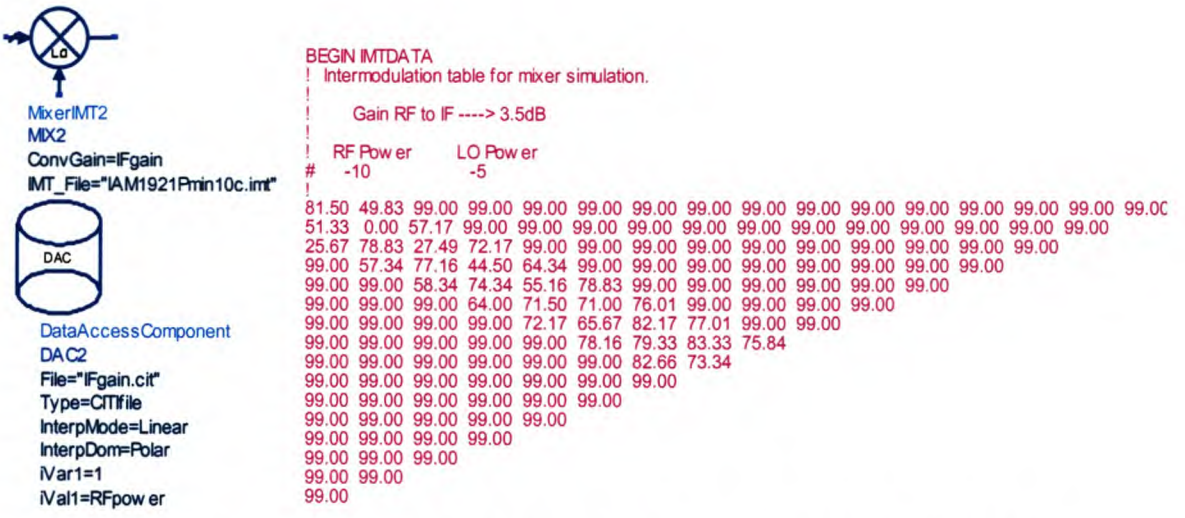


Figure 4.25 This figure show the Mixer IMT model along with the specified IMT file.

While the S-parameters are imported in the same way as the Mixer2 model, the interpretation of the S-parameters and conversion gain is influenced by the IMT data. The MixerIMT leakage terms are specified in two separate ways: the IMT file entries, and the SPij parameters. For example, LO to IF leakage is given by the (M=1, N=0) term in the IMT file as well as the SP23 parameter. When both specifications are given, the total leakage is given by the complex sum of the two specifications. The ADS literature advises the user to omit the specification of SP23 and SP21 in which case the LO to IF and the RF to IF leakages are specified by the IMT file [23].

Another very important aspect of this data based model is the fact that the data in the IMT file is measured data for a specific combination of LO and RF power. These values are specified in the IMT file. The fundamental output term is calculated using the RF input power in the simulation by adding the specified conversion gain. All other signals are then referenced to this output power. This is why the relative power at position M=1, N=1 in the table is zero. For example in Figure 4.25 the output tone at 400MHz corresponds to M=2, N=2. The value at this position in the IMT table is 27.49dBc. The output amplitude for this tone should then be the fundamental output power minus 27.49dB. The input power for the simulation was -10dBm and the gain for this large input signal is 3.5dB. This will bring the output power at the IF frequency to -6.5dBm meaning that the spurious signal at 400MHz should have an amplitude of -33.99dBm. This value is very close to the measured value shown in Figure 4.24. However if the power levels in a simulation are not the exact power levels that the IMT data in the table was measured for, the simulator has to make adjustment to the values in the table. To explain this, the above example is extended as follows:

1. If the RF input signal in the simulation differs from the -10 dBm reference power level listed at the top of the table (Figure 4.25) by a value of X dB, then the number in the table is adjusted. The value is changed by adding (N-1) × X dB to it. According to the ADS literature this manner of adjustment is good for input power levels up to 5 dB greater than the reference signal power [23] .
2. If the local oscillator power level differs from the -5 dBm reference power level listed at the top of the table (Figure 4.25) by X dB, then the number in the table is adjusted. This is

done adding M × X dB to it. According to the ADS literature this manner of adjustment is good for local oscillator power levels from the reference level minus 10 dB to the reference level plus 3 dB.

If these aspects are taken into consideration the MixerIMT model can give very accurate simulations of the spurious responses of a mixer. This will be shown next while the MixerIMT model's performance for a one-tone swept power excitation will be investigated later in this section.

Figure 4.26 shows a portion of the IF spectrum up to 4.5GHz comparing data measured with the spectrum analyzer to the result for a harmonic-balance simulation using the MixerIMT model. The simulation was set up for an RF frequency of 1.9GHz with an LO frequency of 2.1GHz. The setup in Figure 4.19 was used meaning that the IF gain changes for different input power levels. The IF gain in the citi file was taken from a one-tone power sweep while the IMT file was created from a spurious response measurement. The significance of this will be explained later.

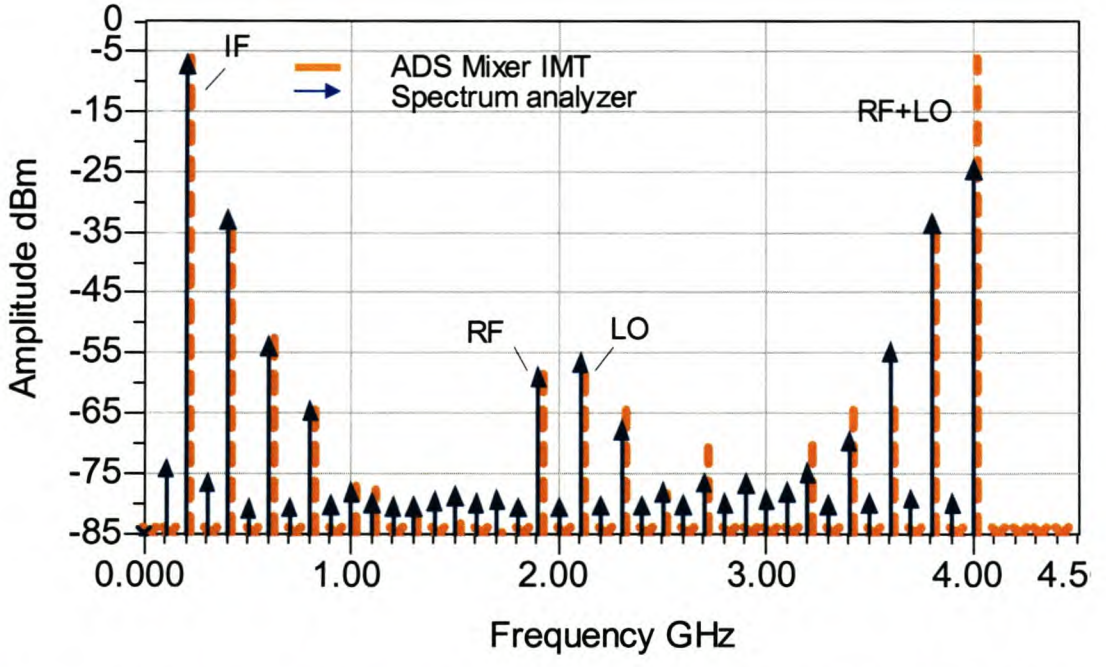


Figure 4.26 This figure shows the output spectrum for the Agilent IAM mixer for the setup of Figure 4.19. While the spurious prediction is vastly superior to that of the parameter-based model, the error is still noticeably large in some cases. The RF input power was -10dBm.

From this figure it can be seen that the MixerIMT model's prediction of the mixer's spurious response is almost identical to the measured data. However there are frequencies where there are some larger errors. These frequencies generally correspond to higher order mixing terms. This is a result of the fact that the conversion gain is not taken from the same measurement that was used to create the IMT file. There will always be a small difference between two measurements of the same device because of the measurement uncertainty. The measured data is specific for a combination of LO and RF signals. However the simulation uses the IMT file as well as the conversion gain specification to produce the various spurious output signals. The IF signal is

produced by adding the conversion gain to the input signal. The rest of the output spectrum at the IF port is calculated relative to this signal by using the IMT file. This will have the effect that the first order IF output signal will be the same as the measurement used to calculate the conversion gain. However the uncertainty between the two measurements will still be present when the spurious responses are calculated. In fact the spurious output signals will be calculated relative to a different IF power level than the one in the IMT file. This means that if the IF resulting from the conversion gain parameter is slightly smaller or larger than the one in the IMT table, this error will not affect the IF output signal but it will affect the higher order mixing terms. However the RF and LO leak signals will be more accurate because of the isolation parameters S21 and S23 as can be seen in the figure. Notice also that the sum term (RF + LO) is exactly the same as the difference term. This is always the case for the MixerIMT model.

The reason for not using the IMT data to calculate the conversion gain is that the mixer in Figure 2.19 is setup for a one-tone power sweep. This is done by changing the conversion gain parameter for different input power levels. Obviously conversion gain parameters for different input signals are not available from one IMT measurement. The conversion gain was specified in this way to enable this model to predict the mixer's behavior under swept power conditions. This technique is used because the MixerIMT model can not receive compression parameters like the Mixer2 model. Figure 4.27 show the result of an identical simulation as for Figure 4.20 performed using the MixerIMT model. It can be seen that the model gives excellent results because its gain was calculated from the spectrum analyzer measurement in the figure. This does however come at the expense of the reduced spurious accuracy discussed in the previous paragraph.

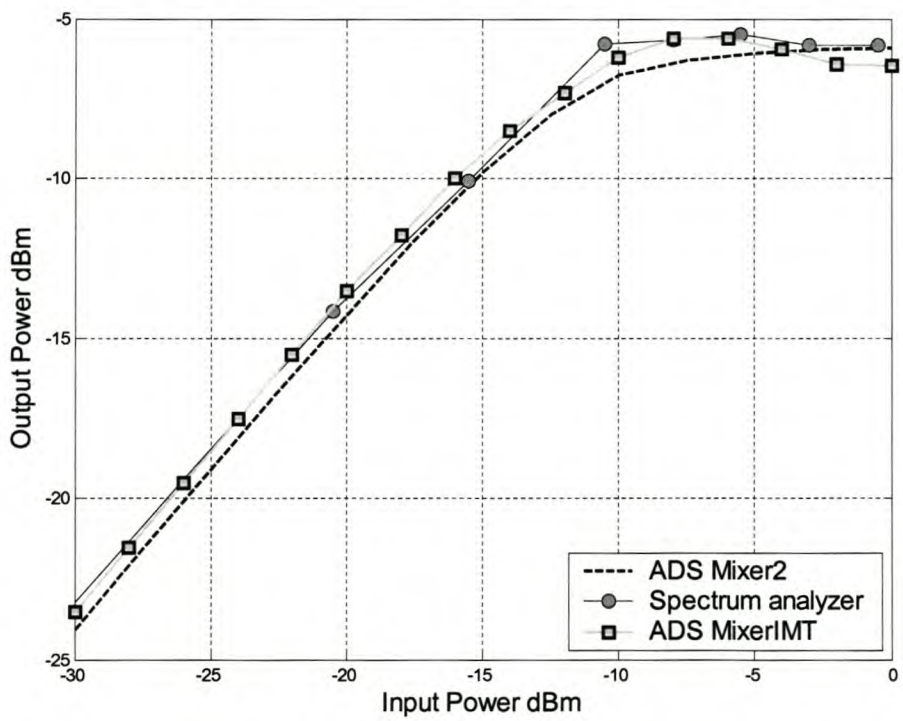


Figure 4.27 This figure compares the two models under swept input power conditions. It can be seen that the MixerIMT model matches the measured data very closely. This is because the swept power conversion gain parameters imported with DAC2 in Figure 4.19 were calculated from this measurement.

While the technique showed in Figure 4.19 gives the IMT model the ability to perform swept power gain compression simulations, it degrades the models spurious response performance which is the model's intended use. The rest of this section will focus on aspects of the models behavior concerning spurious response prediction. While it will be shown that the model can match the measured data exactly if the simulation conditions are equivalent to the conditions of the measurement, the model's ability to adjust to different input signal will be investigated. Figure 4.28 shows the IF output spectrum for the Hittite HMC mixer with an RF signal of -10dBm at 1.9GHz and an LO signal of 13dBm at 2.1GHz. These input signal are in this passive mixers small signal region. In this simulation the setup was identical to the measurement setup used to create the IMT file and it can be seen that the simulated data matches the measured data except for the sum product at 4GHz.

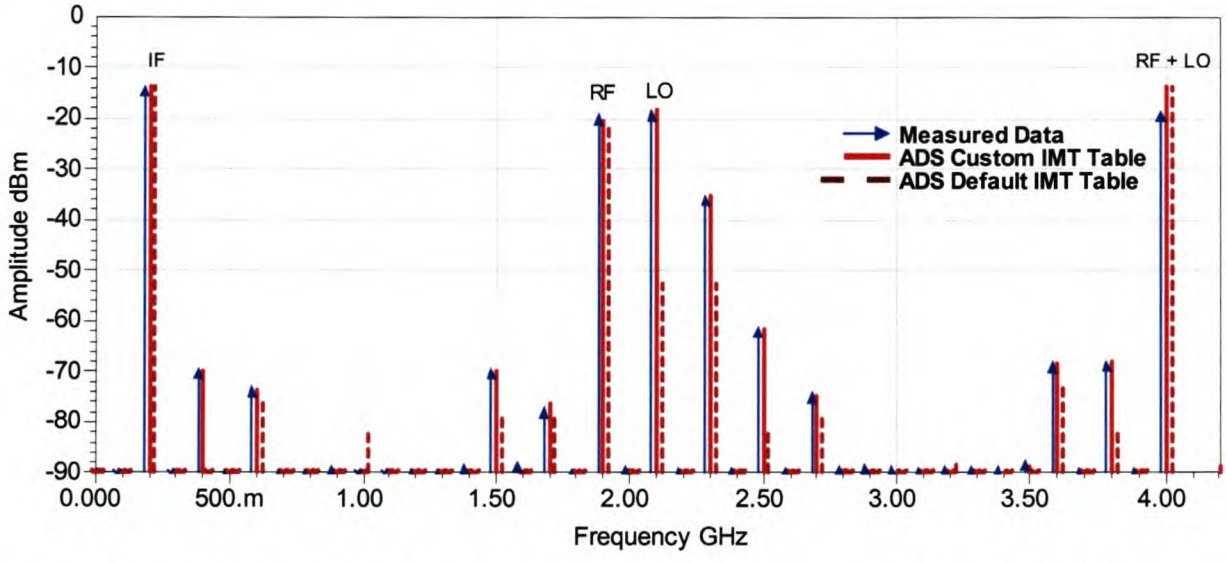


Figure 4.28 This figure shows a portion of the IF output spectrum for the Hittite HMC mixer with an RF input tone of 0dBm at 1.9GHz and an LO input tone of 13dBm at 2.1GHz. The plot compares the measured result to two simulations utilizing different IMT tables.

The default IMT table for a double balanced mixer supplied by ADS does not give very good results. However the simulation using the custom IMT table matches the measured data exceptionally well with the largest error being about 2dB at 1.9GHz caused by the RF to IF isolation issue explained earlier in this section.

While the IMT model can give excellent simulations as shown above, the model's operation is highly dependant on the IMT table. A specific IMT table is ideally only applicable to the input powers and frequencies of the RF and LO signals that it was measured for. It is however impractical to create custom IMT files for every possible input combination. The next two experiments are aimed to test the simulator's ability to adjust the data in the IMT table to accommodate different input signals.

To test the MixerIMT model's ability to predict spurious signals for a different RF input frequency than the frequency the table was created for, the following simulation was performed. The model was setup using the IMT table for an RF signal of 0dBm at 1.9GHz and a LO signal of 13dBm at

2.1GHz. However the simulation was performed with an RF signal at 2GHz and an LO signal at 2.2GHz. This combination will also produce an IF at 200MHz. The result of this simulation is shown in Figure 4.29.

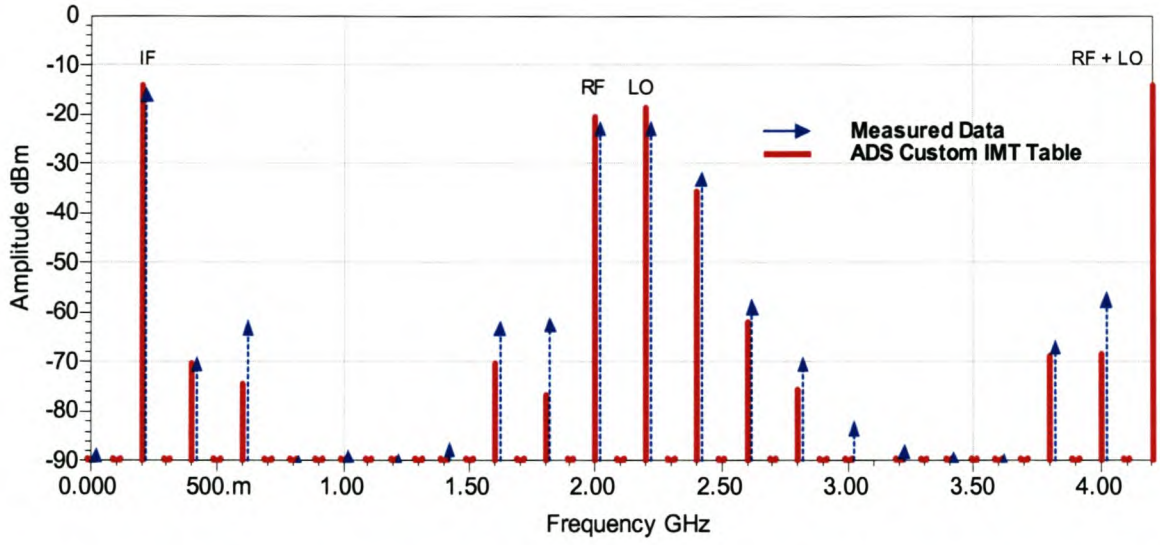


Figure 4.29 This figure shows that the MixerIMT model gives reasonably good results when it is used for a LO and RF input combination that is 100MHz above the frequency the table was created for.

The most important result of this experiment is the fact that although the amplitude values predicted by the IMT table are less accurate, the frequencies where spurious signals occur are accurately predicted. The next experiment used the same setup with a RF signal at 1.9GHz and a LO signal at 2.1GHz. The IMT table was created for an RF input power of 0dBm while the RF power in the simulation was -10dBm.

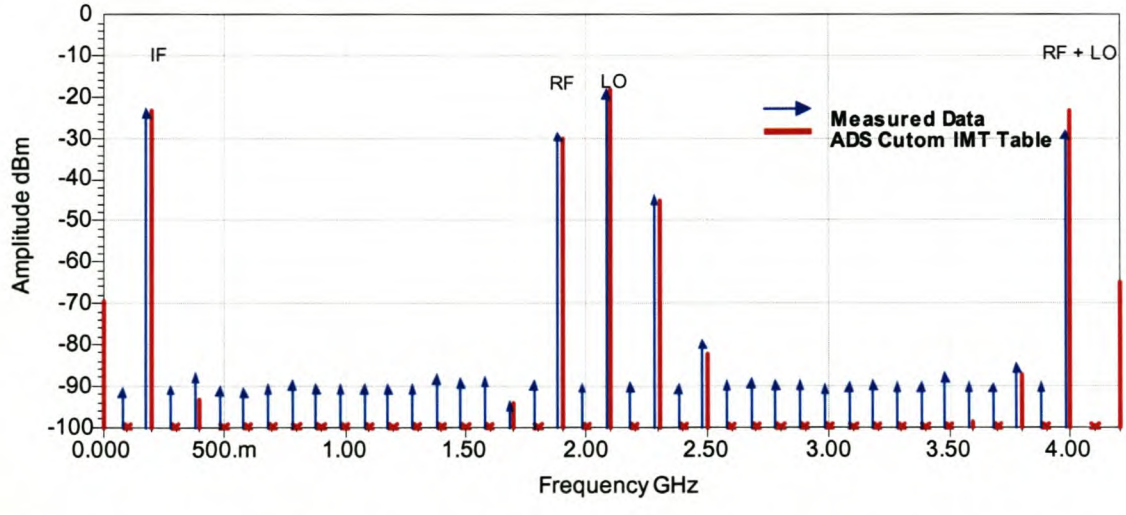


Figure 4.30 This figure shows the model's performance if the RF power is different from the reference RF power that the IMT table was created from. It performs very well if the RF signal is smaller than the reference RF signal.

A final critical aspect to consider when spurious responses are important is the maximum order of the simulation. There are a few places where this can be adjusted. The order of the harmonic-balance simulation determines the number of RF and LO harmonic combinations that will be considered. This is definitely a matter where lower orders will produce faster simulations. Conversely lower order simulations may not include enough harmonics to predict a higher order spur. The order of a simulation is normally set in the simulation component (Harmonic Balance component in this case) where the order of the RF and LO frequencies can be selected. The maximum mixing order can also be specified. In the case of the MixerIMT simulation the RF order basically determines the maximum N value in equation (4.1) while the LO order determines M. These values for M and N are also the indexes for the IMT table and will determine the order of the highest intermodulation product that will be included in the simulation. These values can also be changed in the MixerIMT model. Figure 4.31 shows a spectrum analyzer sweep of the IF output spectrum for the Hittite HMC mixer with the same frequencies that where used in the previous simulations. The RF power was 0dBm. Two HB simulations where performed to predict the mixers spurious responses. One with a RF and LO order of 3 and one with an order of 15.

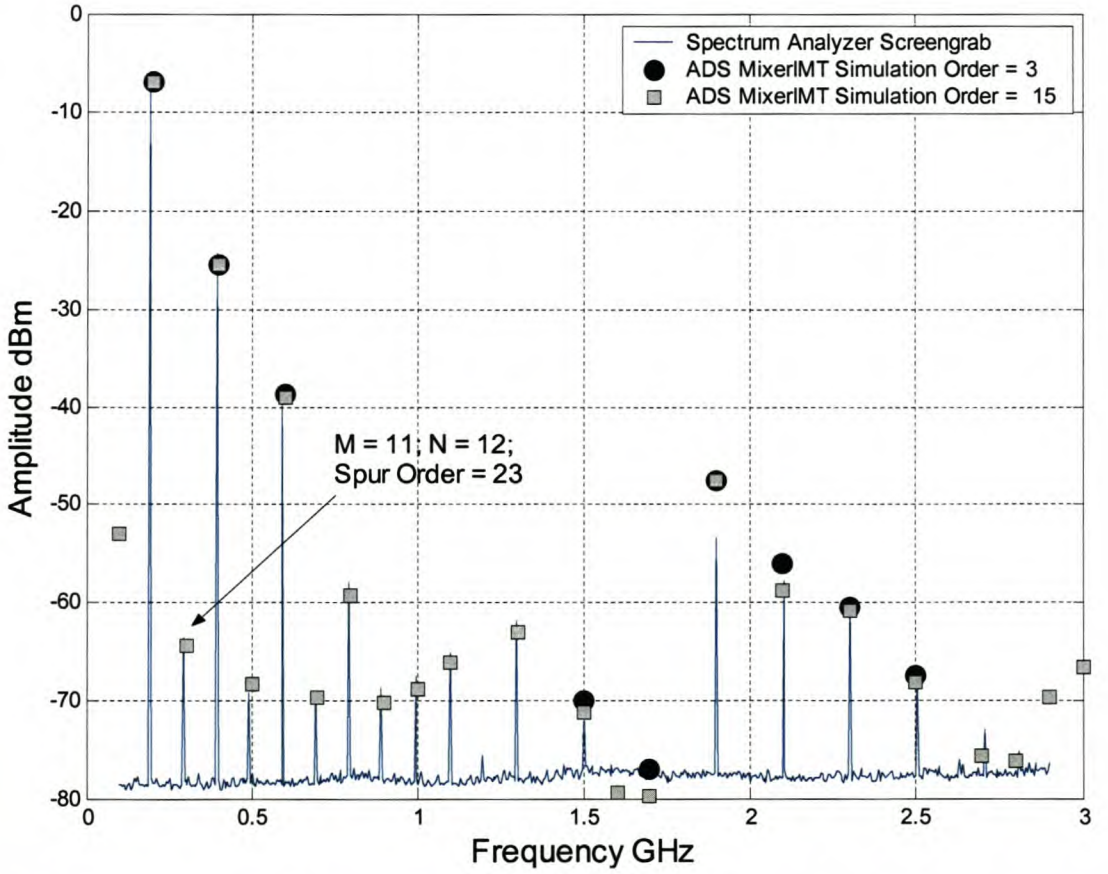


Figure 4.31 The effect of the simulation order can clearly be seen in this figure. The simulation with order 3 can only predict intermodulation spurs up to an order of 6 while the simulation with the RF and LO order = 15 can predict spurs with an order of 30. It can be seen that the spur at 300MHz has an order of 23 which required an IMT table with M and N at least up to 13. The simulation using the higher orders for the RF and LO signals gives far better performance than the lower order simulation.

From Figure 4.31 it can be seen that several spurs where not included for the order 3 simulation. This is because this simulation can only predict spurs up to order 6. As an example the spur at 300MHz is of the order 23 and needed an RF signal of order 11 and an LO signal of order 12. It is also interesting to note that the two simulations give different amplitudes at some frequencies. For instance at 1.5GHz and 2.1GHz. This is because there are more than one spurious response that contribute to the signals at these frequencies. For the lower order simulation these higher order mixing terms are not present resulting in the observed discrepancies.

### 4.2.2 Conclusion

ADS provide two basic mixer models that can be used with measured data. The use of the Mixer2 model is equivalent to the parameter-based amplifier models and gives excellent results for mixer characteristics such as conversion gain, gain compression, isolation and port impedance. The most significant shortcoming of this model is the prediction of higher order mixing terms or spurious responses. The MixerIMT model is specifically designed for this. This model can give excellent spurious prediction when custom measured data is use. The performance of these models is highly dependant on the measured data from which the nonlinear behavior is modeled.

# Chapter 5

# System Simulation

## Introduction

The term system level simulation can be applied to many topics. In this work the term, system, refers to RF receivers consisting off amplifiers and mixers as well as various passive components. Furthermore the models used in these system level simulations are the behavioral models discussed in chapter 2 and chapter 3. The amplifier and mixer models will be used to simulate important receiver characteristics. The previous chapters showed that it is possible to accurately reproduce device behavior from selected measurements using the nonlinear models in ADS. The aim of this chapter is to show the capabilities and shortcomings of nonlinear system level simulation using measurement based behavioral models to predict important receiver parameters. Section (5.1) will discuss receiver gain and gain compression while section (5.2) evaluates the prediction of two-tone intermodulation. The issue of spurs where discussed in chapter 4 and the ability of system simulation to predict spurious signals in a receiver is shown in section (5.3). It has also become increasingly important to evaluate a receiver's effect on a signal with digital modulation and this is the topic of section (5.4).

## 5.1 Gain and Gain Compression

While gain compression was discussed in chapter 3, it should be noted that this phenomena is very important in nonlinear system level simulation. Although it is usually desired that receivers operate in their linear region, the nonlinear behavioral models in ADS rely strongly on gain compression

parameters or data to determine the nonlinear behavior of the device. Gain is also one of the most important parameters for most RF systems and it normally refers to the total power gain of the system under small signal conditions. This section will show that the ADS models can be used to accurately predict the total gain and determine the linear and nonlinear operating regions of a receiver.

Figure 5.1 shows a simple receiver consisting of an ERA6 amplifier and an Agilent IAM-91563 mixer. The receiver was used to downconvert a RF signal at 1.9GHz to an IF frequency of 200MHz. Attenuators were placed at the mixer ports to reduce the effects of mismatch errors between the devices. The attenuators and filters are linear small signal models comprised the measured S-parameters. Note that there are no bandpass filters in either the RF or IF stages of the receiver. While bandpass filters are very important in receiver design they where omitted in this work. This makes it much easier to measure the various spurious signals that are generated in a receiver. The accurate prediction of these spurious signals may be very important in some wideband receivers and will be discussed in section (5.3).

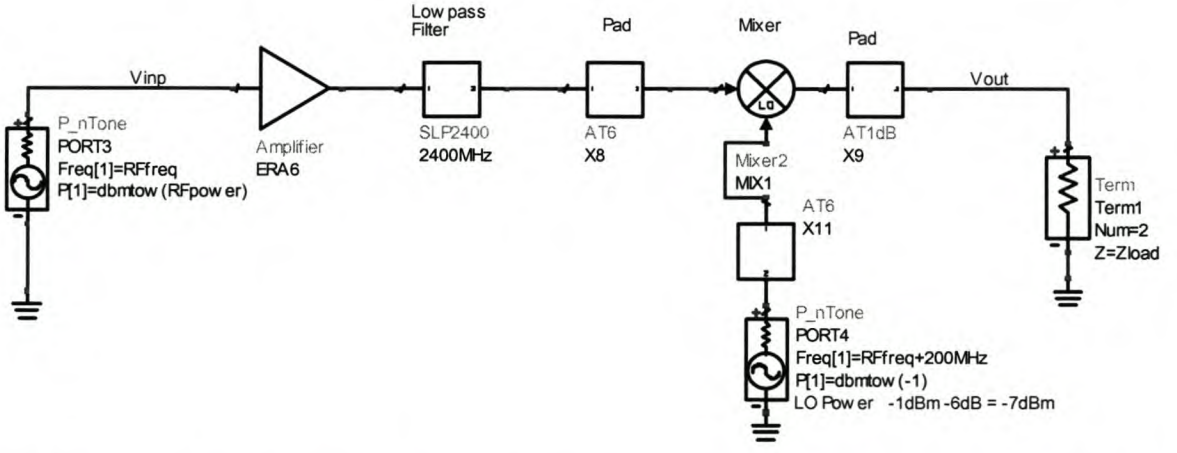


Figure 5.1 Receiver 1 showing the port terminations and signal sources in ADS. Each block is represented by a measurement based model. The filters and attenuators are small signal models consisting of measured scattering parameters.

A power sweep was performed at 1.9GHz to determine the gain of the receiver and this is displayed in Figure 5.2. The gain for the receiver is similar to mixer conversion gain with the gain being the difference in dB between the output power at the IF frequency and the RF input power of the fundamental input tone. The mixer model used for the simulation shown in Figure 5.2 is the Mixer 2 parameter model described in section (4.2.1.1) set up for a fifth order polynomial (parameters are P1dB and TOI). The nonlinear parameters were only included for the specified LO power and frequency (-7dBm and 2.1GHz) and RF frequency (1.9GHz) combination. However the small signal conversion gain is specified from 1.6GHz to 2.5GHz for the appropriate LO power. The amplifier model used is the parameter based polynomial model described in section (3.2.1.1) setup for a ninth order polynomial using measured parameter data. The amplifier's nonlinear parameters where setup to operate from 1.5GHz to 2.5GHz.

From this simulation it can be seen that the small signal gain is within 0.1dB of the measured data. However there is a larger error in the compression region. From the data it can be seen that the compression of the receiver is dominated by the mixer's compression characteristics. The mixer has a 1dB compression point of -10dBm at the output port. This corresponds with a receiver output power of -11dBm because of the 1dB attenuator at the output port.

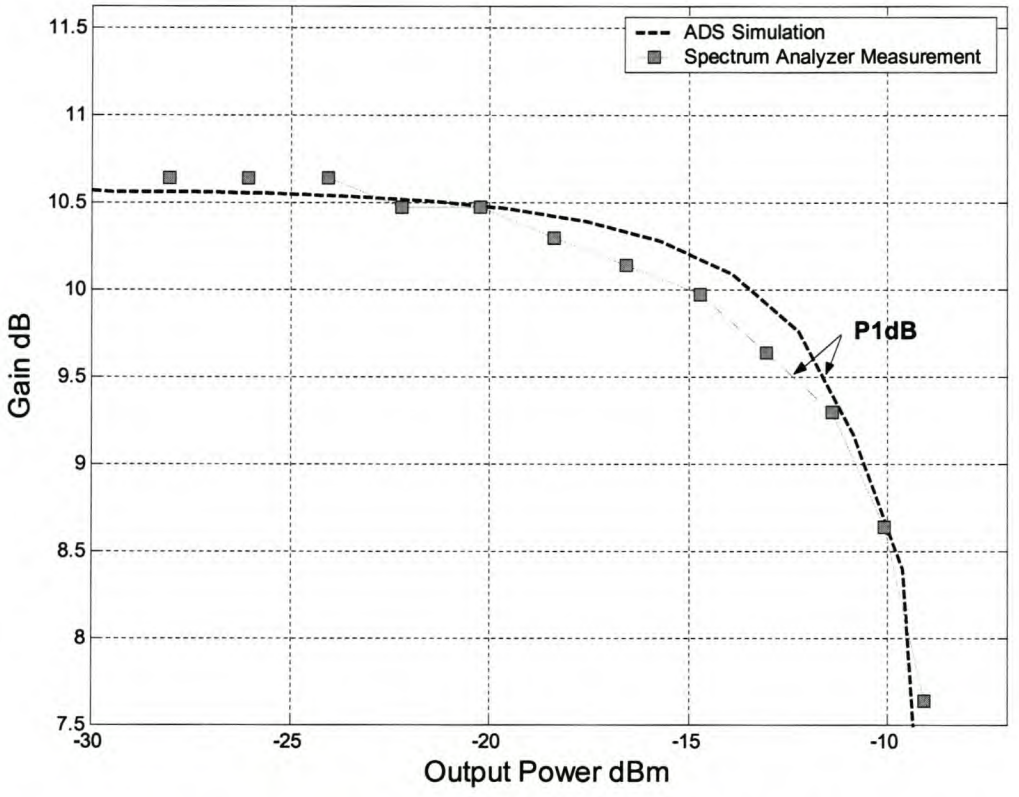


Figure 5.2 This figure shows the gain versus output power for the simulation described in the above paragraph. It can be seen that the results compare well to measured data for the receiver. The small signal gain is within 0.1dB. However the error in the 1dB compression point is approximately 1dB.

It was shown in section (4.2.1.1) that a fifth order polynomial model is only adequate to approximately predict the mixer's behavior in the compression region. The 1dB discrepancy between the measured and simulated data can be ascribed to the mixer model's limited accuracy in this region. It can be seen from this simulation that the receiver has a gain of 10.5dB and a 1dB compression point in the region of -12dBm as a result of the mixer's output power limitations.

Another simulation was performed with a similar receiver, shown in Figure 5.3. The mixer for this receiver is the Hittite passive mixer and has a conversion loss of approximately -12dB. To compensate for this loss another amplifier, the ERA 33, is added to the RF portion of the circuit. While the same measurement based parameter models are used for the amplifiers, the mixer model is the data based MixerIMT model. For this model it is important that the IMT file used in the simulation corresponds to the estimated input power at the mixer's RF port. The IMT file should also be in the range of the LO power and frequency as well as the RF frequency. The same simulation was repeated for this receiver for and RF frequency of 1.9GHz and a LO frequency of

2.1GHz at 13dBm. The simulation was repeated with two different IMT files. The first IMT file was created using data from a measurement with a RF input power of 10dBm while the second IMT file was created from a measurement with an RF input power of 0dBm. The traces for the two simulations are labeled Data1 and Data2 respectively in the Figure 5.4.

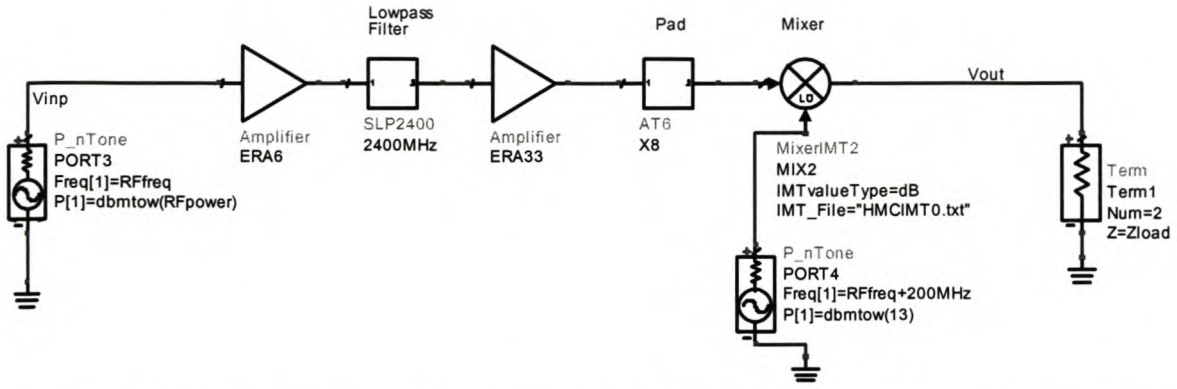


Figure 5.3 Receiver 2 consisting of two parameter-based amplifier models and a data-based IMT mixer model. The passive components in this simulation were modelled using measured scattering parameters.

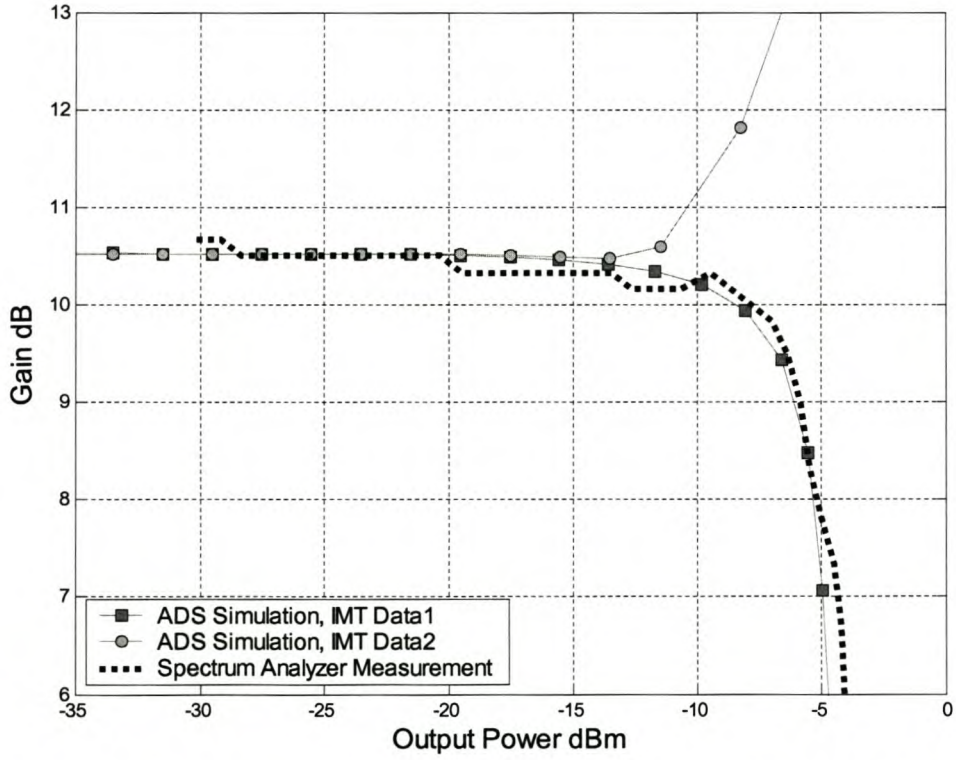


Figure 5.4 This figure shows the results of swept power simulations for Receiver 2. The simulation trace labeled "Data1" was performed with an IMT file for an RF input power of 10dBm while the trace labeled "Data2" was for the same simulation using an IMT file created for a RF input power of 0dBm.

Figure 5.4 shows that the maximum output power for this receiver is limited by the ERA33 amplifier. The compression region corresponds to output power levels of the ERA 33 amplifier in the range of 12dBm which is close to the values found for this amplifier in Chapter 3. Because of this the Hittite mixer, having an input 1dB compression point of 10dBm, will operate in its linear region. The error for the trace with the 0dBm IMT file is a result of the ADS simulator adjusting the values in the IMT table (section (4.2.1.2)) for the input power level present at the mixer's RF port. From this simulation it can be seen that the adjustment is accurate for RF power levels smaller than the RF input power specified by the IMT file. However if the power at the mixer's RF port is larger than the power level in the IMT file the resulting IF output power will be too large. This simulation has shown that the MixerIMT model can give good simulation results if the correct IMT file is supplied. The 1dB compression point for this receiver is accurately predicted by this simulation as -6.7dB which is very close to the measured value of -6.4dBm. The improved accuracy in the compression region can be attributed to the higher order polynomial models used to model the amplifiers which dominate the compression effects in this receiver.

The simulations shown in Figure 5.2 and Figure 5.4 showed that the models can accurately predict the gain of a receiver at a single frequency point. Figure 5.5 shows a swept frequency simulation of Receiver 1. The RF input power for the simulation was -30dBm to ensure that the Receiver was operating in its linear region.

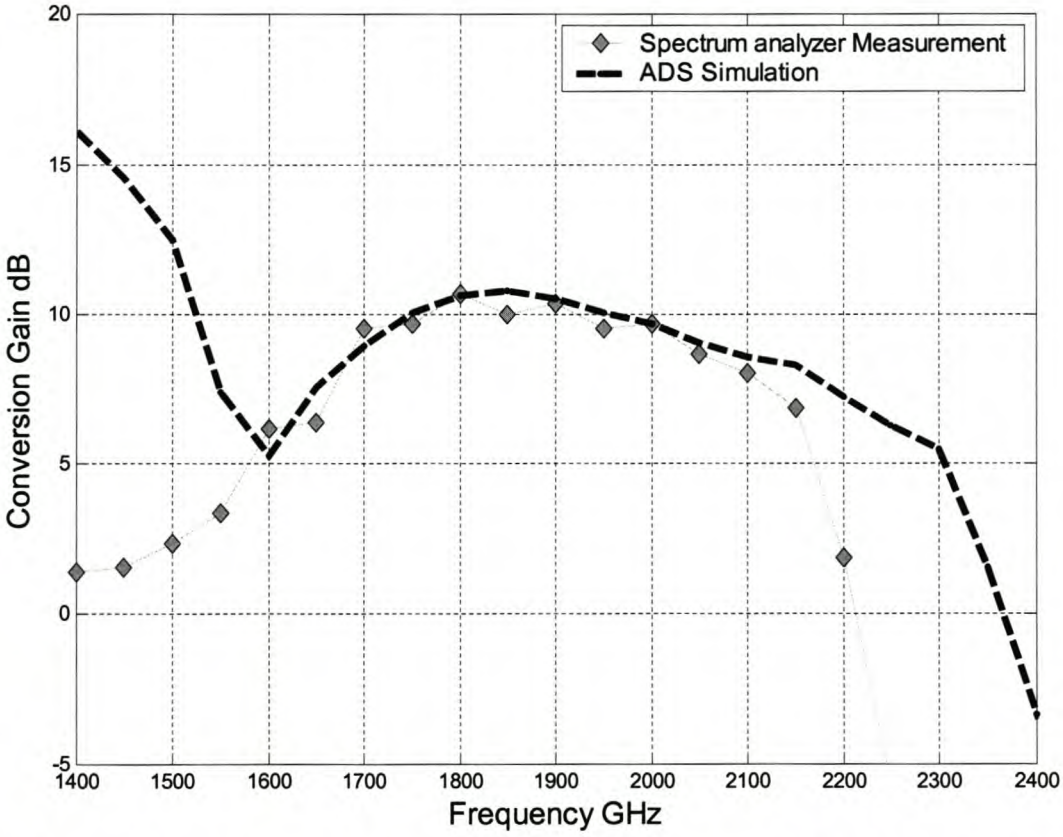


Figure 5.5 This figure shows the result of a swept frequency simulation for Receiver 1. The input power of -30dBm is in the receiver's linear operating region. While the gain is accurately predicted in the region between 1600MHz and 2100MHz there are very large discrepancies between the measured and simulated data at other frequencies.

From this figure it can be seen that there are very large errors for RF frequencies below 1.6GHz and above 2.1GHz. The conversion gain for this model is specified from 1.6GHz up to 2.5GHz in 50MHz steps. The large error below 1600MHz is a result of incorrect extrapolation of the conversion gain for frequencies below this value. However the error above 2100MHz can not be attributed to this because the conversion gain is specified up to 2500MHz. This error is a result of the fact that the compression parameters for this model are only specified at 1.9GHz. The measured data shows that the gain of the receiver falls drastically above 2.1GHz. This drop in gain is as a result of the mixer compression characteristics at the higher frequencies which is different from the compression parameters at 1.9GHz. Figure 4.22 in section (4.2.1.1) showed that the mixer goes into compression for much lower power levels at frequencies above 2GHz than the power level specified at 1.9GHz. This type of problem can be corrected by supplying the appropriate compression parameters for the frequencies that will be simulated.

This section has shown that the gain for these fairly complicated systems can be predicted accurately using these models. The accuracy in the linear region was within ±0.1dB. The gain was also predicted accurately in the compression region with a maximum error of 1.5dB at 5dB gain compression.

## 5.2 Two-Tone Intermodulation

Two-tone intermodulation is a very important measure of the nonlinearity of a component or system. This nonlinear phenomenon is discussed in chapter 3. However where more than one nonlinear device is cascaded to realize a receiver, it becomes even more important. The most obvious reason that intermodulation can be a potential problem is the fact that it causes unwanted in-band spurious products. This problem is increased in the case of a receiver where there is more than one active device that can cause intermodulation. Take for instance Receiver 1 in Figure 5.1. If a two-tone excitation is applied to the input of the receiver the Era 6 amplifier will cause intermodulation products. The resulting spectrum at the input to the mixer will consist of the amplified original two-tones as well as all the intermodulation products cased by the nonlinearity of the amplifier. The original two-tones as well as different combinations of the various intermodulation products will cause intermodulation at the mixers output port. Furthermore the intermodulation products caused by the amplifier will also pass through the mixer and the resulting output from the mixer will be the vector sum of the amplifier's intermodulation as well as the mixer's intermodulation products. This has the effect that the intermodulation accumulates in a system such as a receiver [31, 32]. This effect is degrading to the overall dynamic range of the system. It is also possible that the multi tone input to the mixer will cause additional intermodulation frequencies not caused by a pure two-tone signal. For these reasons it is not only important that a receiver simulation can predict the intermodulation products around the IF tones correctly, but also that it will identify any other unwanted spurious signals that may be a result of the multi tone signals at various points in the receiver.

The first simulation in this section shows the result of a two-tone swept input power excitation applied to Receiver 1. This is essentially the same measurement described in chapter 3 with the only exception that the output power is measured at the IF frequency. The simulation was performed for a two-tone signal at 1.9GHz with a tone spacing of 1MHz. The receiver has an IF frequency of 200MHz. The Mixer2 measurement based parameter model was used for this

simulation. The results are shown in Figure 5.6. This figure shows the input versus output power plot for the upper fundamental and the third order intermodulation ($2\omega_2 - \omega_1$) tones. The figure also shows the third order intercept point determined by the graphical method as well as the values calculated with equation (3.4).

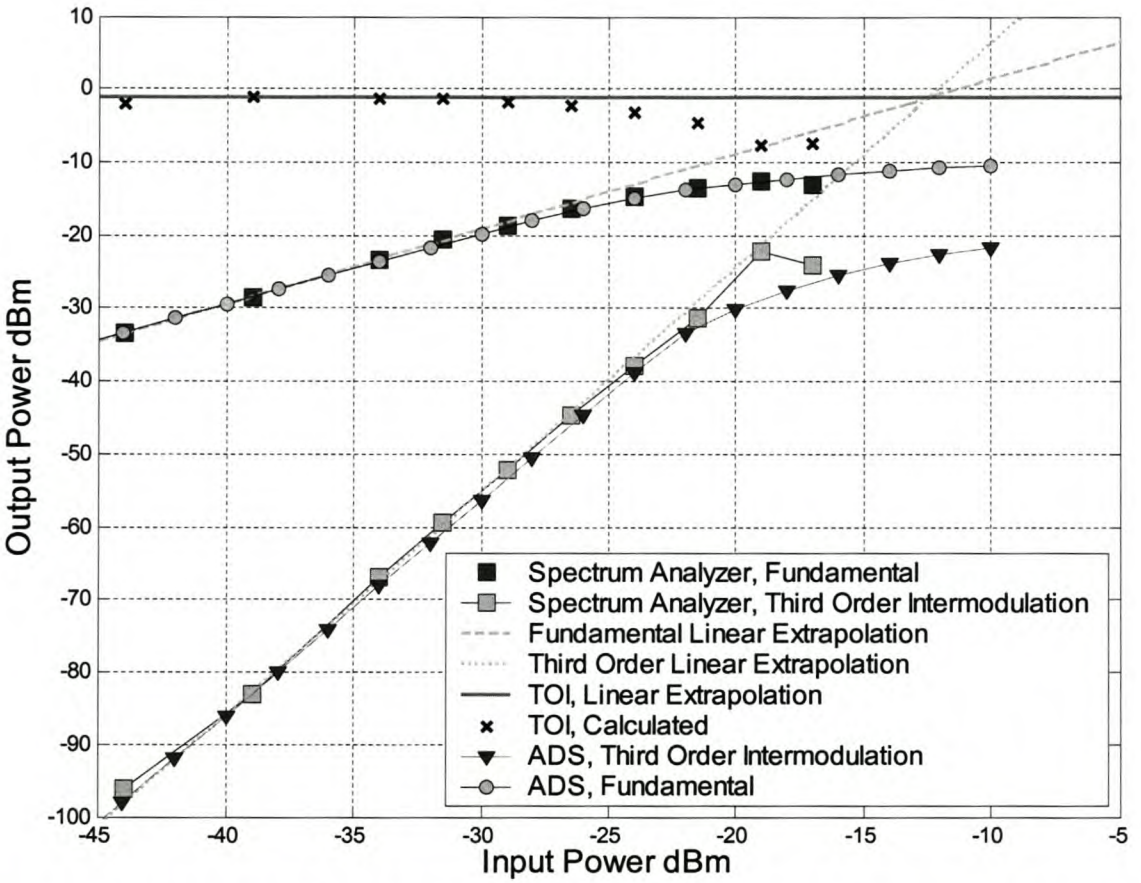


Figure 5.6 This figure shows the fundamental and third order intermodulation tones for a swept input power two-tone simulation of Receiver 1. The simulated data is seen to compare very well with measured data with the third order intermodulation matching the measured data up to approximately -12dBm for the fundamental tone. This is at 2.5dB gain compression. Note that the gain is slightly less than for the one tone case. The TOI point is -1dBm at the receiver's output port.

This figure shows excellent results for the prediction of third order intermodulation even in the compression region. The TOI point for the receiver is -1dBm. The TOI of the mixer alone is approximately 2.5dBm. Including the effect of the 1dB attenuator this should give a TOI of 1.5dBm. However the measured and simulated values obtained for the receiver is -1dBm showing the accumulation effect described earlier. It should also be noted that the conversion gain for the fundamental tones is less for the two-tone excitation than is was in the one tone case. In the two-tone case the receiver has a 1dB compression point at -15dBm instead of -12.5dBm which was the case for the single tone excitation.

The simulation setup that was used to produce the data shown in Figure 5.6 required the harmonic-balance simulator to allow intermodulation up to the ninth order to give the accurate results shown in the figure.

The next figure shows the output spectrum for a two-tone simulation of Receiver 1 with the same setup as the previous simulation. The input power was not swept in this case and an RF input power of -23.5dBm was used. This power level is close to the input1dB compression point of the receiver. Figure 5.7 shows two portions of the resulting output spectrum around 200MHz (IF) and 400MHz.

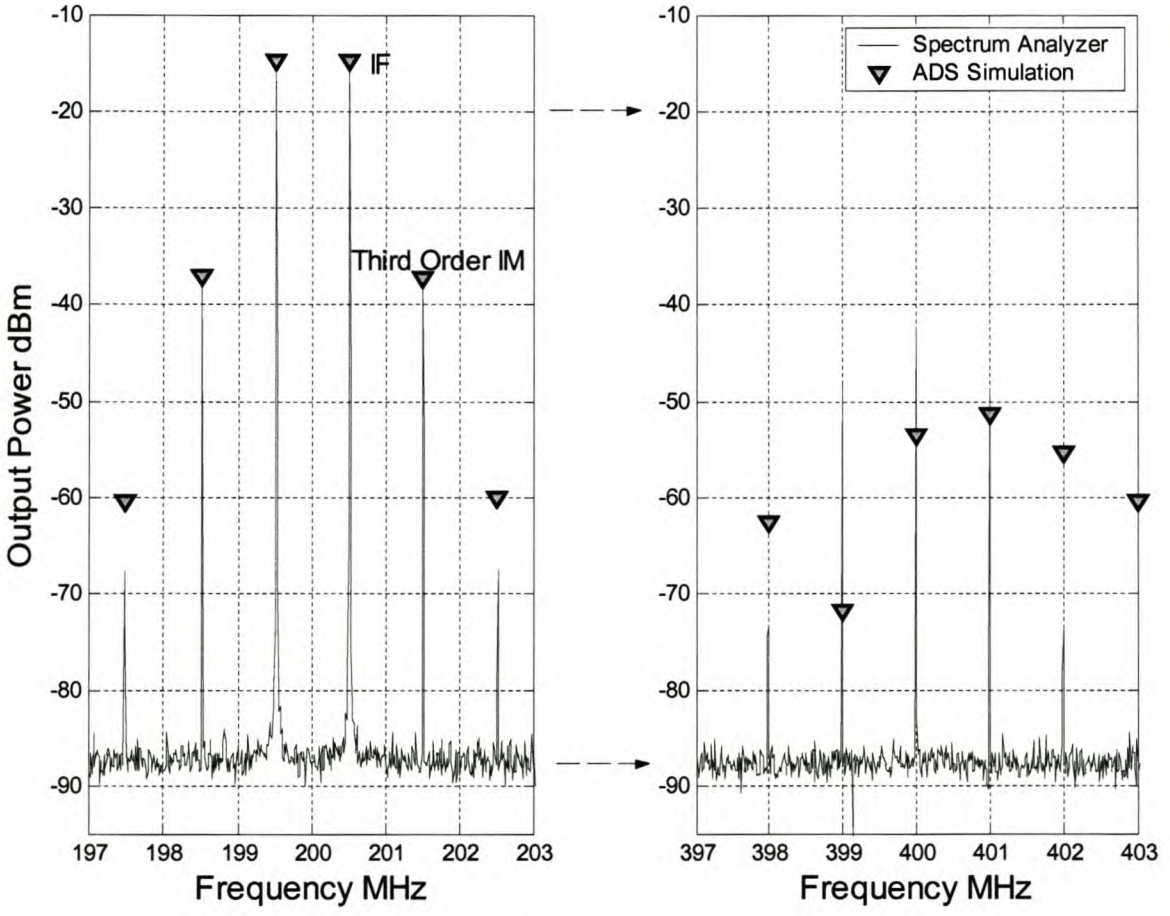


Figure 5.7 This figure shows the output spectrum for a two-tone excitation of Receiver 1 at 200MHz and 400MHz.

For the output spectrum around 200MHz is can be seen that the fundamental and third order tones for the simulation matches the measured values very closely. However the fifth order intermodulation has an error of 6dB. This error can be attributed to the large input tone used in the simulation. The third order assumption described in chapter 3 is usually only applicable in a certain region of the device operation. It was seen in chapter 3 that the fifth order power transfer curve deviates from this assumption for much lower power levels. The portion of the output spectrum around 400MHz was included to show the model's ability to predict intermodulation around frequencies other than the desired IF frequency. A discussion of the possible frequencies

that can be produced for a two-tone excitation of a mixer can be found in [24]. The tones shown in the figure are all intermodulation products with an order of 7 or lower. Even though the amplitude values of these tones are not very accurate they do supply valuable information about these spurious signals that are produced by the receiver. Although more accurate results are usually obtained by including higher intermodulation tones in the harmonic-balance simulation, the simulation time and computer memory required for intermodulation orders higher than 9 becomes impractical.

## 5.3 Spurious Signals

This section will show the ability of the models from chapter 3 and chapter 4 to predict the spurious responses characterized by equation 4.1 when used in a receiver. While this type of spurious signal is normally not a very serious problem in narrowband systems, they may be very important in certain applications such as wide band receivers that may have very large IF bandwidths. The receiver shown in Figure 5.8 is an example of a wideband spectrum monitoring receiver. In a system such as this, the correct prediction of spurious signal products can be critical.

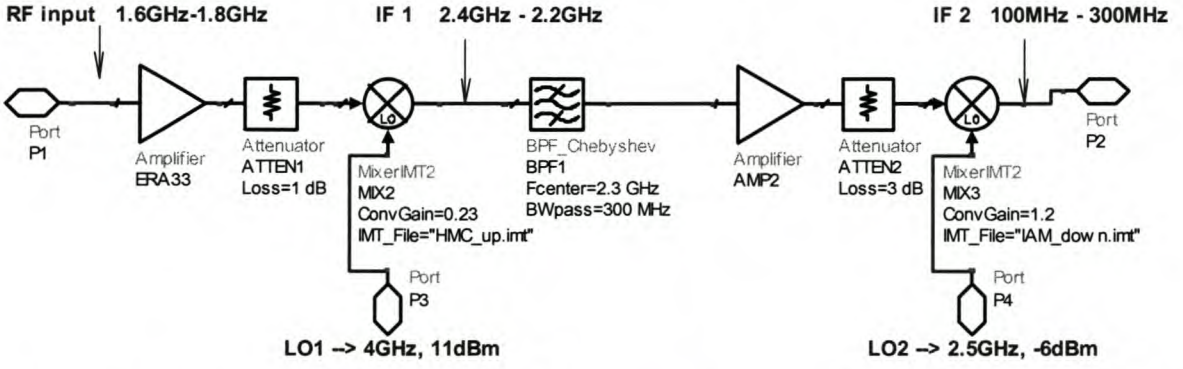


Figure 5.8 This figure shows a wideband receiver designed to downconvert the entire frequency band from 1.6GHz to 1.8GHz simultaneously. Because this receiver has a very wide IF bandwidth (100MHz to 200MHz), spurious responses in the IF band is crucial to the design. The amplifiers are both ERA 33 amplifiers. The first mixer is a Hittite HMC178 passive mixer while the second mixer is the Agilent IAM mixer.

The type of receiver in Figure 5.8 is used in wideband applications where an entire frequency band is downconverted simultaneously. In other words the receiver does not sweep over the band in question but down converts the entire spectrum to a wideband IF where it is normally digitized. Receivers like this one are normally used to monitor a certain frequency band and therefore any in band spurious signals will be mistaken for real world signals. However, because of this wideband architecture, these receivers are vulnerable to spurious responses and careful design is necessary. The purpose of the upconvering stage will be explained with an example. If a receiver like Receiver 1 were to be used, there would be serious problems with image frequency spurious responses. For instance a tone at 1.6GHz would need either a LO frequency of 1.7GHz or 1.5GHz to be down converted to 100MHz. A LO of 1.7GHz is out of the question as it is in the RF bandwidth. For an LO of 1.5GHz the image frequency is 1.7GHz which again is in the RF band and can not be filtered. This type of spurious response is discussed in chapter 4, section (4.1.3.1A).

However, the addition of a second mixer makes the receiver more susceptible to the type of spurious response of chapter 4, section (4.1.3.1B). This will happen because the second mixer will have a multi-tone input signal that may produce even more spurious responses in the IF band than would be the case for a single mixer. This effect can be minimized by the bandpass filter and careful selection of the two LO signals. Because the fist stage uses high side injection to upconvert the desired RF band, most spurious signals will be far removed from the 2.2GHz to 2.4GHz passband of the filter. This happens because a relatively large LO frequency is necessary to accomplish this. The bandpass filter will remove the out of band spurious signals and leak signals and the resulting spectrum is amplified. The second mixer then downconverts the filtered output band to IF 2.

This type of receiver is considerably more complicated than the first two receivers as far as the number of devices and possible frequency components are concerned. Because it is used in applications where knowledge about low level spurious signals is essential, it was used to verify ADS's ability to predict spurious responses in a complicated system. Figure 5.9 shows the measured and simulated output spectrum for a simulation performed for this receiver.

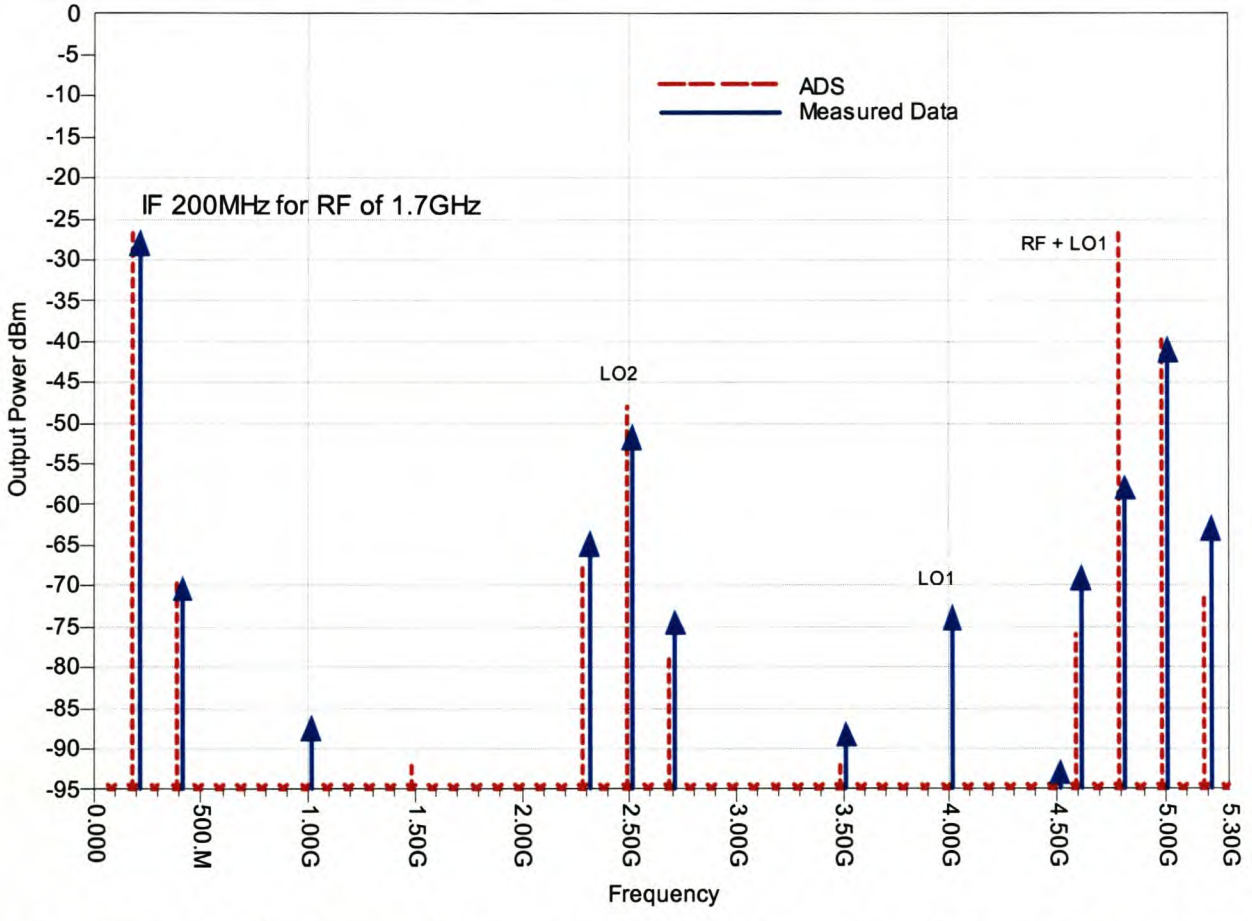


Figure 5.9 This figure shows the output spectrum for the receiver of Figure 5.8 with an RF input of -45dBm at 1.7GHz. It can be seen that the gain for the receiver is 18dB. While the measured data is very close to the simulated data for the IF tone as well as many other of the spurious responses, there are some frequencies where very large discrepancies occur.

The results in Figure 5.9 shows that the simulation gives accurate spurious prediction for the fundamental and spurious signals that may be close to the desired IF frequency. However there are a number of frequencies where there are large errors in the level of the spurious output signals. These errors are the result of a number of aspects of this type of simulation that need to be taken into account.

The first and most obvious error is the large output tone at the sum frequency (4.8GHz) at the output of the second mixer. This was explained in chapter 4 and is a result of the symmetrical intermodulation file. This has the effect that the sum and difference frequencies will have exactly the same amplitude.

It can be seen that many of the other cases where the simulated data does not match the measured data is at higher frequencies and are higher order mixing terms. These errors can be attributed to the fact that the intermodulation tables that are used are created from measurements at one specific combination of RF power and LO power. If the power level in the simulation is not exactly the same as it was in the measurement, the simulator adjusts the data in the IMT file to adapt to the new power level. This effect was described in chapter 4. The adjustment is progressively larger for higher order mixing terms so that spurious signals of a higher order will show a larger error for a small difference in fundamental power. Another reason for the errors at the higher frequencies is the fact that the S-parameters that were used to represent the bandpass filter where only measured up to 3GHz. This has the effect that certain spurious tones are not present in the simulated data while they have significant amplitudes in the measurement. Examples of this can be seen at 1GHz and 4GHz. The extrapolated attenuation of the filter at the higher frequencies is larger than the real world case which has the effect of attenuating certain signals in the simulation more than is the case in reality. This problem can be corrected by using S-parameter data measured up to higher frequencies.

There is another error than can occur in systems such as this one where a mixer is followed by an amplifier. The IMT table usually includes the power levels of spurious mixing terms in dBc relative to the fundamental (second order) mixing term. However if this table is created using measured data there will be a limited dynamic range to the measurement. If a mixing term can not be measured the power level of the noise floor of the measurement is usually used for that mixing term in the IMT table. In a simulation these spurious tones will therefore have power levels higher than the actual power levels because they were too small to measure. While this noise floor power level is usually very low, it can create errors if the mixer is followed by and amplifier. This can be seen in Figure 5.9 at 1.5GHz where a tone is present in the simulated data but not in the measured data. In this case the intermodulation table had a value equal to the noise floor. While this value is lower than the minimum value of -95dBm for this figure, the tone was amplified and can now be seen while it should not be there. This can have the effect that many low level spurious signals are produced from the noise floor of the measurement. This problem can be avoided by manually decreasing the noise floor values in the intermodulation table. It will also not be a problem if the measurement used to create the intermodulation table has a noise floor that is significantly lower than the noise floor that will be considered in the simulation.

The simulation described above showed that the combination of parameter based amplifier models and MixerIMT intermodulation mixer models give excellent spurious prediction. However the accuracy is largely due to the use of custom intermodulation tables measured for a specific excitation. If the simulation parameters deviate from the parameters the data was measured for,

errors will start to get larger. The next simulation was performed with exactly the same setup as the previous simulation for the receiver shown in Figure 5.8 with an additional 3dB attenuator at the output port. The LO signals were the same as well as the RF input power. The input frequency was stepped across the RF input band from 1.6GHz to 1.95GHz in 50MHz steps. However, the same intermodulation tables that were measured for an input frequency of 1.7HGz at -45dBm were used for both mixers at all input frequencies. The purpose of this simulation is to use the intermodulation models for frequencies other than the frequencies of the measured intermodulation data in the IMT tables. This wideband application is an example of the type of simulation where the MixerIMT model can give a designer insight into problems that may arise as a result of spurious signals at several possible frequencies. The results are shown in Figure 5.10 where the simulated results are compared to measured data. The simulation was repeated for each frequency point but the results are displayed on the same plot. The gain is less than in Figure 5.9 because a 3dB attenuator was included at the output port. This receiver downconverts 1.6GHz to 100MHz, 1.7GHz to 200MHz, 1.8GHz to 300MHz and so on.

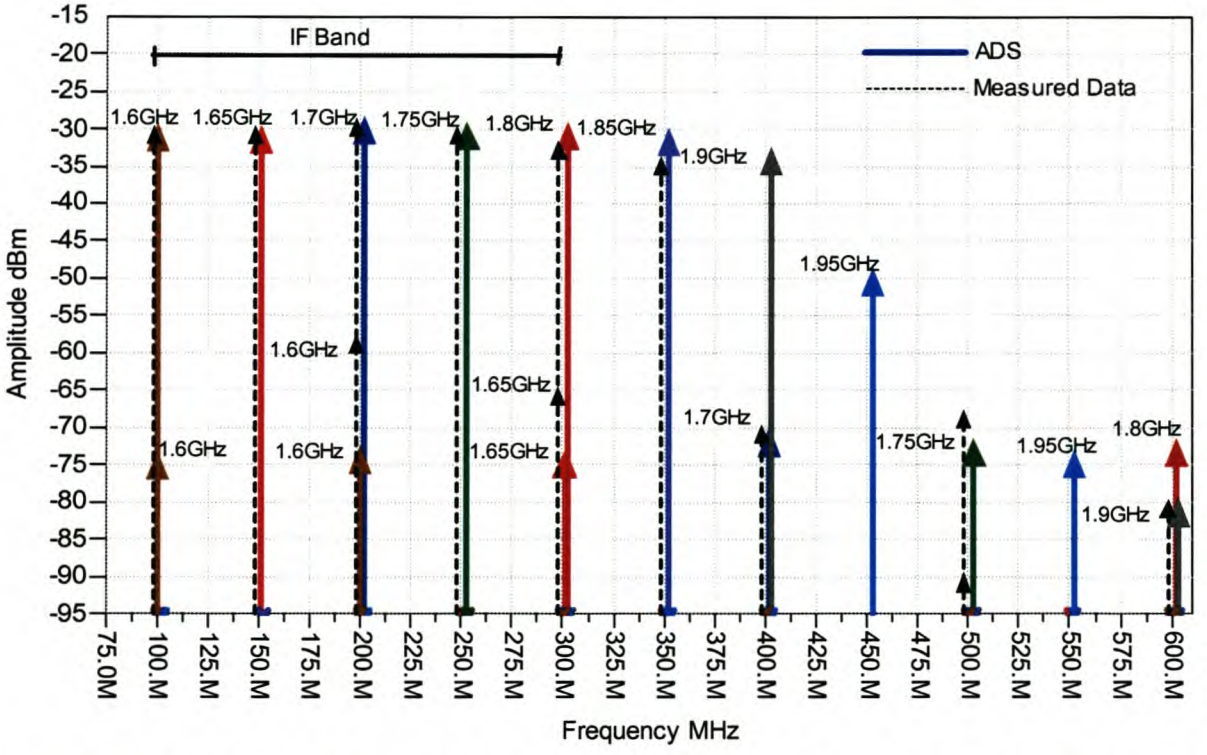


Figure 5.10 This figure shows the results of 8 separate simulations of the receiver shown in Figure 5.8 with the only adjustment being the addition of a 3dB attenuator at the output port. The mixer intermodulation tables where measured for the case where the input frequency was 1.7GHz at -45dBm. The measured and simulated results for this case compare very well as can be seen for the second order mixing term at 200MHz and for the spurious signal at 400MHz. The second order mixing terms for input signals close to 1.7GHz are also very accurate (100MHz to 300MHz) although the spurious signals for these input signals show errors as large as 13dB (spurious signal at 200MHz as a result of a 1.6GHz input tone).

This figure shows that the intermodulation tables measured for a 1.7GHz input frequency does not give accurate results for other input frequencies. The second order input tones are accurate for

signal close to 1.7GHz with the input signals at 1.6GHz to 1.85GHz showing errors of less than 2dB when compared to measured data. However it can be seen that the prediction of spurious signals are not very accurate. The spur at 400MHz is produced by an input signal of 1.7GHz and is therefore accurately predicted. However it can be seen that all the other spurs in the simulation have approximately the same level as this case which is what can be expected from using the same intermodulation table. For instance the spur at 300MHz is a result of the input frequency at 1.65GHz downconverted to 150MHz. This spur shows a 10dBm error when compared to measured data. From this simulation it can be seen that the models are inherently narrowband and are strongly dependant on the measured data.

Even though these results are not very accurate they are still useful to the designer. From Figure 5.10 it is clear that the desired IF bandwidth from 100MHz to 300MHz can not be realized because of spurious signals. This IF band coincides with input frequencies from 1.6GHz to 1.8GHz. From the figure it can be seen that input tones from 1.6GHz to 1.65GHz will generate in band spurious responses. The receiver will only operate as desired for frequencies from 1.65GHz to 1.85GHz. The gain starts to decline above 1.85GHz as a result of the bandpass filter. The setup above was used to determine the origin of the in band spurious signals. It was determined that the second mixer was the case of the spurs giving the designer the choice of changing the IF band or using a different mixer.

This type of simulation is a powerful way of analyzing spurious performance as can be seen from this relatively complicated example. Even though the technique is limited to narrowband applications around custom measurement points, it can give frequency information on possible spurious signals resulting from other input frequencies. The following section will investigate simulations with digitally modulated input signals.

## 5.4 Digitally Modulated Signals

Digital modulation has become a very important field in communication. While the one-tone and two-tone simulations give a good representation of how a receiver will influence an analog signal, digitally modulated signals are different from analog signals in many aspects. This section will investigate the ability of the models characterized with analog signals to predict the effect of a receiver on a digitally modulated signal. Digital signals are generated by modulating a high frequency carrier wave using a base-band digital signal. While there are various digital modulation schemes [31, 33] they all have the effect of changing the time domain signal in discrete steps of phase, frequency or amplitude. Because of this digital signals often occupy large areas of the frequency spectrum. The exact frequency, magnitude and phase at any given time depend on the input data bits and the modulation scheme. Digital tests are usually performed using pseudo-random bit sequences as data input. Digital signals have noise like characteristic in the frequency domain and this makes spectrum analyzer measurement of these signals dependant on the spectrum analyzer's resolution bandwidth. This will be shown in section 5.4.2 along with an example of a receiver simulation. The complicated nature of digitally modulated signals also poses a problem for conventional harmonic-based simulation. Envelope analysis is discussed in section 5.4.1.

### 5.4.1 Envelope Analysis

Envelope analysis was developed to handle modulated signals and is specifically important for simulations using digitally modulation. This technique combines features of time and frequency domain schemes to give efficient and complete analysis of complex signals [34, 35]. The basic idea of envelope analysis is to sample the complex envelope of a signal in the time domain, performing a harmonic-balance simulation at each sampled point in the frequency domain. This can be done because a modulated waveform can be represented by a complex envelope (containing magnitude and phase data of the modulated waveform) and a high frequency carrier component as described by equation (5.1) [3].

$$s(t)=\mathrm{Re}\{s_e(t)\}\,\mathrm{e}^{j\varpi_c t} \qquad 5.1$$

In this equation, $s_e(t)$ is the envelope function modulating a carrier signal of frequency $\omega_c$. If such a waveform is distorted by a nonlinear circuit it will generate harmonics of the carrier. The envelope will also be distorted. The envelope function varies slowly compared to the carrier function and if the waveform is sampled at a rate determined by this envelope function, a much lower sampling rate is required.

The first step in envelope simulation is to sample the envelope of the waveform in the time domain. This can be seen in Figure 5.11. After the time-domain sampling the tone at each time point is applied to the nonlinear circuit resulting in a separate output spectrum at each time point.

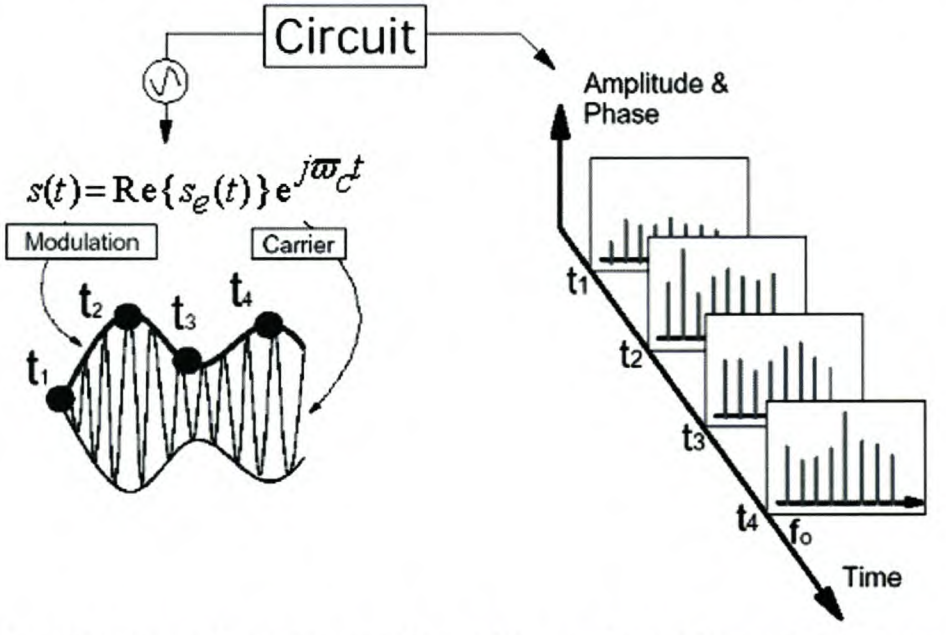


Figure 5.11 This figure shows the sampling of the envelope of the modulated signal in the time domain at time points $t_1$ to $t_4$. At each time sample a harmonic-balance simulation is performed using the tone acquired from the sampling. This tone is applied to the nonlinear circuit (harmonic-balance) in the frequency domain resulting in an output spectrum at each time point. This is shown to the right of the figure [34, 35].

The time varying spectrum can be used to obtain the modulated output spectrum around each harmonic. This is done by constructing a time domain signal by sequentially linking harmonics at the same frequency at different time points. This will give a sampled time domain signal for each frequency point in the spectrum. This process is shown in Figure 5.12.

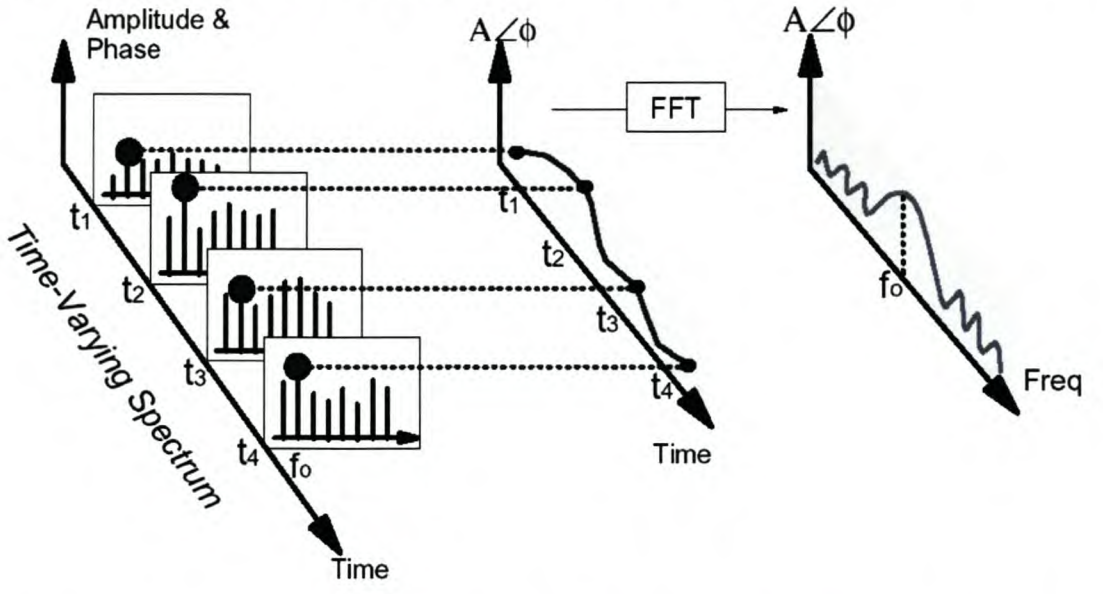


Figure 5.12 The time varying output spectrum obtained from the consecutive harmonic-balance simulations can be seen to the left of this figure. Using the tones a sampled time signal can be constructed at each frequency point. Applying the Fourier transform to this time signal will result in the output spectrum around the frequency [34, 35].

If this time domain signal is converted to the frequency domain, the modulated spectrum around each harmonic component can be calculated. Because the output from an envelope simulation is a time varying spectrum, it is possible to calculate instantaneous magnitude and phase at each harmonic. This makes envelope simulation suited to analyze digitally modulated signals, such as QPSK and QAM. This does however require the nonlinear models used to represent the circuit to have both amplitude and phase descriptions. The following section shows an example of the use of envelope simulation to analyze the effect of a receiver on $\pi$/4DQPSK signal.

### 5.4.2 Envelope Simulation of Digitally Modulated Signals

One of the most common digital modulation techniques is QPSK. The specific variant that was used for this simulation is called $\pi$/4DQPSK. However the specific modulation scheme is not the only important aspect when digital modulation is used. Digital signals are often also required to adhere to certain standards that ensure compatibility of signals and devices manufactured by different companies. In standards like GSM, this type of specification is used to stipulate factors such as maximum bandwidth and channel power to a signal. There are many important aspects depending on the specific application. The communications standards often require that the baseband signal is filtered using a digital technique called baseband filtering. The detail of the

different aspects of digital modulation and standards is a very large topic and not in the scope of this work. The aim of this section is to show an example of this type of simulation. However this poses some practical problems. Most digital modulation schemes rely strongly on phase changes in the time domain. A measurement instrument that can measure digitally modulated signals including phase was not available throughout the duration of this work. However a Rohde&Schwarz FSEK signal analyzer was available for a short time. This instrument is a spectrum analyzer that has the ability to analyze digitally modulated signals. The example in this section is a very basic comparison between measured results and simulated results in this very large and complicated field.

Figure 5.13 shows an ADS schematic of a receiver that downconverts a $\pi$/4DQPSK signal from 1.9GHz to 200MHz. The bandwidth of the signal is determined by the data rate. This is measured in symbols per second. This type of modulation can transmit 2 data bits for every symbol. For this simulation a symbol rate of 2MHz was used resulting in a signal bandwidth of approximately 2MHz around 1.9GHz.

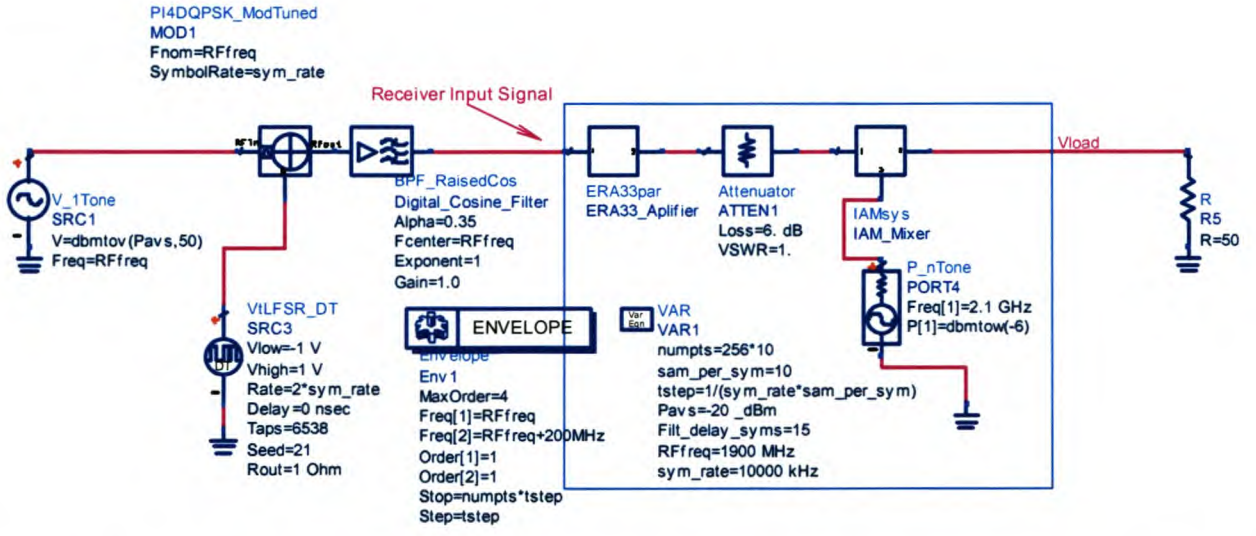


Figure 5.13 This figure shows the setup for a simple simulation using $\pi$/4DQPSK generated by a built-in digital modulator. The data was generated using a pseudo random bit generator that repeats every 8191 bits. This number is significantly larger than the 512 (256 symbols) bits that were considered in the simulation. The mixer and amplifier models are parameter based models created using measured data. The model parameters are specified in 50MHz steps.

The digital filter that is used to shape the signal in Figure 5.13 is a raised-cosine digital filter. It has the effect of suppressing sidebands that are outside of the 2MHz modulation bandwidth. The signal at the input to the ERA33 amplifier is a typical digital signal. It can be seen that the time duration of the envelope simulation, as well as the time steps between harmonic-balance simulations, are linked to the symbol rate in this simulation. The simulation was set up to take 10 time samples per symbol and the maximum time is calculated as 256 times the samples per symbol. In other words the simulator will consider enough time to transmit 256 symbols taking 10 samples per symbol. The time step can be calculated using this information and the symbol rate. The RF frequency as

well as the LO frequency have to be specified as well to be used in the consecutive harmonic-balance simulations. The available source power was -20dBm. The maximum intermodulation order that was considered in the simulation was 4. For further information on digital signal simulation and filters see the ADS literature [33]. The most significant difference between the measurement setup and the simulation setup is the fact that the pseudo-random generators of the respective setups where not configured to give the same bit sequence.

Figure 5.14 shows the input signal and output signals for this simulation. The measured output signal is shown in Figure 5.15. To be able to do this type of measurement requires a signal generator that can generate digitally modulated signals. The Rohde&Schwarz SMIQ has this ability. The measurement was performed with a borrowed Rohde&Schwarz FSEK signal analyzer. This measurement does not include any phase data and can purely show the receiver's effect on the amplitude of the digital signal. This is however an important measurement because the nonlinearity of the receiver generates intermodulation sidebands that have to be below a certain level, depending on the modulation standard. There is however a problem with measuring digitally modulated signals with spectrum analyzers. Because of the noise like nature of digital signals, the IF bandwidth of the spectrum analyzer influences the level of the signal considerably. This problem is not present in the simulation because the spectrum is directly calculated from time-domain data using the Fourier transform. The video filter of the spectrum analyzer can also have an averaging effect on the signal that influences the power level. In this case a resolution bandwidth of 30KHz was used with a video bandwidth of 100KHz. This minimizes the effect of the video filter. Because of this problem the absolute power levels in the two figures are not equal but the relative power levels between the fundamental output power and the intermodulation sidebands are closely matched.

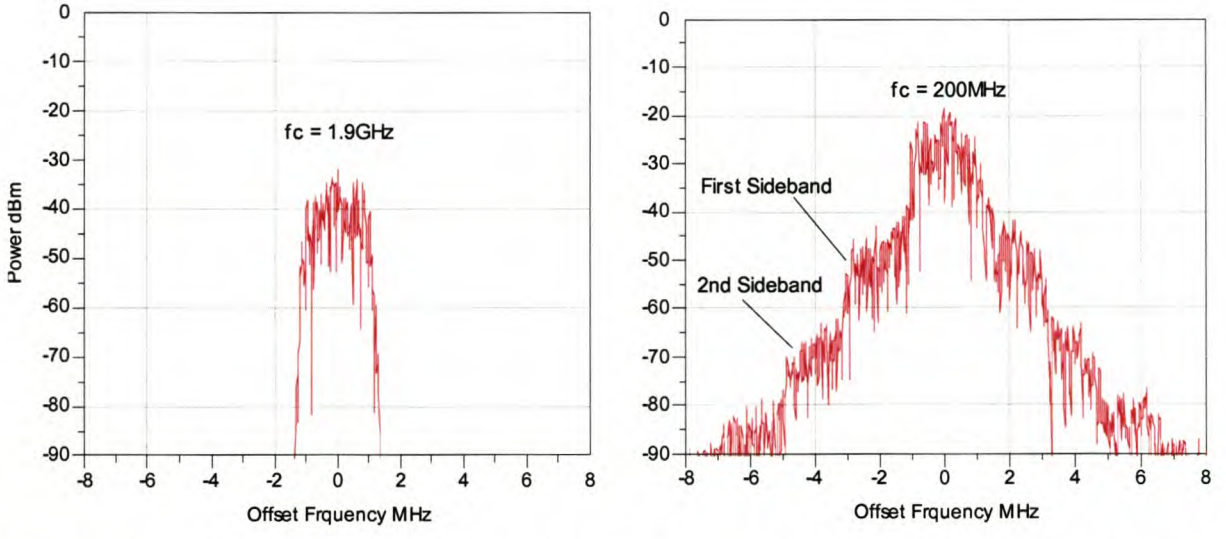


Figure 5.14 ADS simulation showing the input spectrum at 1.9GHz (left) and the output spectrum at 200MHz (right) for the circuit shown in Figure 5.13. It can be seen that the gain is approximately 15dB. The first set of intermodulation sidebands is at -50dBm and the second set at -70dBm.

It can be seen that the first intermodulation sideband is situated approximately 20dB below the fundamental and the second sideband is 40dB below the fundamental.

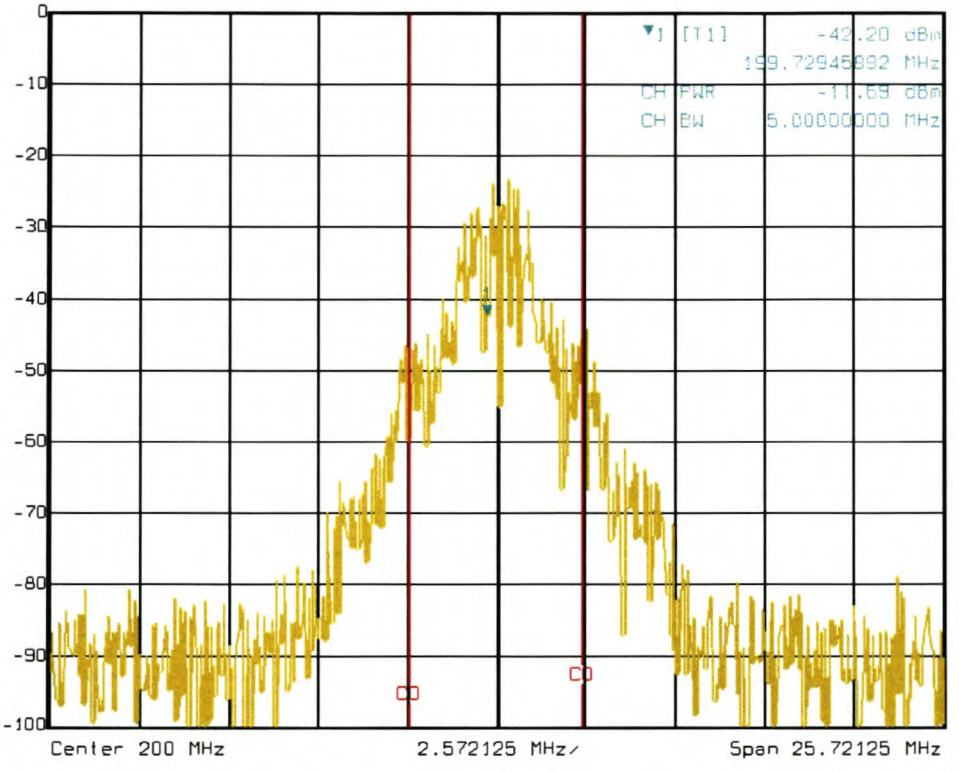


Figure 5.15 The spectrum analyzer measurement shown in this figure compares very well with the simulation data shown in Figure 5.14. The first sidebands are at -50dBm and the second sidebands are at -70dBm.

This figure shows a reasonably good match with the simulated results. The result of this type of distortion on the digital signal is usually measured with a figure of merit called bit error rate however this was not done in this work. A more intuitive type of plot, called the trajectory plot, was used to give a visual idea of the effect of the distortion. This technique plots the real component of the output voltage against the imaginary component to create a pattern. Figure 5.16 shows the trajectory plots for the input and output signals for the same simulation. The effect of the distortion on the symbols can clearly be seen.

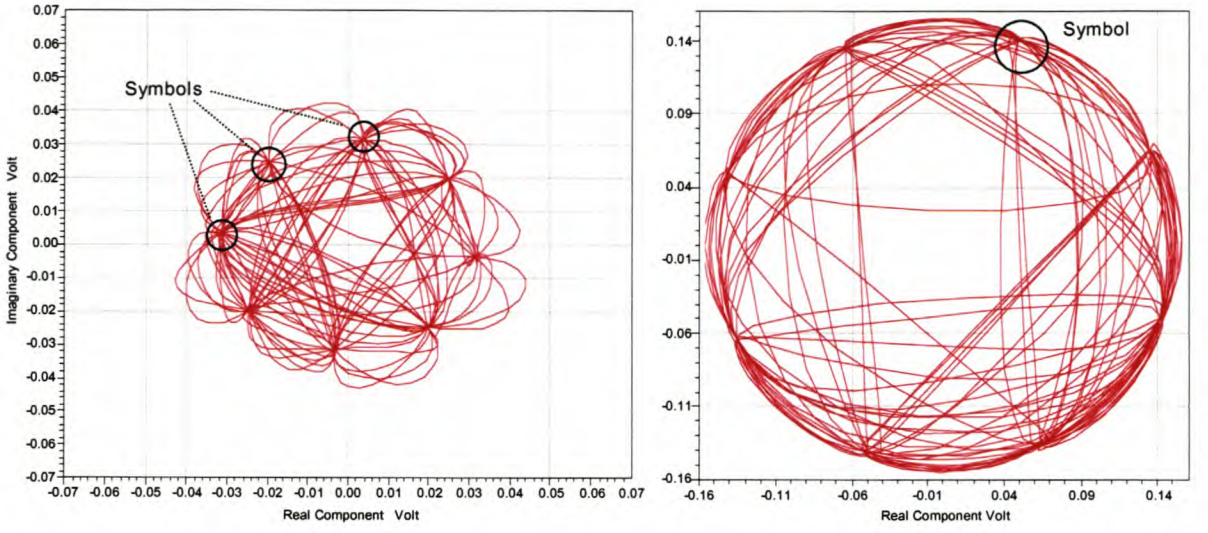


Figure 5.16 This figure shows the input and output trajectory plots for the simulation in Figure 5.13. Note that the two plots are not on the same scale. It can clearly be seen that the input trajectory is significantly amplified to give the trajectory in the second plot. The effect of the distortion is that the symbols are spread out which makes them less recognizable. It is also clear from the output plot that the receiver is operating in the saturation region.

The trajectory plots show the effects of distortion on the quality of the digital signal. The symbols in the input plot are clearly defined while they are spread out in the output plot. This type of spreading out makes the symbols less recognizable increasing the chance of errors. A phase shift can also be seen from the angular position of the symbols while amplification can be seen from the radial position of the symbols. Similar results where obtained from measurements but these techniques where not compared quantitatively and a more detailed investigation of this topic will be necessary.

## 5.5 Conclusion

The results of this chapter showed the use of the nonlinear system models of chapter 3 and chapter 4 in receiver simulations. The aim was to investigate the interactions between models as well as the prediction of some receiver characteristics.

The first section showed that the accuracy of gain and gain compression simulations are in the same region as the results obtained in chapter 3. The performance in this type of one-tone simulation is excellent giving accurate receiver gain and gain compression results providing the models are configured for the simulation conditions.

The two-tone simulations also showed accurate results. The prediction of high order intermodulation products in a frequency translating example was also very accurate. This section

showed that the models are capable of predicting a large number of two-tone intermodulation tones at spurious frequencies accurately.

The generation of unwanted spurious responses is a very important topic in receiver design and this section showed excellent results for simulations using the MixerIMT model. This type of simulation can be very useful although amplitude accuracy is dependant on custom IMT files.

The section on digitally modulated signals is a very short introduction into this type of simulation. However it was shown that the nonlinear models can give accurate amplitude results. The prediction of intermodulation sidebands was also very accurate. Although this section showed a very limited application of envelope simulation, it was seen that this technique can give valuable information regarding system behavior using digitally modulated signals. A final point to consider is the signal bandwidth of 2MHz. This was limited because of the measurement equipment. The accuracy of this type of simulation will be dependant on the signal bandwidth as it was seen that the models are relatively narrow band representations. Modern communications systems often have signal bandwidths much greater than 2MHz. The effect of model bandwidth may be a limitation in this regard and will require careful investigation.

# Chapter 6

# Conclusions

## 6.1 Introduction

The most important theme of this thesis was to develop an understanding of the capabilities and limitations of current behavioral level models and simulation techniques. The work focused on the system level models in ADS using the powerful harmonic-balanced capabilities of ADS. A very large portion of the work was aimed at developing the necessary infrastructure required to perform experiments. Measurement automation software was also developed to ensure fast and accurate implementation of models. This chapter will give a brief overview of the content and outcomes of each chapter. It will also make some recommendations regarding future research.

## 6.2 Overview and Conclusions

The second chapter in this thesis discusses the various measurement instruments that were used to characterize devices in this work. The complicated nature of nonlinear behavior often requires a comprehensive knowledge of the phenomenon as well as the measurement instruments necessary to measure it. Chapter 2 is a detailed study of the different instruments including their basic operation, capabilities and shortcomings as well as important cases where different instruments may interact. This chapter also describes the basis for the measurement automation software that was developed. This is a very important aspect of this work because the models rely on measured data. The software that was developed enables fast and repeatable measurement of device characteristics such as gain compression and intermodulation. The chapter also shows the error correction that was formulated to reduce the effects of the measurement setup on the measured

data. This chapter provides the basis for the measurements that are shown in the later chapters, and it shows that accurate measurement of nonlinear phenomenon can require significant effort and knowledge.

Chapter 3 discusses nonlinear amplifier behavior. The knowledge and software developed in Chapter 2 is employed in this chapter to characterize the nonlinear behavior of two amplifiers. This includes detailed descriptions of both one-tone and two-tone measurements. The final part of this chapter describes behavioral level, measurement based amplifier modeling in ADS. This section shows that the models can give excellent performance using the accurate measurement techniques described in the previous part of the chapter. This chapter shows the different models that are available as well as testing the performance of the models against measured data. The measurement techniques, as well as the different techniques that where used to implement these models are described. The effects of data extrapolation and interpolation are also shown. Important areas where the models can be improved are: inaccurate harmonic generation, phase prediction, gain under multi tone excitation and the generation of symmetrical intermodulation tones.

The topic of Chapter 4 is mixers. This chapter includes detailed descriptions of nonlinear behavior in mixers including measurement techniques and automation software. The topic of spurious responses is discussed in detail and some of the available spurious prediction techniques are discussed. The chapter proceeds on to mixer models showing the options that are available in ADS. The chapter compares the parameter based model to the MixerIMT intermodulation table model. It is shown that the parameter based gives excellent results for conversion gain, gain compression, isolation and port impedance. While it predicts spurious signals the amplitudes are not very accurate. The intermodulation table mixer is specifically designed for this purpose and gives excellent prediction of high order spurious signals. There are some issues concerning the use of the mixer models. The most significant is the fact that the mixers are extremely sensitive to changes in the excitation tones. Both the RF and LO signals influence the device operation which limits the application of the mixers to areas where the parameters or data were measured.

The models developed in Chapter 3 and Chapter 4 are combined n Chapter 5 to create receivers. Important receiver characteristics such as gain compression, intermodulation and spurious signals are discussed. The simulated data is compared to measured data to show the accuracy of the system simulations. It is shown that the receiver simulations give excellent results providing the models are set-up for the correct operating regions. It is shown that issues such as extrapolation and simulation order can have an important effect on the simulation accuracy. Finally the use of intermodulation mixers along with parameter based amplifiers is shown in a fairly complicated example that shows the bandwidth limitations of such a setup.

While the experiments in these chapters showed that the models can give very accurate results (as accurate as the measurement uncertainty in most cases), there are some important aspects of behavioral level simulation in ADS that need to be considered.

Firstly the models require data. This data can be supplied from various sources such as data-sheets, measured data or from transistor level simulations. While the data-sheet is the easiest, this source of data can be inadequate. Data-sheets are often very limited and most importantly they measure parameters under unknown conditions. If measured data is used, the user knows the substrate, bias, connector type and any external devices such as DC-blocking caps that will be used in the design

and can use custom measurements for the exact conditions. Transistor level modeling simulation is an excellent choice providing the necessary information is available. However in all of these cases the models are only accurate in the region of the data that is supplied. These models are not general models and the range of application around a set of nonlinear data is dependant on the specific characteristics of each device.

The models can be set up to use frequency or power dependant parameters but this requires a large amount of measured data. The accuracy and bandwidth of the models is strongly dependant on the range of data supplied. The effect of this is that a lot of effort and time is necessary to create a reasonably general model that can be used for different applications. For the case of the intermodulation models, each combination of input tones will require a custom measured intermodulation table if accurate amplitude results are required. To conclude, the performance of the models is usually directly related to the amount of time and effort used to develop the application.

However the receiver simulations of Chapter 5 showed that the models developed in the preceding chapters can be used in a wide variety of combinations where the only critical problems being the intermodulation tables and the issues related to the LO signal.

ADS supplies a comprehensive and flexible environment that can be of great help to a designer even though there are limitations in some areas.

## 6.3 Future Work and Recommendations

The entire topic of behavioral modeling is still relatively new and there are numerous fields that need further work. Within the constraints of this thesis the following areas where identified as areas where the abilities are not sufficient.

The issue of phase is becoming increasingly important in digitally modulated communications systems. Because the measurement instruments that where available limited the accuracy with which AM-to-PM could be measured, this was not investigated as thoroughly as the amplitude effects. There is still a lot of scope for improvement in this area.

ADS has the ability to build custom models. There are various options to do this. The first is the Model Development Kit that enables user to create custom analog models implemented in C-code. The other two similar options are the Symbolically-Defined Devices (SDD) and Frequency-Defined Devices (FDD). However all three these methods will require significant effort from the user. All of these techniques supply the user with the necessary interface to implement a mathematical model that has already been developed. These abilities can be employed in case where the available system level models do not meet the necessary requirements.

The models developed in this work can also be used in simulations using digitally modulated signals to verify communications systems requirements. This is a very large and powerful section of ADS that was not explored in this work and the use of nonlinear models in this type of simulation can prove to be very valuable.

# References

[1] *The New OXFORD Dictionary of English*, Clarendon Press, OXFORD, 1998

[2] Agilent EEsof EDA, *Advanced Design System Circuit Simulation*, Agilent Technologies, CA, 1999

[3] Stephen A. Maas, *Nonlinear Microwave and RF Circuits*, Second Edition, Artech House, Norwood MA, 2003

[4] Applied Wave Research, *Microwave Office 2002 User Guide*, CA, 2002

[5] David M. Pozar, *Microwave Engineering*, Second Addition, John Wiley and Sons, Canada, 1998

[6] Steve C. Cripps, *Advanced Techniques in RF Power Amplifier Design*, Artech House, Norwood MA, 2002

[7] Daniel Faria, Lawrence Dunleavy, Terje Svensen, "The Use of Intermodulation Tables for Mixer Simulations", University of South Florida, FL

[8] David Ballo, "Network Analyzer Basics", Hewlett-Packard Back to Basics Seminar, U.S.A, 1998

[9] Agilent Product Note 8753-1, "RF Component Measurements: Amplifier Measurements Using the Agilent 8753 Network Analyzer", Agilent Technologies

[10] Doug Rytting, "Network Analyzer Error Models and Calibration Methods", Agilent Technologies

[11] C van Niekerk, "3 Day Training Course in Network Analyzer Measurements", University of Stellenbosch, 2003

[12] *HP 8753C Network Analyzer Operating Manual,* Hewlett-Packard Company, CA, 1988

[13] Christie Brown, "Spectrum Analyzer Basics", Hewlett-Packard Back to Basics Seminar, U.S.A, 1997

[14] *MS462XX Vector Network Measurement System Operating Manual*, Anritsu Company, CA

[15] *HP436A Power Meter Operating and Service Manual,* Hewlett-Packard Company, U.S.A, 1984

[16] Application Note 64-1, "Fundamentals of RF and Microwave Power Measurements", Hewlett-Packard Company, U.S.A, 1977

[17] Application Note 1306-1, "8 Hints for Making Better Measurements Using Analog RF signal Generators", Agilent Technologies, CA

[18] Application Note 388, "Agilent Signal Generator Spectral Purity", Agilent Technologies, CA

[19] "Signal Source Basics", Slide Presentation, Agilent Technologies, CA

[20] C. van Niekerk, Dominique Schreurs, P. Meyer, "An Overview of Current and Future Non-Linear Device Modelling Techniques", University of Stellenbosch

[21] Bob Meyers, "Measuring IP3", Design Tip, Agilent Technologies, CA

[22] Keith Barkley, "Two-Tone IMD Measurement Techniques", www.RFdesign.com

[23] Agilent EEsof EDA, System Models, ADS 2003 Documentation, 2003

[24] Daniel Gandhi, Christopher Lyons, "Mixer Spur Analysis with Concurrently Swept LO, RF and IF: Tools and Techniques", Hittite Corp. Chelmsford, MA, 2003

[25] Product Note 8753-2, "RF Component Measurements: Mixer Measurements Using the HP 8753B Network Analyzer", Hewlett-Packard Company, U.S.A

[26] L. Dunleavy, T. Weller, E. Grimes, J. Cluver, "Mixer Measurements Using Network and Spectrum Analysis", University of South Florida, FL

[27] Application Note 1287-7, "Improving Network Analyzer Measurements of Frequency Translating Devices", Agilent Technologies, CA

[28] Agilent IAM-91563 Data Sheet, Agilent Technologies

[29] R.S. Carson, *Radio Concepts Analog*, Wiley, 1990

[30] Application note 1838, "Mixer 2x2 Spurious Response and IP2 Relationship", MAXIM, Dallas, 2002

[31] David M. Pozar, *Microwave and RF Design of Wireless Systems,* John Wiley and Sons, Canada, 2001

[32] Stephen A. Maas, "How to Model Intermodulation distortion", IEEE Microwave Theory and Tech, 1991

[33] Refresher Topic, "Digital Modulation and Mobile Radio", Rohde & Schwarz, Germany

[34] How-Siang Yap, HP EEsof Division, Hewlett-Packard, "Designing to Digital Wireless Specifications Using Circuit Envelope Simulation", Hewlett Packard, CA

[35] Agilent EEsof EDA, "Circuit Envelope Simulation", Agilent Technologies, 2003

[36] Data-Sheet, "Mini-Circuits RF Design Guide", Mini-Circuits, NY

[37] Data-Sheet, "0.8 to 6GHz Down Converter: IAM 91563", Agilent Technologies, CA

[38] Data-Sheet, "GaAs MMIC SMT Double Balanced Mixer 2.5 to 4GHz HMC170C8", Hittite Microwave Corporation

# Appendix A

## Mixer and Amplifier Circuits

Two amplifiers and two mixers where used throughout this work. They are the ERA33, ERA6 [36], Agilent IAM 91563 [37] and the Hittite 170C8 [38].

The two amplifiers and the Agilent mixer are active devices and they where biased using a low noise power supply. The supply used an LM317 voltage regulator chip with tantalum capacitors to convert 15V DC to the required output voltage for each device. The circuit layout was done in ADS and an example of this is shown in Figure A.1.

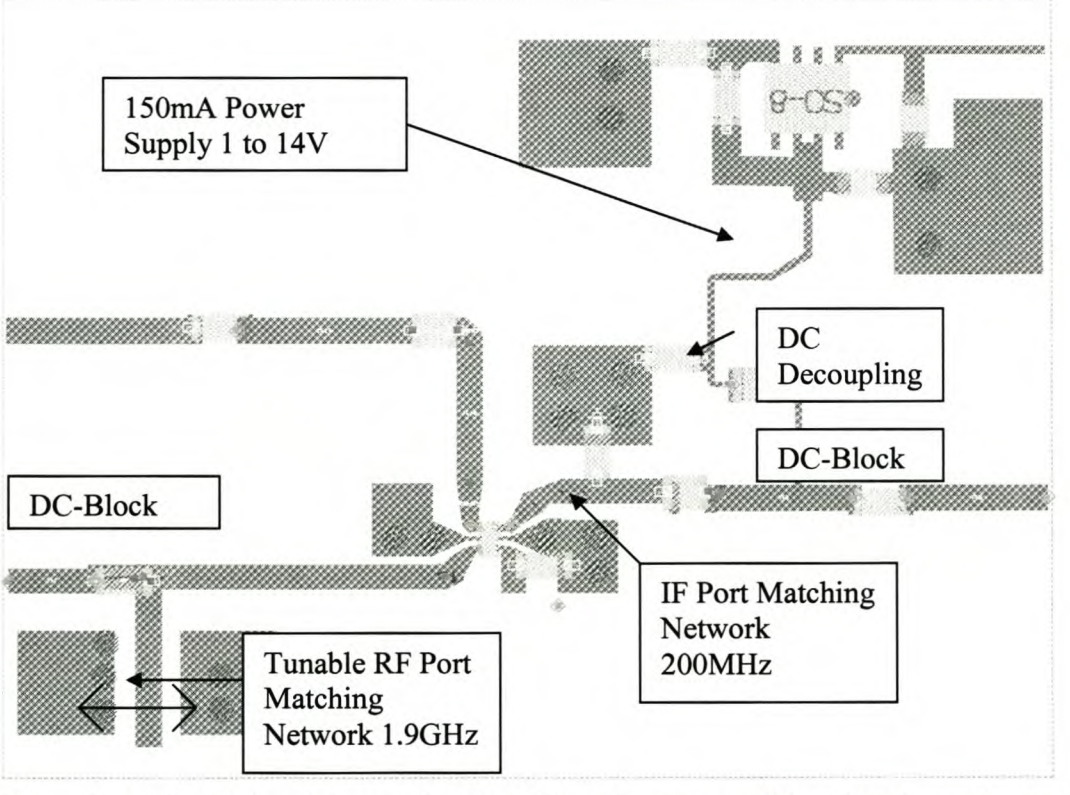


Figure A.1 Example of circuit layout in ADS. The RF port matching circuit can be tuned by adjusting the position of the shot to earth. The power supply decoupling capacitors are tantalum capacitors and the DC blocking capacitors are wideband DC blocks from Dielectric Laboratories.

The setup was designed to ensure that the different components could be used in a number of setups. The designs are compatible with any SMA filters, attenuators etc. The design ensured easy manipulation and handling of circuits to be able to create different receiver configurations quickly.

An example of a receiver is shown in Figure A.2. The figure photo shows a two-tone intermodulation setup. The SMA attenuators and filters are from Mini-Circuits as well as the power combiner. The LO input is filtered at the signals generator's output port. Any receiver combination can be realized by different combinations of the components. Note that the DC power source is not shown in this figure.

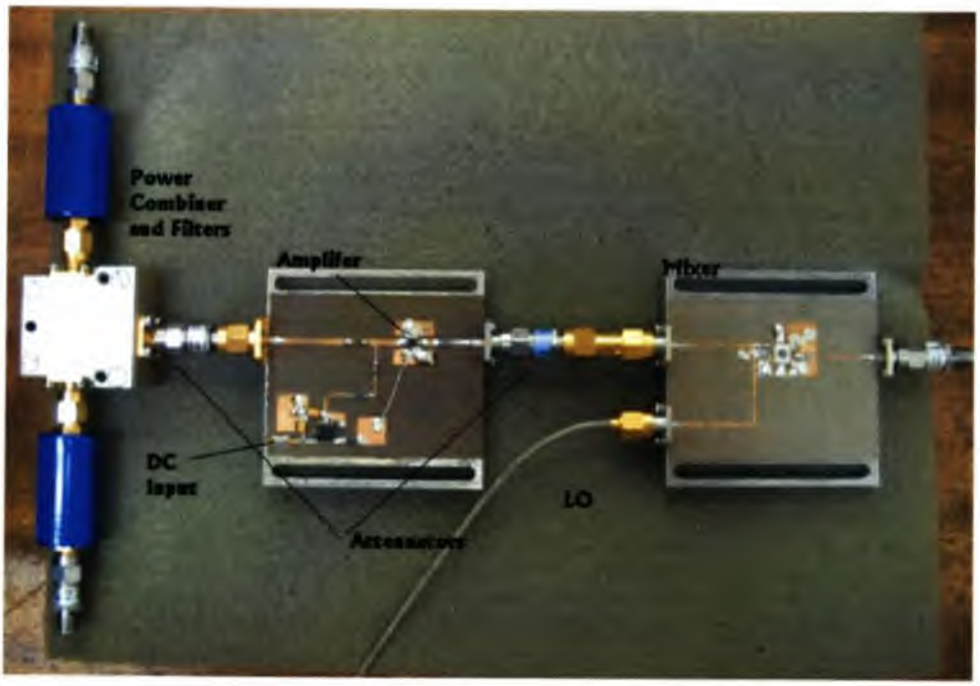


Figure A.2 This photo shows the component design that was used to realize different receivers. This specific setup is to measure two-tone intermodulation for a receiver showing the filters, attenuators and power combiner that is necessary for this measurement. Attenuators are also included to reduce the mismatch at the mixer ports.